

Amino acid metabolism under drought stress in *Arabidopsis thaliana*

Von der Naturwissenschaftlichen Fakultät der
Gottfried Wilhelm Leibniz Universität Hannover

zur Erlangung des Grades

Doktor der Naturwissenschaften (Dr. rer. nat.)

genehmigte Dissertation

von

Björn Heinemann, M. Sc.

2021

Referent: Prof. Dr. rer. nat. Hans-Peter Braun

Korreferent: Prof. Dr. rer. nat. Stefan Binder

Korreferent: Dr. rer. nat. Sascha Offermann

Tag der Promotion: 22.01.2021

Contributing publications

The following publications contributed to this thesis:

1. Batista-Silva, W.* , **Heinemann, B.***, Rugen, N., Nunes-Nesi, A., Araújo, W.L., Braun, H.P., Hildebrandt, T.M. (2019):
The role of amino acid metabolism during abiotic stress release
Plant, Cell & Environment, Vol. 42, Issue 5, Pages 1630-1644
DOI: 10.1111/pce.13518
* Equally contributing first authors
2. **Heinemann, B.**, Künzler, P., Eubel, H., Braun, H.P., Hildebrandt, T.M. (2021):
Estimating the number of protein molecules in a plant cell: protein and amino acid homeostasis during drought
Plant Physiology, Vol. 185, Issue 2, Pages 385–404
DOI: 10.1093/plphys/kiaa050
3. **Heinemann, B.**, Hildebrandt, T.M. (2021):
The role of amino acid metabolism in signaling and metabolic adaptation to stress induced energy deficiency in plants
Journal of Experimental Botany, Vol. 72, Issue 13, Pages 4634–4645
DOI: 10.1093/jxb/erab182

Abstract

Due to climate change, drought periods will occur more frequently in the future. They will have a strong negative impact on crop yields. Drought stress leads to an osmotic imbalance and causes the closure of stomata to reduce water loss of transpiration. However, this reduces photosynthesis and ultimately leads to the formation of oxygen radicals, which may damage cell structure and function. If drought stress continues, a dramatic lack of energy is caused, which threatens plant life. To prevent irreversible damage, plants adapt their entire metabolism to resist drought stress at an early stage.

This dissertation is dedicated to the adaptation of plants upon drought stress and the specific contribution of amino acid metabolism during this process. An *in vitro* experiment was performed to investigate the implications of a short but severe water deficit (**Chapter 2.1**). The *Arabidopsis* seedlings showed a strong decrease in protein content within 24h and at the same time a strong accumulation of the amino acids L-proline and GABA. Proteome analyses revealed that the aromatic amino acids were primarily used for the synthesis of stress mitigating secondary metabolites, such as flavonoids and anthocyanins, which are known to scavenge reactive oxygen species. Furthermore, a general induction of amino acid catabolism was observed, which provides sufficient amounts of L-glutamate for the synthesis of L-proline and GABA. Simultaneously, the catabolic pathways could represent an alternative source of reduction equivalents, which may fuel mitochondrial ATP production under carbon starvation conditions.

In soil experiments were performed to investigate the plant drought stress response in a more physiological context (**Chapter 2.2**). In both, the *in vitro* and the *in soil* system, the plant stress response can be divided into distinct phases. The osmotically active amino acids, L-proline and GABA, are already produced in early phases of the water deficit and allow keeping the cellular water content constant for several days. Shortly before plants become irreversibly impaired by drought, a massive protein degradation takes place. This marks the beginning of the severe stress phase. Based on the proteome data and theoretical considerations, an experimental strategy was developed, which allows calculating absolute contents, concentrations and even copy numbers of individual proteins per leaf cell. As a result, the dynamic interconnection of protein homeostasis and amino acid homeostasis could be monitored and quantified on absolute scales. Our approach reveals the energy content of the released amino acids and indicates that their complete oxidation would cover the energy demand of the plant for several hours.

In a review article, the regulatory properties of amino acids during the plant stress response were summarized and discussed (**Chapter 2.3**): Amino acids can be used as signal molecules, e.g. for inducing stomatal closure, as sensors of the nutrient content of cells or regulators for inducing their own catabolism. Our findings contribute to a general understanding of the effects of drought stress on the plant metabolism and shed light on the versatile and important roles of amino acids beyond their role in representing building blocks for protein biosynthesis.

Keywords: drought stress, amino acid metabolism, proteomics, *Arabidopsis thaliana*

Zusammenfassung

Aufgrund des Klimawandels werden zukünftig vermehrt Trockenperioden auftreten. Diese Phasen werden die Erträge unserer Nutzpflanzen stark beeinträchtigen. Trockenstress führt zu einem osmotischen Ungleichgewicht und zur Schließung der Spaltöffnungen der Blätter, um den Wasserverlust durch Transpiration zu reduzieren. Dies verringert die Photosynthese-Leistung und führt letztendlich zur Entstehung von Sauerstoffradikalen, die Zellstrukturen beschädigen und nur unter Energieaufwand beseitigt werden können. Hält der Trockenstress an, führt dies zu einem sukzessiven Energiemangel. Um irreversible Schäden zu verhindern, passen Pflanzen ihren kompletten Stoffwechsel bereits früh an den Trockenstress an. Welche Anpassungen in welchem Ausmaß induziert werden und welche Rolle der Aminosäurestoffwechsel dabei spielt, war das Hauptthema dieser kumulativen Dissertation. Mithilfe eines *in vitro* Experiments wurde ein kurzes, aber unmittelbares und sehr starkes Wasserdefizit erzeugt (**Kapitel 2.1**). Die *Arabidopsis* Keimlinge zeigten eine starke Abnahme des Proteingehalts innerhalb von 24h und gleichzeitig eine starke Anreicherung der Aminosäuren L-Prolin und GABA. Eine Proteomanalyse ergab, dass die aromatischen Aminosäuren primär für die Synthese von hilfreichen Sekundärmetaboliten, wie Flavonoiden und Anthocyanen benutzt werden, um oxidative Schäden vorzubeugen. Weiterhin zeigte die Proteomanalyse, dass der Aminosäurekatabolismus generell induziert wurde. Dadurch kann ausreichend L-Glutamat für die Synthese von L-Prolin und GABA bereitgestellt werden. Gleichzeitig könnte der Abbau von Aminosäuren eine alternative Quelle für Reduktionsäquivalente darstellen, um die ATP Produktion der Mitochondrien während einer Kohlenhydratmangelsituation anzutreiben. Um die *in vitro* identifizierten Anpassungen der Pflanzen in einen physiologischen Kontext einordnen zu können, wurde ein progressives Stressexperiment *in soil* durchgeführt (**Kapitel 2.2**). Der Stressverlauf konnte auf Basis der beiden Experimente in Phasen eingeteilt werden. Die osmotisch aktiven Aminosäuren L-Prolin und GABA, werden bereits in der frühen Trockenstressphasen produziert und konnten den zellulären Wassergehalt für einige Tage konstant halten. Erst wenige Stunden bevor die Pflanzen irreversibel ausgetrocknet waren, wurde ein massiver Proteinabbau detektiert, welcher den Beginn der schwerwiegenden Stressphase einleitet. Basierend auf den Proteomdaten wurde eine Berechnungsmethode entwickelt, die es ermöglicht, den absoluten Gehalt, die Konzentrationen und die Anzahl der in einer Zelle vorhandenen Moleküle für individuelle Proteine abzuschätzen. Somit konnte die Dynamik zwischen der Proteinhomöostase und der Aminosäurehomöostase analysiert werden. Wir konnten die freigesetzte Aminosäuremenge abschätzen und berechnen, dass diese die Energieversorgung der Pflanze für einige Stunden decken könnten. In einem abschließenden Review-Artikel wurden die neusten Erkenntnisse zur Rolle der Aminosäuren als Signalmoleküle bei der Anpassung des Stoffwechsels an abiotischen Stress zusammengestellt (**Kapitel 2.3**). In Stresssituationen wirken Aminosäuren als Signalmoleküle, um z.B. Spaltöffnungen zu schließen, um die Pflanze über den Nährstoffgehalt der Zellen zu informieren oder um den eigenen Katabolismus zu induzieren. Unsere Erkenntnisse tragen zum generellen Verständnis der Auswirkungen von Trockenstress auf den pflanzlichen Stoffwechsel bei und beleuchten gleichzeitig die vielseitigen und bedeutsamen Rollen des Aminosäuremetabolismus.

Schlagworte: Trockenstress, Aminosäuremetabolismus, Proteomik, *Arabidopsis thaliana*

Abbreviations

Table 1: Explanation of relevant terms and acronyms used in this dissertation.

Abbreviation	Explanation
2-OB	2-Oxobutanoate
2-OG	2-Oxoglutarate
2-PG	2-Phosphoglycolate
3-MOB	3-Methyloxobutanoate
3-MOP	3-Methyloxopentanoate
3-PG	3-Phosphoglycerate
4-MOP	4-Methyloxopentanoate
AAA	Aromatic amino acids
ABA	Abscisic acid
Ala	L-Alanine
AlaAT	Alanine aminotransferase
APS	Adenosine-5-phosphosulfate
Arg	L-Arginine
Asn	L-Asparagine
Asp	L-Aspartic acid
BCAA	Branched-chain amino acids
Cit	Citrulline
Cys	L-Cysteine
Cysn	Cystine
D2HGDH	D-2-Hydroxyglutarate dehydrogenase
DW	Dry weight
EAA	Essential amino acids
ETC	Electron transport chain
ETF	Electron-transfer flavoprotein
ETFQO	Electron-transfer flavoprotein ubiquinone oxidoreductase
GABA	γ -Aminobutyrate
GABA-T	γ -Aminobutyrate transaminase
GDH	Glutamate dehydrogenase
Gln	L-Glutamine
GLS	Glucosinolates
Glu	L-Glutamic acid
Glx	Glyoxylate
Gly	Glycine
GOGAT	Glutamin-Oxoglutarate aminotransferase
GS	Glutamine synthetase
His	L-Histidine

Table 1: Continued.

Abbreviation	Explanation
iBAQ	Intensity-based absolute quantification
Ile	L-Isoleucine
IVDH	Isovaleryl-CoA dehydrogenase
Leu	L-Leucine
LFQ	Label free quantification
LS	Large subunit
Lys	L-Lysine
MDH	Malate dehydrogenase
Met	L-Methionine
MS	Mass spectrometry
MW	Molecular weight
NEAA	Non-essential amino acids
OA	Oxaloacetate
OST1	Open stomata 1
Orn	Ornithine
P5C	Pyrroline-5-carboxylate
PAL-4	Phenylalanine ammonia lyase 4
PEG	Polyethylene glycol
Phe	L-Phenylalanine
PRM	Parallel reaction monitoring
Pro	L-Proline
Pyr	Pyruvate
RBOHD	Respiratory burst oxidase homolog D
ROS	Reactive oxygen species
RubisCO	Ribulose-1,5-bisphosphate carboxylase/oxygenase
SAM	S-adenosyl methionine
Ser	L-Serine
SnRK	Sucrose non-fermentation-related kinase
SSA	Succinic semialdehyde
TCA	Tricarboxylic acid cycle
Thr	L-Threonine
TOR	Target of rapamycin
Trp	L-Tryptophan
TRX	Thioredoxin
Tyr	L-Tyrosine
Val	L-Valine
WHO	World Health Organization

Contents

Contributing publications.....	I
Abstract	II
Zusammenfassung.....	III
Abbreviations.....	IV
1 Introduction	7
1.1 Plant amino acid metabolism	8
1.1.1 Glutamate related amino acids	8
1.1.2 The aspartate family	10
1.1.3 Aromatic amino acids	12
1.1.4 Alanine and the branched-chain amino acids	13
1.2 Physiological and metabolic consequences of drought stress.....	14
1.3 Drought prevention and cellular counteractions	16
1.4 Major functions of amino acid metabolism during drought stress	17
1.4.1 Experimental approaches to study drought stress in Arabidopsis	18
1.4.2 A quantitative angle on amino acid metabolism during drought stress	20
1.4.3 Proteostasis and amino acid homeostasis during progressive drought stress.....	22
1.4.4 Amino acids as osmolytes.....	24
1.4.5 Amino acids as precursors for secondary metabolites	24
1.4.6 Amino acids as alternative respiratory substrates	25
1.4.7 Amino acids as signaling molecules and cellular benchmarks.....	27
1.5 References	29
2 Publications and Manuscripts.....	34
2.1 The role of amino acid metabolism during abiotic stress release.....	35
2.2 Estimating the number of protein molecules in a plant cell: protein and amino acid homeostasis during drought.....	54
2.3 The role of amino acid metabolism in signaling and metabolic adaption to stress induced energy deficiency in plants.....	82
3 Appendix	95
3.1 Curriculum Vitae	96
3.2 List of publications	97
3.3 Conference contribution	98

1 Introduction

People know amino acids as nutritional parts of their food or of animal feed. Due to promotion by food companies, amino acids are nowadays connected to a healthy and responsible lifestyle. Amino acids are added to food products to improve their nutritional value and the attractiveness for consumers. Especially, athletes and hobby sportsmen like to supplement their diet with amino acids to achieve optimal nitrogen supply and muscle growth. Twenty different amino acids are needed for protein biosynthesis. They are called proteinogenic amino acids and are divided into two subcategories: the essential amino acids (EAA) and non-essential amino acids (NEAA) (Figure 1).

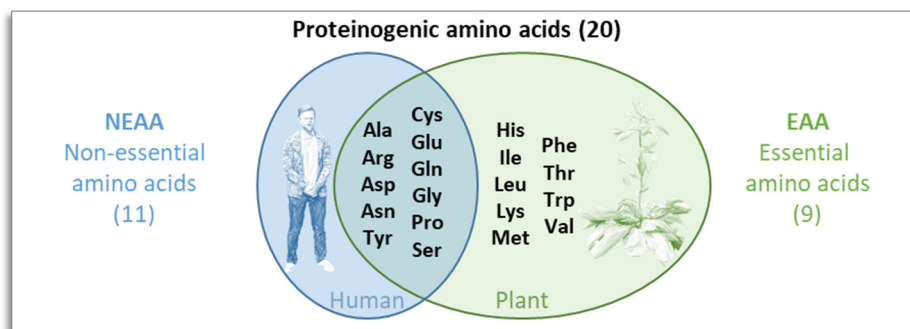


Figure 1: Overlap of the endogenous amino acids of humans and plants. Humans are only capable of building eleven amino acids (non-essential amino acids, NEAA), while plants are also synthesizing the missing nine proteinogenic amino acids (essential amino acids, EAA).

In contrast to humans, plants and fungi are capable of synthesizing all twenty amino acids. During early evolution, a wide variety of eukaryotes such as animals and parasites lost the feature of EAA synthesis, because they existed in a nutrition-rich environment and evolved the ability to feed on other organisms (Payne and Loomis, 2006). These eukaryotes could save the energy required for EAA synthesis but had to take them up through their regular diet (e.g. plant- or animal-source foods). During food digestion, EAA and NEAA are released and transported via the blood stream to serve the protein biosynthesis of the cells. A long-term unbalanced diet or malnutrition can result in EAA deficiency causing health problems such as vomiting, emotional disorders, insomnia and anemia (Hou and Wu, 2018). In 2010 the World Health Organization estimated that about 167 million children in developing countries suffered growth retardation caused by postnatal protein-deprived malnutrition (Onis *et al.*, 2012). Although this number is decreasing since 1990, the increase of the global temperature and the changing climate however may severely impair agricultural yield and aggravate food shortage in developing countries again. In the past years, plant scientist addressed these problems by genetically modifying crop plants to increase drought tolerance and EAA content (Martignago *et al.*, 2019; Yang *et al.*, 2020). However, the complexity and the tight regulation of amino acid metabolism posed some challenges in increasing single amino acid contents. Despite several recent contributions, regulation mechanisms of the amino acid network under drought-stress remain widely elusive. The following chapters describe background information about the amino acid metabolism in plants and the general consequences of drought stress for plants. After that, the research topic of this dissertation will be addressed by discussing the major functions of the amino acid metabolism during drought stress. Thereby, the findings of the two research publications and the review article are summarized and set into context.

1.1 Plant amino acid metabolism

Nitrogen is an essential macronutrient for plants, and is required as a component of secondary metabolites, nucleotides, amino acids and thus proteins. The availability of nitrogen and the biochemical processes of nitrogen uptake and assimilation are important for plant growth (Hirel *et al.*, 2007; Liu *et al.*, 2011). In brief, ammonia or nitrate from the rhizosphere can be imported through low and high affinity transporter systems (Krapp, 2015). Nitrate and ammonia can be metabolized in roots, but are mainly transported and loaded into the xylem. Within the leaf cells, nitrate is reduced and incorporated into amino acids. All amino acids contain an amino group (NH₂) and a carboxyl group (COOH) plus individual functional groups. These side chains confer various biochemical properties to amino acids like size, polarity, charge and reactivity. Amino acids are further classified into proteinogenic and non-proteinogenic amino acids. The group of non-proteinogenic amino acids is vast (>700) and diverse (Hunt, 1985). These amino acids are rather low abundant and some of them function as precursor for the proteinogenic amino acids of the primary metabolism. However, they are mostly specific to the plant species and are often used as stress defense compounds or toxins. In contrast, the proteinogenic amino acids, are less in number (20) but highly abundant. This thesis focuses on the proteinogenic amino acids and their functions during drought stress. Amino acids are the constituents of proteins but they also accumulate in free pools. The free amino acid pool sizes depend on (1) protein homeostasis (proteostasis), (2) free amino acid homeostasis and (3) the demand for amino acids as precursors for the synthesis of secondary of metabolites (Figure 2).

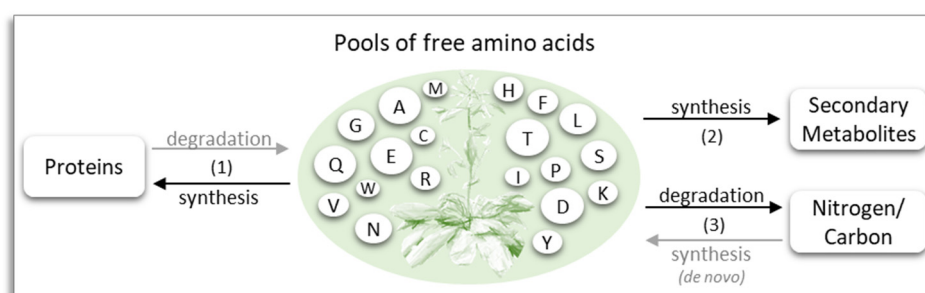


Figure 2: Three metabolic equilibria affect the concentration of free amino acids in a plant cell. Pool sizes increase by protein degradation or *de novo* amino acid synthesis. Pool sizes decrease by protein synthesis, synthesis of secondary metabolites and amino acids degradation.

1.1.1 Glutamate related amino acids

Glutamate (Glu) can be considered as precursor of all other amino acids. The *de novo* amino acid synthesis starts when cytosolic nitrate is reduced to nitrite via nitrate reductase. Nitrite is subsequently imported into the plastids where it is further reduced to ammonia by nitrite reductase. The chloroplastic isoform of glutamine synthetase facilitates the actual assimilation of ammonia by condensing ammonia with Glu to Glutamine (Gln). The amino group of Gln is transferred to a 2-oxoglutarate (2-OG) molecule yielding two Glu molecules. This transamination step is catalyzed by glutamine-oxoglutarate aminotransferase (Forde and Lea, 2007; Lea and Mifflin, 2011). Another glutamine synthetase isoform in the cytoplasm is in charge of re-assimilating ammonia released by other metabolic pathways such as protein degradation (Thomsen *et al.*,

2014). Most of the characterized aminotransferases (18 out of 25) generate or use Glu as amino group donor (Liepman and Olsen, 2004). Figure 3 gives an overview of the amino acid metabolism focusing on Glu.

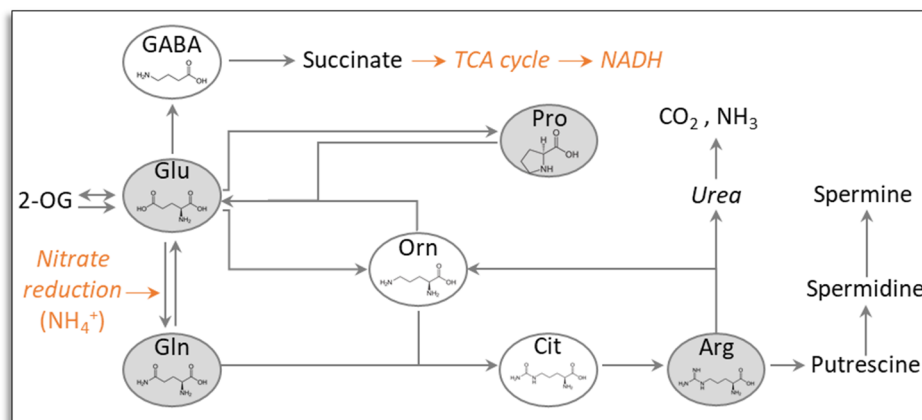


Figure 3: Metabolism of glutamate-derived amino acids. Proteinogenic amino acids are highlighted in grey. Arrows may stand for multiple enzymatic steps (Figure from Hildebrandt *et al.*, (2015), modified). Orange caption show further metabolic connections (2-OG: 2-Oxoglutarate; TCA cycle: Tricarboxylic acid cycle).

Glu decarboxylase decarboxylates Glu to γ -aminobutyrate (GABA), a non-proteinogenic amino acid that plays an important role in abiotic stress defense. It can be further transaminated by the GABA transaminase, which transfers the amino group of GABA to pyruvate or glyoxylate to produce either Ala or Gly and succinic semialdehyde. Subsequently, succinic semialdehyde is oxidized to succinate, which can enter the tricarboxylic acid cycle (TCA cycle) to generate reducing equivalents. This connection highlights the central role of Glu. An ubiquitous and especially important enzyme is Glu dehydrogenase (GDH). It regulates the Glu and 2-OG homeostasis and is therefore important for the TCA cycle (export of 2-OG), the nitrogen assimilation and the production of Glu as precursor for stress relevant amino acids such as Proline (Pro) (Lehmann *et al.*, 2010). Under optimal conditions, the content of free Pro is low. Interestingly, Pro accumulates in the cytosol and in chloroplasts under osmotic stress several hundred folds. Pro synthesis starts with the reduction of Glu to Glu-semialdehyde, followed by a spontaneous conversion to pyrroline-5-carboxylate (P5C). Finally, P5C is reduced to Pro catalyzed by the P5C-reductase. The catabolic enzymes ProDH and P5CR are located in mitochondria, facilitating the use of recovered reduction equivalents, like NADH and FADH to fuel the respiratory electron transport chain (Schertl and Braun, 2014).

Another Glu-derived, but non-proteinogenic amino acid is Ornithine (Orn). Orn is only present in low cellular concentrations. Majumdar *et al.* (2013) suggested that Orn is primarily an intermediate of the synthesis of more abundant amino acids such as Pro, Arginine (Arg) and also polyamines. In line with this, the Orn-transcarbamylase as well catalyzes the conversion to Citrulline (Cit), another non-proteinogenic amino acid, which is in turn precursor of Arg (Winter *et al.*, 2015).

Arg is synthesized in plastids and is the amino acid with the highest nitrogen to carbon ratio (4N : 6C). This makes Arg an efficient nitrogen store. However, Arg can also be used as precursor for the cytosolic polyamine synthesis. Polyamines, like putrescine (diamine),

spermidine (triamine) and spermine (tetraamine) are linear molecules of two or more amines and categorized as secondary metabolites (Alcázar *et al.*, 2010; Planchais *et al.*, 2014). For degradation, Arg is transported into mitochondria. The catabolism leads to the release of Cit and urea, which is finally hydrolyzed to ammonium and carbon dioxide by an Urease (Witte, 2011).

1.1.2 The aspartate family

Like Gln and Glu, the main tasks of Asparagine (Asn) and Aspartate (Asp) are the distribution and storage of nitrogen. Asn is especially efficient, because of its high nitrogen to carbon ratio (2N : 4C). Asn was the first molecule, which was classified as an amino acid when it was isolated from the sap of asparagus plants in 1806 (Wisniak, 2013). The Asp metabolism is the origin of the essential amino acids: Lysine (Lys), Threonine (Thr), Methionine (Met) and Isoleucine (Ile), and is further connected to Glycine (Gly), Serine (Ser) and Cysteine (Cys) (Figure 4). This anabolic pathway involves particularly many enzymatic steps, that are regulated by feedback inhibition of the initial Asp phosphorylation. Deriving metabolites and amino acids, like Lys, Thr or *s*-adenosylmethionine inhibit the activities of all three Asp kinases (Jander and Joshi, 2009). Asp is found in especially high concentrations in plant cells, because of its central function as precursor for the other amino acids mentioned above. The Asp aminotransferase generates Asp by transferring the amino group of Glu to oxaloacetate (OA). Therefore, Asp is the third amino acid by which nitrogen is mainly assimilated. Besides GS, also Asn synthetase can facilitate the assimilation of ammonia using Asp to form Asn in the cytosol (Coruzzi, 2003). Starting from Asp there are two branches leading to either Lys or Thr, Met and Ile. Free Lys is found in low concentrations, probably due to its cell toxicity (Batista-Silva *et al.*, 2019). Its degradation starts with the condensation of Lys and 2-OG to form saccharopine, which is subsequently oxidized to amino adipate. Thompson *et al.* (2020) proposed that the GABA transaminase transaminates amino adipate to 2-oxoadipate. 2-oxoadipate is subsequently converted to hydroxyglutarate by a newly characterized Hydroxyglutarate synthase. A second path was recently described by Ding *et al.* (2016), where Lys serves as a precursor of hydroxyl pipercolic acid, which is an important signal molecule for the induction of systemic acquired resistance upon pathogen attack (Hartmann and Zeier, 2018).

Proceeding from Asp, the second main branch splits into the anabolic pathways of Met and Thr, which both derive from *o*-phospho-homoserine (Lee *et al.*, 2005). Thr is used as a precursor for the branched-chain amino acid Ile and can also be cleaved to form Gly. *O*-phospho-homoserine can also be conjugated with Cys by cystathionine- γ -synthase to form cystathionine. Cystathionine is further converted to homocysteine, which is the direct precursor of Met. It also represents the entry into the Met-SAM (*s*-adenosyl methionine) cycle. The Met-SAM cycle is closely linked to the Met salvage cycle. Together they provide SAM for several methylation reactions of the cell and simultaneously recycle the side product methylthioadenosine to Met (Sauter *et al.*, 2013). SAM provides methyl groups for several stress related pathways like the ethylene biosynthesis, polyamine biosynthesis, glucosinolate metabolism, Cys synthesis and DNA methylation (Mäkinen and De, 2019).

Met and Cys are the only two proteinogenic amino acids carrying sulfur. The synthesis of Cys completes the sulfur assimilation process in plants. In brief, sulfate is taken up by the roots and loaded into the xylem. Driven by transpiration, it is transported to the shoot.

After the import into the cell, sulfate can be stored in vacuoles or directly transported into the chloroplast, where it is activated by conjugation with ATP. Adenosine-5-phosphosulfate is formed and in further consecutive enzymatic steps it is reduced to Sulfide using reducing power of glutathione and ferredoxin. Sulfide is finally assimilated with o-acetylserine to Cys by the o-acetylserine-(thiol)-lyase (Hell and Wirtz, 2011). O-acetylserine originates from Ser, an amino acid known to be involved in the recycling of carbon during photorespiration.

There are three processing routes of Cys in different compartments. (1) In mitochondria, it can be transaminated to 2-Mercaptopyruvate by an unknown Cys aminotransferase, and subsequently detoxified to pyruvate and thiosulfate. (2) Ubiquitous Cys desulfyrases can use the reduced sulfur to assemble Fe-S clusters, producing Alanine as by product. (3) In the cytosol, Cys can be desulfhydrated by another class of Cys desulfhydrases producing ammonia, pyruvate and hydrogen sulfide (Hildebrandt *et al.*, 2015). An additional Cys sink may be the formation of a cysteine dimer called cystine (Cysn). So far, there are no enzymes known, which catalyze this dimerization. However Jones *et al.* (2003) reported the first cystine lyase, catalyzing the cleavage of cystine into thiocysteine and pyruvate. The spontaneous generation of disulfide bonds may be affected by environmental stressors and part of sensing the redox state of the cell (Pivato *et al.*, 2014).

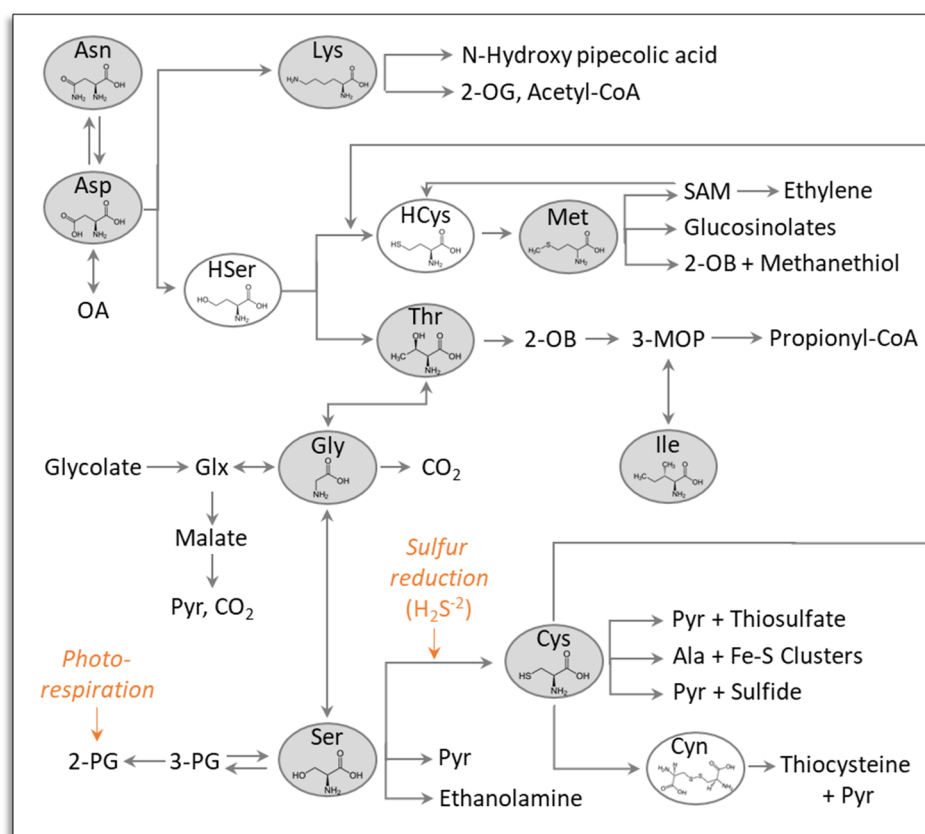


Figure 4: Metabolism of aspartate family amino acids. Proteinogenic amino acids are highlighted in grey. Arrows may stand for multiple enzymatic steps (Figure from Hildebrandt *et al.*, (2015), modified). Orange caption show further metabolic connections. OA: Oxaloacetate, 2-OG: 2-Oxoglutarate, 2-OB: 2-Oxobutanoate, HSer: Homoserine, HCys: Homocysteine, Cysn: Cystine, 3-MOB: 3-Methyloxobutanoate, Glx: Glyoxylate, Pyr: Pyruvate, 2-PG: 2-phosphoglycolate, 3-PG: 3-phosphoglycerate).

1.1.3 Aromatic amino acids

Aromatic amino acids (AAA) possess aromatic rings as functional groups and are rather less abundant in plant cells. A reason for that may be the energy-consuming biosynthesis of the aromatic structures. Aromatic amino acids are mainly used as precursors for secondary metabolites like flavonoids, glucosinolates, terpenes, hormones or alkaloids, but are also building blocks for proteins (Figure 5). In plants, the aromatic amino acids Tryptophan (Trp), Tyrosine (Tyr) and Phenylalanine (Phe) derive from chorismate, which originates from the shikimate pathway located in plastids (Maeda and Dudareva, 2012). Chorismate is catalyzed to prephenate and is either oxidized to 4-hydroxyphenylpyruvate (Tyr precursor) or oxidized to phenylpyruvate (Phe precursor). Corresponding intermediates can subsequently be aminated to Tyr and Phe, catalyzed by the respective transaminases. The transamination reaction can also happen first, forming aroenate directly from prephenate. Aroenate can be used for the synthesis of both amino acids, and is subsequently oxidized to either Tyr or Phe (Rippert *et al.*, 2009). Similar to the Asp-related amino acid metabolism, also AAA levels are regulated by feedback inhibition (Maeda and Dudareva, 2012).

The AAA biosynthesis is primarily induced when there is a need for secondary metabolites. In the course of this, an important enzyme is the Phe ammonia lyase, which converts Phe to cinnamate. Cinnamate is hydroxylated to p-coumaroyl-CoA by cinnamate 4-hydroxylase. A similar but unverified biochemical route to p-coumaroyl-CoA is proposed for Tyr. P-coumaroyl-CoA is a central intermediate of the phenylpropanoid pathway, which is the source of diverse compounds like coumarins, flavonoids, lignin, isoflavonoids, suberins, stilbenes, cutins, anthocyanins, phenylpropenes, acylated polyamines and other alkaloid derivatives (Fraser and Chapple, 2011). Trp is synthesized by six enzymatic steps also starting from chorismate. Many metabolic routes to secondary metabolites are proposed, but rarely investigated in Arabidopsis. Furthermore, the catabolic route of Trp is also not known to date.

Histidine (His) appears to be a special case in amino acid research. While the synthetic pathway is completely known in Arabidopsis, neither the degradation nor the conversion to secondary metabolites have been revealed in any plant. His derives from ribose 5-phosphate and has connections to folate and the purine metabolism (Stepansky and Leustek, 2006). The synthesis of His is energy-intensive, involving eleven reactions, eight enzymes and requiring 41 ATP molecules (Swire, 2007). In humans, the first two steps of histidine degradation are catalyzed by a histidase (*NM_001258333*) and an urocanase (*NM_144639*). So far, alignment studies of both proteins failed to find corresponding homologs in Arabidopsis. The closest homolog, with 29% identity, turned out to be the phenylalanine ammonia lyase-4 (PAL-4). However, a His-catalyzing activity of Arabidopsis PAL-4 was not confirmed yet. Reports of a histidase-like enzyme of the algae *Chlamydomonas* and an urocanase-like enzyme of white clover were not reproducible and should be reviewed (unpublished data).

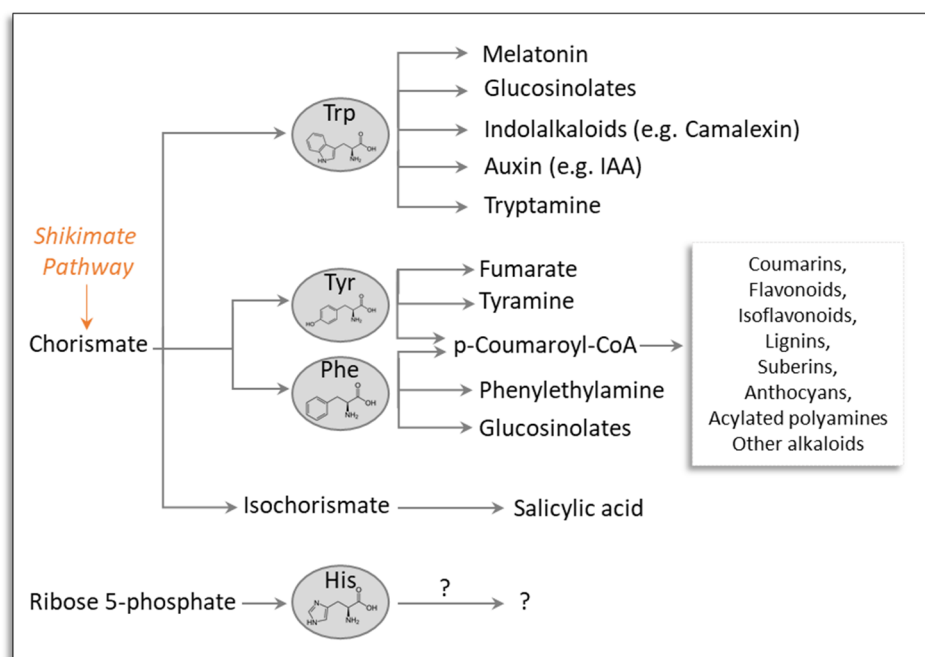


Figure 5: Metabolisms of aromatic amino acids. Proteinogenic amino acids are highlighted in grey. Arrows may stand for multiple enzymatic steps (Figure from Hildebrandt *et al.*, 2015, modified). Orange caption show further metabolic connections.

1.1.4 Alanine and the branched-chain amino acids

The oxidation of pyruvate represents the entry to the TCA cycle. However, pyruvate is also linked to amino acid metabolism by being precursor of Ala (Figure 6). Within a single reaction, the Ala aminotransferase (AlaAT) catalyzes the reversible transamination of pyruvate and Glu to Ala and 2-OG (Liepman and Olsen, 2004). Therefore, AlaAT may be seen as a switch valve for balancing the pyruvate availability for the generation of reduction equivalents through the TCA cycle and the intermediate flux to synthesize other amino acids like the branched-chain amino acids. This feature becomes important during hypoxic situations, when pyruvate accumulates and sensible regulation of the energy- and amino acid metabolism is required (Miyashita *et al.*, 2007).

Isoleucine (Ile), Valine (Val) and Leucine (Leu) are known as the branched-chain amino acids (BCAA), the name originates from the characteristic aliphatic side-chains. While 2-oxobutanoate is the initial substrate for Ile, Val and Leu are deriving from pyruvate (Figure 6). A transamination step, catalyzed by a BCAA aminotransferase (BCAT) completes the synthesis (Binder, 2010). In this step, the amino group of Glu is transferred to the individual precursor, resulting in the respective amino acid: 4-Methyloxopentanoate (4-MOP) to Leu, 3-Methyloxobutanoate (3-MOB) to Val and 3-Methyloxopentanoate (3-MOP) to Ile. The initial degradation step is also catalyzed by a BCAT but is located in mitochondria. There are six BCAT isoforms in Arabidopsis, located in mitochondria and plastids, but their individual roles are not completely understood. Laborious effort was put into the identification of the rather complex BCAA degradation pathways, which could recently be updated (Latimer *et al.*, 2018; Gipson *et al.*, 2017; Schertl *et al.*, 2017).

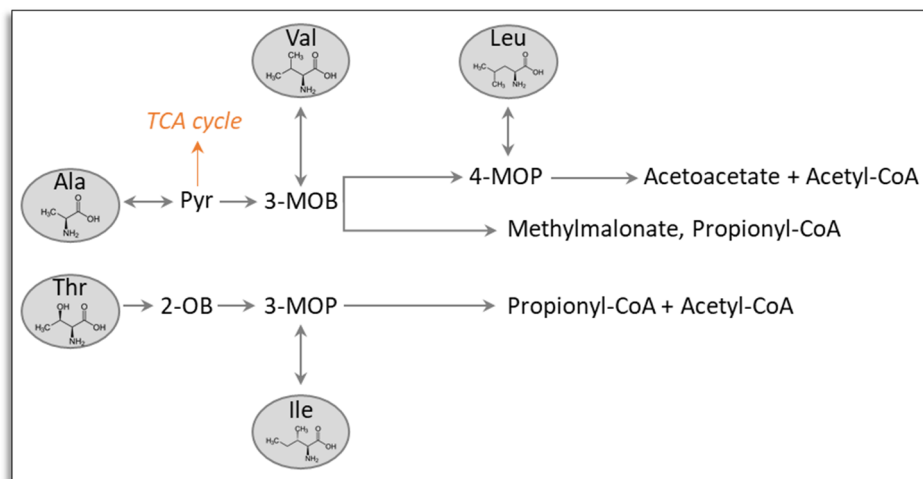


Figure 6: Simplified metabolisms of branched chain amino acids. Proteinogenic amino acids are highlighted in grey. Arrows may stand for multiple enzymatic steps (Figure from Hildebrandt *et al.*, (2015), modified). Double arrow symbolizes single, but reversible transamination step. Orange caption show further metabolic connections. (Pyr: Pyruvate, 3-MOB: 3-Methyloxobutanoate, 4-MOP: 4-Methyloxopentanoate, 3-MOP: 3-Methyloxopentanoate, 2-OB: 2-Oxobutanoate).

1.2 Physiological and metabolic consequences of drought stress

Under optimal conditions, the average water content is about 80% to 90% of the plant's total weight (Heinemann *et al.*, 2020). Plants need a high water content to generate a sufficient cellular turgor, which enables the expansion of the leaves. The permanent pressure promotes cell proliferation and enhances general stability of plants (Kroeger *et al.*, 2011). A controlled evaporation of water through the stomata on the downside of the leaves creates a water stream from the roots to the shoot, which enables the transport of nutrients as nitrogen and sulfur, which are taken up from the soil. Furthermore, the stomata ensure a sufficient gas exchange between the leaves and the surrounding air, so that carbon dioxide can be fixed in the Calvin cycle. In the initial step, RubisCO is binding carbon dioxide to Ribulose-1,5-bisphosphate. The resulting phosphorylated six-carbon intermediate decays into two molecules of 3-phosphoglycerate (3-PG). These molecules are used for the production of glucose molecules, which fuel the energy demand of the plants to build up macromolecules. Remaining glucose is stored as starch for the energy supply during night.

There are several environmental conditions such as lack of rainfalls, high temperatures, high light intensities or dry winds that can reduce the availability of water for plants and can lead to drought stress. When plant roots sense a lowered water content of the soil, the production of the endogenous plant hormone abscisic acid (ABA) is induced. ABA is loaded into the xylem and transported to the leaves (Jiang and Hartung, 2008). The increased ABA level triggers the closure of stomatal cells to avoid additional water loss through transpiration (Figure 7). This is an important adjustment, because plants transpire up to 97% of the water taken up from the soil (Raven and Edwards, 2001). However, closed stomatal cells in turn inhibit the gas exchange of the underlying mesophyll cells. The ongoing light reaction accumulates oxygen (O_2), while less atmospheric CO_2 reaches the mesophyll cells. Therefore, the oxygenase side-reaction of

Ribulose-1,5-bisphosphate carboxylase/oxygenase (RubisCO) happens with increasing frequency. The fixation of O_2 generates the unfavorable intermediate 2-phosphoglycolate (2-PG), which needs to be recycled to 3-PG. This happens partly in the peroxisomes because the process produces hydrogen peroxide (H_2O_2), which then in turn needs to be detoxified. The whole process is a complex series of carbon recycling and detoxification reactions and designated as photorespiration. Under high energy consumption photorespiration is able to recover 75% of the carbon of 2-PG into 3-PG and is releasing the residual 25% in form of carbon dioxide (Peterhansel *et al.*, 2010). Although the oxygenase activity is reducing the photosynthetic efficiency, the dissipation of plant-available energy in the photorespiration is however useful to prevent the overreduction of the electron transport chain under drought stress for example.

The Calvin cycle usually uses NADPH generated by photosystem I as reducing power to produce triose phosphates for the sugar synthesis. In this process, $NADP^+$ is recycled and can take up new reducing power (electrons) from the light reaction. As water deficit reduces the photosynthetic efficiency, which implies that simultaneously fewer carbohydrates are produced, less NADPH is needed and less $NADP^+$ can be regenerated. At some point, the plastidic $NADP^+/NADPH$ equilibrium is overreduced, causing a backlog of electrons at the photosystems. The electrons start to reduce O_2 as alternative electron acceptor, generating reactive oxygen species (ROS) (Figure 7).

High concentrations of ROS are harmful for cells, because they can lead to oxidative damages of cellular structures (e.g. photosystems, protein complexes and membranes). Stressed cells need to invest additional energy into the production of ROS scavenging antioxidants and the induction of ROS detoxifying pathways to mitigate the oxidative stress level (Laxa *et al.*, 2019).

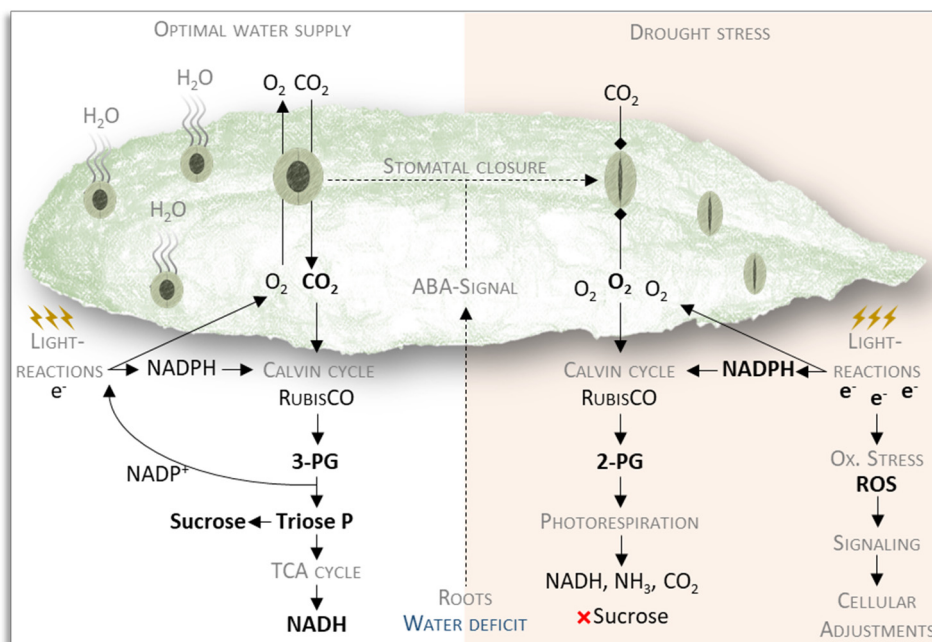


Figure 7: Consequences of drought stress for the plant. **Left:** Photosynthesis under sufficient water supply leads to fixation of CO_2 and results in the production of carbohydrates. **Right:** Drought-induced stomatal closure enhances photorespiration. Missing electron acceptors (CO_2) lead to an overreduction of the photosystems and oxidative stress. This causes a significant energy lack and triggers defensive adjustments of the cell. 3-PG: 3-Phosphoglycerate, 2-PG: 2-Phosphoglycolate, ABA: Abscisic acid, ROS: Reactive oxygen species. Schematic illustration: stomata are at the underside of a leaf.

1.3 Drought prevention and cellular counteractions

Some plant species have adjusted their leaf anatomy and developed biochemical mechanisms to improve water usage and photosynthesis efficiency to occupy arid landscapes (Sage, 2004). They were classified as C_4 plants and crassulacean acid metabolism (CAM) plants (Bräutigam *et al.*, 2017; Bräutigam and Gowik, 2016). Without going into details, there are three major adjustments. (1) Pre-fixation: Both classes initially bind CO_2 into the 4-carbon molecule oxaloacetate (OA) in the mesophyll cells, but export these molecules via the OA/malate shuttle into the bundle sheath cells. (2) Spatial arrangement: In C_4 plants, RubisCO is not located in the mesophyll cells, but in bundle sheath cells. Imported malate is degraded and CO_2 is released in proximity to RubisCO, promoting its carboxylation reaction. The whole process prevents energy loss due to photorespiration and enables lower stomatal conductance, which can save water more efficiently. (3) Timing: CAM plants open their stomatal cells at low temperatures during the night day to accumulate C_4 metabolites, which can be used for photosynthesis during the day. The adjustments prevent water loss and allow plants to exist in dry habitats. However, about 95% of the land plant biomass is represented by C_3 plants (Sowjanya *et al.*, 2019). Like *Arabidopsis thaliana*, these plants directly fixate CO_2 by RubisCO in the mesophyll cells. Their photosynthetic efficiency is highly dependent on an adequate gas exchange and sufficient water availability. The photosynthetic electron transport chain is regulated by the linear and cyclic electron transport. While the linear pathway generates both NADPH and ATP, the cyclic pathway only contributes to the proton gradient for ATP generation. In brief, when PS I receives electrons from the plastoquinone pool, it transfers them to ferredoxin, which omits the electron transfer to the Ferredoxin-NADP reductase but interacts with the NADH dehydrogenase-like complex. The electrons are redirected into the plastoquinone pool, where electron transfer reactions are coupled with pumping protons into the thylakoid lumen (Yamori and Shikanai, 2016). The drought-induced overreduction is counteracted by the induction of the cyclic electron transport to maintain the photosynthetic ATP production. Oxidative stress is sensed by the ubiquitous thioredoxin (TRX) system. TRX are disulfide reductases, which regulate enzyme activity and transcription factors and are involved in redox signaling (Vieira Dos Santos and Rey, 2006). TRX activates the NADPH-dependent malate dehydrogenase (MDH). This special MDH reduces oxaloacetate (OA) to malate by oxidizing NADPH and triggers the translocation of malate from chloroplasts to mitochondria via the reversible malate/OA shuttle. This process is known as light malate valve (Selinski and Scheibe, 2019). In mitochondria, imported malate is oxidized with NAD^+ to OA and NADH. With this mechanism, the overreduction of the plastidic $NADP^+/NADPH$ equilibrium can be shifted to the mitochondrial $NAD^+/NADH$ pool, where it can enter the ETC. In case of the overreduction of the mitochondrial ETC, alternative oxidases and uncoupling proteins can dissipate the excess electrons. However, the plastidic $NADP^+/NADPH$ pool makes just 10 % of the mitochondrial $NAD^+/NADH$ pool and neither the malate shuttle nor the cyclic electron transfer can compensate the energy loss of the inhibited photosynthesis under severe drought stress (Noctor *et al.*, 2006). Symptoms of drought stress are a decreased water content and a reduced cellular turgor. Without a sufficient turgor, cell division and cell expansion are inhibited, leading to an arrested growth of the whole plant. Therefore, the plant accumulates high amounts of osmotically active compounds to stabilize the water content as long as possible. The efficiency of the photosynthesis is inhibited leading to carbon starvation and the generation of ROS. Total biomass of the shoot decreases, while energy is invested into the root system to optimize water uptake. Consequently,

prolonged drought stress is a multidimensional stress situation, which leads to energy deprivation and oxidative stress. However, plants have developed a sophisticated stress network of stress responses to partially compensate and longer withstand drought stress. The amino acid metabolism plays an important role in drought tolerance as it is a target of major metabolic changes. The key functions of these changes will be described in the following paragraphs supported by experimental findings of the three research publications of this thesis.

1.4 Major functions of amino acid metabolism during drought stress

Weather continuously affects a plant's life cycle. Since plants are sessile, they need to develop strategies to overcome temporary stress situations. During drought periods, plants sense the water deficit, evaluate the severity and respond in an energetically appropriate way. They have to adjust their metabolism constantly and accurately, because progressive drought becomes more critical and the energy resources are limited. As mentioned in earlier chapters, the consequences of prolonged drought stress are oxidative stress and energy deprivation caused by the water deficit and the excess of sunlight. When stress effects overload the plant's defensive strategies, desiccation will be irreversible. Therefore, surviving demands drastic cellular adjustments.

The general metabolism is shifted towards energy saving and stress defense, which leads to an arrest of growth and development. Plants start to invest their energy resources into the production of protective secondary metabolites and osmolytes to counteract the effects of drought stress. As precursors, alternative respiratory substrates and osmolytes, some amino acids represent useful compounds during this emergency. The role of the amino acid metabolism during drought stress was addressed by three publications. They focus major on functions of amino acids during drought stress (Figure 8).

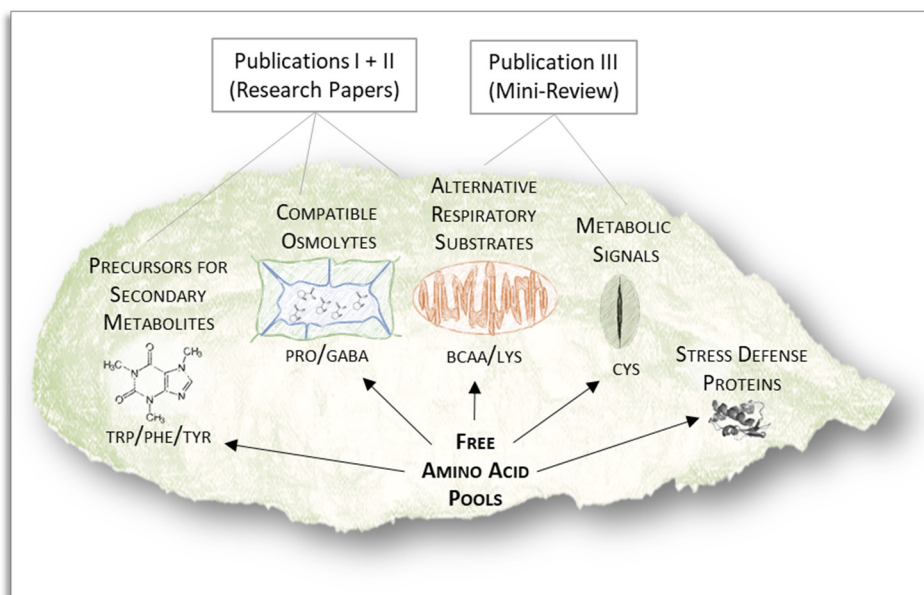


Figure 8: Roles of free amino acids during drought stress and contributions by the three publications of this thesis. **Chapter 2.1:** The role of amino acid metabolism during abiotic stress release, **Chapter 2.2:** Estimating the number of protein molecules in a plant cell: A quantitative perspective on proteostasis and amino acid homeostasis during progressive drought stress, **Chapter 2.3:** The role of amino acid metabolism in signaling and metabolic adaptation to stress induced energy deficiency in plants.

1.4.1 Experimental approaches to study drought stress in Arabidopsis

Drought stress is a widespread problem that is becoming increasingly important with climate change. Therefore, many data sets of drought stress experiments are available in literature. However, there is no standard experimental procedure for drought treatments and very different approaches were used, often lacking a detailed description of the parameters. This makes it difficult to compare data sets of drought stress experiments. Especially, the aspect of physiology is sometimes a matter of interpretation and always a compromise between the validity of the scientific outcome and the controllability of the experimental parameters. Drought stress effects can be investigated by using field experiments, soil-based phytochamber experiments, *in vitro* approaches and even by drying separated leaves. These setups have their own benefits and drawbacks regarding the physiology, stress consistency and the experimental controllability. A consistent drought stress application to a larger plant group *in soil* can be quite challenging, but reveals physiological stress effects and plant responses. Plants of all developmental stages can be tested. *In vitro* approaches are rather artificial and less physiological, but enable the accurate adjustment of distinct water potentials or other osmotic treatments. The growth media can be quickly replaced, enabling the investigations of heavy short-term stress phases. The same applies for releasing the stress or the influence of a treatment, making *in vitro* setups suitable approaches for the investigation of stress release situations. However, the sizes of the *in vitro* containers limit the plant material to young seedlings.

Here, *in vitro* and *in soil* experiments were designed to examine the drought stress responses from different angles (Figure 9). The first publication mainly focused on the effects of low water content ($\Psi_s = -1$ MPa) on young Arabidopsis plants (Batista-Silva *et al.*, 2019). Seedlings were grown on sieves on MS media for 14 days. The sieves holding the seedlings were transferred into liquid media supplemented with polyethylene glycol (PEG). PEG was used to reduce the water availability in the growth media. With this approach, we could rapidly apply severe drought conditions. Samples of control, 24h stress and stress release situations were taken to investigate the behavior of the amino acid metabolism and other stress relevant parameters in the seedlings.

The second experimental approach of this thesis focused on the physiological investigation of the balances between proteostasis and amino acid homeostasis during progressive drought stress (Heinemann *et al.*, 2020). The experiment started by saturating the pots of two weeks old soil-grown Arabidopsis plants with water. After that, water was withheld and the pot positions were daily rotated within the long-day phytochamber (16h light/8h darkness). This procedure enabled an equal desiccation across all plants. After ten days without water, growth arrested and the first group was harvested (S1). To test plant viability at each harvesting time point, three additional plants were re-watered to see, whether they can recover from the applied drought stress. Subsequently, plants were grouped according to their stress phenotype (number of wrinkled leaves) and harvested until recovery was no longer possible. We collected seven stressed sample groups (S1-S7) ranging from moderate to very severe drought stress.

To face the full picture of the amino acid metabolism, the free amino acid contents of both experimental approaches were quantified by HPLC, while the enzymes involved in amino acid metabolism were monitored by shotgun mass spectrometry proteome analysis. The proteome analysis also provided an overview of other stress-adjusted metabolic pathways. Changes of the amino acid metabolism and the free amino acid

pools revealed the dimensions of the stress-relevant purposes of individual amino acids. Other parameters as the total protein content and the relative water content were additionally measured, as they are also affected by drought stress. We combined the results to describe the order of adjustments to successive drought stress. Two major phases became visible, which nicely correlated with the impression of the stress phenotype (Figure 9). An extended period of moderate drought stress, where plants manage to maintain their water content, was followed by a short phase of severe drought stress, in which the plants lost a significant amount of water and died, if not re-watered. At first, the growth was arrested and a slight decrease of the relative water content was observed, indicating that the stomatal cells were already closed to stop further water loss. In the early phase of drought the accumulation of cellular osmolytes such as free sugars, Pro and GABA was induced. The osmolytes stabilized the water content for several days during moderate drought stress conditions. When all leaves were wrinkled, the water content dropped again and a massive protein degradation was detected. Consequently, free amino acids accumulated, and there was a particularly strong increase in Pro and the normally low abundant amino acids BCAA and Lys. According to the proteome data, the catabolic pathways of these amino acids were also strongly induced during drought stress. This supports the assumption, that their degradation provides alternative respiratory substrates during severe stress situations. These aspects will be discussed in more detail below. The effects of severe drought stress were also observed after 24h PEG treatment *in vitro*, confirming the treatment to induce severe drought stress with the respective PEG concentration.

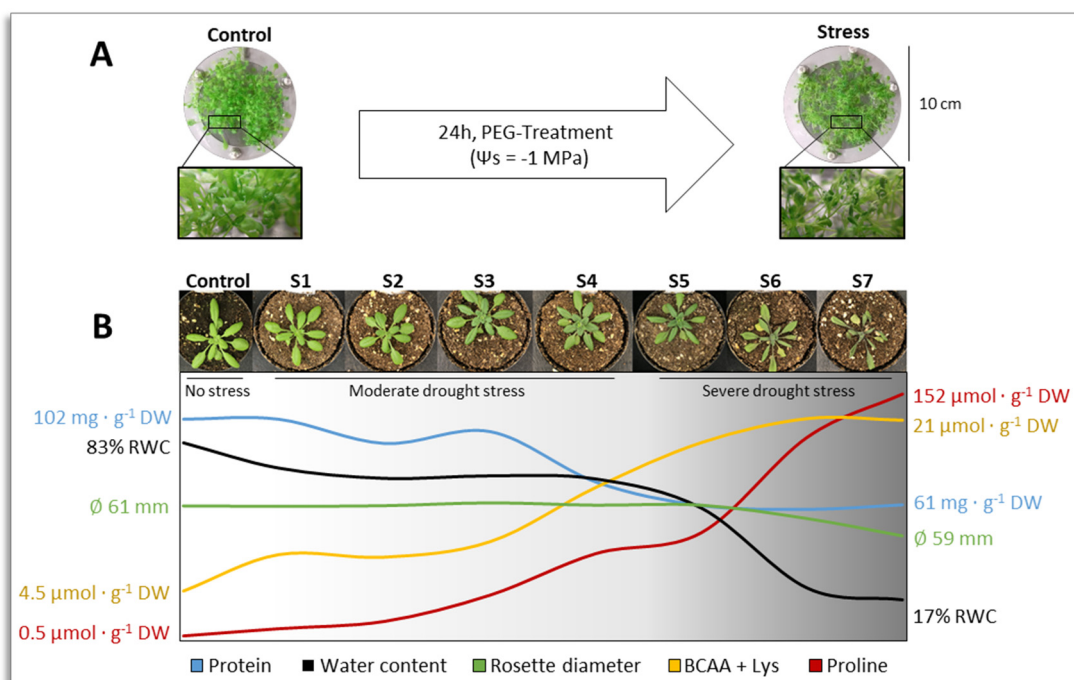


Figure 9: Experimental systems, which were used for the investigation of drought stress effects. A. Arabidopsis seedlings were grown on sieves *in vitro* and treated with PEG for 24h to induce drought stress. B. Soil-grown Arabidopsis plants were subjected to progressive drought stress by withholding the water. (Control – S7) and the effects on growth, relative water content (RWC), protein content and selected amino acid contents. Original data can be found in [Heinemann et al. \(2020\)](#).

1.4.2 A quantitative angle on amino acid metabolism during drought stress

Data sets of proteome-, metabolome- or genome-wide changes are often given as fold-changes to express the difference between two samples. Interesting changes are instantly visible, no prior calibrations are necessary and the relative values are easy to calculate. However, by using relative values the quantitative context is lost. That makes the comparison of fold-changes across different protein or metabolite species less conclusive. Furthermore, enormous fold-changes of a compound might be interpreted as highly important. Fold-changes can be misleading as the absolute abundance might be just very low in one sample.

Therefore, we were interested in the quantitative analysis of the proteome of *Arabidopsis* during drought stress. We developed a calculation method to estimate absolute contents of individual proteins, based on the shotgun proteome data set. This enabled us to combine the results of the proteomic composition, the total protein content and the contents of free amino acids and to put the drought stress roles of the amino acid metabolism in a larger physiological context.

Shotgun MS proteome analysis requires equal amounts of extracted protein. It does not take into account, how much leaf material has been used for protein extraction and thus provides only relative protein abundances, which is not ideal when studying leaves of severely stressed plants with a much lower protein content than control leaves (Figure 10a). Considering these circumstances, we had to exclude the use of “label free quantification (LFQ) intensities”, which are usually provided by the MS data evaluation software (MaxQuant). LFQ intensities are normalized relative protein intensities and they are usually used to compare the abundance of individual proteins in two samples by building LFQ ratios. However, LFQ intensities can be biased during massive proteolysis. For example, a relative increase could have two reasons: (1) the protein is induced by *de novo* synthesis or (2) all other proteins decrease more strongly in abundance and artificially elevate the abundance of the protein of interest. Besides that, we were interested in absolute protein amounts, which were necessary to calculate the absolute amount of protein bound amino acids. Therefore, a calculation method was established using individual intensity based absolute quantification (iBAQ) values, the molecular weight and the total protein content of the plant. With these parameters, it was possible to calculate absolute contents of individual proteins ($\text{mg protein} \cdot \text{g}^{-1} \text{DW}$).

The accuracy was verified by the quantification of the RubisCO large subunit (LS) in a separate experiment as proof of concept. In brief, isotope-labeled unique peptides of the RubisCO LS were spiked into the existing MS samples. A targeted parallel reaction monitoring (PRM) MS analysis showed that our theoretical quantification method covers 82% of the total protein mass. In other words, the absolute amounts of the detected proteins were overestimated by 18%. This is caused by the summed protein mass of many low abundant proteins (e.g. signaling molecules, transcription factors), which were below the detection limit of our MS detector (Heinemann *et al.*, 2020). However, the results still provide realistic impressions of the proteome. This method enabled the estimation of absolute amounts and molar concentrations of the 1400 most abundant proteins, which were identified in our shotgun MS analysis of the *Arabidopsis* leaf proteome. To further increase the understanding of the cellular dimensions, we related the protein concentrations to single cells and even individual subcellular compartments (Figure 10b).

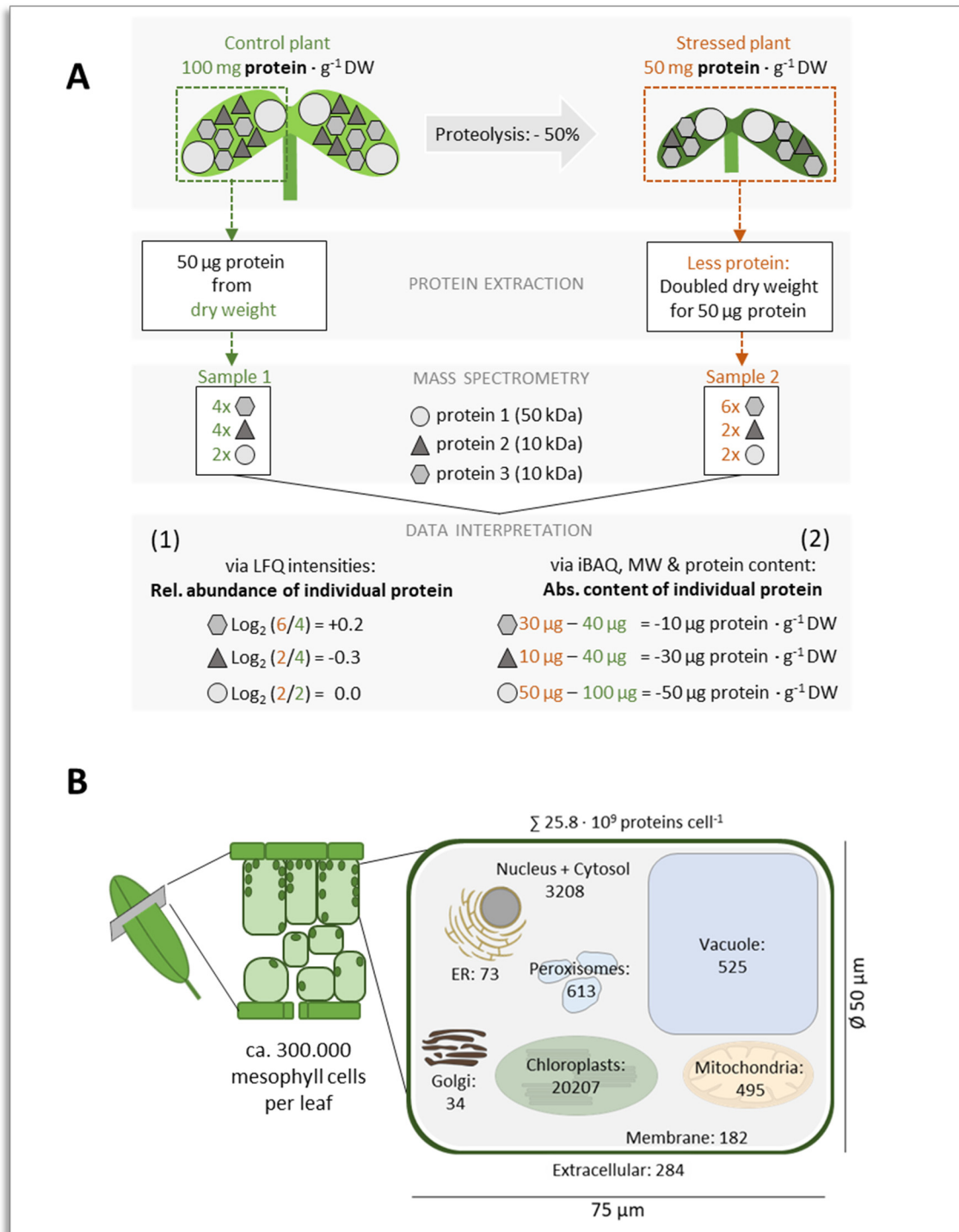


Figure 10: Calculation of absolute amounts of individual proteins.

A. Schematic example of the two approaches for the interpretation of a proteomic MS dataset. (1) The relative abundance of individual proteins in the protein extracts used for MS analysis can be calculated based on LFQ ratios. However, LFQs are not suitable when the total protein content is drastically changed. (2) iBAQ values, the molecular weight of the individual protein and the total protein content of the plant can be used to calculate absolute amounts of individual protein to monitor their dynamics during proteolysis. LFQ: label-free quantification, iBAQ: intensity-based absolute quantification, MW: molecular weight. **B.** Calculated protein copy numbers of an average mesophyll cell of *Arabidopsis thaliana*. Copy numbers represent the sum of protein molecules present in all chloroplasts (ca. 100; Königer *et al.*, 2008), mitochondria (300-450; Preuten *et al.*, 2010), or peroxisomes in the cell. Copy numbers for all individual proteins detected in our MS approach are given in Heinemann *et al.*, (2020), Supp. Dataset S1.

1.4.3 Proteostasis and amino acid homeostasis during progressive drought stress

The absolute individual protein contents were categorized according to their cellular functions and merged to so-called "PROTEOMAPS" to visualize the quantitative composition of the leaf proteome under control conditions and severe drought stress (Figure 11a). The most abundant protein of *Arabidopsis thaliana* and on our planet is the large subunit (LS) of RubisCO (Bar-On and Milo, 2019). We could support that fact with our proteomic data set, where RubisCO LS takes a share of 16% of the total protein content. It even remains the most abundant protein after the massive proteolysis during severe drought stress as the complete photosynthesis-related protein fractions still dominate the proteome. We observed that severely drought-stressed plants decreased their total protein content by 40%. All protein categories, except the proteases, decrease in absolute abundance. However, when comparing the relative compositions, several categories seem to be less degraded than others. The plant cell has two independent systems to control concentrations of individual proteins, either by regulating the gene expression or by inhibiting the degradation of proteins. For example by selective autophagy of subcellular compartments or the induction of specific proteases (Wang and Schippers, 2019). We investigated, whether the bulk degradation is a non-selective process to accumulate free amino acids or still a regulated recycling procedure of the least essential proteins by comparing the proteome data sets of the sample groups of the progressive drought stress experiment. We calculated degradation rates of all identified proteins and used gene expression data, retrieved from the GENEVESTIGATOR database, to perform enrichment analysis. With this approach, we found different degrees of the drought-induced proteolysis in respect to compartments and protein categories.

Our results showed that mainly plastidic, cytosolic, membrane proteins were degraded, while extracellular and mitochondrial proteins were potentially protected. This can be explained by considering the high abundance of the photosynthetic apparatus, which is impaired under drought stress and rather causing oxidative damages. Plants might mitigate the constant ROS formations at the plastidic ETC, by recycling the photosystems and damaged proteins.

Gene expression of enzymes involved in secondary metabolism, stress signaling, protein degradation, amino acid degradation and lipid degradation was actively induced, which counteracted the proteolysis and lead to an increase in relative abundance during drought stress. In contrast, the gene expression of the biosynthetic pathways of lipids and chlorophyll were down regulated, while the proteins were additionally degraded. Interestingly, gene expression of mitochondrial ETC components was not regulated. Their protein abundances remained stable during stress and thus increased in relation to the overall decreasing total protein content. This observation is in accordance with our hypothesis that the mitochondrial ETC must remain active, even during the drought-caused carbon starvation.

By combining the absolute changes of the proteome with the amino acid sequences of the identified proteins, we were able to calculate the protein-bound amounts of amino acids (Figure 11b). Together with the contents of the free amino acids, we could analyze the changes of the total amino acid composition of the protein-bound and free amino acids during the stress phase. Deduced from that, we calculated the individual amounts of the proteinogenic amino acids, which were released and degraded during the drought stress. The largest part of this proteolysis is the degradation of the highly abundant RubisCO LS. Consequently, this protein represents the main source of released amino

acids and therefore biases the sizes of the free amino acid pools. Interestingly, drought-stressed plants showed a different composition of the free amino acid pools than calculated from proteolysis (Figure 11C). Correlating to the proteolysis, a sudden increase of free Pro was observed (Figure 9). Therefore, we hypothesize, that the released amino acids are primarily degraded for the Pro production. However, about 28% of the theoretically released amino acids were missing. They must have been converted to secondary metabolites or degraded as an alternative energy source during the drought period. The fact that pool sizes of free amino acids did not change according to the calculated amino acid composition released by proteolysis indicates a tight regulation.

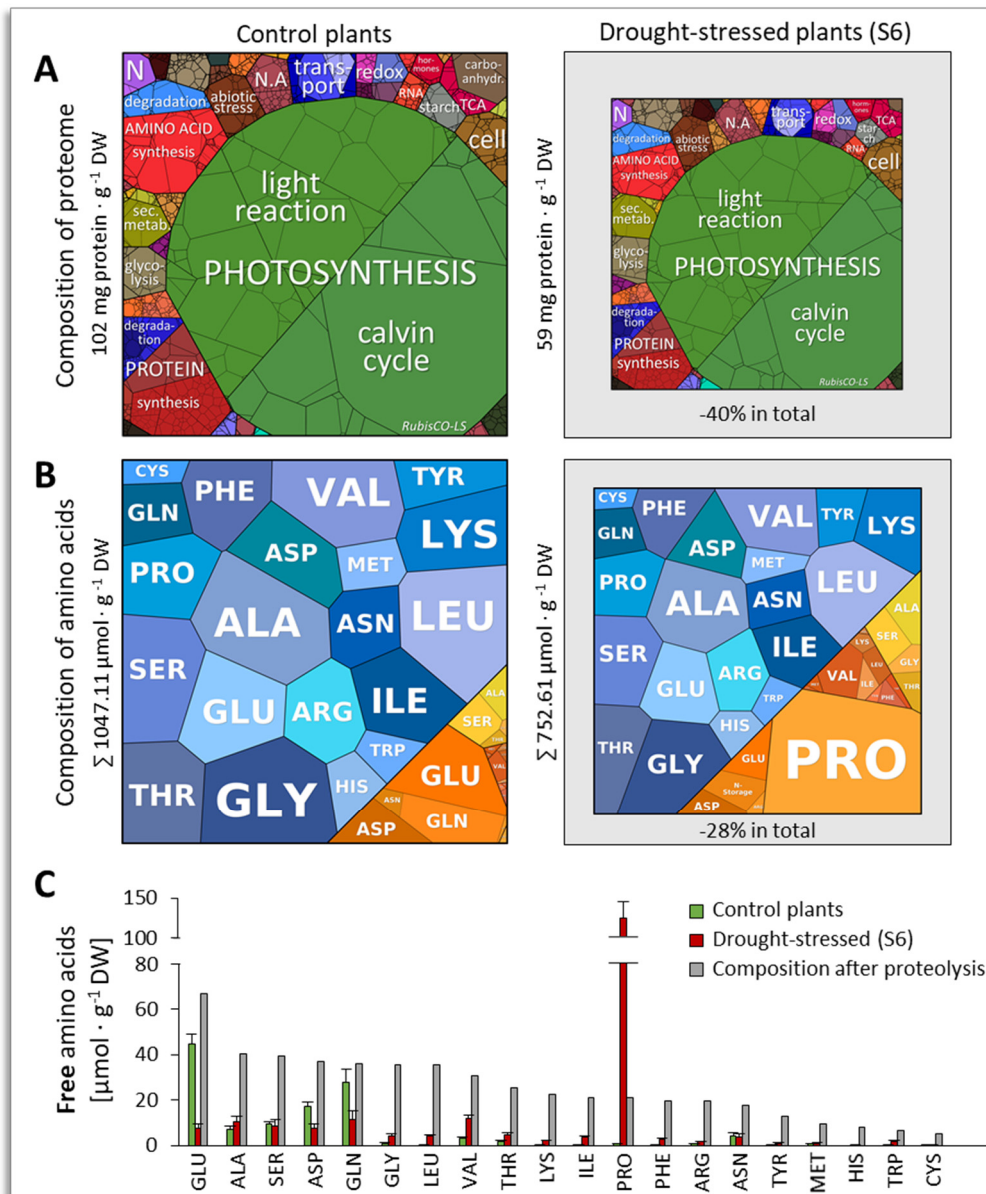


Figure 11: Interconnection of amino acid pools during progressive drought stress. **A.** Proteomaps: Proteins are shown as polygons whose sizes represent the mass fractions. Proteins involved in similar cellular functions according to MapMan (Thimm *et al.*, 2004) are arranged in adjacent locations and by colors. **B.** Aminomaps: Pool sizes and compositions of the free (orange colors) and protein-bound (blue colors) amino acid pools. Polygons represent the molar fractions. **C.** Effect of proteolysis on free amino acid homeostasis. The quantitative composition of the degraded proteins were used to calculate the theoretical composition of the free amino acid pool (grey bars) that would result from massive proteolysis during drought stress without any metabolic conversion of the amino acids produced. The actual free amino acid profiles in the leaves of control plants (green bars) and of severely stressed plants (red bars) were analyzed by HPLC.

1.4.4 Amino acids as osmolytes

Pro and the non-proteinogenic amino acid GABA accumulate already during the early drought stress phase, indicating their importance and reliability as osmoprotectants (Fig 9, Heinemann *et al.*, 2020). They are not harmful in high concentrations and help the plant to keep the water content stable for several days, The proteome analysis confirmed the induction of biosynthetic pathways of GABA and Pro in the *in vitro* as well as the *in soil* approach, while most catabolic pathways of other amino acid were induced (Heinemann *et al.*, 2020; Batista-Silva *et al.*, 2019). We hypothesize, that other free amino acids were degraded or converted to Glu to provide precursors for the bulk synthesis of the osmotically active Pro and GABA. The free Glu content constantly decreased during the whole stress phase, possibly due to the massive flux to Pro and GABA. GABA also acts as ROS scavenger, preventing oxidative stress at the plastidic ETC (Liu *et al.*, 2011). Since drought stress leads to an overreduction of the plastidic NADPH pool, the massive NADPH-dependent biosynthesis of Pro partly regenerates the NADP⁺ pool, which in turn releases the electron backlog at the plastidic ETC (Christensen *et al.*, 2017). Interestingly, the Pro degrading “delta-1-pyrroline-5-carboxylate dehydrogenase” and the GABA degrading “GABA transaminase” were already induced during stress. This could be observed in both proteome data sets of the *in soil* and *in vitro* approach. However, since both amino acids were still accumulating, the activity of the anabolic enzymes might overturn the catabolic enzymes. The early induction of the catabolic enzymes could be preventive, to avoid high contents of osmolytes during re-watering conditions. This would probably disturb the recovery process and might cause additional osmotic stress due to a rapid water influx. During recovery, Pro and GABA contents indeed dropped rapidly, supporting the hypothesis of a primed degradation. The early adjustment of the amino acid metabolism is focused on the fast mass production of osmolytes. The Pro production might be helpful to regenerate the overreduced NADPH pool of the plastids and is extremely effective in delaying severe stress consequences.

1.4.5 Amino acids as precursors for secondary metabolites

The proteomic analysis further revealed an induction of the secondary metabolism. Secondary metabolites are small organic compounds, which can have multifunctional roles in regulating plant growth and stress adjustment processes (Erb and Kliebenstein, 2020). Especially, the pathways of the AAA derived secondary metabolites, like anthocyanins, lignin and flavonoids were induced by osmotic stress (Batista-Silva *et al.*, 2019). Flavonoids and anthocyanins are known ROS scavengers, which mitigate oxidative stress and enhance drought stress tolerance (Nakabayashi *et al.*, 2014). Another group of stress-relevant secondary metabolites is represented by the Arg-derived polyamines. Using polyamine-deficient mutants, several research groups could prove their mediating role during abiotic stress situations (Alcázar *et al.*, 2010). Polyamine contents were not quantified in this thesis, but proteome MS analysis showed an elevated abundance of polyamine synthesizing enzymes during both water-deficit and re-watering situation (Batista-Silva *et al.*, 2019). Similar roles were described for the Met-derived aliphatic glucosinolates (GLS). The preservation of GLS contents was identified to be important for drought stress tolerance (Salehin *et al.*, 2019). The authors assume that products of the GLS degradation are involved in stomatal closure, suspending further water loss. This assumption is supported by the results of Batool *et al.* (2018), who demonstrated that

sulfate, which is a product of GLS degradation, serves as a drought stress signal, transported from the roots to the stomatal guard cells of leaves. Sulfate is subsequently assimilated into Cys, which promotes the final step of ABA production in the guard cells. ABA then finally triggers stomatal closure.

Since the *de novo* synthesis of the aromatic amino acids is rather expensive for the cell, a stress-induced degradation does not seem reasonable. Instead, our proteome analysis of both *in vitro* and *in soil* approaches suggest that, the aromatic amino acids are likely used for the production of secondary metabolites such as ROS scavenging flavonoids and UV protecting anthocyanins. However, the absolute dimension is not clear and cannot be rated.

1.4.6 Amino acids as alternative respiratory substrates

Both experimental approaches, *in vitro* and *in soil*, showed strong degradation (40%) of the total protein content. This releases a vast amount of free amino acids and leads to the accumulation of mostly all proteinogenic amino acids. It was shown that this activates “sucrose non-fermentation-related protein kinase 1” (SnRK1), which in turn activates the transcription factors, which induce the transcription of the respective catabolic pathways (Pedrotti *et al.*, 2018). SnRK1 is known to activate autophagy and catabolic pathways of the primary metabolism to maintain metabolic homeostasis during disruptive stress situations and to supply precursors for the metabolic stress adaptation. However, the regulatory mechanism, how SnRK1 senses the accumulated amino acids is still unclear. Especially, the catabolic enzymes of the BCAA and Lys were strongly induced during our drought stress approaches. Published gene expression data sets of other energy deprivation situations revealed a conserved response of the same set of enzymes. This feature helped to identify additional enzymes participating in these pathways. A lot of work was put into the identification of participating enzymes and in completing these catabolic pathways in the last years. In our review, we summarized the updates of the degradation pathways for BCAA and Lys and discussed possible connections to the SnRK/TOR network (Heinemann and Hildebrandt 2021; Gipson *et al.*, 2017; Schertl *et al.*, 2017; Thompson *et al.*, 2020).

The degradation of amino acids such as BCAA and Lys can provide alternative respiratory substrates, serving the stressed plant as additional energy source during the energy deprivation situation (Araújo *et al.*, 2011). After deamination, the carbon skeletons can fuel the drought-impaired TCA cycle at multiple entry sites, generating NADH and ATP along their oxidative degradation (Figure 12). The degradation of complex amino acids, as the AAA and the BCAA, includes more enzymatic steps and might yield more reduction equivalents than simpler amino acids. According to that, the amount of net ATP varies from 2.5 (Gly) to 34 (Tyr) molecules per amino acid molecule (Hildebrandt *et al.*, 2015). An alternative option, which directly transfers electrons into the respiratory chain is represented by the electron transfer flavoprotein/electron-transfer flavoprotein:ubiquinone oxidoreductase (ETF/ETFQO) system (Araújo *et al.*, 2010). Catabolic amino acid dehydrogenases, such as the isovaleryl-CoA dehydrogenase (IVDH; BCAA catabolism) and the D-2-hydroxyglutarate dehydrogenase (D2HGDH; Lys catabolism) can directly donate electrons to this carrier system. The ETF/ETFQO system then transfers the electrons to the ubiquinol pool of the mitochondrial ETC. Interestingly,

the Pro dehydrogenase is also suspected to transfer electrons directly to ubiquinone, which would represent a rapid and profitable way to recycle the invested energy (Schertl and Braun, 2014). However, experimental evidence about the dimension of amino acids as alternative energy sources was rather unclear. As mentioned in earlier chapters, we were able to estimate the amounts of protein bound amino acids, which were released during the drought-induced proteolysis. By comparing the actual free amino acid content with the theoretically released amount, we observed that 28% of the amino acids were missing, and probably degraded. However, we further calculated that this amount could only fuel the mitochondrial ETC for seven hours. This led to the assumption that amino acids are rather used as precursors for stress mitigating compounds and only used as alternative energy resource during very severe drought stress, shortly before death.

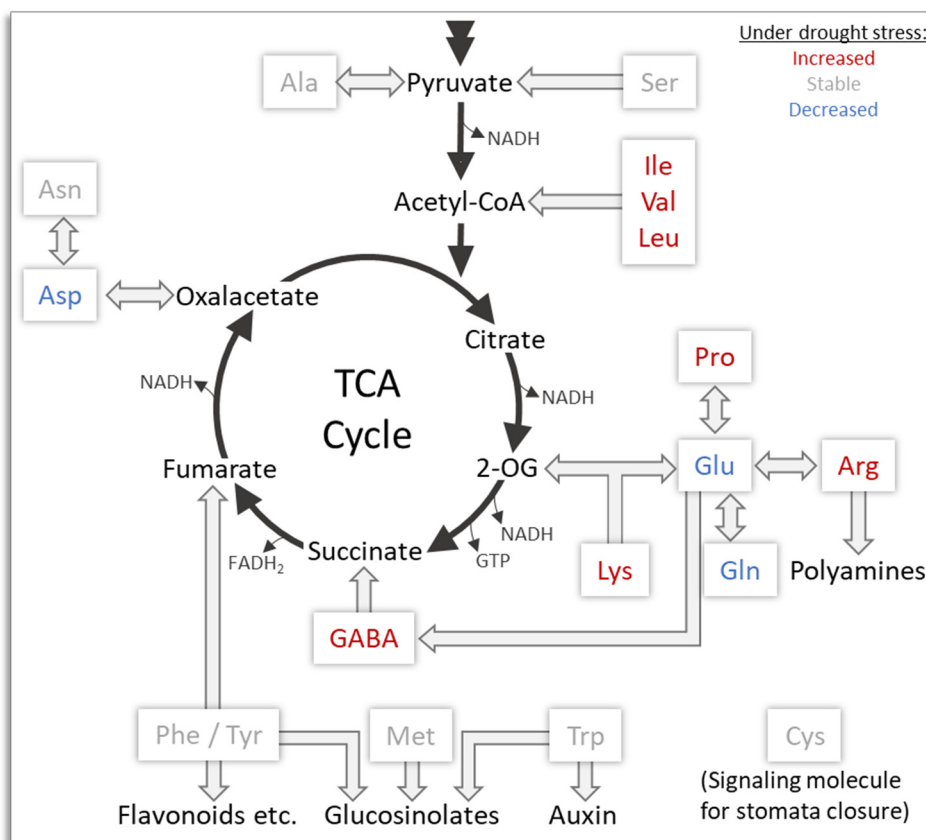


Figure 12: Purposes of free amino acids during drought stress. Carbon skeletons (e.g. keto acids) of several amino acids can enter the tricarboxylic acid (TCA) cycle and provide alternative energy in form of reducing equivalents. Others can be used as precursors for secondary metabolites. Colors indicate increased (red), stable (grey) or decreased (blue) amino acid content during drought stress in [Batista-Silva et al. \(2019\)](#) and [Heinemann et al., \(2020\)](#). 2-OG: 2-Oxoglutarate.

1.4.7 Amino acids as signaling molecules and cellular benchmarks

The plant free amino acid composition consists of twenty individual pools. The contents of individual pools vary widely according to the developmental stage as well as the nutritional status and they respond strongly to environmental stresses. Furthermore, plants can adjust these pools remarkably by regulating their degradation or *de novo* synthesis. Recently, the usually low abundant amino acids Pro, BCAA and Cys have been discussed as signaling molecules. Signaling molecules need to be tightly regulated during control conditions, and show distinct changes in their concentration only under specific conditions, when the signal is required. This characteristic makes several amino acids suitable as signaling molecules for environmental influences and in general for the nutritional status of the plant cell.

In 2002, a homolog of the “target of rapamycin” (TOR) protein kinase, the central hub for processing nutrient information and master regulator of growth in mammals was identified in *Arabidopsis thaliana* (Menand *et al.*, 2002). Protein kinases transfer phosphate groups of ATP molecules to a target protein, (e.g. enzyme or transcription factor) and can thus change characteristics such as its activity, substrate affinity, substrate specificities or the protein stability. As in mammals, the TOR kinase complex in *Arabidopsis* activates growth-relevant pathways of the plants metabolism (e.g. amino acid synthesis, protein synthesis & sugar metabolism). TOR activation is multifaceted and depends on the availability of nutrients including nitrogen, carbon and sulfur (Fu *et al.*, 2020). Cao *et al.* (2019) observed an up-regulated TOR activity in a BCAA over-accumulating *Arabidopsis* mutant and assumed increased BCAA concentration as signal for the protein biosynthesis. In line with that, O'Leary *et al.* (2020) recently showed that increased levels of free Ala and Pro can activate their mitochondrial degradation pathways, which can be prevented by other amino acids (e.g. Met, Ile) via the TOR signaling pathway. Although the mechanism is unclear yet, amino acids can also be sensed by the sucrose non-fermentation-related protein kinases (SnRK 1 and 2). They were identified as having an antagonistic role within the TOR kinase network. Like its homologue in yeast, SnRK1 is assumed to sense metabolic signals and activate autophagy and amino acid degradation to maintain amino acid homeostasis and adapt to environmental stress (Pedrotti *et al.*, 2018). Several basic region/leucine zipper motif (bZIP) transcription factors, which regulate several enzymes of the amino acid degradation pathways, were revealed to interact with SnRK1 (Pedrotti *et al.*, 2018). More is known about the role of a member of the SnRK2 class, also known as Open stomata 1 kinase (OST1) or SnRK2.6. Batool *et al.* (2018) demonstrated that sulfate, which serves as a mobile drought stress signal from roots into the guard cells, is incorporated into Cys. The local increase of Cys induces the ABA synthesis, which in turn induces the Cys desulfhydrase 1 (DES1) (Chen *et al.*, 2020; Shen *et al.*, 2020). DES1 catalyzes the production of H₂S and promotes the persulfidation of SnRK2.6 and the NADPH oxidase respiratory burst oxidase homolog D (RBOHD). The persulfidated enzymes then promote stomatal closure. Simultaneously, SnRK2.6 inhibits the TOR activity, as the TOR kinase continuously phosphorylates ABA receptors to suppress unwanted stress responses under optimal conditions (Wang *et al.*, 2018).

As part of this thesis, we reviewed the roles of amino acids as signal molecules for the plant TOR/SnRK network during stress situations (Heinemann and Hildebrandt 2021). Therefore, we compiled online-accessible gene expression data on carbon starvation, drought stress and of plants with manipulated TOR/SnRK mechanisms (Baena-González

et al., 2007; Dong *et al.*, 2017; Pedrotti *et al.*, 2018; Xiong *et al.*, 2013). Interestingly, we observed that the amino acid catabolism showed an induction during carbon starvation and in plants with inhibited TOR kinase activity or an overexpressed SnRK1. In contrast, gene expression of the amino acid biosynthesis pathways was decreased under these conditions. However, they were up-regulated when the TOR kinase was induced or SnRK1 was knocked out. Especially, enzymes of Lys, Tyr, Met, Pro and BCAA metabolism showed a conserved co-regulation across the transcriptomic data sets, highlighting their role during energy deprivation as mentioned in previous chapters of this thesis. However, how plant cells sense and quantify the free amino acids and how they interact with SnRK and TOR kinase remains unknown.

1.5 References

- Alcázar, R., Altabella, T., Marco, F., Bortolotti, C., Reymond, M., Koncz, C., Carrasco, P. and Tiburcio, A.F. (2010) Polyamines: molecules with regulatory functions in plant abiotic stress tolerance. *Planta*, 231, 1237–1249.
- Araújo, W.L., Ishizaki, K., Nunes-Nesi, A., Larson, T.R., Tohge, T., Krahnert, I., Witt, S., Obata, T., Schauer, N., Graham, I.A., Leaver, C.J. and Fernie, A.R. (2010) Identification of the 2-hydroxyglutarate and isovaleryl-CoA dehydrogenases as alternative electron donors linking lysine catabolism to the electron transport chain of Arabidopsis mitochondria. *The Plant cell*, 22, 1549–1563.
- Araújo, W.L., Tohge, T., Ishizaki, K., Leaver, C.J. and Fernie, A.R. (2011) Protein degradation - an alternative respiratory substrate for stressed plants. *Trends in plant science*, 16, 489–498.
- Baena-González, E., Rolland, F., Thevelein, J.M. and Sheen, J. (2007) A central integrator of transcription networks in plant stress and energy signalling. *Nature*, 448, 938–942.
- Bar-On, Y.M. and Milo, R. (2019) The global mass and average rate of rubisco. *Proceedings of the National Academy of Sciences of the United States of America*, 116, 4738–4743.
- Batista-Silva, W., Heinemann, B., Rugen, N., Nunes-Nesi, A., Araújo, W.L., Braun, H.-P. and Hildebrandt, T.M. (2019) The role of amino acid metabolism during abiotic stress release. *Plant, cell & environment*, 42, 1630–1644.
- Batool, S., Uslu, V.V., Rajab, H., Ahmad, N., Waadt, R., Geiger, D., Malagoli, M., Xiang, C.-B., Hedrich, R., Rennenberg, H., Herschbach, C., Hell, R. and Wirtz, M. (2018) Sulfate is incorporated into cysteine to trigger ABA production and stomatal closure. *The Plant cell*, 30, 2973–2987.
- Binder, S. (2010) Branched-chain amino acid metabolism in *Arabidopsis thaliana*. *The Arabidopsis book*, 8, e0137.
- Bräutigam, A. and Gowik, U. (2016) Photorespiration connects C3 and C4 photosynthesis. *Journal of experimental botany*, 67, 2953–2962.
- Bräutigam, A., Schlüter, U., Eisenhut, M. and Gowik, U. (2017) On the evolutionary origin of CAM photosynthesis. *Plant physiology*, 174, 473–477.
- Cao, P., Kim, S.-J., Xing, A., Schenck, C.A., Liu, L., Jiang, N., Wang, J., Last, R.L. and Brandizzi, F. (2019) Homeostasis of branched-chain amino acids is critical for the activity of TOR signaling in Arabidopsis. *eLife*, 8.
- Chen, S., Jia, H., Wang, X., Shi, C., Wang, X., Ma, P., Wang, J., Ren, M. and Li, J. (2020) Hydrogen sulfide positively regulates abscisic acid signaling through persulfidation of SnRK2.6 in guard cells. *Molecular plant*, 13, 732–744.
- Christensen, E.M., Patel, S.M., Korasick, D.A., Campbell, A.C., Krause, K.L., Becker, D.F. and Tanner, J.J. (2017) Resolving the cofactor-binding site in the proline biosynthetic enzyme human pyrroline-5-carboxylate reductase 1. *The Journal of biological chemistry*, 292, 7233–7243.
- Coruzzi, G.M. (2003) Primary N-assimilation into amino acids in Arabidopsis. *The Arabidopsis book*, 2, e0010.
- Ding, P., Rekhter, D., Ding, Y., Feussner, K., Busta, L., Haroth, S., Xu, S., Li, X., Jetter, R., Feussner, I. and Zhang, Y. (2016) Characterization of a pipercolic acid biosynthesis pathway required for systemic acquired resistance. *The Plant cell*, 28, 2603–2615.
- Dong, Y., Silbermann, M., Speiser, A., Forieri, I., Linster, E., Poschet, G., Allboje Samami, A., Wanatabe, M., Sticht, C., Teleman, A.A., Deragon, J.-M., Saito, K., Hell, R. and Wirtz, M. (2017) Sulfur availability regulates plant growth via glucose-TOR signaling. *Nature communications*, 8, 1174.
- Erb, M. and Kliebenstein, D.J. (2020) Plant secondary metabolites as defenses, regulators, and primary metabolites: The blurred functional trichotomy. *Plant physiology*, 184, 39–52.
- Forde, B.G. and Lea, P.J. (2007) Glutamate in plants: metabolism, regulation, and signalling. *J Exp Bot*, 58, 2339–2358.

- Fraser, C.M. and Chapple, C. (2011) The phenylpropanoid pathway in Arabidopsis. *The Arabidopsis book*, 9, e0152.
- Fu, L., Wang, P. and Xiong, Y. (2020) Target of rapamycin signaling in plant stress responses. *Plant physiology*, 182, 1613–1623.
- Gipson, A.B., Morton, K.J., Rhee, R.J., Simo, S., Clayton, J.A., Perrett, M.E., Binkley, C.G., Jensen, E.L., Oakes, D.L., Rouhier, M.F. and Rouhier, K.A. (2017) Disruptions in valine degradation affect seed development and germination in Arabidopsis. *The Plant journal : for cell and molecular biology*, 90, 1029–1039.
- Hartmann, M. and Zeier, J. (2018) l-lysine metabolism to N-hydroxy-pipecolic acid: an integral immune-activating pathway in plants. *The Plant journal : for cell and molecular biology*, 96, 5–21.
- Heinemann, B., Künzler, P., Eubel, H., Braun, H.-P. and Hildebrandt, T.M. (2020) Estimating the number of protein molecules in a plant cell: protein and amino acid homeostasis during drought. *Plant physiology*.
- Hell, R. and Wirtz, M. (2011) Molecular biology, biochemistry and cellular physiology of cysteine metabolism in *Arabidopsis thaliana*. *The Arabidopsis book*, 9, e0154.
- Hildebrandt, T.M., Nunes Nesi, A., Araújo, W.L. and Braun, H.-P. (2015) Amino acid catabolism in plants. *Molecular plant*, 8, 1563–1579.
- Hirel, B., Le Gouis, J., Ney, B. and Gallais, A. (2007) The challenge of improving nitrogen use efficiency in crop plants: towards a more central role for genetic variability and quantitative genetics within integrated approaches. *J Exp Bot*, 58, 2369–2387.
- Hou, Y. and Wu, G. (2018) Nutritionally essential amino acids. *Advances in nutrition (Bethesda, Md.)*, 9, 849–851.
- Hunt, S. (1985) The Non-Protein Amino Acids. In *Chemistry and biochemistry of the amino acids* (Barrett, G.C., ed). London, New York: Chapman and Hall, pp. 55–138.
- Jander, G. and Joshi, V. (2009) Aspartate-derived amino acid biosynthesis in *Arabidopsis thaliana*. *The Arabidopsis book*, 7, e0121.
- Jiang, F. and Hartung, W. (2008) Long-distance signalling of abscisic acid (ABA): the factors regulating the intensity of the ABA signal. *Journal of experimental botany*, 59, 37–43.
- Jones, P.R., Manabe, T., Awazuhara, M. and Saito, K. (2003) A new member of plant CS-lyases. A cystine lyase from *Arabidopsis thaliana*. *The Journal of biological chemistry*, 278, 10291–10296.
- Königer, M., Delamaide, J.A., Marlow, E.D. and Harris, G.C. (2008) *Arabidopsis thaliana* leaves with altered chloroplast numbers and chloroplast movement exhibit impaired adjustments to both low and high light. *Journal of experimental botany*, 59, 2285–2297.
- Krapp, A. (2015) Plant nitrogen assimilation and its regulation: a complex puzzle with missing pieces. *Current opinion in plant biology*, 25, 115–122.
- Kroeger, J.H., Zerkour, R. and Geitmann, A. (2011) Regulator or driving force? The role of turgor pressure in oscillatory plant cell growth. *PLoS one*, 6, e18549.
- Latimer, S., Li, Y., Nguyen, T.T.H., Soubeyrand, E., Fatihi, A., Elowsky, C.G., Block, A., Pichersky, E. and Basset, G.J. (2018) Metabolic reconstructions identify plant 3-methylglutaconyl-CoA hydratase that is crucial for branched-chain amino acid catabolism in mitochondria. *The Plant journal : for cell and molecular biology*, 95, 358–370.
- Laxa, M., Liebthal, M., Telman, W., Chibani, K. and Dietz, K.-J. (2019) The role of the plant antioxidant system in drought tolerance. *Antioxidants (Basel, Switzerland)*, 8.
- Lea, P.J. and Mifflin, B.J. (2011) Nitrogen assimilation and its relevance to crop improvement. In *Annual plant reviews* (Foyer, C.H. and Zhang, H., eds). Oxford, Hoboken, NJ: Wiley-Blackwell, pp. 1–40.
- Lee, M., Martin, M.N., Hudson, A.O., Lee, J., Muhitch, M.J. and Leustek, T. (2005) Methionine and threonine synthesis are limited by homoserine availability and not the activity of homoserine kinase in *Arabidopsis thaliana*. *The Plant journal : for cell and molecular biology*, 41, 685–696.

- Lehmann, S., Funck, D., Szabados, L. and Rentsch, D. (2010) Proline metabolism and transport in plant development. *Amino acids*, 39, 949–962.
- Liepmann, A.H. and Olsen, L.J. (2004) Genomic analysis of aminotransferases in *Arabidopsis thaliana*. *Critical Reviews in Plant Sciences*, 23, 73–89.
- Liu, C., Zhao, L. and Yu, G. (2011) The dominant glutamic acid metabolic flux to produce γ -amino butyric acid over proline in *Nicotiana tabacum* leaves under water stress relates to its significant role in antioxidant activity. *Journal of integrative plant biology*, 53, 608–618.
- Maeda, H. and Dudareva, N. (2012) The shikimate pathway and aromatic amino acid biosynthesis in plants. *Annual review of plant biology*, 63, 73–105.
- Majumdar, R., Shao, L., Minocha, R., Long, S. and Minocha, S.C. (2013) Ornithine: the overlooked molecule in the regulation of polyamine metabolism. *Plant & cell physiology*, 54, 990–1004.
- Mäkinen, K. and De, S. (2019) The significance of methionine cycle enzymes in plant virus infections. *Current opinion in plant biology*, 50, 67–75.
- Martignago, D., Rico-Medina, A., Blasco-Escámez, D., Fontanet-Manzaneque, J.B. and Caño-Delgado, A.I. (2019) Drought Resistance by Engineering Plant Tissue-Specific Responses. *Frontiers in plant science*, 10, 1676.
- Menand, B., Desnos, T., Nussaume, L., Berger, F., Bouchez, D., Meyer, C. and Robaglia, C. (2002) Expression and disruption of the Arabidopsis TOR (target of rapamycin) gene. *Proceedings of the National Academy of Sciences of the United States of America*, 99, 6422–6427.
- Miyashita, Y., Dolferus, R., Ismond, K.P. and Good, A.G. (2007) Alanine aminotransferase catalyses the breakdown of alanine after hypoxia in *Arabidopsis thaliana*. *The Plant journal : for cell and molecular biology*, 49, 1108–1121.
- Nakabayashi, R., Yonekura-Sakakibara, K., Urano, K., Suzuki, M., Yamada, Y., Nishizawa, T., Matsuda, F., Kojima, M., Sakakibara, H., Shinozaki, K., Michael, A.J., Tohge, T., Yamazaki, M. and Saito, K. (2014) Enhancement of oxidative and drought tolerance in Arabidopsis by overaccumulation of antioxidant flavonoids. *The Plant journal : for cell and molecular biology*, 77, 367–379.
- Noctor, G., Queval, G. and Gakière, B. (2006) NAD(P) synthesis and pyridine nucleotide cycling in plants and their potential importance in stress conditions. *Journal of experimental botany*, 57, 1603–1620.
- O'Leary, B.M., Oh, G.G.K., Lee, C.P. and Millar, A.H. (2020) Metabolite regulatory interactions control plant respiratory metabolism via target of rapamycin (TOR) kinase activation. *The Plant cell*, 32, 666–682.
- Onis, M. de, Blössner, M. and Borghi, E. (2012) Prevalence and trends of stunting among pre-school children, 1990–2020. *Public health nutrition*, 15, 142–148.
- Payne, S.H. and Loomis, W.F. (2006) Retention and loss of amino acid biosynthetic pathways based on analysis of whole-genome sequences. *Eukaryotic Cell*, 5, 272–276.
- Pedrotti, L., Weiste, C., Nägele, T., Wolf, E., Lorenzin, F., Dietrich, K., Mair, A., Weckwerth, W., Teige, M., Baena-González, E. and Dröge-Laser, W. (2018) Snf1-RELATED KINASE1-Controlled C/S1-bZIP signaling activates alternative mitochondrial metabolic pathways to ensure plant survival in extended darkness. *The Plant cell*, 30, 495–509.
- Peterhansel, C., Horst, I., Niessen, M., Blume, C., Kebeish, R., Kürkcüoğlu, S. and Kreuzaler, F. (2010) Photorespiration. *The Arabidopsis book*, 8, e0130.
- Pivato, M., Fabrega-Prats, M. and Masi, A. (2014) Low-molecular-weight thiols in plants: functional and analytical implications. *Archives of biochemistry and biophysics*, 560, 83–99.
- Planchais, S., Cabassa, C., Toka, I., Justin, A.-M., Renou, J.-P., Saviouré, A. and Carol, P. (2014) BASIC AMINO ACID CARRIER 2 gene expression modulates arginine and urea content and stress recovery in Arabidopsis leaves. *Frontiers in plant science*, 5, 330.
- Preuten, T., Cincu, E., Fuchs, J., Zoschke, R., Liere, K. and Börner, T. (2010) Fewer genes than organelles: extremely low and variable gene copy numbers in mitochondria of somatic plant cells. *The Plant journal : for cell and molecular biology*, 64, 948–959.

- Raven, J.A. and Edwards, D. (2001) Roots: evolutionary origins and biogeochemical significance. *J Exp Bot*, 52, 381–401.
- Rippert, P., Puyaubert, J., Grisollet, D., Derrier, L. and Matringe, M. (2009) Tyrosine and phenylalanine are synthesized within the plastids in *Arabidopsis*. *Plant physiology*, 149, 1251–1260.
- Sage, R.F. (2004) The evolution of C 4 photosynthesis. *The New phytologist*, 161, 341–370.
- Salehin, M., Li, B., Tang, M., Katz, E., Song, L., Ecker, J.R., Kliebenstein, D.J. and Estelle, M. (2019) Auxin-sensitive Aux/IAA proteins mediate drought tolerance in *Arabidopsis* by regulating glucosinolate levels. *Nature communications*, 10, 4021.
- Sauter, M., Moffatt, B., Saechao, M.C., Hell, R. and Wirtz, M. (2013) Methionine salvage and S-adenosylmethionine: essential links between sulfur, ethylene and polyamine biosynthesis. *The Biochemical journal*, 451, 145–154.
- Schertl, P. and Braun, H.-P. (2014) Respiratory electron transfer pathways in plant mitochondria. *Frontiers in plant science*, 5, 163.
- Schertl, P., Danne, L. and Braun, H.-P. (2017) 3-Hydroxyisobutyrate dehydrogenase is involved in both, valine and isoleucine degradation in *Arabidopsis thaliana*. *Plant physiology*, 175, 51–61.
- Selinski, J. and Scheibe, R. (2019) Malate valves: old shuttles with new perspectives. *Plant biology (Stuttgart, Germany)*, 21 Suppl 1, 21–30.
- Shen, J., Zhang, J., Zhou, M., Zhou, H., Cui, B., Gotor, C., Romero, L.C., Fu, L., Yang, J., Foyer, C.H., Pan, Q., Shen, W. and Xie, Y. (2020) Persulfidation-based modification of cysteine desulphydrase and the NADPH oxidase RBOHD controls guard cell abscisic acid signaling. *The Plant cell*, 32, 1000–1017.
- Sowjanya, B.A., Narayana, B.D. and Shreyas, S. (2019) Enhancement of photosynthetic efficiency of C3 plants. *Int.J.Curr.Microbiol.App.Sci*, 8, 775–786.
- Stepansky, A. and Leustek, T. (2006) Histidine biosynthesis in plants. *Amino acids*, 30, 127–142.
- Swire, J. (2007) Selection on synthesis cost affects interprotein amino acid usage in all three domains of life. *Journal of molecular evolution*, 64, 558–571.
- Thimm, O., Bläsing, O., Gibon, Y., Nagel, A., Meyer, S., Krüger, P., Selbig, J., Müller, L.A., Rhee, S.Y. and Stitt, M. (2004) MAPMAN: a user-driven tool to display genomics data sets onto diagrams of metabolic pathways and other biological processes. *The Plant journal : for cell and molecular biology*, 37, 914–939.
- Thompson, M.G., Blake-Hedges, J.M., Pereira, J.H., Hangasky, J.A., Belcher, M.S., Moore, W.M., Barajas, J.F., Cruz-Morales, P., Washington, L.J., Haushalter, R.W., Eiben, C.B., Liu, Y., Skyrud, W., Benites, V.T., Barnum, T.P., Baidoo, E.E.K., Scheller, H.V., Marletta, M.A., Shih, P.M., Adams, P.D. and Keasling, J.D. (2020) An iron (II) dependent oxygenase performs the last missing step of plant lysine catabolism. *Nature communications*, 11, 2931.
- Thomsen, H.C., Eriksson, D., Møller, I.S. and Schjoerring, J.K. (2014) Cytosolic glutamine synthetase: a target for improvement of crop nitrogen use efficiency? *Trends in plant science*, 19, 656–663.
- Vieira Dos Santos, C. and Rey, P. (2006) Plant thioredoxins are key actors in the oxidative stress response. *Trends in plant science*, 11, 329–334.
- Wang, H. and Schippers, J.H.M. (2019) The role and regulation of autophagy and the proteasome during aging and senescence in plants. *Genes*, 10.
- Wang, P., Zhao, Y., Li, Z., Hsu, C.-C., Liu, X., Fu, L., Hou, Y.-J., Du, Y., Xie, S., Zhang, C., Gao, J., Cao, M., Huang, X., Zhu, Y., Tang, K., Wang, X., Tao, W.A., Xiong, Y. and Zhu, J.-K. (2018) Reciprocal regulation of the TOR kinase and ABA receptor balances plant growth and stress response. *Molecular cell*, 69, 100–112.e6.
- Winter, G., Todd, C.D., Trovato, M., Forlani, G. and Funck, D. (2015) Physiological implications of arginine metabolism in plants. *Frontiers in plant science*, 6, 534.
- Wisniak, J. (2013) Pierre-Jean Robiquet. *Educación Química*, 24, 139–149.
- Witte, C.-P. (2011) Urea metabolism in plants. *Plant science : an international journal of experimental plant biology*, 180, 431–438.

- Xiong, Y., McCormack, M., Li, L., Hall, Q., Xiang, C. and Sheen, J.** (2013) Glucose-TOR signalling reprograms the transcriptome and activates meristems. *Nature*, 496, 181–186.
- Yamori, W. and Shikanai, T.** (2016) Physiological functions of cyclic electron transport around photosystem I in sustaining photosynthesis and plant growth. *Annual review of plant biology*, 67, 81–106.
- Yang, Q., Zhao, D. and Liu, Q.** (2020) Connections between amino acid metabolisms in plants: Lysine as an example. *Frontiers in plant science*, 11, 928.

2 Publications and Manuscripts

2.1 The role of amino acid metabolism during abiotic stress release

Batista-Silva, W.^{1,2*}, Heinemann, B.^{2*}, Rugen, N.², Nunes-Nesi, A.¹, Araújo, W.L.¹, Braun, H.P.², Hildebrandt, T.M.²




¹Max - Planck Partner Group at the Departamento de Biologia Vegetal, Universidade Federal de Viçosa, Brazil

²Institute of Plant Genetics, Leibniz Universität Hannover, Hannover, Germany

*contributed equally to this study

Type of authorship:	Shared first author
Type of article:	Research article
Share of the work:	35 %
Contribution to the publication:	Performed experiments, analyzed data, prepared figures, participated in writing the manuscript
Journal:	Plant Cell & Environment
Impact factor:	5.970 (2019)
Date of publication:	10.01.2019
Number of citations (Google Scholar, 23.06.2021)	61
DOI:	10.1111/pce.13518
PubMed-ID:	30632176

The role of amino acid metabolism during abiotic stress release

Willian Batista-Silva^{1,2*} | Björn Heinemann^{2*} | Nils Rugen² | Adriano Nunes-Nesi¹ |
Wagner L. Araújo¹  | Hans-Peter Braun²  | Tatjana M. Hildebrandt² 

¹Max-Planck Partner Group at the Departamento de Biologia Vegetal, Universidade Federal de Viçosa, Viçosa, Brazil

²Institut für Pflanzengenetik, Leibniz Universität Hannover, Hannover, Germany

Correspondence

Tatjana M. Hildebrandt, Institut für Pflanzengenetik, Leibniz Universität Hannover, Herrenhäuser Str. 2, 30419 Hannover, Germany.
Email: hildebrandt@genetik.uni-hannover.de

Funding information

National Council for Scientific and Technological Development; Coordenação de Aperfeiçoamento de Pessoal de Nível Superior, Grant/Award Number: PROBRAL #423/14

Abstract

Plant responses to abiotic stress include various modifications in amino acid metabolism. By using a hydroponic culture system, we systematically investigate modification in amino acid profiles and the proteome of *Arabidopsis thaliana* leaves during initial recovery from low water potential or high salinity. Both treatments elicited oxidative stress leading to a biphasic stress response during recovery. Degradation of highly abundant proteins such as subunits of photosystems and ribosomes contributed to an accumulation of free amino acids. Catabolic pathways for several low abundant amino acids were induced indicating their usage as an alternative respiratory substrate to compensate for the decreased photosynthesis. Our results demonstrate that rapid detoxification of potentially detrimental amino acids such as Lys is a priority during the initial stress recovery period. The content of Pro, which acts as a compatible osmolyte during stress, was adjusted by balancing its synthesis and catabolism both of which were induced both during and after stress treatments. The production of amino acid derived secondary metabolites was up-regulated specifically during the recovery period, and our dataset also indicates increased synthesis rates of the precursor amino acids. Overall, our results support a tight relationship between amino acid metabolism and stress responses.

KEYWORDS

Arabidopsis thaliana, drought, hydroponic culture, proteomics, salinity

1 | INTRODUCTION

Higher plants are sessile and therefore cannot escape adverse environmental conditions that are a constant threat throughout their life cycle. Unfavourable growth conditions such as extreme temperatures (heat, cold, and freezing), drought (deficient precipitation and drying winds), and contamination of soils with high salt concentrations are considered the major abiotic environmental stressors that can not only limit plant growth and development but they also determine the geographic distribution of plant species and directly affect agronomical yield (Krasensky & Jonak, 2012). Early effects of high salinity and drought on plant metabolism are relatively similar because both restrict the availability of water to plant cells and impose osmotic

stress that can lead to turgor loss. To cope with that, plants react with stomatal closure, which inhibits CO₂ assimilation and thus triggers a chain of events including accumulation of reducing equivalents, overreduction of plastidial and mitochondrial electron transport chains and as a consequence increased production of reactive oxygen species (ROS) which in turn damage proteins, lipids, and nucleic acids. Prolonged salt stress in addition induces hyperionic stress and secondary deficiencies in K⁺ and NO₃⁻ (Chaves, Flexas, & Pinheiro, 2009; Mahajan & Tuteja, 2005). Under field conditions, this may even be the predominant factor affecting plant performance (Verslues, Agarwal, Katiyar-Agarwal, Zhu, & Zhu, 2006).

Plants have evolved different strategies to minimize the adverse effects of abiotic stress conditions and several of them are connected to amino acid metabolism (Hildebrandt, 2018; Madhava Rao, Janardhan Reddy, & Raghavendra, 2006). For instance, osmotic

*Willian Batista-Silva and Björn Heinemann contributed equally to this study.

adjustment is achieved by the accumulation of compatible osmolytes that do not interfere with plant metabolism even at high concentrations and may also act as ROS scavengers such as Pro and GABA. Pro synthesis is strongly induced during osmotic stress leading to an accumulation of Pro to high millimolar levels (Verslues & Sharma, 2010). Thus, increased Pro concentrations can be used as a metabolic stress indicator. Pro content is determined by the balance between synthesis and degradation, and its accumulation capacity has been shown to correlate with abiotic stress tolerance (Szabados & Savouré, 2010).

Several amino acids can act as precursors for the synthesis of secondary metabolites and signalling molecules. Polyamines are derived from Arg (Alcázar et al., 2006), the plant hormone ethylene is synthesized from Met (Amir, 2010), and immune signalling requires conversion of Lys to N-hydroxy pipercoline (Chen et al., 2018; Hartmann et al., 2018). A broad spectrum of secondary metabolites with multiple biological functions and health promoting properties are further derived from the aromatic amino acids Phe, Tyr, and Trp or from intermediates of their synthesis pathways (Tzin & Galili, 2010). A general accumulation of free amino acids has usually been observed in different plants exposed to abiotic stress (Aleksza, Horváth, Sándor, & Szabados, 2017; Barnett & Naylor, 1966; Draper, 1972; Ferreira Júnior, Gaion, Sousa Júnior, Santos, & Carvalho, 2018; Fougère, Le Rudulier, & Streeter, 1991; Huang & Jander, 2017; Lugan et al., 2010). Extensive amino acid accumulation in response to drought stress has been reported for maize, cotton, tomato, and the resurrection plant (Martinelli et al., 2007; Perez-Alfocea, Estan, Caro, & Guerrier, 1993; Ranieri, Bernardi, Lanese, & Soldatini, 1989; Showler, 2002). Recent studies also suggested that autophagy and abscisic acid-induced protein turnover contribute to the increase in free amino acids (Barros et al., 2017; Hildebrandt, 2018; Hirota, Izumi, Wada, Makino, & Ishida, 2018; Huang & Jander, 2017). In situations of insufficient carbohydrate supply due to a decrease in photosynthesis rates that usually occur during stress conditions, plants can use amino acids as alternative substrates for mitochondrial respiration (Araújo, Tohge, Ishizaki, Leaver, & Fernie, 2011; Hildebrandt, 2018; Hildebrandt, Nunes Nesi, Araújo, & Braun, 2015). The degradation pathways for Lys and the branched-chain amino acids Val, Leu, and Ile have already been identified as essential factors for dehydration tolerance in *Arabidopsis* (Pires et al., 2016), but the specific role of other catabolic pathways remains unclear. After return to more favourable growth conditions, plants have to reprogram their metabolism and switch back from survival to active growth. Thus, not only metabolic adjustments to the stress conditions but also the efficiency of resuming growth and seed production after stress release will affect plant fitness and consequently crop yield.

By using a hydroponic culture system, here, we investigate the response of amino acid metabolism during the recovery phase following low water potential and salt stress in *Arabidopsis thaliana* under controlled environmental conditions. Our results provide novel insight into the dynamic behaviour of individual pathways and their potential functions during stress tolerance. They demonstrate that the usage of a relatively simple experimental system is suitable for investigating the mechanisms and regulatory networks associated with efficient recovery from stress.

2 | MATERIALS AND METHODS

2.1 | Plant growth conditions and stress treatment

Seeds of *A. thaliana* Col-0 (10 mg) were sterilized by incubation in 50% ethanol for 1 min, followed by manual shaking for 2 min. After that, the ethanol was replaced by 6% of hypochlorite and shaken for another 2 min. Subsequently, the seeds were washed five times by adding 1 ml sterilized water, inverting the tubes for 2 min and spinning the seeds down. In a final step, 2 ml Agarose (0.15% w/v; Sigma-Aldrich, Hamburg, Germany) were added to the sterilized seeds. The seed suspension was diluted to a final concentration of 2.5 mg ml⁻¹ of agarose per tube. Plant cultivation took place in specialized glass jars, which include a stainless steel wire mesh platform (125 µm mesh size) that is fixed between two flat rings and held in place by three legs (as developed by Schlesier, Bréton, & Mock, 2003). One millilitre of the seed/agarose suspension was dispensed on each wire mesh platform. The glass jars were filled to the height of the platform with ~150 ml of a solution including 2.2 g L⁻¹ Murashige and Skoog (MS) basal medium (Murashige & Skoog, 1962; Sigma-Aldrich, Hamburg, Germany) and 0.4% Agar (Agar Type A, Sigma-Aldrich). Plants were cultivated in a growth chamber at long-day conditions (16 hr light [85 µmol photon m⁻² s⁻¹] and 8 hr dark), a temperature of 23 ± 2°C and a humidity of 60 ± 5%. For the initial plant cultivation, the abovementioned medium was supplemented with 1% (w/v) sucrose. During continued cultivation at stress conditions (see below), supplementation of sucrose was omitted.

Fourteen days after sowing, the wire mesh platforms with seedlings were transferred into new glass jars including liquid medium (150 ml of 2.2 g L⁻¹ of MS) supplemented with either (a) 150 mM NaCl (salt stress), (b) PEG 6000 (water stress; $\Psi_s = -1.0$ MPa; 290.92 g L⁻¹), or (c) none of the two compounds (control). The medium supplemented with NaCl was autoclaved together with the MS medium before use, whereas PEG-6000 was added to the MS medium after autoclaving. Stress treatment was started 1 hr after the beginning of the light period. The seedlings were maintained at the stress conditions for the next 24 hr. To investigate the recovery from NaCl and PEG stress, wire mesh platforms with seedlings were returned to glass jars containing ½ MS medium without supplements and cultivated for another 18 hr. Leaf material of the plants was harvested at four time points (Figure 1): At the beginning of the stress treatment (immediately before transferring to the new glass jars), at the end of the stress treatment, and after 6 and 18 hr of recovery. Leaves of all plants growing in the same glass jar were pooled. For each time point and condition plant material from four individual glass jars was analysed. Samples were frozen in liquid nitrogen, ground to a fine powder, and stored at -80°C until further use.

2.2 | Determination of hydrogen peroxide content

The hydrogen peroxide (H₂O₂) content of plant extracts was measured after reaction with KI (potassium iodide) as described by Gharibi, Tabatabaei, Saeidi, and Goli (2016). In brief, extraction was performed using 30 mg of plant material. The powder was resolved in 1 ml of

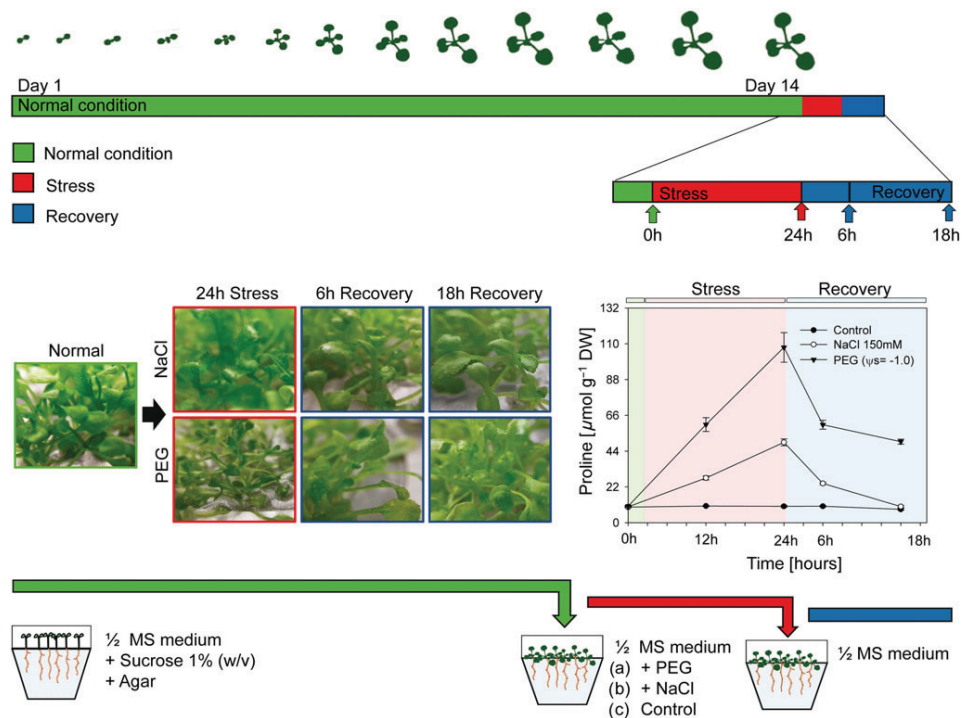


FIGURE 1 Scheme of the experimental set-up for investigating the stress and stress recovery responses in Arabidopsis. Throughout the experiment, plants were cultivated at long-day conditions (16 hr light and 8 hr dark; see Section 2 for details). Germination and initial cultivation of plants took place on semi-solid ½ MS medium containing 1% sucrose (green bar). Fourteen days after sowing (DAS), plants were transferred, to liquid ½ MS medium without sucrose 1 hr after the beginning of the light period and subjected to stress (addition of either 150 mM NaCl or PEG6000) for 24 hr (red bar). Finally, plants were transferred to liquid ½ MS medium without additions for stress recovery for 18 hr (blue bar). Plants were harvested and used for all further experiments at the four time points indicated by the colour arrows. Representative pictures of the plants before and after the stress treatments and during the recovery phase are shown. The inserted graph presents leaf proline contents at the time points indicated [Colour figure can be viewed at wileyonlinelibrary.com]

0.6% (w/v) of thiobarbituric acid (Sigma-Aldrich) in 10% (w/v) of trichloroacetic acid. Then, the mixture was heated at 100°C for 15 min and centrifuged at 2,400 g for 10 min. Afterwards, the supernatant (20 µl) was combined with 200 µl of 100 mM K-phosphate buffer, pH 7.0, and 80 µl of KI 1% (w/v). The blank probe consisted of the same compounds except that the protein extract was omitted. The reaction took place for 1 hr in the dark. Subsequently, absorbance was measured at 390 nm. The amount of H₂O₂ was determined according to a standard curve prepared with known concentrations of H₂O₂.

2.3 | Assays of antioxidant enzyme activities

About 0.25 g of leaf material was solubilized in 0.5 ml 50 mM potassium phosphate buffer (pH 7.0) containing 1 mM ethylenediaminetetraacetic acid (EDTA), 1% polyvinylpyrrolidone, and 1 mM ascorbic acid. The homogenate was centrifuged at 15,000 g for 20 min at 4°C, and the supernatant was used for the following enzyme assays. The total protein content was determined as previously described (Bradford, 1976).

Catalase (CAT; EC1.11.1.6) activity was determined as described before with some modifications (Aebi, 1984). In brief, CAT activity was assayed by H₂O₂ consumption (extinction coefficient 39.4 mM

⁻¹ cm⁻¹) at 240 nm. The reaction was carried out in a volume of 200 µl (20 µl supernatant of the plant extract plus 180 µl of a solution containing 50 mM potassium phosphate buffer (pH 7.0) and 10 mM H₂O₂). Ascorbate peroxidase (APX; EC1.11.1.11) activity was determined by following the decrease in A₂₉₀ (extinction coefficient 2.8 mM⁻¹ cm⁻¹). The reaction volume was 200 µl (20 µl supernatant of the plant extract plus 180 µl of 50 mM potassium phosphate [pH 7.0], 0.5 mM ascorbic acid, and 0.1 mM of H₂O₂ as described in Nakano & Asada, 1981). Glutathione reductase (GR; EC1.6.4.2) activity was determined by measuring NADPH oxidation at 340 nm (extinction coefficient 6.2 mM⁻¹ cm⁻¹). The assay mixture (volume: 200 µl) included 20 µl supernatant of the plant extract plus 180 µl of a solution containing 50 mM potassium phosphate buffer (pH 7.8), 2 mM of Na₂EDTA, 0.15 mM glutathione disulphide, and 0.15 mM NADPH. The reaction was initiated by adding NADPH as described previously by Schaedle and Bassham (1977). The reaction was monitored for 3 min. Superoxide dismutase (SOD; EC1.15.1.1) was assayed by monitoring the inhibition of the photochemical reduction of nitro blue tetrazolium (NBT) at 560 nm (100 µmol photons m⁻² s⁻¹) as previously described by Giannopolitis and Ries (1977). The reaction mixture (300 µl) contained 20 µl of supernatant of the plant extract plus 280 µl a solution containing 50 mM of potassium phosphate buffer (pH 7.8), 75 µM nitroblue tetrazolium, 13 mM methionine, 0.1 mM EDTA, and 2 µM riboflavin.

2.4 | Determination of metabolite levels

Photosynthetic pigments were determined according to Porra, Thompson, and Kriedemann (1989). Total proteins were determined as described before (Cross et al., 2006).

2.5 | Amino acid quantification

Amino acid profiles were quantified using a modified version of the procedure described by Fürst, Pollack, Graser, Godel, and Stehle (1990). Leaf material was lyophilized using an Alpha 1-2 LD+ freeze dryer (Christ, Osterode, Germany). About 10 mg plant powder was used for the extraction of free amino acids. Samples were solubilized in 800 μ l of 0.1 M HCl (Roth, Karlsruhe, Germany). After 15 min of incubation at room temperature, the samples were centrifuged at 16,100 g for 5 min. Supernatants were mixed with equal volume of 0.5 M potassium borate buffer (pH 11), incubated for 15 min at room temperature, and centrifuged at 16,100 g for 5 min. The supernatants were collected and stored at -20°C . Shortly before the analysis, 50 μ l of the extracts were diluted with 300 μ l 0.5 M potassium borate buffer (pH 11) and 280 μ l 0.1 M HCl. As internal standard for the derivatization of primary amino acids 5 μ l of 0.5 mM beta-aminobutyrate (Sigma-Aldrich, Hamburg, Germany) was added. For the normalization of the derivatization of the secondary amino acids, 5 μ l of 0.5 mM sarcosine (Sigma-Aldrich, Hamburg, Germany) was added to the dilution.

During the precolumn derivatization, 7 μ l of samples were mixed with 18 μ l 0.1 M borate buffer (Agilent, Waldbronn, Germany) and 3.5 μ l ortho-phthaldialdehyde (Agilent, Waldbronn, Germany). After 60 s, 2.8 μ l 9-fluorenylmethoxycarbonyl chloride (Agilent, Waldbronn, Germany) were added, and subsequently, the derivatization was stopped by adding 90 μ l of 15 mM acetic acid. Finally, 1 μ l were injected onto a 100 \times 2.1 mm Acclaim RSLC 120 C18, 2.2 μ m (Thermo Fisher, Dreieich, Germany), driven by the Ultra High-Performance Liquid Chromatography (UHPLC) System Ultimate 3000 (Thermo Fisher, Dreieich, Germany) at 40°C . The gradient was composed of solvent A (10 mM sodium phosphate and 10 mM sodium tetraborate decahydrate [pH 8.2]) and solvent B (methanol:acetonitrile:water [45:45:10]) with a flow rate of 0.71 ml min $^{-1}$. The gradient programme started with a composition of 98:2 (solvent A:B), which changed linearly from 0 to 4.4 min to 71.5:28.5, followed by an isocratic step for 0.3 min. From 4.7 to 6.9 min, solvent A reduced further to 43%, followed again by an isocratic step till 9 min. At 9.8 min, the composition reached 0:100 (A:B) and remained for 5.7 min, to wash the column. At 15.7 min, the initial composition of 98:2 (A:B) was used for 4.3 min to re-equilibrate the column for the next run. Amino acids were detected using a Fluorescence detector 3400 RS and UV-Detector 3100 (Thermo Fisher, Dreieich, Germany). Primary amino acids were excited with 337 nm wavelength, whereas the emitted light at 442 nm was measured. Secondary amino acids were excited with 266 nm, and the emitted signals detected at 305 nm. Standards were prepared using the amino acid standard solution from Sigma-Aldrich (AAS18-5ML), stacked with L-Asparagine, L-Glutamine, gamma-Aminobutyrate, beta-Aminobutyrate, L-Tryptophan and

Sarcosine (each from Sigma-Aldrich, Hamburg, Germany). Evaluation of the peak areas was done with the software Chromeleon 7.2 SR4 (Thermo Fisher, Dreieich, Germany).

2.6 | Proline quantification

The proline content was measured as previously described by Abrahám, Hourton-Cabassa, Erdei, and Szabados (2010), with modifications. A total of 10 mg lyophilized plant powder was used for proline extraction as described above for amino acid extraction. The sample extract was prepared in a reaction mixture containing 100 μ l of sulfosalicylic acid (3%, w/v), 200 μ l of acidic ninhydrin, (1.25 g ninhydrin (1,2,3-indantrione monohydrate), 30 ml glacial acetic acid, 20 ml of 6 M orthophosphoric acid), 200 μ l of glacial acetic acid. To start the reaction, 100 μ l of sample extract was added to the reaction mixture, incubated at 96°C for 60 min in the dark. Transfer on ice stopped the reaction. After that, 1 ml of toluene (Sigma-Aldrich) was added, vortexed and kept at room temperature for 5 min to allow the separation of the organic and the water phase. A total of 200 μ l of the chromophore phase (200 μ l) containing the toluene was transferred into a fresh quartz 96-well plate and read by a microplate reader at 520 nm. The system was calibrated by measuring known proline concentrations.

2.7 | Label-free quantitative shotgun mass spectrometry

Protein extraction and sample preparation for label-free quantitative shotgun mass spectrometry analysis were performed as described by Thal, Braun, and Eubel (2018). Tandem mass spectrometry (MS/MS) analysis was performed using a Q-Exactive mass spectrometer coupled to an Ultimate 3000 UPLC (Thermo Fisher Scientific, Dreieich, Germany) as described in Fromm, Göing, Lorenz, Peterhänsel, and Braun (2016).

For MS data interpretation, the software MaxQuant (Version 1.5.5.1) was used, including the Andromeda search engine (Cox & Mann, 2008) against the TAIR 10 database. Max Quant and Andromeda settings were selected as described in Thal et al. (2018). The final analysis and comparison of the protein identification lists were done with Perseus (Version 1.5.5.3; Tyanova et al., 2016). In brief, MaxQuant LFQ (Label Free Quantification) values were imported and proteins only identified by a single peptide containing a modification, decoy entries, as well as common contaminations were removed. The data were transformed to log $_2$ and grouped (40 samples: four biological replicates for 0 hr stress, 24 hr stress (PEG, NaCl, control), 6 hr recovery (PEG, NaCl, control), and 18 hr recovery (PEG, NaCl, control), respectively). Protein entries were classified as "valid" if they were identified in at least three replicates of at least one group.

Proteins were assigned to functional categories according to the MapMan annotation file (version Ath_AGI_LOCUS_TAIR10_Aug2012). Enrichment of specific categories within the proteins with significantly changed abundance in the individual treatments compared with the control was calculated as the relative abundance of

the category in the analysed group divided by the relative abundance in the complete proteomics dataset.

2.8 | Root toxicity test

The toxicity of certain amino acids to *A. thaliana* was tested in vitro by analysing the root growth in the presence of the respective amino acid. The experiment was performed in a growth chamber at 22°C, 85 $\mu\text{mol s}^{-1} \text{m}^{-2}$ light, 16 hr light, and 8 hr darkness. For the initial rooting, seeds were sterilized and placed on ½ MS Medium with 1% sucrose and 1% agar for 3 days. Ten similarly developed seedlings were then transferred to squared agar plates supplemented with 100 μM of the respective amino acid. Plates were placed upstanding to let the roots grow vertically along the medium. After 8 days, the roots were measured with the AxioVison software (Carl-Zeiss, Jena).

2.9 | Statistical analysis

The experiment was performed in a completely randomized design, with four replicates per treatment. Additionally, the complete set-up was repeated at least four times with similar phenotypes observed each time. Statistical analysis of the MS dataset was performed in Perseus using two-sample *t* tests ($P < 0.05$). For amino acid profiles, the averages of the treatments were compared by the Tukey's test ($P < 0.05$) using the GENES software (Cruz, 2013). Statistical analysis of root lengths was performed using the Mann-Whitney *U* test.

3 | RESULTS

3.1 | Investigation of stress and stress release in a hydroponic culture system

We adapted a hydroponic culture system previously developed (Schlesier et al., 2003) to investigate changes in amino acid metabolism in *Arabidopsis* during osmotic stress as well as in the early recovery period. Plants were cultivated under controlled environmental conditions in sealed glass jars (Figure 1). Seeds were placed on platforms covered with steel mesh allowing to quickly modify the conditions in the growth medium by transferring the platform to a new glass jar. Preliminary experiments were conducted to establish the optimal experimental conditions including (a) the time point for the beginning of the stress treatment, (b) the intensity and duration of the stress period, and (c) the duration of the recovery phase. Leaf Pro content was monitored as a marker for osmotic stress response. We selected plants that were severely stressed but still able to recover completely. The final set-up included cultivating plants under control conditions for 2 weeks, followed by the exposition to stress treatments (150 mM NaCl; 291 g L⁻¹ PEG; control without stress) for 24 hr and afterwards return to control conditions (Figure 1; see Section 2 for details). Shoots were harvested before and at the end of the stress treatment as well as after 6 and 18 hr of recovery.

The plants were apparently severely stressed after 24 hr of PEG or NaCl treatment as reflected by shrivelled leaves and in case of PEG even a brownish colour (Figure 1). They recovered almost

completely within the first 6 hr of stress release with only individual leaves still showing necrotic lesions. In order to assess the general condition of the plants, we analysed oxidative stress parameters as well as the chlorophyll, amino acid, and protein content (Figure 2). Principal component analysis illustrates the significant impact of the stress treatment on these variables and the gradual return to control levels during recovery (Figure S1). Both hydrogen peroxide content and the activities of enzymes involved in the antioxidative system were consistently increased after the stress period, an effect that was stronger for PEG than for NaCl treatment (Figures 2 and S2). Catalase, glutathione reductase, and superoxide dismutase activity returned to control levels after 6 hr of stress release in the NaCl treated samples indicating a quick recovery from oxidative stress. The decrease in antioxidative enzyme activities was slower after PEG treatment, and ascorbate peroxidase activity remained at higher levels throughout the recovery phase. PEG stress led to a decrease in leaf chlorophyll and protein content, which were completely (protein) or partially (chlorophyll) restored within 18 hr of release. By contrast, the protein but not the chlorophyll content was affected by salt stress.

3.2 | Global responses of the Arabidopsis leaf proteome during stress and stress release

Total leaf protein fractions were isolated from plants harvested before and after the stress treatment and after 6 and 18 hr of recovery and subjected to label-free shotgun proteomics. A total of 1,839 proteins were detected in at least three replicates of one group and on that basis selected for further analysis (Table S1). In order to obtain a general overview regarding the proteomic stress response, we grouped all proteins into functional categories according to MapMan (Thimm et al., 2004). This dataset was used for enrichment analysis to identify the most relevant pathways during stress and/or recovery (Figure 3), and in addition, protein abundance profiles were calculated for all functional categories (Figure 4). A total of 707 proteins were significantly changed after PEG stress and a large fraction of them remained increased or decreased also during the recovery phase (Figure 3a, dark grey bars; Figure 3b, top box). In comparison, high salinity led to rather short-term proteome modifications. Aminotransferases as well as heat shock proteins were consistently increased during stress and recovery in both, PEG and NaCl stress, whereas ribosomal and photosystems proteins were of lower abundance indicating increased turnover of such highly abundant proteins. Enrichment analysis as well as the heatmaps also demonstrated that other categories related to photosynthesis including light reactions, Calvin-Benson cycle, photorespiration, and tetrapyrrole synthesis were strongly down-regulated following the stress treatment. As a potential compensation, PEG treatment led to an induction of pathways involved in heterotrophic energy metabolism such as the degradation of lipids, proteins and cell walls, glycolysis, and the tricarboxylic acid (TCA) cycle. There was a biphasic oxidative stress response in PEG treated plants with an initial peak in catalase and glutathione-S-transferase abundance during the stress period followed by a gradual increase in peroxidase abundance during the recovery phase.

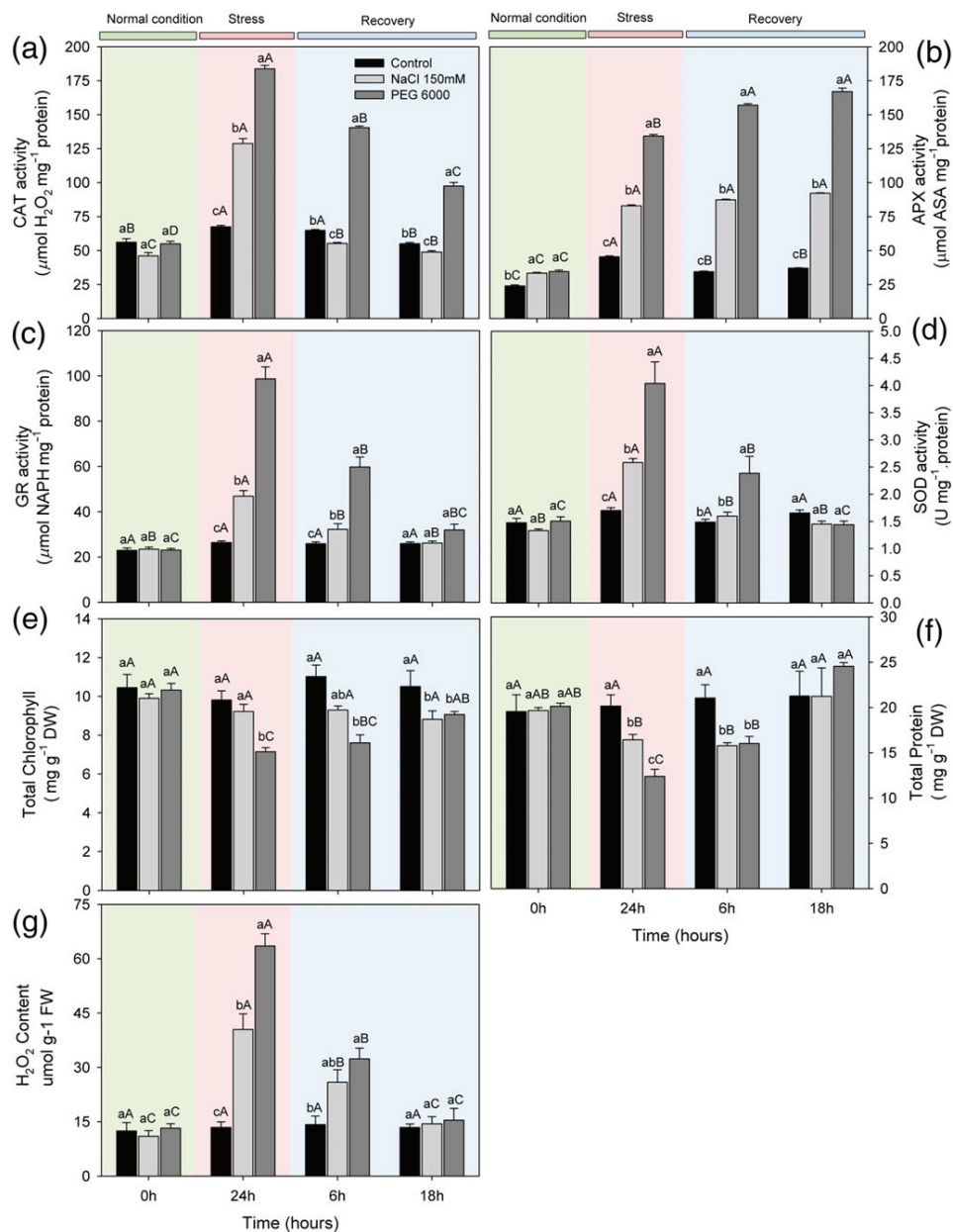


FIGURE 2 Physiological and biochemical properties of Arabidopsis plants during stress and stress recovery. Plants were characterized before stress (0 hr; indicated by green colour), at the end of the stress period (24 hr; red), and during stress recovery (6 and 18 hr; blue). Activities of selected enzymes involved in the antioxidative system. (a) CAT: catalase. (b) APX: ascorbate peroxidase. (c) GR: glutathione reductase. (d) SOD: superoxide dismutase. Additionally, were measured (e) total chlorophyll, (f) total protein, and the (g) contents of H_2O_2 with respect to fresh weight (FW) or dry weight (DW) as indicated. Data presented are means \pm SE ($n = 4$). Different letters represent average values that were judged to be statistically different between samples ($P < 0.05$, Tukey test). Small letters refer to the comparison between treatments at the same time points and capital letter to comparisons between individual treatments over time [Colour figure can be viewed at wileyonlinelibrary.com]

3.3 | Amino acid metabolism during stress and stress release

Enrichment analysis also revealed a prominent role of amino acid metabolism during stress and stress release (Figure 3b). In addition to the sustained induction of aminotransferases, the synthesis pathways for Arg and aromatic amino acids were significantly up-regulated on a protein level specifically during the recovery phase following both PEG and salt stress. In contrast, the abundance of branched-chain amino acid biosynthetic enzymes was significantly decreased after

the stress. In order to understand the interactions of amino acid metabolism and stress response in more detail, we additionally measured leaf amino acid profiles (Tables S2 and S3) and integrated all the information in a comprehensive metabolic pathway map (Figure 5). This map represents all currently known enzymatic steps involved in plant amino acid synthesis (arrows pointing at the amino acids) and amino acid degradation (arrows pointing away from the amino acids; Hildebrandt, 2018). In addition, committed steps leading to the synthesis of secondary metabolites are also shown (in italics).

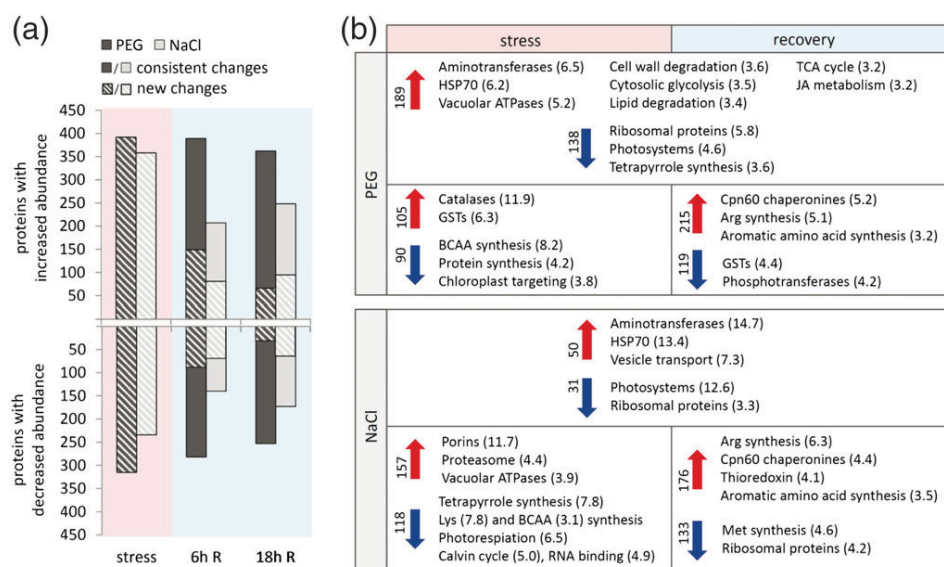


FIGURE 3 Significant changes in the Arabidopsis leaf proteome during stress and recovery period. Total protein fractions were isolated from plants harvested at the time points indicated in Figure 1 and subjected to label-free shotgun proteomics (see Section 2 for details). Log₂-fold changes in protein abundances were calculated for the stress treated versus control plants, and significant changes in abundance were identified by Student *t* test ($P < 0.05$). (a) Number of proteins with significantly increased or decreased abundance in stress treated versus control plants after the stress treatment (stress), after 6 hr of recovery (6 hr R), and after 18 hr of recovery (18 hr R). Proteins with consistently changed abundance during the stress and recovery phase are represented by filled bars, whereas significant changes that were not present in the previous time points are shown as striped areas. (b) Enrichment analysis to identify functional protein categories that are consistently regulated during the stress and recovery period (shown in the upper part of the boxes) or specific for either stress or stress release (shown at the bottom). Numbers next to the arrows indicate the total number of significantly increased (red arrows) or decreased (blue arrows) proteins. The enrichment factors are given in parentheses after the names of the categories. The full shotgun proteome dataset is given in Table S1 [Colour figure can be viewed at wileyonlinelibrary.com]

Pro accumulation during the stress treatment followed by a decrease in the recovery phase had been used as a marker for osmotic stress response for establishing the experimental set-up, and our dataset further confirms that the synthesis pathway for Pro was induced during salt as well as PEG stress (Figure 5d; Table S4). This response was stronger and more persistent with PEG than with NaCl. Interestingly, the abundance of delta-1-pyrroline-5-carboxylate dehydrogenase, an enzyme involved in Pro degradation, was already induced during the stress treatment and remained on a high level during stress release (Figure 5d; Table S4). Overall, the effect of salt stress on the leaf amino acid profile was less pronounced than for PEG treatment. Only four of the 20 amino acids analysed significantly changed their contents after salt stress, and three additional ones changed only during the recovery phase (Table S3). In contrast, four amino acids remained completely unaffected by PEG stress, whereas 10 were increased throughout the entire experiment. The total free amino acid content, calculated as the sum of all amino acids in our profile, increased during stress and showed a second peak during late recovery (Table S3). Gly was the only amino acid with a consistently lower content in stressed plants compared with controls. Gln and Ala strongly accumulated during the recovery period from PEG treatment. After salt stress, there was an initial reduction in the contents of Gln, Arg, and Asn after 6 hr of recovery before they returned to control levels after 18 hr. Arg decreased significantly during recovery from PEG, which might be explained by a high demand for precursors of polyamine synthesis, because this pathway was induced (Figure 5d). Amino acid derived secondary metabolism was generally up-regulated

during stress and recovery with the exception of ethylene production from Met. This finding is in good agreement with the observed induction of aromatic amino acid synthesis because these are precursors for a diverse set of secondary metabolites such as glucosinolates, alkaloids, and phenylpropanoids.

Concentrations of the low abundant amino acids (branched-chain amino acids, Lys, Met, His, and aromatic amino acids) showed the strongest relative increase after PEG treatment, whereas there was no significant change compared with the control after NaCl stress. The synthesis pathways of these amino acids were generally down-regulated during both stress conditions investigated and gradually returned to control levels during recovery. In contrast, the degradation pathways were strongly induced and in several cases peaked during early recovery before decreasing again (Figure 5a–c; Table S4). Looking at the absolute amino acid concentrations in the leaves, it becomes obvious that some of the low abundant amino acids such as Lys and Leu accumulated during PEG stress but were degraded very fast after stress release, whereas others (Val, Ile, His) remained elevated (Figure 6a). Proteomics show that LKR/SDH and aldehyde dehydrogenase 7B4 catalysing the first steps in Lys degradation were strongly induced during PEG treatment and remained on a high level also throughout the recovery phase (Figure 6b). Induction of enzymes involved in branched-chain amino acid catabolism seemed to be less pronounced and of a more transient nature.

To test whether toxic effects could be the reason for preferential degradation of specific amino acids, we further performed a root growth inhibition assay (Figure 6c). Indeed, Lys turned out to be the

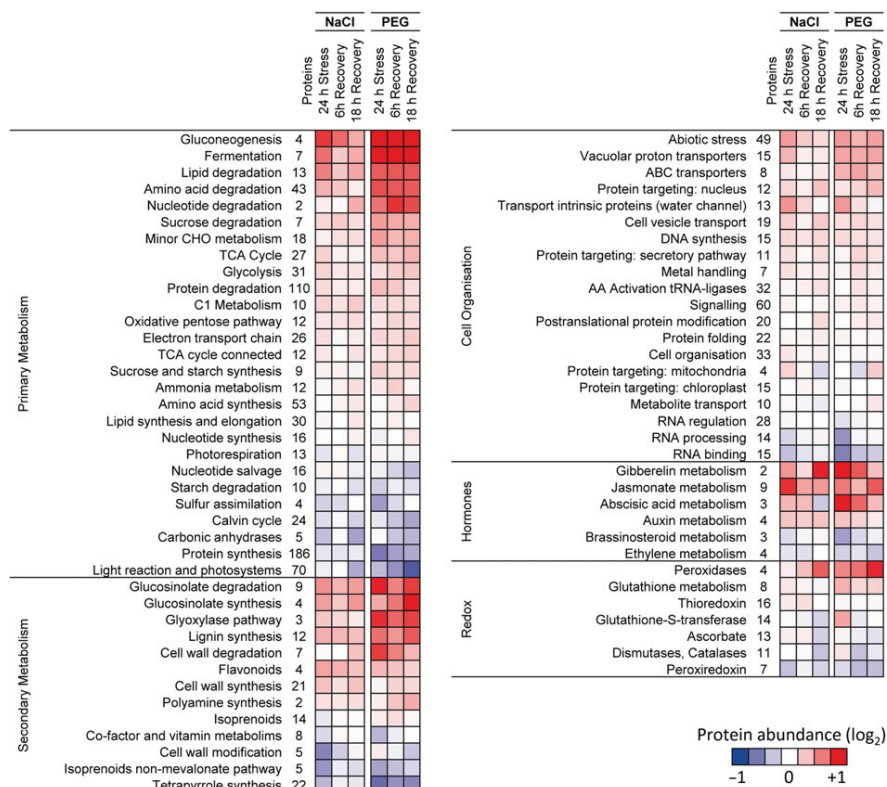


FIGURE 4 Heatmap representing protein abundance profiles during stress and recovery period. Total protein fractions were isolated from plants harvested at the time points indicated in Figure 1 and subjected to label-free shotgun proteomics (see Section 2 for details). Log₂-fold changes in protein abundances were calculated for the stress treated versus control plants. The colour gradient represents the means of all log₂-ratios (scaling: -1 to +1) for proteins included in the functional categories listed according to the MapMan annotation file (version Ath_AGI_LOCUS_TAIR10_Aug2012). Red colours: increased abundance with respect to the reference fraction. Blue colours: decreased abundance with respect to the reference fraction. The full shotgun proteome dataset is given in Table S1 [Colour figure can be viewed at wileyonlinelibrary.com]

most toxic amino acid and inhibited the growth of *Arabidopsis* roots by 80% at a concentration of 100 μ M followed by Leu (62% inhibition) and Met (44% inhibition). By sharp contrast, Val and Ile showed only mild toxic effects, whereas His addition even slightly promoted root growth.

4 | DISCUSSION

Our approach aimed at specifically addressing the behaviour of amino acid metabolism during the recovery phase from high salinity and low water potential in the model plant *A. thaliana*. Our in vitro experimental system provided reliable and reproducible conditions during stress and more importantly in the recovery period. In contrast to soil-based techniques, it allows rapid and accurate modification of the water potential and the salt concentration in the medium. The advantages of PEG as a drought stress inducer have been repeatedly demonstrated (Frolov et al., 2017; van der Weele, Spollen, Sharp, & Baskin, 2000; Verslues et al., 2006). Although caution must be taken when analysing such results due to potential effects of the artificial growth conditions such as crowding, hypoxia, or the supply of sucrose in the initial growth medium, our experimental system had very little effect on amino acid metabolism in control plants. Therefore, we conclude that our approach is highly suitable for investigating the effect of

stress and stress release on amino acid metabolism in order to complement the results obtained with soil-based systems.

4.1 | Stress recovery: Re-establishing photosynthesis and fighting ROS

Photosynthesis is one of the primary processes affected by drought and salt stress (Chaves, 1991; Munns, James, & Läuchli, 2006). The decreased availability of CO₂ due to diffusion limitations directly restrict photosynthesis rates but also leads to secondary effects such as photo-oxidative damage and increased protein turnover (Chaves et al., 2009). The carbon balance of a recovering plant may thus depend on both the degree of damage induced during stress as well as the velocity and extent of photosynthetic recovery. Our results confirm a sharp increase in oxidative stress after PEG as well as NaCl treatment leading to an induction of protective enzymes such as chaperones, catalase, and glutathione S-transferase. Although plants were able to eliminate ROS levels within 18 hr of recovery, the chlorophyll content as well as the abundance of proteins from the photosystems still remained low, indicating an incomplete recovery of the photosynthetic activity. In addition, ribosomal proteins were clearly enriched in the group of proteins with consistently reduced abundance after stress treatments as well as during the recovery period. Preferential

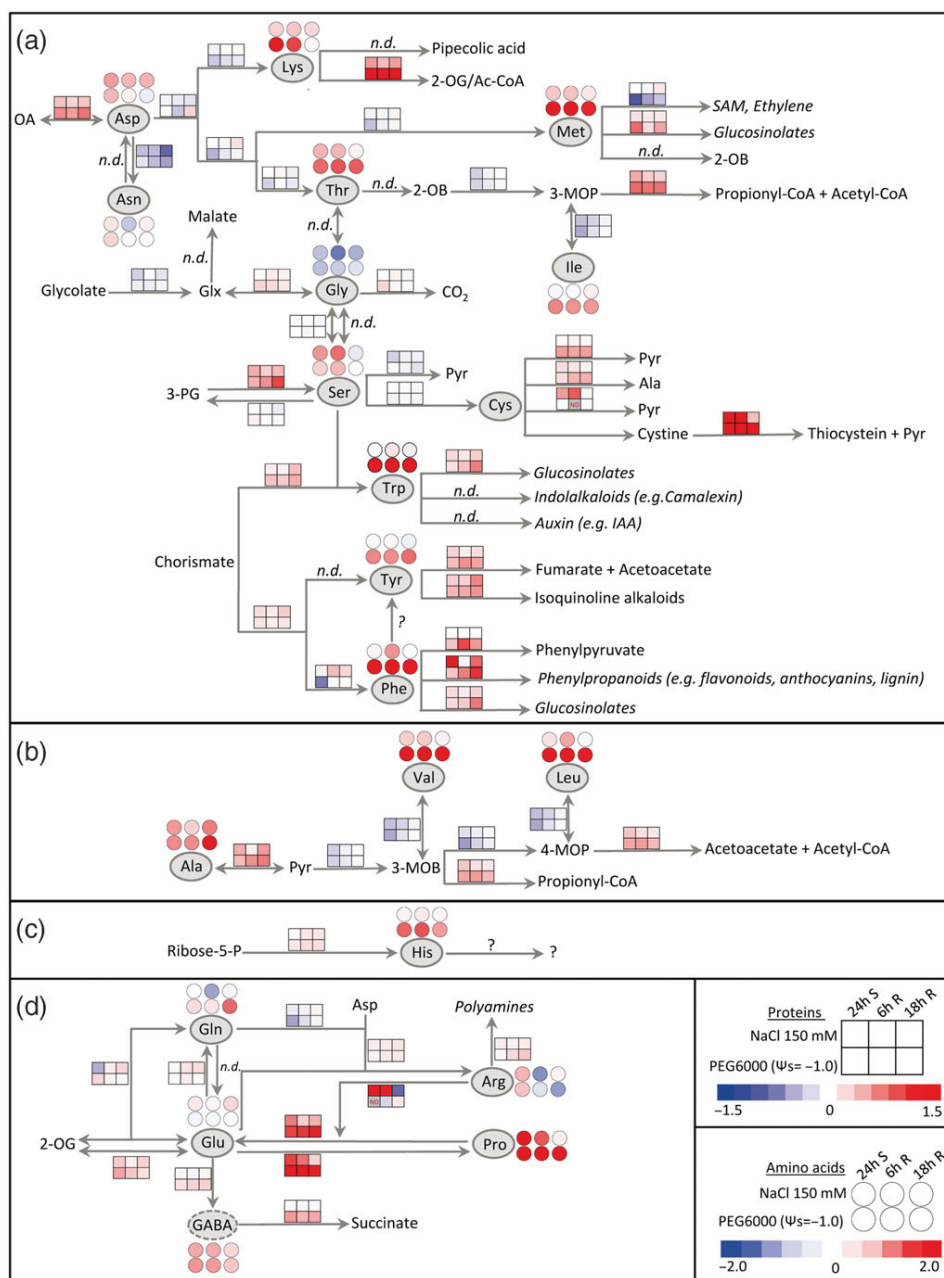


FIGURE 5 Amino acid metabolism during stress and stress release. Log₂-fold changes in amino acid contents (heatmap circles) and abundances of enzymes involved in amino acid metabolism (heatmap squares). Red colours: increased with respect to the control fraction. Blue colours: decreased with respect to the control fraction. All values are means from four biological replicates. The complete amino acid profile including statistical analysis can be found in Table S3. Log₂-fold changes in the abundance of currently known enzymes involved in amino acid synthesis and degradation pathways as well as of the enzymes catalysing committed steps leading to the synthesis of amino acid derived secondary metabolites were extracted from the proteomics dataset (Table S1). The coloured squares represent the means of all changes in the abundance of enzymes involved in the respective branch of the pathway. Arrows leading to amino acids represent the synthesis pathways, arrows pointing away from the amino acid show catabolic reactions, and metabolites that can be interconverted by a single set of enzymes are connected by arrows pointing in both directions. Pathways and metabolites marked by a question mark are presently unknown. The complete enzyme list including the proteomics results as well as the position of each enzyme within the pathway scheme is shown in Table S4 and Figure S3. 2-OB: 2-oxobutyrate; 2-OG: 2-oxoglutarate; 3-MOB: 3-methyl-2-oxobutanoate; 3-MOP: 3-methyl-2-oxopentanoate; 3-PG: 3-phosphoglycerate; 4-MOP: 4-methyl-2-oxopentanoate; GABA: γ -aminobutyric acid; Glx: glyoxylate; IAA: indole-3-acetic acid; n.d.: not detected; OA: oxaloacetic acid; Pyr: pyruvate; SAM: S-adenosyl methionine [Colour figure can be viewed at wileyonlinelibrary.com]

degradation of the photosystems proteins might be associated with a high frequency of photo-oxidative damage. Ribosomal proteins are highly abundant and thus sequester a large amount of the cell's resources. In addition, protein synthesis consumes a considerable

fraction of the cells' ATP and precursor supply. Consequently, cells react to various stresses by translation arrest to release energy and resources for stress responses (Cebollero, Reggiori, & Kraft, 2012). Selective degradation of ribosomes (ribophagy) under nutrient

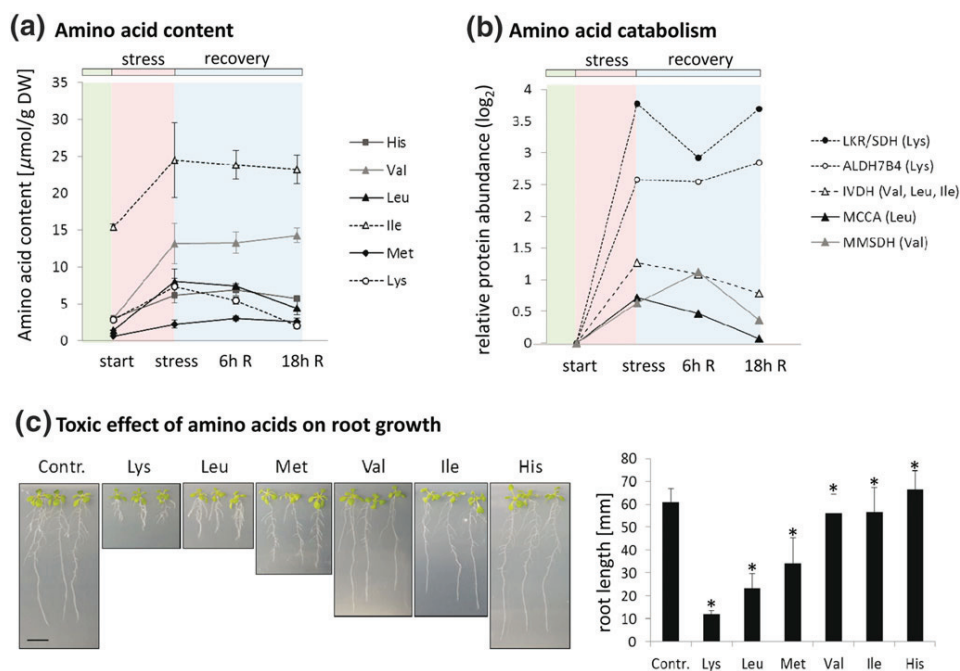


FIGURE 6 Rapid degradation of toxic amino acids during PEG stress and stress release. (a) Leaf contents ($\mu\text{mol g DW}^{-1}$) of low abundant amino acids during PEG stress and recovery. Please note that lines have been added for eye guidance only. (b) Relative abundance (\log_2 treatment/control) of enzymes involved in the degradation of low abundant amino acids during stress and recovery. LKR/SDH: lysine-ketoglutarate reductase/saccharopine dehydrogenase bifunctional enzyme (AT4G33150, Lys catabolism); ALDH7B4: aldehyde dehydrogenase 7B4 (AT1G54100, Lys catabolism); IVDH: isovalery-CoA carboxylase alpha chain (AT3G45300, BCAA degradation); MCCA: methylcrotonyl-CoA carboxylase alpha chain (AT1G03090, Leucine degradation); MMSD4: methylmalonate semialdehyde dehydrogenase (AT2G14170, valine degradation). Lines are for eye guidance only. (c) Root toxicity test: Arabidopsis plants were grown on vertical agar plates containing no amino acid (control) or 100 μM Lys, Leu, Met, Val, Ile, or His. Scale bar: 1 cm. Mean root lengths were calculated from 40 plants per treatment (see Tables S1–S3 for primary data) [Colour figure can be viewed at wileyonlinelibrary.com]

starvation conditions has been first described in yeast cells (Kraft, Deplazes, Sohrmann, & Peter, 2008) and a similar process has also been proposed for plants (Floyd, Morriss, Macintosh, & Bassham, 2012). Our results indicate that ribosomes are degraded within the first 24 hr of salt stress or low water potential, and control levels are not restored within 18 hr of recovery. As a consequence, protein synthesis might still be limited for a considerable period after the stress has been alleviated potentially affecting the replacement of damaged photosystems and slowing down the complete recovery process.

4.2 | Stress recovery: The significance of amino acid metabolism

In general, the content of free amino acids in plants increases considerably during different abiotic stress conditions. The reason for this accumulation might be different for individual amino acids. Synthesis rates of the amino acid can be up-regulated, degradation down-regulated, and in addition, it can be produced by proteolysis or consumption can be restricted due to a decrease in protein synthesis or secondary metabolite production. Our study provides insight into the direction of metabolism for different proteinogenic amino acids during stress and stress release and their potential function in stress tolerance. The main results are summarized in Figure 7 and are discussed below.

4.2.1 | Pro homeostasis as a balance between synthesis and degradation

The role of Pro as a compatible osmolyte during abiotic stress conditions associated with low water availability has been extensively demonstrated (Liang, Zhang, Natarajan, & Becker, 2013; Szabados & Savaure, 2010). We also observed a strong induction of Pro synthesis after NaCl as well as PEG treatment. Mitochondrial Pro catabolism contributes to ATP production by directly transferring electrons into the respiratory chain and also produces Glu that can be converted into the TCA cycle intermediate 2-oxoglutarate by glutamate dehydrogenase (Schertl & Braun, 2014). This pathway is seemingly relevant for increased drought resistance and can act as a buffer of the cellular redox status (Bhaskara, Yang, & Verslues, 2015; Shinde, Villamor, Lin, Sharma, & Verslues, 2016). Delta-1-pyrroline-5-carboxylate dehydrogenase (P5CDH) is induced by high Pro concentrations most likely to prevent accumulation of the toxic degradation intermediate Δ^1 -pyrroline-5-carboxylate, which might serve as a signalling molecule promoting programmed cell death (Deuschle et al., 2001; Deuschle et al., 2004). The regulation of proline dehydrogenase (ProDH), the initial enzyme of the Pro degradation pathway, seems to be more complex. Expression of the main isoform ProDH1 is strongly induced by Pro, but high salinity or PEG treatment can prevent this induction (Peng, Lu, & Verma, 1996; Sharma & Verslues, 2010). Our proteomics dataset does not include ProDH but demonstrates that P5CDH is already up-regulated on a protein level during stress, which in the

Amino acid	Direction of metabolism		Amino acid profile		Role in stress response
	Stress	Recovery	PEG	NaCl	
Pro	Synthesis + Degradation	Synthesis + Degradation			compatible osmolyte
Ala Gln	Synthesis	Synthesis			nitrogen store
Trp,Phe,Tyr Ser Arg	Synthesis (+ Degradation*)	Synthesis (+ Degradation*)			precursor for secondary metabolites
Leu, Val, Ile, Lys (Thr, Met)	Degradation	Degradation			ATP production, detoxification

FIGURE 7 Schematic summary of amino acid metabolism during osmotic stress and stress release. The dominant direction of amino acid metabolism during stress and recovery, which was similar for PEG and NaCl, is indicated in the red and blue fields. Mean relative protein abundances (treatment vs. control) of all enzymes involved in the synthesis and degradation pathways, respectively, were calculated for each individual amino acid in order to estimate up- or down-regulation of the pathway. Pathways that were on average induced are listed in the figure. Thr and Met are shown in parentheses because catabolic enzymes were not detected in our proteomics dataset and thus increased catabolism can only be postulated on the basis of amino acid contents and down-regulation of the synthesis pathways. The symbol “*” indicates only some of the degradation pathways were induced. The amino acid profiles are summarized by line plots. Red lines indicate the development of amino acid contents during stress treatment and blue lines represent the recovery phase [Colour figure can be viewed at wileyonlinelibrary.com]

presence of sufficient amounts of ProDH could lead to simultaneous synthesis and degradation of Pro and thus waste valuable resources. However, a regulatory protein (DFR1) has been recently identified as able to inhibit mitochondrial Pro degradation during drought stress and freezing by directly interacting with the two catabolic enzymes ProDH and delta-1-pyrroline-5-carboxylate dehydrogenase (Ren et al., 2018). Thus, one possible scenario would be that plants already prepare themselves during stress for rapid removal of Pro in the recovery phase by increasing the amount of catabolic enzymes and at the same time prevent a futile cycle via post-translational regulation.

4.2.2 | Amino acid synthesis for nitrogen storage and secondary metabolite production

The biosynthetic pathways of certain additional amino acids, namely, aromatic amino acids, Ser, Arg, Gln, and Ala were also up-regulated during PEG as well as salt stress and stress release (Figure 7). The content of free Ala and Gln continuously increased in particular during recovery from PEG stress indicating that these amino acids might be used for storage of the amino groups liberated during degradation of other amino acids. This is in line with the consistent induction of aminotransferases, most of which use either Pyr or 2-oxoglutarate as a substrate to produce Ala and Glu. Thus, accumulation of specific amino acids might be associated with storage of precursors for protein synthesis to prepare for rapid recovery of plant metabolism following stress. It seems reasonable to suggest that this situation also occurs in response to less severe stress conditions experienced by most plants at some stage during their life cycle. Interestingly, we observed a transient decrease in the content of nitrogen storage amino acids during early recovery from salt stress and also a reduction in total free amino

acids for both stress conditions analysed. These findings indicate a high demand for nitrogen during initial stress release potentially for increased production of non-protein amino acids or other nitrogen containing metabolites that are not detected in our HPLC approach.

Secondary metabolites of the phenylpropanoid group are synthesized through the shikimate pathway by phenylalanine ammonia lyase (PAL), which is induced by several adverse environmental conditions (Tzin & Galili, 2010). We detected increased amounts of PAL 1 during salt stress and stress release. There was also a consistent induction of trans-cinnamate 4-monooxygenase involved in phenylpropanoid synthesis and tyrosine aminotransferase required for the conversion of Tyr to isoquinoline alkaloids during stress as well as in the following recovery period for both stress conditions used here. Leaf contents of the aromatic amino acids were significantly increased (two to five-fold) after PEG treatment and remained on a high level throughout the recovery period (18 hr). The enzymes involved in aromatic amino acid synthesis were generally induced indicating that during osmotic stress as well as for efficient recovery Phe, Tyr, and Trp have to be produced by de novo synthesis most likely in order to provide sufficient substrates for secondary metabolite production. Our finding that Ser synthesis is also up-regulated during the entire period is in line with a high demand for Ser as a precursor of Trp synthesis. During salt stress, which in general had a less severe effect on amino acid metabolism than PEG treatment, there was no increase in free Phe, Tyr, or Trp indicating that the control steady state levels were sufficient to support secondary metabolite synthesis.

We also observed a significant depletion of free Arg during recovery from low water potential although Arg synthesis was up-regulated. These results indicate that large amounts of Arg might be required for polyamine synthesis and/or an increased production of the gasotransmitter NO particularly during the recovery process. This

hypothesis is in line with the induction of spermidine synthase involved in polyamine metabolism and nitrate reductase 2 producing NO during stress release (Table S1). Polyamines as well as NO have been implicated in salt and drought tolerance (Alcázar et al., 2006, Alcázar et al., 2010; Domingos, Prado, Wong, Gehring, & Feijo, 2015; Krasensky & Jonak, 2012).

4.2.3 | Amino acid degradation for ATP production and detoxification

During senescence but also under stress situations restricting photosynthesis, proteins are degraded into free amino acids before they are remobilized to other parts of the plant or used as alternative substrates for mitochondrial ATP production (Araújo et al., 2011; Hildebrandt, 2018; Huang & Jander, 2017). The in vitro approach used for this study also led to massive stress-induced proteolysis demonstrated by a drop in total protein content after PEG and salt treatment (Figure 2). At the same time, the total content in free amino acids increased. Both effects were more pronounced during PEG than during salt stress. The significant induction of catabolic pathways for the branched-chain amino acids, Lys, and Cys is well in line with their postulated role as an alternative substrate for mitochondrial respiration. The accumulation of these normally low abundant amino acids during PEG treatment is most likely the result of proteolysis because the synthesis pathways were down-regulated. During salt stress, catabolism was obviously fast enough to quantitatively remove surplus amino acids produced by protein degradation because we did not detect significant changes in the content of Val, Leu, Ile, Lys, or Met. A previous study using Arabidopsis plants grown on an artificial substrate also came to the conclusion that drought-induced accumulation of branched-chain amino acids was caused by ABA-regulated protein degradation (Huang & Jander, 2017), and published transcriptome and metabolome datasets reveal a similar trend for other low abundant amino acids (Hildebrandt, 2018). The functional relevance of branched-chain amino acid and Lys catabolism for drought stress tolerance becomes obvious in mutant lines for different enzymatic steps that show early symptoms of wilting, necrosis, and higher rates of water loss during dehydration (Pires et al., 2016).

Our results indicate that there might be a preference for fast degradation of specific amino acids to return to control levels as soon as possible after stress release. Because amino acid degradation rates correlated with their inhibitory effect on root growth, the need for rapid detoxification might be the reason for this finding. In fact, Lys degradation was strongly induced after PEG stress, and it was also the most toxic amino acid. The high efficiency of Lys catabolism has been demonstrated before in different plant species (Stepansky et al., 2006). Because Lys is an essential amino acid for human nutrition that is present in particularly low levels in crop plants, extensive efforts have been made to increase the Lys content in Arabidopsis and different crops such as rice and maize (Wang, Xu, Wang, & Galili, 2017). However, this approach was only moderately successful because plants were able to eliminate additional Lys produced by increased synthesis rates very efficiently, whereas an additional block in Lys catabolism led to growth inhibition and an abnormal seed composition (Galili & Amir, 2013; Karchi, Shaul, & Galili, 1994; Yang et al.,

2018). Manipulation of Lys metabolism also induces changes in photosynthesis and amino acid metabolism similar to the effect of stress treatments observed here (Cavalcanti et al., 2018). Similar drawbacks have been reported from attempts to increase seed contents of Met, which is also essential for human nutrition (Galili & Amir, 2013). A possible reason for the need to strictly regulate the concentrations of specific amino acids might be that they act as a signalling molecule, which has been postulated for Leu (Hannah et al., 2010). In addition, some amino acids are precursors for metabolic signals such as Lys producing N-hydroxy pipecoline and α -amino adipic acid as mediators in pathogen response and Met required for the synthesis of the phytohormone ethylene (Chen et al., 2018; Hartmann et al., 2018; Zeier, 2013). Signals are normally present in low and strictly controlled concentrations, so that a sudden increase will most likely have detrimental effects.

5 | CONCLUSIONS

Our results provide to our knowledge the first combined metabolomic and proteomic analysis of the regulation of amino acid metabolism during stress release in plants. The data obtained here provide evidence for a rapid regulation of both amino acid levels and enzymes that mediate the developmental switch to cope with stress and the likely resumption of growth following stress release. Our analysis reveals that during stress release plants acclimate their entire metabolism involving a proteomic and metabolic response that has to be tightly regulated. Further, combined analysis of mutant and wild type plants will help to elucidate the detailed mechanism involved in the crucial significance of amino acid metabolism in response to biotic and abiotic stress.

ACKNOWLEDGEMENTS

We thank Christa Ruppelt for excellent technical assistance in performing the root toxicity tests. This work was supported by the binational science funding programme "PROBRAL" of the Deutsche Akademische Austauschdienst (DAAD; funds provided by the Bundesministerium für Bildung und Forschung—BMBF) and the Coordenação de Aperfeiçoamento de Pessoal de Nível Superior (CAPES), Refs: Project-ID PROBRAL #423/14. Research fellowships granted by the National Council for Scientific and Technological Development (CNPq-Brazil) to A.N.N. and W.L.A. are gratefully acknowledged.

ORCID

Wagner L. Araújo  <https://orcid.org/0000-0002-4796-2616>

Hans-Peter Braun  <https://orcid.org/0000-0002-4459-9727>

Tatjana M. Hildebrandt  <https://orcid.org/0000-0002-3562-5241>

REFERENCES

- Abrahám, E., Hourton-Cabassa, C., Erdei, L., & Szabados, L. (2010). Methods for determination of proline in plants. *Methods in Molecular Biology*, 639, 317–331. https://doi.org/10.1007/978-1-60761-702-0_20
- Aebi, H. (1984). Catalase in vitro. *Methods in Enzymology*, 105, 121–126. [https://doi.org/10.1016/S0076-6879\(84\)05016-3](https://doi.org/10.1016/S0076-6879(84)05016-3)
- Alcázar, R., Altabella, T., Marco, F., Bortolotti, C., Reymond, M., Koncz, C., ... Tiburcio, A. F. (2010). Polyamines: Molecules with regulatory

- functions in plant abiotic stress tolerance. *Planta*, 231, 1237–1249. <https://doi.org/10.1007/s00425-010-1130-0>
- Alcázar, R., Marco, F., Cuevas, J. C., Patron, M., Ferrando, A., Carrasco, P., ... Altabella, T. (2006). Involvement of polyamines in plant response to abiotic stress. *Biotechnology Letters*, 28, 1867–1876. <https://doi.org/10.1007/s10529-006-9179-3>
- Aleksza, D., Horváth, G. V., Sándor, G., & Szabados, L. (2017). Proline accumulation is regulated by transcription factors associated with phosphate starvation. *Plant Physiology*, 175, 555–567. <https://doi.org/10.1104/pp.17.00791>
- Amir, R. (2010). Current understanding of the factors regulating methionine content in vegetative tissues of higher plants. *Amino Acids*, 39, 917–931. <https://doi.org/10.1007/s00726-010-0482-x>
- Araújo, W. L., Tohge, T., Ishizaki, K., Leaver, C. J., & Fernie, A. R. (2011). Protein degradation—An alternative respiratory substrate for stressed plants. *Trends in Plant Science*, 16, 489–498. <https://doi.org/10.1016/j.tplants.2011.05.008>
- Barnett, N. M., & Naylor, A. W. (1966). Amino acid and protein metabolism in Bermuda grass during water stress. *Plant Physiology*, 41, 1222–1230. <https://doi.org/10.1104/pp.41.7.1222>
- Barros, J. A. S., Cavalcanti, J. H. F., Medeiros, D. B., Nunes-Nesi, A., Avin-Wittenberg, T., Fernie, A. R., & Araújo, W. L. (2017). Autophagy deficiency compromises alternative pathways of respiration following energy deprivation in *Arabidopsis thaliana*. *Plant Physiology*, 175, 62–76. <https://doi.org/10.1104/pp.16.01576>
- Bhaskara, G. B., Yang, T.-H., & Verslues, P. E. (2015). Dynamic proline metabolism: Importance and regulation in water limited environments. *Frontiers in Plant Science*, 6, 484.
- Bradford, M. M. (1976). A rapid and sensitive method for the quantitation of microgram quantities of protein utilizing the principle of protein-dye binding. *Analytical Biochemistry*, 72, 248–254. [https://doi.org/10.1016/0003-2697\(76\)90527-3](https://doi.org/10.1016/0003-2697(76)90527-3)
- Cavalcanti, J. H. F., Kirma, M., Barros, J. A. S., Quinhones, C. G. S., Pereira-Lima, Í. A., Obata, T., ... Araújo, W. L. (2018). An LL-diaminopimelate aminotransferase mutation leads to metabolic shifts and growth inhibition in *Arabidopsis*. *Journal of Experimental Botany*, 69, 5489–5506. <https://doi.org/10.1093/jxb/ery325>
- Cebollero, E., Reggiori, F., & Kraft, C. (2012). Reticulophagy and ribophagy: Regulated degradation of protein production factories. *International Journal of Cell Biology*, 2012, 182834.
- Chaves, M. M. (1991). Effects of water deficits on carbon assimilation. *Journal of Experimental Botany*, 42, 1–16. <https://doi.org/10.1093/jxb/42.1.1>
- Chaves, M. M., Flexas, J., & Pinheiro, C. (2009). Photosynthesis under drought and salt stress: Regulation mechanisms from whole plant to cell. *Annals of Botany*, 103, 551–560. <https://doi.org/10.1093/aob/mcn125>
- Chen, Y.-C., Holmes, E. C., Rajniak, J., Kim, J.-G., Tang, S., Fischer, C. R., ... Sattely, E. S. (2018). N-hydroxy-pipecolic acid is a mobile metabolite that induces systemic disease resistance in *Arabidopsis*. *Proceedings of the National Academy of Sciences of the United States of America*, 115, E4920–E4929. <https://doi.org/10.1073/pnas.1805291115>
- Cox, J., & Mann, M. (2008). MaxQuant enables high peptide identification rates, individualized p.p.b.-range mass accuracies and proteome-wide protein quantification. *Nature Biotechnology*, 26, 1367–1372. <https://doi.org/10.1038/nbt.1511>
- Cross, J. M., von Korff, M., Altmann, T., Bartzetko, L., Sulplice, R., Gibon, Y., ... Stitt, M. (2006). Variation of enzyme activities and metabolite levels in 24 *Arabidopsis* accessions growing in carbon-limited conditions. *Plant Physiology*, 142, 1574–1588. <https://doi.org/10.1104/pp.106.086629>
- Cruz, C. D. (2013). GENES—A software package for analysis in experimental statistics and quantitative genetics. *Acta Scientiarum Agronomy*, 35, 271–276.
- Deuschle, K., Funck, D., Forlani, G., Stransky, H., Biehl, A., Leister, D., ... Frommer, W. B. (2004). The role of Δ^1 -pyrroline-5-carboxylate dehydrogenase in proline degradation. *The Plant Cell*, 16, 3413–3425. <https://doi.org/10.1105/tpc.104.023622>
- Deuschle, K., Funck, D., Hellmann, H., Däschner, K., Binder, S., & Frommer, W. B. (2001). A nuclear gene encoding mitochondrial Δ^1 -pyrroline-5-carboxylate dehydrogenase and its potential role in protection from proline toxicity. *The Plant Journal*, 27, 345–356. <https://doi.org/10.1046/j.1365-313X.2001.01101.x>
- Domingos, P., Prado, A. M., Wong, A., Gehring, C., & Feijo, J. A. (2015). Nitric oxide: A multitasked signaling gas in plants. *Molecular Plant*, 8, 506–520. <https://doi.org/10.1016/j.molp.2014.12.010>
- Draper, S. R. (1972). Amino acid changes associated with low temperature treatment of *Lolium perenne*. *Phytochemistry*, 11, 639–641. [https://doi.org/10.1016/0031-9422\(72\)80025-6](https://doi.org/10.1016/0031-9422(72)80025-6)
- Ferreira Júnior, D. C., Gaion, L. A., Sousa Júnior, G. S., Santos, D. M. M., & Carvalho, R. F. (2018). Drought-induced proline synthesis depends on root-to-shoot communication mediated by light perception. *Acta Physiologiae Plantarum*, 40, 363.
- Floyd, B. E., Morriss, S. C., Macintosh, G. C., & Bassham, D. C. (2012). What to eat: Evidence for selective autophagy in plants. *Journal of Integrative Plant Biology*, 54, 907–920. <https://doi.org/10.1111/j.1744-7909.2012.01178.x>
- Fougère, F., Le Rudulier, D., & Streeter, J. G. (1991). Effects of salt stress on amino acid, organic acid, and carbohydrate composition of roots, bacteroids, and cytosol of alfalfa (*Medicago sativa* L.). *Plant Physiology*, 96, 1228–1236. <https://doi.org/10.1104/pp.96.4.1228>
- Frolov, A., Bilova, T., Paudel, G., Berger, R., Balcke, G. U., Birkemeyer, C., & Wessjohann, L. A. (2017). Early responses of mature *Arabidopsis thaliana* plants to reduced water potential in the agar-based polyethylene glycol infusion drought model. *Journal of Plant Physiology*, 208, 70–83. <https://doi.org/10.1016/j.jplph.2016.09.013>
- Fromm, S., Göing, J., Lorenz, C., Peterhänsel, C., & Braun, H.-P. (2016). Depletion of the “gamma-type carbonic anhydrase-like” subunits of complex I affects central mitochondrial metabolism in *Arabidopsis thaliana*. *Biochimica et Biophysica Acta*, 1857, 60–71. <https://doi.org/10.1016/j.bbabi.2015.10.006>
- Fürst, P., Pollack, L., Graser, T. A., Godel, H., & Stehle, P. (1990). Appraisal of four pre-column derivatization methods for the high-performance liquid chromatographic determination of free amino acids in biological materials. *Journal of Chromatography A*, 499, 557–569. [https://doi.org/10.1016/S0021-9673\(00\)97000-6](https://doi.org/10.1016/S0021-9673(00)97000-6)
- Gallii, G., & Amir, R. (2013). Fortifying plants with the essential amino acids lysine and methionine to improve nutritional quality. *Plant Biotechnology Journal*, 11, 211–222. <https://doi.org/10.1111/pbi.12025>
- Gharibi, S., Tabatabaei, B. E. S., Saeidi, G., & Goli, S. A. H. (2016). Effect of drought stress on total phenolic, lipid peroxidation, and antioxidant activity of *Achillea* species. *Applied Biochemistry and Biotechnology*, 178, 796–809. <https://doi.org/10.1007/s12010-015-1909-3>
- Giannopolitis, C. N., & Ries, S. K. (1977). Superoxide dismutases: I. Occurrence in higher plants. *Plant Physiology*, 59, 309–314. <https://doi.org/10.1104/pp.59.2.309>
- Hannah, M. A., Caldana, C., Steinhauser, D., Balbo, I., Fernie, A. R., & Willmitzer, L. (2010). Combined transcript and metabolite profiling of *Arabidopsis* grown under widely variant growth conditions facilitates the identification of novel metabolite-mediated regulation of gene expression. *Plant Physiology*, 152, 2120–2129. <https://doi.org/10.1104/pp.109.147306>
- Hartmann, M., Zeier, T., Bernsdorff, F., Reichel-Deland, V., Kim, D., Hohmann, M., ... Zeier, J. (2018). Flavin monooxygenase-generated N-hydroxypipecolic acid is a critical element of plant systemic immunity. *Cell*, 173, 456–469.e16. <https://doi.org/10.1016/j.cell.2018.02.049>
- Hildebrandt, T. M. (2018). Synthesis versus degradation: Directions of amino acid metabolism during *Arabidopsis* abiotic stress response. *Plant Molecular Biology*, 98, 121–135. <https://doi.org/10.1007/s11103-018-0767-0>

- Hildebrandt, T. M., Nunes Nesi, A., Araújo, W. L., & Braun, H.-P. (2015). Amino acid catabolism in plants. *Molecular Plant*, 8, 1563–1579. <https://doi.org/10.1016/j.molp.2015.09.005>
- Hirota, T., Izumi, M., Wada, S., Makino, A., & Ishida, H. (2018). Vacuolar protein degradation via autophagy provides substrates to amino acid catabolic pathways as an adaptive response to sugar starvation in *Arabidopsis thaliana*. *Plant and Cell Physiology*, 59, 1363–1376. <https://doi.org/10.1093/pcp/pcy005>
- Huang, T., & Jander, G. (2017). Abscisic acid-regulated protein degradation causes osmotic stress-induced accumulation of branched-chain amino acids in *Arabidopsis thaliana*. *Planta*, 246, 737–747. <https://doi.org/10.1007/s00425-017-2727-3>
- Karchi, H., Shaul, O., & Galili, G. (1994). Lysine synthesis and catabolism are coordinately regulated during tobacco seed development. *Proceedings of the National Academy of Sciences of the United States of America*, 91, 2577–2581. <https://doi.org/10.1073/pnas.91.7.2577>
- Kraft, C., Deplazes, A., Sohrmann, M., & Peter, M. (2008). Mature ribosomes are selectively degraded upon starvation by an autophagy pathway requiring the Ubp3p/Bre5p ubiquitin protease. *Nature Cell Biology*, 10, 602–610. <https://doi.org/10.1038/ncb1723>
- Krasensky, J., & Jonak, C. (2012). Drought, salt, and temperature stress-induced metabolic rearrangements and regulatory networks. *Journal of Experimental Botany*, 63, 1593–1608. <https://doi.org/10.1093/jxb/err460>
- Liang, X., Zhang, L., Natarajan, S. K., & Becker, D. F. (2013). Proline mechanisms of stress survival. *Antioxidants and Redox Signaling*, 19, 998–1011. <https://doi.org/10.1089/ars.2012.5074>
- Lugan, R., Niogret, M.-F., Lepout, L., Guégan, J.-P., Larher, F. R., Savouré, A., ... Bouchereau, A. (2010). Metabolome and water homeostasis analysis of *Thellungiella salsuginea* suggests that dehydration tolerance is a key response to osmotic stress in this halophyte. *The Plant Journal*, 64, 215–229. <https://doi.org/10.1111/j.1365-313X.2010.04323.x>
- Madhava Rao, K. V., Janardhan Reddy, K., & Raghavendra, A. S. (Eds.) (2006). *Physiology and molecular biology of stress tolerance in plants*. Dordrecht: Springer.
- Mahajan, S., & Tuteja, N. (2005). Cold, salinity and drought stresses: An overview. *Archives of Biochemistry and Biophysics*, 444, 139–158. <https://doi.org/10.1016/j.abb.2005.10.018>
- Martinelli, T., Whittaker, A., Boichchio, A., Vazzana, C., Suzuki, A., & Masclaux-Daubresse, C. (2007). Amino acid pattern and glutamate metabolism during dehydration stress in the 'resurrection' plant *Sporobolus stapfianus*: A comparison between desiccation-sensitive and desiccation-tolerant leaves. *Journal of Experimental Botany*, 58, 3037–3046. <https://doi.org/10.1093/jxb/erm161>
- Munns, R., James, R. A., & Läuchli, A. (2006). Approaches to increasing the salt tolerance of wheat and other cereals. *Journal of Experimental Botany*, 57, 1025–1043. <https://doi.org/10.1093/jxb/erj100>
- Murashige, T., & Skoog, F. (1962). A revised medium for rapid growth and bio assays with tobacco tissue cultures. *Physiologia Plantarum*, 15, 473–497. <https://doi.org/10.1111/j.1399-3054.1962.tb08052.x>
- Nakano, Y., & Asada, K. (1981). Hydrogen peroxide is scavenged by ascorbate-specific peroxidase in spinach chloroplasts. *Plant and Cell Physiology*, 22, 867–880.
- Peng, Z., Lu, Q., & Verma, D. P. S. (1996). Reciprocal regulation of Δ^1 -pyrroline-5-carboxylate synthetase and proline dehydrogenase genes controls proline levels during and after osmotic stress in plants. *Molecular Genetics and Genomics*, 253, 334–341.
- Perez-Alfocea, F., Estan, M. T., Caro, M., & Guerrier, G. (1993). Osmotic adjustment in *Lycopersicon esculentum* and *L. pennellii* under NaCl and polyethylene glycol 6000 iso-osmotic stresses. *Physiologia Plantarum*, 87, 493–498. <https://doi.org/10.1111/j.1399-3054.1993.tb02498.x>
- Pires, M. V., Pereira Júnior, A. A., Medeiros, D. B., Daloso, D. M., Pham, P. A., Barros, K. A., ... Fernie, A. R. (2016). The influence of alternative pathways of respiration that utilize branched-chain amino acids following water shortage in *Arabidopsis*. *Plant, Cell and Environment*, 39, 1304–1319. <https://doi.org/10.1111/pce.12682>
- Porra, R. J., Thompson, W. A., & Kriedemann, P. E. (1989). Determination of accurate extinction coefficients and simultaneous equations for assaying chlorophylls a and b extracted with four different solvents: Verification of the concentration of chlorophyll standards by atomic absorption spectroscopy. *Biochimica et Biophysica Acta*, 975, 384–394. [https://doi.org/10.1016/S0005-2728\(89\)80347-0](https://doi.org/10.1016/S0005-2728(89)80347-0)
- Ranieri, A., Bernardi, R., Lanese, P., & Soldatini, G. F. (1989). Changes in free amino acid content and protein pattern of maize seedlings under water stress. *Environmental and Experimental Botany*, 29, 351–357. [https://doi.org/10.1016/0098-8472\(89\)90009-9](https://doi.org/10.1016/0098-8472(89)90009-9)
- Ren, Y., Miao, M., Meng, Y., Cao, J., Fan, T., Yue, J., ... Cao, S. (2018). DFR1-mediated inhibition of proline degradation pathway regulates drought and freezing tolerance in *Arabidopsis*. *Cell Reports*, 23, 3960–3974. <https://doi.org/10.1016/j.celrep.2018.04.011>
- Schaedle, M., & Bassham, J. A. (1977). Chloroplast glutathione reductase. *Plant Physiology*, 59, 1011–1012. <https://doi.org/10.1104/pp.59.5.1011>
- Scherlt, P., & Braun, H.-P. (2014). Respiratory electron transfer pathways in plant mitochondria. *Frontiers in Plant Science*, 5, 163.
- Schlesier, B., Bréton, F., & Mock, H.-P. (2003). A hydroponic culture system for growing *Arabidopsis thaliana* plantlets under sterile conditions. *Plant Molecular Biology Reporter*, 21, 449–456. <https://doi.org/10.1007/BF02772594>
- Sharma, S., & Verslues, P. E. (2010). Mechanisms independent of abscisic acid (ABA) or proline feedback have a predominant role in transcriptional regulation of proline mechanism during low water potential and stress recovery. *Plant, Cell and Environment*, 33, 1838–1851. <https://doi.org/10.1111/j.1365-3040.2010.02188.x>
- Shinde, S., Villamor, J. G., Lin, W., Sharma, S., & Verslues, P. E. (2016). Proline coordination with fatty acid synthesis and redox metabolism of chloroplast and mitochondria. *Plant Physiology*, 172, 1074–1088. <https://doi.org/10.1104/pp.16.01097>
- Showler, A. T. (2002). Effects of water deficit stress, shade, weed competition, and kaolin particle film on selected foliar free amino acid accumulations in cotton, *Gossypium hirsutum* (L.). *Journal of Chemical Ecology*, 28, 631–651. <https://doi.org/10.1023/A:1014556515489>
- Stepansky, A., Less, H., Angelovici, R., Aharon, R., Zhu, X., & Galili, G. (2006). Lysine catabolism, an effective versatile regulator of lysine level in plants. *Amino Acids*, 30, 121–125. <https://doi.org/10.1007/s00726-005-0246-1>
- Szabados, L., & Savouré, A. (2010). Proline: A multifunctional amino acid. *Trends in Plant Science*, 15, 89–97. <https://doi.org/10.1016/j.tplants.2009.11.009>
- Thal, B., Braun, H.-P., & Eubel, H. (2018). Proteomic analysis dissects the impact of nodulation and biological nitrogen fixation on *Vicia faba* root nodule physiology. *Plant Molecular Biology*, 97, 233–251. <https://doi.org/10.1007/s11103-018-0736-7>
- Thimm, O., Bläsing, O., Gibon, Y., Nagel, A., Meyer, S., Krüger, P., ... Stitt, M. (2004). MAPMAN: A user-driven tool to display genomics data sets onto diagrams of metabolic pathways and other biological processes. *The Plant Journal*, 37, 914–939. <https://doi.org/10.1111/j.1365-313X.2004.02016.x>
- Tyanova, S., Temu, T., Sinitcyn, P., Carlson, A., Hein, M. Y., Geiger, T., ... Cox, J. (2016). The Perseus computational platform for comprehensive analysis of (prote)omics data. *Nature Methods*, 13, 731–740. <https://doi.org/10.1038/nmeth.3901>
- Tzin, V., & Galili, G. (2010). New insights into the shikimate and aromatic amino acids biosynthesis pathways in plants. *Molecular Plant*, 3, 956–972. <https://doi.org/10.1093/mp/ssq048>
- van der Weele, C. M., Spollen, W. G., Sharp, R. E., & Baskin, T. I. (2000). Growth of *Arabidopsis thaliana* seedlings under water deficit studied by control of water potential in nutrient-agar media. *Journal of Experimental Botany*, 51, 1555–1562. <https://doi.org/10.1093/jexbot/51.350.1555>
- Verslues, P. E., Agarwal, M., Katiyar-Agarwal, S., Zhu, J., & Zhu, J.-K. (2006). Methods and concepts in quantifying resistance to drought, salt and

- freezing, abiotic stresses that affect plant water status. *The Plant Journal*, 45, 523–539. <https://doi.org/10.1111/j.1365-313X.2005.02593.x>
- Verslues, P. E., & Sharma, S. (2010). Proline metabolism and its implications for plant-environment interaction. *Arabidopsis Book*, 8, e0140. <https://doi.org/10.1199/tab.0140>
- Wang, G., Xu, M., Wang, W., & Galili, G. (2017). Fortifying horticultural crops with essential amino acids: A review. *International Journal of Molecular Sciences*, 18, 1306. <https://doi.org/10.3390/ijms18061306>
- Yang, Q.-Q., Zhao, D.-S., Zhang, C.-Q., Wu, H.-Y., Li, Q.-F., Gu, M.-H., ... Liu, Q.-Q. (2018). A connection between lysine and serotonin metabolism in rice endosperm. *Plant Physiology*, 176, 1965–1980. <https://doi.org/10.1104/pp.17.01283>
- Zeier, J. (2013). New insights into the regulation of plant immunity by amino acid metabolic pathways. *Plant, Cell and Environment*, 36, 2085–2103. <https://doi.org/10.1111/pce.12122>

SUPPORTING INFORMATION

Additional supporting information may be found online in the Supporting Information section at the end of the article.

Figure S1. Principal component analysis of stress parameters.

Figure S2. In situ detection of H₂O₂ by DAB staining and O₂⁻ by NBT staining.

Figure S3. Scheme of all currently known reaction steps involved in amino acid synthesis and degradation pathways as well as of the enzymes catalyzing committed steps leading to the synthesis of amino acid derived secondary metabolites.

Table S1. Shotgun proteomics dataset of shoots harvested before stress treatment, after 24h of control, NaCl (150 mM) or PEG (291 g L⁻¹) stress, and after 6h and 18h of recovery.

Table S2. Amino acid contents in control samples of Arabidopsis seedlings.

Table S3. Amino acids profile of Arabidopsis seedlings during stress and recovery.

Table S4. Complete list of Arabidopsis enzymes involved in amino acid metabolism including the shotgun-MS dataset.

How to cite this article: Batista-Silva W, Heinemann B, Rugen N, et al. The role of amino acid metabolism during abiotic stress release. *Plant Cell Environ*. 2019;1–15. <https://doi.org/10.1111/pce.13518>

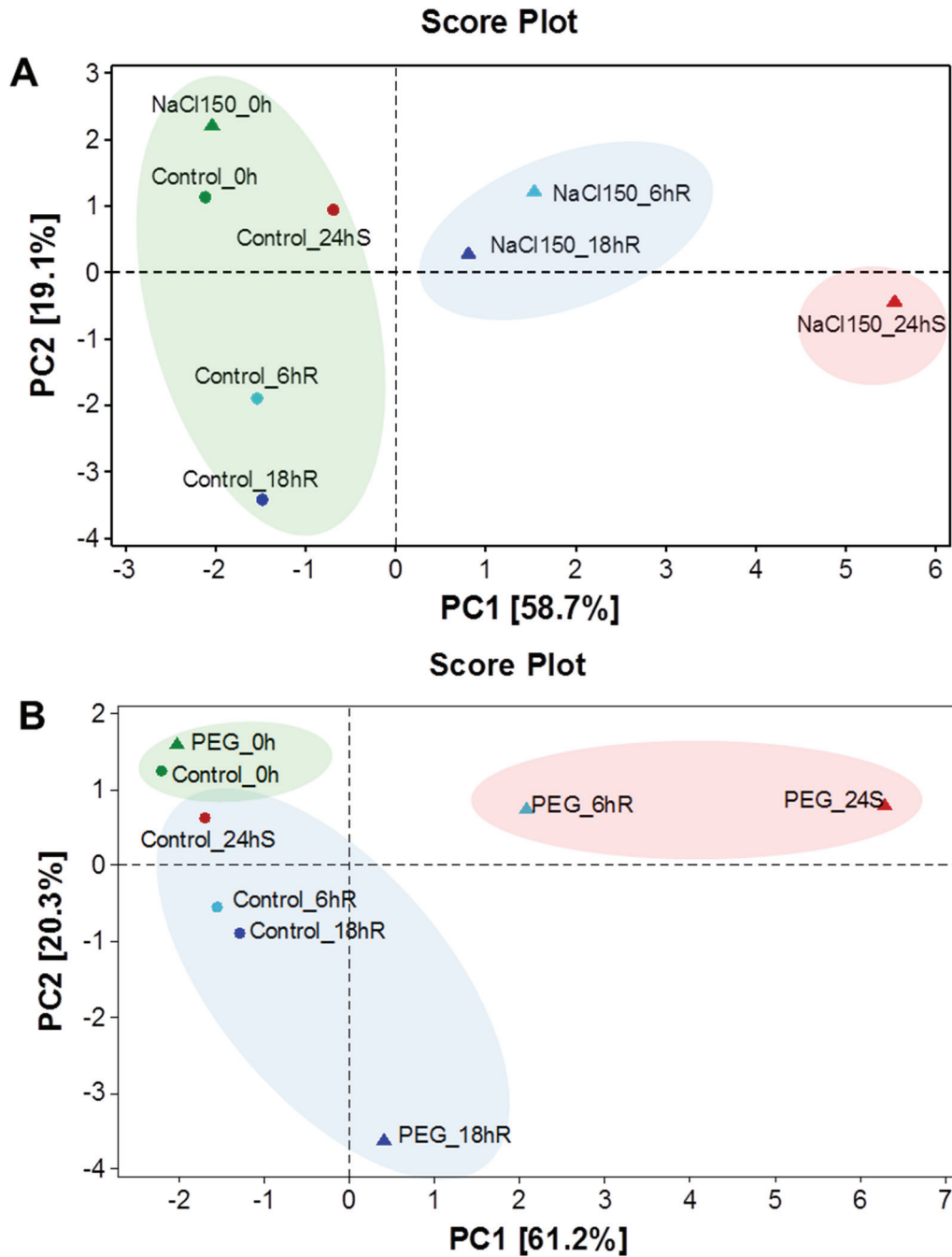


Figure S1: Principal component analysis (PCA) of stress parameters. The score plots of *A. thaliana* under different osmotic stress as Control (circle), NaCl (square) and PEG (triangle) during stress and recovery phase 0h (green), 24h stress (red), 6h recovery (light blue) and 18h recovery (dark blue) are shown individually for both NaCl (A) and PEG (B). The large circles represent the three clusters formed by the Euclidean distance method. The analysis was performed by Minitab Statistical Software version 17 using the average of the each variable shown in Figure 2.

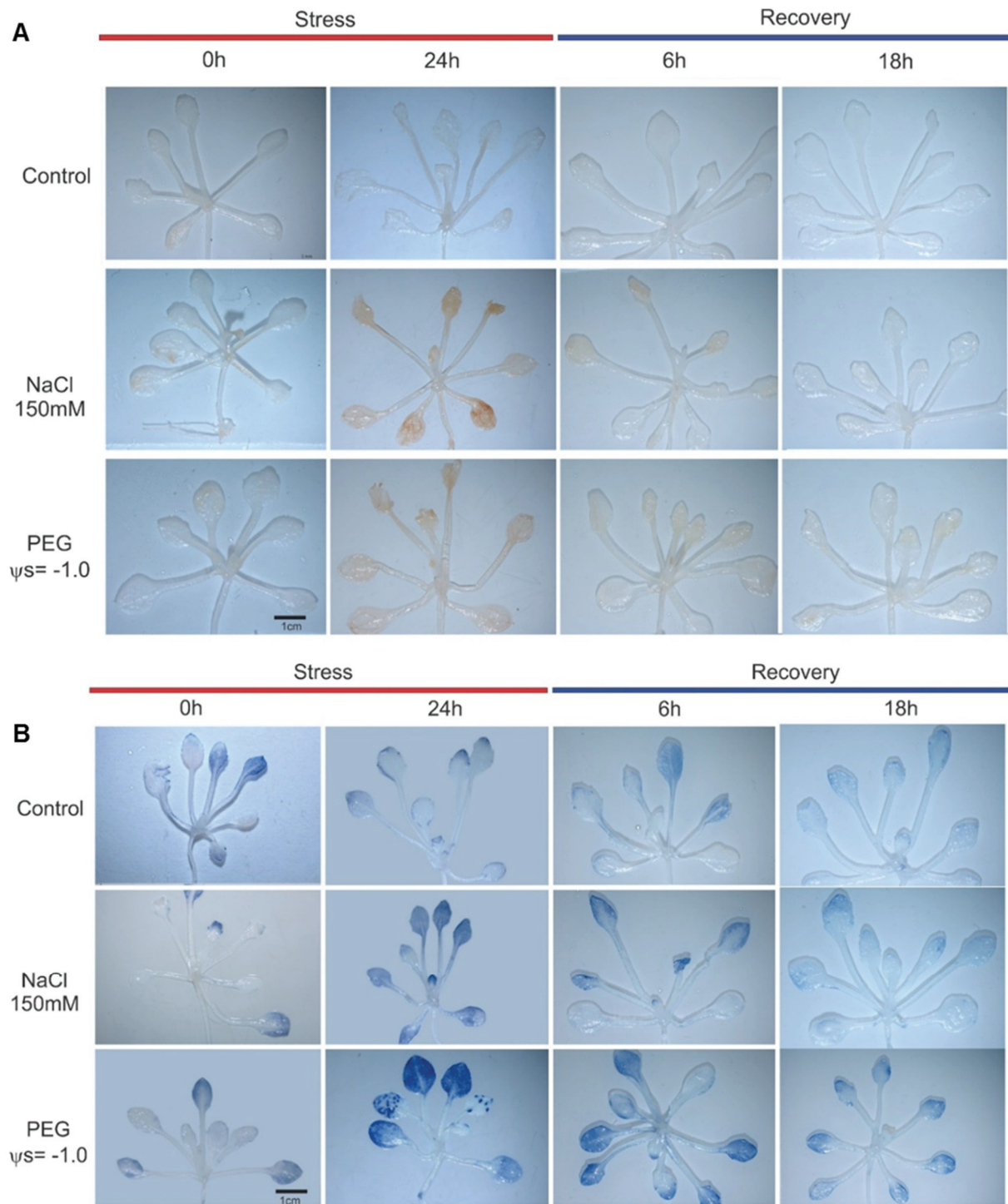


Figure S2: In situ detection of H_2O_2 by DAB staining (A) and O_2^- by NBT staining (B). Plants were grown under control conditions for 14 days, treated with 150 mM NaCl or PEG ($\psi_s = -1.0$) for 24h and then transferred to the recovery solution.

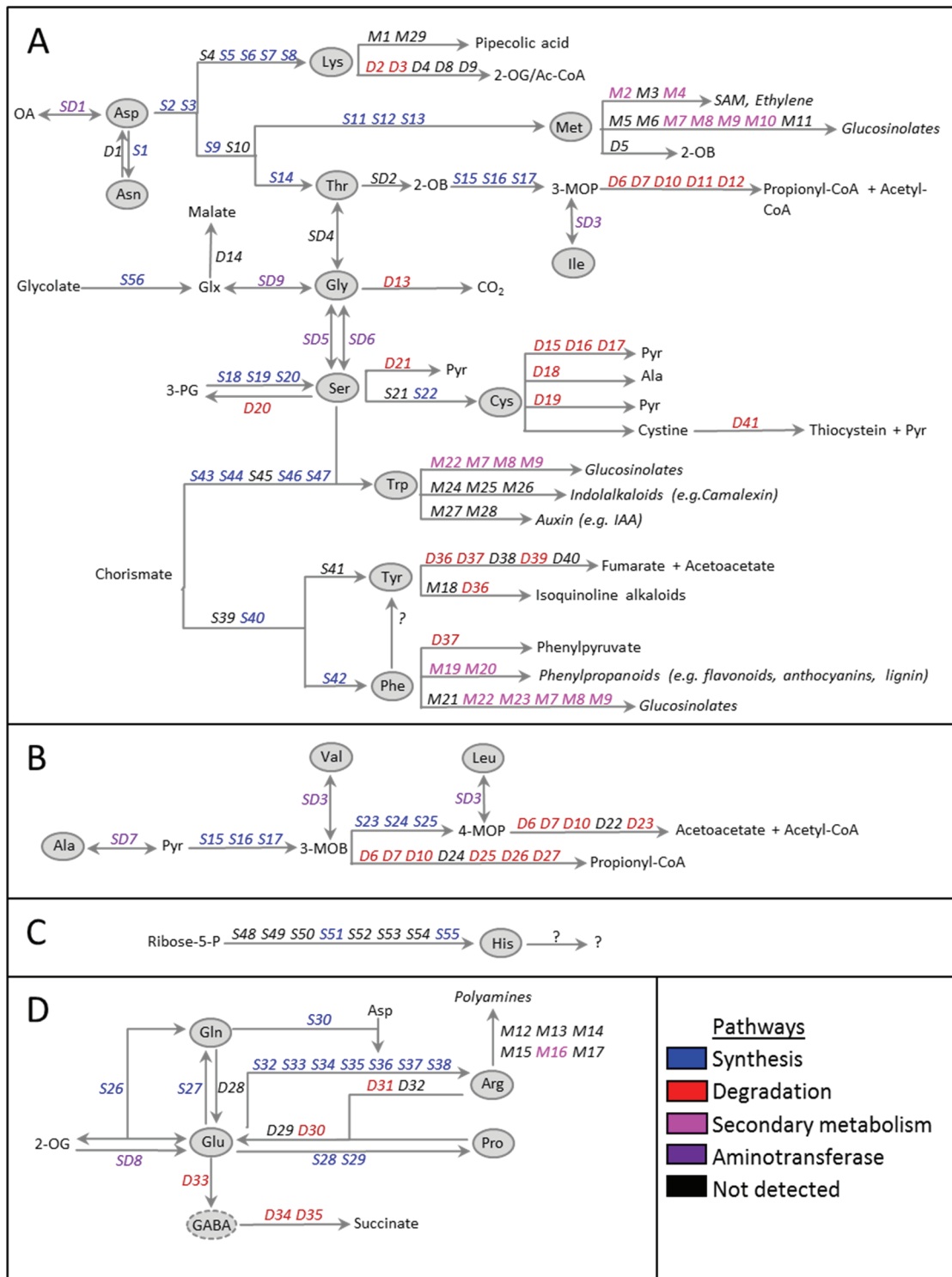


Figure S3: Scheme of all currently known reaction steps involved in amino acid synthesis and degradation pathways as well as of the enzymes catalyzing committed steps leading to the synthesis of amino acid derived secondary metabolites (shown in italics). Arrows leading to amino acids represent the synthesis pathways (numbers S1-S56), arrows pointing away from the amino acid show catabolic reactions (numbers D1-D41), and metabolites that can be interconverted by a single set of enzymes are connected by arrows pointing in both directions (numbers SD1-SD9). Initial steps of secondary metabolite synthesis are numbered M1-M29. Pathways and metabolites marked by a question mark are presently unknown. The complete enzyme list is included in Supplemental Table S4. 2-OB, 2-oxobutyrate; 2-OG, 2-oxoglutarate; 3-MOB, 3-methyl-2-oxobutanoate; 3-MOP, 3-methyl-2-oxopentanoate; 3-PG, 3-phosphoglycerate; 4-MOP, 4-methyl-2-oxopentanoate; GABA, γ -aminobutyric acid; Glx, glyoxylate; IAA, indole-3-acetic acid; OA, oxaloacetic acid; Pyr, pyruvate; SAM, S-adenosyl methionine.

2.2 Estimating the number of protein molecules in a plant cell: protein and amino acid homeostasis during drought

Heinemann, B., Künzler, P., Eubel, H., Braun, H.P., Hildebrandt, T.M.

Institute of Plant Genetics, Leibniz Universität Hannover

Type of authorship:	First author
Type of article:	Research article
Share of the work:	65 %
Contribution to the publication:	Planned and performed all experiments, analyzed data, prepared figures, participated in writing the manuscript
Journal:	Plant Physiology
Impact factor:	6.420 (2019)
Date of publication:	07.12.2020
Number of citations (Google Scholar, 23.06.2021)	1
DOI:	10.1093/plphys/kiaa050
PubMed-ID:	33721903

Estimating the number of protein molecules in a plant cell: protein and amino acid homeostasis during drought

Björn Heinemann,¹ Patrick Künzler,¹ Holger Eubel,¹ Hans-Peter Braun¹ and Tatjana M. Hildebrandt^{1,*†}

¹ Department of Plant Proteomics, Institute of Plant Genetics, Leibniz Universität Hannover, Herrenhäuser Str. 2, 30419 Hannover, Germany

*Address for communication: hildebrandt@genetik.uni-hannover.de

†Senior author.

T.M.H. and H.-P.B. initiated the project. T.M.H. designed the research, wrote the manuscript with support from H.-P.B. and B.H., and agreed to serve as the author responsible for contact and to ensure communication. B.H. performed most experiments. B.H. and P.K. performed the shotgun proteomics experiments. B.H. and H.E. performed the absolute Rubisco quantification. T.M.H. and B.H. analyzed the data.

The author responsible for distribution of materials integral to the findings presented in this article in accordance with the policy described in the Instructions for Authors (<https://academic.oup.com/plphys>) is: Tatjana M. Hildebrandt (hildebrandt@genetik.uni-hannover.de).

Abstract

During drought stress, cellular proteostasis on the one hand and amino acid homeostasis on the other hand are severely challenged, because the decrease in photosynthesis induces massive proteolysis, leading to drastic changes in both the proteome and the free amino acid pool. Thus, we selected progressive drought stress in *Arabidopsis* (*Arabidopsis thaliana*) as a model to investigate on a quantitative level the balance between protein and free amino acid homeostasis. We analyzed the mass composition of the leaf proteome based on proteomics datasets, and estimated how many protein molecules are present in a plant cell and its subcellular compartments. In addition, we calculated stress-induced changes in the distribution of individual amino acids between the free and protein-bound pools. Under control conditions, an average *Arabidopsis* mesophyll cell contains about 25 billion protein molecules, of which 80% are localized in chloroplasts. Severe water deficiency leads to degradation of more than 40% of the leaf protein mass, and thus causes a drastic shift in distribution toward the free amino acid pool. Stress-induced proteolysis of just half of the 340 million RubisCO hexadecamers present in the chloroplasts of a single mesophyll cell doubles the cellular content of free amino acids. A major fraction of the amino acids released from proteins is channeled into synthesis of proline, which is a compatible osmolyte. Complete oxidation of the remaining fraction as an alternative respiratory substrate can fully compensate for the lack of photosynthesis-derived carbohydrates for several hours.

Introduction

Proteostasis (protein homeostasis) is essential for maintaining normal cellular functions, which rely on an appropriate composition as well as correct folding of the proteome. Plant cells contain several thousand different proteins that are highly diverse—not only in terms of their function but also in size and abundance. RubisCO has to be present in

large quantities in leaf cells due to its low enzymatic activity and carbon fixation efficiency, whereas hardly detectable amounts of, e.g. signaling molecules or transcription factors efficiently fulfil their functions. The protein composition of other tissues, such as roots or seeds, again, is completely different (Baerenfaller et al., 2008; Mergner et al., 2020). In addition, 1 mg of a large protein such as glutamate synthase

contains only 4 nmol active sites compared with 83 nmol for the small protein glutaredoxin. Thus, the investment of resources (energy and nutrients) required for the synthesis of large and/or high abundance proteins is by several magnitudes higher than for small proteins of low abundance.

Not surprisingly, cells contain several sophisticated systems to control proteostasis and are able to recycle the resources needed for new growth. Protein synthesis is catalyzed by the ribosomes in the cytosol, plastids, and mitochondria. The synthesis rate is regulated on different levels in response to the energy status of the cell, e.g. via mRNA availability, the GDP and GTP pools, and posttranslational modifications of the ribosome (Merchante et al., 2017). The two major protein recycling systems in eukaryotes are autophagy and the ubiquitin-proteasome system (reviewed by Vierstra, 2009; Dikic, 2017; Marshall and Vierstra, 2018). During autophagy, cytoplasmic constituents, including large protein and nucleic acid aggregates, lipid bodies, and even entire organelles, are sequestered into a double membrane vesicle, the autophagosome, and delivered to the vacuole for breakdown. Thus, autophagy, in addition to proteins, digests nucleic acids, lipids, and carbohydrates. Autophagosome formation is controlled by a highly conserved set of 40 autophagy-related (ATG) proteins. These include receptors that recognize specific cellular components and tether them to the enveloping autophagic membrane to target them for destruction. In contrast, the ubiquitin-proteasome system localized in the cytosol catabolizes proteins individually. Substrates are marked for degradation by a poly ubiquitin tag that enables their recognition and hydrolysis by the proteasome, a large protein complex composed of a 20S catalytic core and two regulatory 19S lids. Several molecules of the 8.5-kDa protein ubiquitin are covalently conjugated to a lysine residue of the target protein by an enzymatic cascade consisting of ubiquitin activating (E1), conjugating (E2), and ligating (E3) enzymes. Substrate specificity is provided by a high number of different E3 ubiquitin ligases (> 1,400 in the Arabidopsis genome). In addition to the bulk degradation systems, plants contain hundreds of individual proteases from several unrelated families. They can be grouped into four major classes according to the nature of the nucleophile used for proteolytic cleavage of the peptide bond. Cysteine and serine proteases use a Cys or Ser activated by His as a nucleophile whereas metalloproteases and aspartic proteases activate water using a metal ion or Asp, respectively (van der Hoorn, 2008). Proteases are present in all the different subcellular compartments. Plastids and mitochondria contain distinctive proteolytic systems from prokaryotic origin such as AAA-class (ATPases associated with diverse cellular activities), Lon, FtsH (filamentation temperature sensitive H), and Clp (caseinolytic protease) proteases (Kwasniak et al., 2012; Nishimura et al., 2016).

The accumulation of non-functional and misfolded proteins would lead to the formation of large protein aggregates that are detrimental to cellular function (McClellan et al., 2005). Thus, damaged proteins are efficiently detected

and eliminated by the two main protein quality control systems, the ubiquitin-proteasome system and autophagy, to avoid proteotoxic stress (Dikic, 2017). Even under steady-state conditions, the turnover rates of individual proteins are highly diverse: a more than 150-fold variation in protein degradation has been reported (Li et al., 2017). The D1 protein localized in the reaction center of photosystem II is replaced on a daily basis since it is frequently damaged by reactive oxygen species as a result of photosynthetic activity. Also, regulatory proteins such as hormone response factors usually have a short half-life to allow rapid responses to a changing environment (Nelson and Millar, 2015). In contrast, ribosomal subunits are among the most stable proteins in Arabidopsis and remain functional for several months (Li et al., 2017). Protein stability is defined by different factors such as the physical location of the protein, interactions with cofactors or other proteins, and post-translational modifications (Nelson and Millar, 2015).

Proteostasis is closely connected to amino acid homeostasis since protein synthesis requires a sufficient supply of loaded t-RNAs whereas proteolysis releases free amino acids. The effect of protein metabolism on the relative contents of free amino acids can be substantial, in particular, for low abundance amino acids such as the sulfur containing, aromatic, and branched chain amino acids (Hildebrandt, 2018). In yeast and animal cells, proteasome inhibition leads to cell death, which is primarily caused not by the accumulation of misfolded proteins, but by a detrimental deficiency in free amino acids (Suraweera et al., 2012). Apart from serving as building blocks for proteins, free amino acids have several additional functions in plant metabolism. They are precursors for the synthesis of secondary metabolites, hormones, and signaling molecules, and also act as transport and storage forms for organic nitrogen (Lam et al., 2003; Alcázar et al., 2006; Tzin and Galili, 2010). During drought and salt stress, Pro and the non-proteinogenic amino acid γ -aminobutyric acid (GABA) function as compatible osmolytes (Krasensky and Jonak, 2012). Proteolysis is increased in response to adverse environmental conditions to provide amino acids as precursors for these defense-related metabolites and also as alternative substrates for ATP production when photosynthetic activity is low (Araújo et al., 2011; Hildebrandt et al., 2015). In this study, we use progressive drought stress in Arabidopsis as a model to investigate the balance between protein and free amino acid homeostasis on a quantitative level. We estimate the molecular as well as the mass protein composition of an average rosette leaf and an individual mesophyll cell. How many protein molecules are present in a plant cell and its subcellular compartments? Which fraction of their leaf proteome do plants degrade maximally under severe drought stress? How is proteostasis controlled under these conditions? Do cells just eat anything when they are really starved or are they still picky? Are the proteins that are essential for stress tolerance synthesized or, rather, spared from degradation? Which proteins contribute

to the free amino acid pool and what happens to the amino acids released during proteolysis?

Results

Quantitative composition of the leaf proteome

As a starting point for investigating protein homeostasis during drought stress, we focused on the proteome of control plants grown under optimal conditions to gain an impression of their status in the absence of stress (Figure 1, A). Intensity-based absolute quantification (iBAQ; Schwanhäusser et al., 2011) was used for calculating the absolute content [$\mu\text{g protein} \cdot \text{g}^{-1}$ dry weight (DW)] of each of the 1,399 different proteins detected by our shotgun-mass spectrometry (MS) approach. The complete MS dataset, as well as detailed information on the calculation methods, can be found in the Supplemental Material (Supplemental Dataset S1, A and Supplemental Figure S1). In order to estimate which mass fraction of the total leaf proteome is covered by our MS dataset, we used labeled peptides for absolute quantification of RubisCO large subunit (Supplemental Dataset S2 and Supplemental Figure S2). This approach revealed that the 1,399 proteins in our dataset represent 82.4% of the leaf protein mass. We included this factor in all calculations to provide the best possible estimation of individual protein contents (Supplemental Dataset S1, B). However, some questions, such as calculating the total number of protein molecules in a cell or the amount of amino acids produced by protein degradation during stress, require making the best possible assumptions about the composition of the 17.6% of the leaf proteome not visible in our proteomics dataset. For these aspects we assumed that the composition of this invisible portion corresponds to the rest of the proteome, and thus used the original dataset as a basis for calculations (Supplemental Dataset S1, A).

The leaf proteome is dominated by a limited number of very high abundance proteins (Figure 1, B). RubisCO alone, which is well known for being one of the most abundant proteins on earth (Bar-On and Milo, 2019), constitutes about one-fifth of the leaf protein mass, corresponding to $21 \text{ mg} \cdot \text{g}^{-1}$ DW under control conditions (Supplemental Dataset S1, B). Another fifth consists of 11 other photosynthesis-related proteins, and in total, about 80% of the leaf protein mass is found in the chloroplasts (Figure 1, C, top; subcellular protein localization predicted by SUBA4, Hooper et al., 2017). Without taking absolute quantities into account, the distribution of the proteins detected by MS on subcellular compartments looks markedly different, with only 37% chloroplast protein species (Figure 1, C, bottom). It also has to be considered that the 18% of protein mass not covered by our MS approach contains a high number of very low abundance proteins. The protein investment of a leaf cell into different functions can be visualized on a PROTEOmap (Figure 1, D; Liebermeister et al., 2014). Under control conditions, the major part of the leaf protein mass (66%) is dedicated to photosynthesis, followed by protein

metabolism (7.5%) and amino acid metabolism (6%; the relative values [%] for all pathways shown are listed in Supplemental Dataset S3).

Estimating protein copy numbers in a plant cell

We used two different approaches to estimate how many protein molecules are actually present in a plant cell, based on cell number and cell size, respectively (Supplemental Figure S1). We selected mesophyll cells as the representative leaf cell for this estimation, since they are photosynthetically active and constitute the major part of the leaf volume. Total protein copy numbers have already been reported for yeast cells and different animal cell lines. A haploid cell of budding yeast (*Saccharomyces cerevisiae*) has a volume of $42 \mu\text{m}^3$ (Jorgensen et al., 2002) and contains about 42 million proteins (Ho et al., 2018), whereas for human cells with a volume of about $4,200 \mu\text{m}^3$, three billion protein molecules have been calculated (Kulak et al., 2014). Thus, yeast and human cells contain 1.0 and 0.7 million proteins per μm^3 , respectively. An average mature leaf cell has a volume of approximately $150,000 \mu\text{m}^3$ (Supplemental Figure S1). Assuming an average protein abundance of 0.85×10^6 molecules per μm^3 and subtracting the volume of the central vacuole that typically covers about 80% of a plant cell we postulate that a leaf mesophyll cell contains close to 25 billion proteins (Table 1 and Supplemental Figure S1).

An alternative, completely independent way to calculate protein copy numbers is based on an average number of 300,000 mesophyll cells (Wuyts et al., 2010) in a mature rosette leaf of 5 mg DW with a protein content of $102 \text{ mg} \cdot \text{g}^{-1}$ DW. A total of 1.7-ng protein per cell would add up to 20.5 billion protein molecules with an average molecular weight of 50 kDa. Quantitative proteomics, irrespective of its intrinsic limitations, makes it possible to deduce a more precise estimate of 25.8 billion proteins per cell. In addition, this approach provides information about the copy numbers of individual proteins (Figure 1, E, Table 1, and Supplemental Dataset S1, B). It has to be kept in mind that these results are estimations based on the average characteristics of an Arabidopsis mesophyll cell combined with the proteome composition of total rosette leaf material, and thus cannot be regarded as exact, statistically firm numbers. Clearly, the largest share of the protein molecules in a mesophyll cell (~ 20 billion) are located in the chloroplasts, 3.2 billion in the cytosol, and 0.5 billion in the mitochondria. Copy numbers range from 3.2 billion molecules of RubisCO large subunit to 2,039 acetyl-CoA carboxylase 1 molecules, which is the detection limit of our MS approach. Thus, an average Arabidopsis leaf mesophyll cell contains about 340 million RubisCO hexadecamers under optimal growth conditions.

Severe drought stress leads to a massive decrease in leaf protein content

We carefully established an experimental setup that mimicked physiological drought stress conditions as closely as possible and at the same time led to a highly reproducible

Table 1 Total number of protein molecules in an average Arabidopsis leaf mesophyll cell and its subcellular compartments under control conditions (C) and during progressive drought stress (S3, moderate stress; S5, severe stress; and S6, maximum tolerable stress)

Subcellular compartment	Protein numbers ($\times 10^6$)			
	C	S3	S5	S6
Number of proteins in a mesophyll cell	25,766	24,309	15,262	15,337
Number of proteins in all chloroplasts (~100) in a cell	20,208	18,984	11,603	11,468
Number of RubisCO LS (AtCg00490) per cell	3,191	3,393	2,024	1,724
Number of proteins in an individual chloroplast	202	190	116	115
Number of RubisCO LS (AtCg00490) per chloroplast	32	34	20	17
Number of proteins in all mitochondria (~400) in a cell	495	480	385	407
Number of serine hydroxymethyltransferase 1 (At4g37930) per cell	54	42	26	24
Number of proteins in an individual mitochondrion	1.2	1.2	1.0	1.0
Number of serine hydroxymethyltransferase 1 (At4g37930) per mito.	0.14	0.11	0.06	0.06
Number of proteins in the cytosol per cell	2,782	2,575	1,602	1,696
Number of GTP binding EF Tu (At5g60390) per cell	116	108	62	69
Number of proteins in the vacuole	526	443	326	310
Number of tonoplast intrinsic protein 2 (At3g26520) per cell	161	122	92	75
Number of proteins in the extracellular space per cell	285	313	287	338
Number of germin-like protein 1 (At1g72610)	89	50	38	37
Number of proteins per nucleus	160	206	93	131
Number of ubiquitin 5 (At3g62250) per nucleus	31	41	18	18
Number of proteins in all peroxisomes of a cell	614	650	498	533
Number of Aldolase-type TIM barrel protein (At3g14415) per cell	68	57	27	26
Number of proteins in the endoplasmic reticulum per cell	74	70	58	57
Number of ADP-ribosylation factor 1 (At1g70490) per cell	17	12	8	6
Number of proteins in the Golgi apparatus per cell	34	35	23	24
Number of RGP2; UDP-arabinose mutase (At5g15650) per cell	4	5	5	5
Number of proteins in the plasma membrane per cell	183	179	130	104
Number of plasma membrane intrinsic protein 2A (At3g53420)	32	29	17	12

For each compartment, the copy number of the most abundant protein is listed individually. All numbers are based on estimations as discussed in the text (see also Supplemental Figure S1). The total number of proteins in a cell/subcellular compartment is highlighted in bold.

stress phenotype (Figure 2, a detailed description of the drought treatment is given in the “Materials and methods” section). In brief, plants were grown under long-day control conditions for 2 weeks and watered to the same level. The dehydration process was then monitored on a daily basis and leaf samples were taken at different time points during the desiccation process from beginning to moderate and severe drought stress until recovery was no longer possible. Rosette growth gradually declined and stopped after 10 d without water (Figure 2, C). We defined this time point as stress level S1 and numbered the following days of progressive drought stress consecutively. First indications of a loss in leaf turgor became visible in some of the plants after 12 d without water (S3) and complete wilting until death occurred within the following 72 h. These late stages of severe drought stress (S4–S7) were classified according to their leaf phenotype: number of rolled leaves, relative water content (RWC), and potential to recover after re-watering. The leaf protein content remained stable ($109 \pm 13 \text{ mg} \cdot \text{g}^{-1}$ DW) during the first 12 d without watering (S1–S3), but then rapidly decreased by 39% within 24 h (S5).

Patterns of stress-induced proteome changes in subcellular compartments

Four stress levels were selected for leaf proteome analysis by shotgun MS (Figure 3, A, Supplemental Dataset S1, and Supplemental Figure S3): control (RWC = $88 \pm 5\%$), S3 (moderate stress, no wilting, RWC = $69 \pm 5\%$), S5 (severe

stress, RWC = $55 \pm 7\%$), and S6 (maximum tolerable stress, RWC = $22 \pm 5\%$). Statistical evaluation of the proteomics dataset based on label-free quantification (LFQ)-values indicates significant changes in the relative abundance of 291, 523, and 517 protein species in relation to the control at stress levels S3, S5, and S6, respectively (Supplemental Dataset S1, columns X-AC). These results are provided in the Supplemental Material and can be used for data mining. However, since the major focus of this study is a quantitative perspective, we will not evaluate significant changes in individual protein levels in detail. To provide a first impression of quantitative changes in the leaf proteome during progressive drought stress, we sorted all detected proteins according to their absolute content under control conditions for each compartment individually. The contents of each individual protein during progressive drought stress were then plotted in superimposing graphs (Figure 3, B). The fraction of proteins degraded in the course of the stress treatment becomes visible as green or orange area. Interestingly, there are clear differences between the compartments. A large fraction of proteins localized in chloroplasts, the cytosol, the plasma membrane, or the Golgi apparatus shows roughly homogenous decrease rates. In contrast, hardly any green areas are visible for mitochondrial and extracellular proteins, indicating a lower degradation rate (Supplemental Figure S4). In order to quantify this observation, we calculated fold change ratios of individual protein contents in stressed versus control plants using

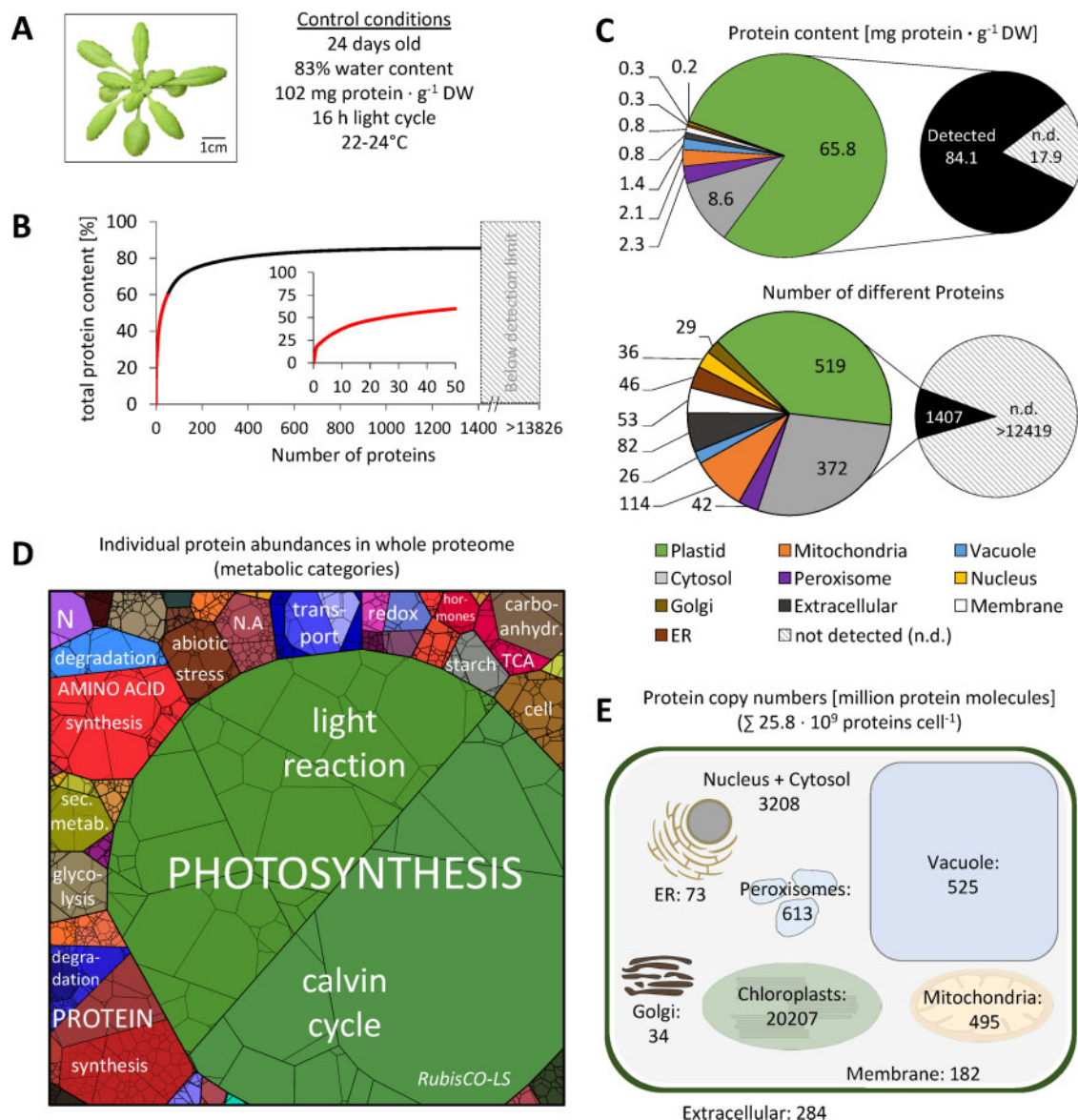


Figure 1 Quantitative composition of the Arabidopsis leaf proteome. (A) Phenotype of a representative control plant used for MS analysis (the rosette was digitally extracted from the soil background). (B) Fraction of total protein content contributed by each of the 1,399 proteins detected by shotgun proteomics. Proteins were sorted according to their absolute content in descending order and added up. The 50 most abundant proteins (red graph) are shown in the inset (the axis label is identical to the main graph). (C) Distribution of the proteins detected in control samples in the different subcellular compartments according to SUBA4 prediction (Hooper et al., 2017). Protein content (sum of all individual protein contents calculated from iBAQs) versus number of different protein species per subcellular compartment. Hatched areas in B and C indicate the protein mass and estimated number of protein groups not detectable by our MS approach. The invisible mass fraction has been calculated on the basis of labeled peptides (Supplemental Figure S2 and Supplemental Dataset S2); the estimated number of leaf protein groups is taken from Mergner et al. (2020). (D) Proteomap illustrating the quantitative composition of the leaf proteome under control conditions. Proteins are shown as polygons whose sizes represent the mass fractions (protein abundances obtained by MS [iBAQ], multiplied with protein molecular weight). Proteins involved in similar cellular functions according to the MapMan annotation file (version Ath_AGI_LOCUS_TAIR10_Aug2012, Thimm et al., 2004) are arranged in adjacent locations and visualized by colors. Mass fractions of the functional categories [%] are provided in Supplemental Dataset S3. (E) Number of protein molecules [million proteins] present in the subcellular compartments of an average Arabidopsis mesophyll cell. Copy numbers represent the sum of protein molecules present in all chloroplasts (ca. 100 per cell; Königler et al., 2008), mitochondria (300–450 per cell; Preuten et al., 2010), or peroxisomes in the cell. Copy numbers for all individual proteins detected in our MS approach are given in Supplemental Dataset S1. Only proteins with unambiguous assignments are shown. N.A., not annotated; N, nitrogen metabolism; LS, large subunit.

the iBAQ-based protein contents shown in Figure 3, B, and sorted them in ascending order for each stress level individually (Figure 3, D and E and Supplemental Figure S5). The total leaf protein content decreased to 94% of control

values at stress level S3, to 61% at S5, and to 58% at S6 (Figure 3, C). Therefore, individual proteins with an average decrease rate during stress are localized at approximately 0.94, 0.61, and 0.58 (marked by vertical green, yellow, and

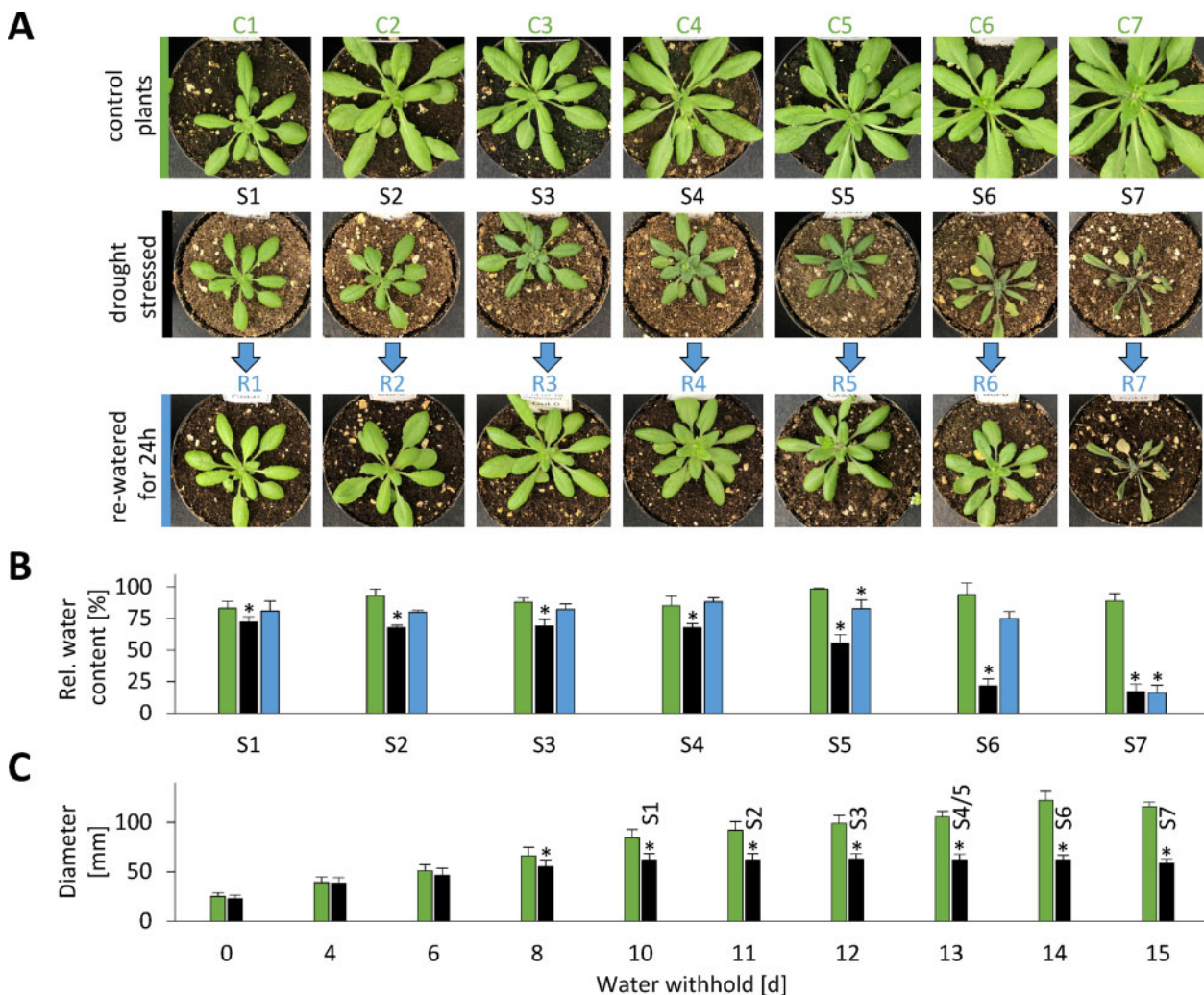


Figure 2 Complete setup of the progressive drought stress experiment. Arabidopsis plants were grown in soil under long-day conditions for 2 weeks. All pots were then brought to the same weight and the stress group was not watered for up to 15 d while the control group was kept at a constant water level. Leaf samples were first collected after 10 d without water (stress level S1) and continued each following day until recovery of the plants was no longer possible (stress level S7). (A) Phenotype of representative plants (pot diameter = 8 cm). (B) RWC (%) in rosette leaves of control plants (green bars), stressed plants (black bars), and stressed plants 24 h after re-watering (blue bars) at the different stress levels. (C) Rosette diameter [mm] of control plants (green bars) and stressed plants (black bars) at 0–15 d after the beginning of the stress treatment. The corresponding stress levels of the plants are indicated on top of the black bars. A detailed description of the drought treatment is given in the “Materials and methods” section. Values are means \pm SD of the biological replicates. S1–S7, $n = 7$; C1–C7, $n = 3$; R1–R7, $n = 3$. Significant differences were determined by Student’s t test $P < 0.01$. Starting material (stress levels) for experimental analyses: S1, 10 d after end of watering; S2, 11 d after end of watering; S3, 12 d after end of watering, first signs of stress (rolled/wrinkled leaves); S4, 13 d after end of watering, 4–7 rolled leaves; S5, ~13 d after end of watering, 8–10 rolled leaves; S6, ~14 d after end of watering, > 10 rolled leaves; recovery of plants still possible; S7, ~15 d after end of watering, > 10 rolled leaves; recovery of plants not possible; C1–C7, control plants (watering continued); R1–R7: same as S1–S7, but re-watered for 24 h.

red lines in Figure 3, D and E). In the complete dataset (Figure 3, D), and in the subsets of plastid and cytosolic proteins (Figure 3, E), there is a large area with almost horizontal graphs representing proteins with roughly average degradation rates. In contrast, the slopes of the mitochondrial and extracellular graphs are much steeper and only 11–12% of the proteins show average or increased degradation rates in severely stressed plants (Figure 3, E, vertical red lines in the graphs “Mito” and “Apoplast”).

Regulation of protein abundance via synthesis and degradation

Protein abundance can be regulated at the level of synthesis and/or degradation. We used genevestigator (Hruz et al., 2008) to estimate gene expression levels during drought stress and combined this information with the relative protein abundances detected by our proteomics approach (Supplemental Dataset S4). We filtered the proteomics dataset for proteins of consistently increased abundance and divided the resulting list of 332 proteins in two subgroups:

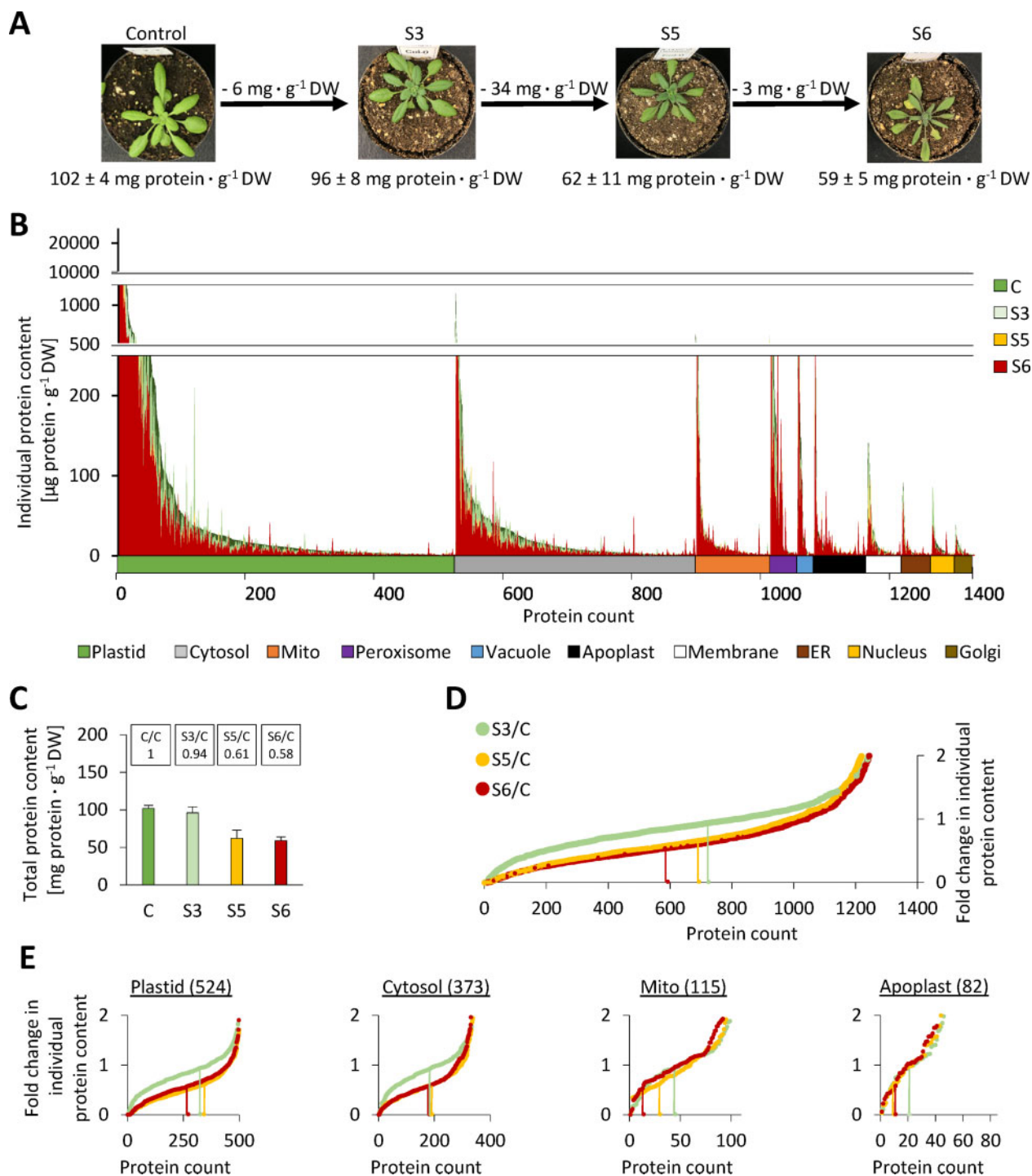


Figure 3 Compartment-specific patterns of stress-induced changes in individual protein abundances. (A) Phenotype and protein content of the plants used for proteome analysis. The representative images are the same as in Figure 2. Complete rosettes of four plants were harvested at the beginning of the stress treatment (parallel to S1–S3) (control), and at three defined stress stages (S3, S5, and S6), respectively. (B) Absolute contents [$\mu\text{g protein} \cdot \text{g}^{-1} \text{ DW}$] of all individual proteins detected by shotgun proteomics in descending order (under control conditions), sorted by subcellular compartments according to SUBA4 prediction (Hooper et al., 2017). Protein contents under control and stress conditions are shown in superimposed graphs. Individual plots for each subcellular compartment are shown in Supplemental Figure S4. (C) Total leaf protein contents [$\text{mg protein} \cdot \text{g}^{-1} \text{ DW}$] at the different stress levels. Values are means \pm SD ($n = 4$). The relative protein contents compared with the control group are indicated at the top. (D) and (E) Fold change ratios of individual protein contents in stressed versus control plants for all proteins (D) and individual subcellular compartments (E). In order to visualize the fraction of proteins with average, high, or low degradation rates, changes in individual protein contents were sorted in ascending order for each stress level. Vertical lines indicate proteins that correspond exactly to the decrease in total protein content, i.e. 0.94 for stress level S3 (light green), 0.61 for S5 (orange), and 0.58 at S6 (red). Changes in individual protein contents were calculated using the absolute protein contents shown in B (Supplemental Dataset S1), and are thus based on iBAQ data. Additional individual plots for subcellular compartments are provided in Supplemental Figure S5.

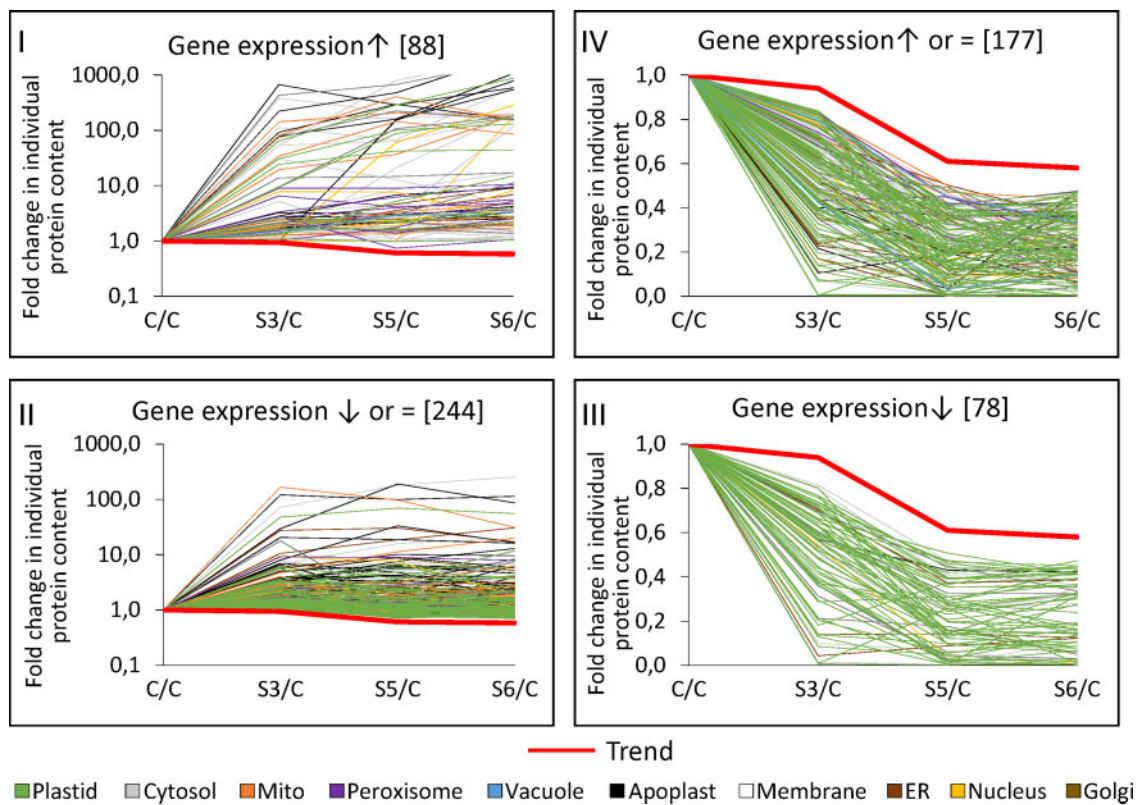


Figure 4 Transcriptional and post-translational regulation of protein abundances during progressive drought stress. Fold change ratios (stress/control) of individual protein contents during progressive drought stress. Red graphs (trend lines) indicate the fold change in total leaf protein content at each stress level (S3/C: 0.94; S5/C: 0.61; S6/C: 0.58). Three microarray datasets available via Genevestigator were used to estimate gene expression levels during drought stress (see the “Materials and methods” section). The proteomics dataset was filtered for proteins that were of increased relative abundance according to both iBAQ-based and LFQ-based data interpretation at each stress level (more details on the filter criteria are provided in [Supplemental Dataset S4](#)). These proteins of increased abundance (left part of the figure) were divided into two groups: proteins with increased gene expression levels according to the microarray datasets (group I) and proteins with unaffected or decreased expression levels during drought stress (group II). Proteins of consistently decreased abundance (right part of the figure) were also filtered for decreased (group III) and increased or unaffected expression levels (group IV). Colors indicate the subcellular localization of the individual proteins according to SUBA4 prediction ([Hooper et al., 2017](#)). Enrichment of compartments and functional categories in the different regulation groups is listed in [Table 2](#).

Group I contained the proteins with significantly increased expression levels (88 proteins) and group II contained proteins with decreased or unaffected expression levels (244 proteins), indicating that regulation might rather be achieved at a posttranscriptional level, e.g. via decreased proteolysis ([Figure 4](#)). In order to determine the metabolic pathways preferentially regulated by these strategies, ratios between the observed frequencies in each group and the observed frequency in the whole MS dataset were calculated ([Table 2](#)). The proteins up-regulated via gene expression (group I) were mainly involved in protein, lipid, or amino acid degradation; stress response; and secondary metabolism. Energy metabolism (glycolysis and respiratory chain) and extracellular proteins required for cell wall metabolism and proteolysis were prevalent in group II, and thus might be regulated by decreased degradation rates. The proteins of consistently decreased relative abundance (255 proteins) were also subdivided into those with decreased expression rates (group III, 78 proteins) and those with increased or

unaffected expression rates (group IV, 177 proteins; [Figure 4](#), right part). Group III (down-regulation on expression level) contains specific vacuolar proteins and enzymes catalyzing lipid or tetrapyrrole synthesis ([Table 2](#)). No particular enrichment in subcellular compartments or functional categories was detected for proteins potentially down-regulated by increased proteolysis (group IV).

Adaptations of the protein synthesis and degradation machineries during progressive drought stress

Under control conditions ~5.4% of the leaf proteome detected by our MS approach is dedicated to protein synthesis (ribosomal proteins, translation initiation, and elongation factors) compared with 1.4% involved in proteolysis (proteasomes, autophagy proteins, proteases, and regulatory proteins; [Figure 5, A and C](#)). During progressive drought stress a majority of the proteins involved in protein synthesis (~75%) decreased more than average ([Figure 5, B](#),

Table 2 Estimating the enrichment of specific compartments (left) or metabolic pathways (right) in groups of proteins regulated on a transcriptional (I, III) or post-translational (II, IV) level

Compartment	I	II	III	IV	Pathway	I	II	III	IV
Cytosol	1.0	0.8	0.5	1.1	AA degradation	2.6	0.6	0.6	1.0
ER	1.5	1.9	0.8	0.7	Cell wall	0.7	2.6	0.8	1.3
Extracellular	2.3	3.1	0.2	0.4	Glycolysis	1.0	2.2	0.0	0.0
Golgi	0.0	0.8	0.6	1.6	Lipid degradation	6.4	1.9	0.0	0.0
Mitochondria	1.3	1.8	0.0	0.3	Lipid synthesis	0.6	1.2	2.2	1.0
Nucleus	2.3	0.8	0.5	0.7	mETC	0.0	2.2	0.0	0.3
Peroxisome	3.2	0.8	0.0	1.1	Protein degradation	2.0	1.5	0.0	0.8
Plasma membrane	2.5	1.0	1.6	1.6	Protein handling	0.5	2.3	0.0	1.2
Chloroplast	0.3	0.6	1.7	1.1	Secondary metabolism	2.3	1.1	1.3	0.6
Vacuole	0.6	1.1	2.7	0.6	Stress	3.0	1.5	0.3	0.4
					Tetrapyrrole synthesis	0.0	0.0	9.0	1.2

Numbers indicate the quotient of the fraction of proteins localized in specific compartments (left) or attributed to metabolic pathways (right) in the regulation groups (I–IV) divided by the fraction of the respective proteins in the total proteomics dataset. Group I: increased protein abundance, increased expression; Group II: increased protein abundance, unaffected or decreased expression; Group III: decreased protein abundance, decreased expression; Group IV: decreased protein abundance, unaffected or increased expression. Only metabolic pathways with quotients ≥ 2 (bold) in at least one regulation group are shown. The complete dataset used for enrichment analysis is provided in [Supplemental Dataset S4](#).

proteins on the left side of the vertical lines that mark the average fold changes in leaf protein content). In particular, the large group of ribosomal proteins (125 proteins, contributing 3.3 mg protein \cdot g⁻¹ DW under control conditions) had strikingly homogenous degradation rates (mass ratio S6/C = 0.5 \pm 0.2; [Figure 5, C](#)). In contrast, the total leaf content of proteolytic enzymes remained stable (0.8–0.9 mg protein \cdot g⁻¹ DW; [Figure 5, C](#)) but changed drastically in its composition, reflected by variations in the total mass content of the different classes of proteolytic enzymes and also by the high number of significant changes in the abundance of individual protease species ([Figure 5, C](#); the proteomics dataset for all individual proteins involved in protein synthesis and degradation is provided in [Supplemental Dataset S5](#)). Protease copy numbers in the cytosol, the vacuole, and in the apoplast increased progressively ([Figure 6, A and E](#)), and after severe stress, most of the vacuolar and extracellular proteases were of significantly increased abundance compared with control conditions indicating their specific relevance for drought response ([Figure 6, B and E](#) and [Supplemental Dataset S5](#)). In order to estimate the mean workload of the proteolytic system in the individual subcellular compartments, we calculated the number of proteases per 1,000 protein molecules ([Figure 6, C](#)) on the basis of the estimated total numbers of protein molecules and protease molecules in each subcellular compartment ([Figure 6, E](#)). The relative abundance of proteases per potential substrate was at least 10-fold higher in the apoplast than in any other compartment, even under control conditions, and further increased during moderate stress (S3; [Figure 6, C](#)). Vacuolar proteases strongly accumulated during severe stress, and also in the cytosol plus nucleus, the relative capacity of proteases approximately doubled (from 8.6 to 16.4 proteases per 1,000 protein molecules), although only a specific subset of proteolytic enzymes (mainly subunits of the proteasome) was significantly increased ([Figure 6, B and C](#) and [Supplemental Dataset S5](#)). Due to their high abundance, chloroplasts contained the major fraction of cellular

proteases (58%) in the leaves of non-stressed plants ([Figure 6, A and E](#)). However, proteases constituted less than 0.5% of all plastid proteins (compared with 9–13% in the apoplast, [Figure 6, E](#)) and decreased during stress to a similar extent as the majority of chloroplast proteins, resulting in a low number of significant changes in the relative abundance of plastid proteases during severe drought stress ([Figure 6, B and E](#)). The largest increase in protease copy numbers during stress (from 14.9 to 22.8 million molecules per cell) can be attributed to the aspartate class of proteases, which includes mainly extracellular subtilases ([Figure 6, D and Supplemental Dataset S5](#)).

Dynamics in free and protein-bound amino acid pools

Massive proteolysis during severe drought stress inevitably leads to liberation of large amounts of amino acids. We thus changed perspective and focused on the fate of the degraded part of the proteome and its effect on free amino acid homeostasis. For each individual protein, we calculated the difference in absolute content in control versus stressed plants ([Figure 7, A](#), top and [Supplemental Dataset S1](#)). It immediately becomes obvious that the amino acids added to the free pool are quantitatively derived from a limited number of very high abundance proteins (blue bars). Degradation of about 170 million RubisCO hexadecamers per cell alone accounts for 23% of the total amino acid release during stress. The profiles of free amino acids in the leaves of control and stressed plants were quantified by HPLC ([Supplemental Dataset S6](#)). In addition, we estimated the total amount of each individual amino acid bound in proteins on the basis of the leaf protein content and the quantitative composition of the proteome ([Supplemental Dataset S7](#)). The pool sizes and compositions of the free and protein-bound amino acid pools can be visualized using a modified version of PROTEOmaps ([Figure 7, B](#), orange: free pool, blue: protein-bound pool). Under control conditions, the Arabidopsis

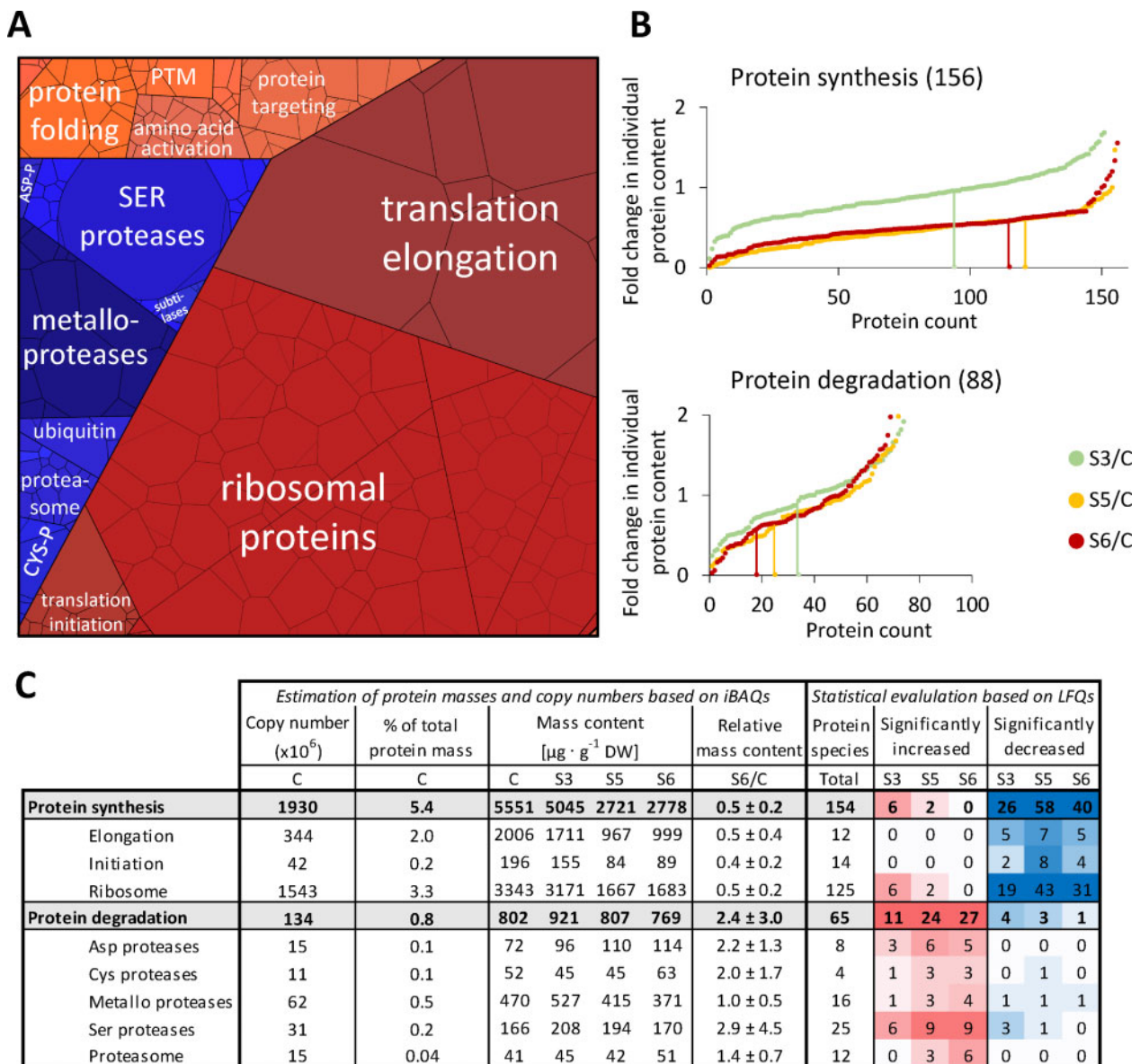


Figure 5 Abundance of the proteostasis apparatus during drought stress. **(A)** Proteomap illustrating the quantitative composition of the proteostasis apparatus under control conditions. Proteins are shown as polygons whose sizes represent the mass fractions (protein abundances obtained by MS [iBAQ], multiplied by protein molecular weight). Proteins involved in similar cellular functions according to the MapMan annotation file (version Ath_AGI_LOCUS_TAIR10_Aug2012) are arranged in adjacent locations and visualized by colors. The total protein fraction represented in the Proteomap is $6.9 \text{ mg} \cdot \text{g}^{-1}$ DW, corresponding to 6.7% of the leaf proteome. **(B)** Fold change ratios of the individual contents of proteins involved in protein synthesis (top) or proteolysis (bottom) in stressed versus control plants. In order to visualize the fraction of proteins with average, high, or low degradation rates, changes in individual protein contents were sorted in ascending order for each stress level. Vertical lines indicate proteins that correspond exactly to the decrease in total protein content, i.e. 0.94 for stress level S3 (light green), 0.61 for S5 (orange), and 0.58 at S6 (red). **(C)** Accumulated copy numbers and mass contents of proteins assigned to the functional sub-categories of protein metabolism. Significant changes in the relative abundance of individual protein species during stress were identified based on LFQ values (Student's *t* test, $P < 0.05$). Color intensities correspond to the number of significant changes (red shading: increase, blue shading: decrease). PTM, post-translational modification; ASP-P, aspartate protease; and CYS-P, cysteine protease.

leaves contained $1.05 \text{ mmol} \cdot \text{g}^{-1}$ DW amino acids of which $0.93 \text{ mmol} \cdot \text{g}^{-1}$ DW were bound in proteins (Supplemental Dataset S7). Drought stress led to a decrease of the total amino content by 28% (to $0.75 \text{ mmol} \cdot \text{g}^{-1}$ DW at stress level S6; Supplemental Dataset S7). Also, the ratio between free and protein-bound amino acids (orange/blue area in Figure 7, B; data provided in Supplemental

Dataset S7) shifted from 0.13 to 0.39 due to massive proteolysis. The amino acid composition of the proteome did not change considerably during stress. The molar share of the 20 proteinogenic amino acid was in the range of 1.3% (Cys) to 9.0% (Ala; Supplemental Figure S6, A). In contrast, the free amino acid pool strongly reacted to drought stress (orange areas in Figure 7, B, Supplemental Figure S6, B, and

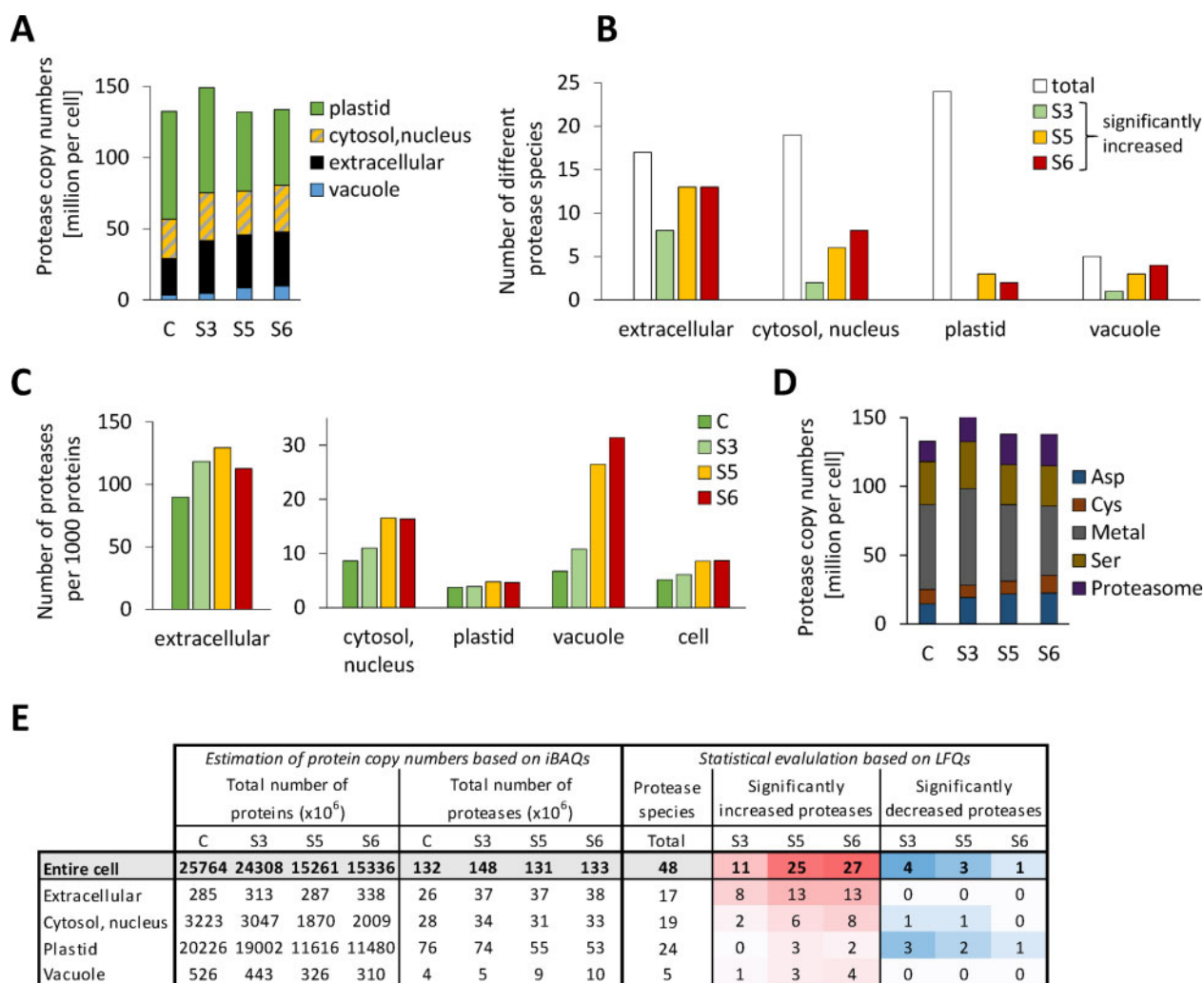


Figure 6 Adaptation of the proteolytic apparatus during progressive drought stress. **(A)** Estimated total number and subcellular distribution of protease molecules in an average leaf mesophyll cell under control conditions and during stress. The proteomics dataset (Supplemental Dataset S1) was filtered for the MapMan category “protein.degradation” (Thimm et al., 2004, the filtered list is provided in Supplemental Dataset S5). Protein copy numbers of all enzymes with proteolytic activity (without regulatory proteins and inhibitors) were added up for each subcellular compartment individually (see also E). **(B)** Significant increase in the abundance of individual protease species during drought stress in the different subcellular compartments. White bars indicate the total number of different proteases detected and colored bars illustrate how many of them were significantly increased based on LFQ values at the respective stress level (Student’s *t* test, $P < 0.05$, see also E). **(C)** Copy numbers of protease molecules per 1,000 proteins in the subcellular compartments of an average mesophyll cell under control conditions and during stress. The protease copy numbers (A) were divided by the total number of protein molecules in the respective subcellular compartment (see E) and multiplied by 1,000. **(D)** Number of protease molecules sorted by their functional classes. **(E)** Accumulated copy numbers of all detected proteins and of proteases in the different subcellular compartments. Significant changes in the relative abundance of individual protease species during stress were identified based on LFQ values (Student’s *t* test, $P < 0.05$). Color intensities correspond to the number of significant changes (red shading: increase, blue shading: decrease).

Supplemental Dataset S7), and also the concentrations of high and low abundance amino acids differed up to 460-fold ($0.27 \pm 0.11 \mu\text{mol} \cdot \text{g}^{-1} \text{DW}$ Cys versus $125 \pm 20 \mu\text{mol} \cdot \text{g}^{-1} \text{DW}$ Pro at stress level S6; Supplemental Figure S6, B and Supplemental Dataset S6). Under control conditions, the free amino acid pool was dominated by Glu, Gln, and Asp (Figure 7, B and Supplemental Dataset S6). Water deficiency led to progressive accumulation of Pro (Figure 7, B), which in the leaves of severely stressed plants represented 59% of the free and 20% of the total amino acid pool (Supplemental Dataset S7).

In order to estimate the role of proteolysis in amino acid homeostasis, we calculated the theoretical composition of the free amino acid pool that would result from partial degradation of the proteome (as detected by our proteomics approach) without any metabolic conversion of the amino acids produced (Figure 7, A, gray bars). With the clear exception of Pro, the free amino acid contents actually detected in severely stressed leaves (Figure 7, A, red bars) were several fold lower than the calculated ones, indicating their degradation or conversion to other metabolites. Enzymes involved in the degradation of branched-

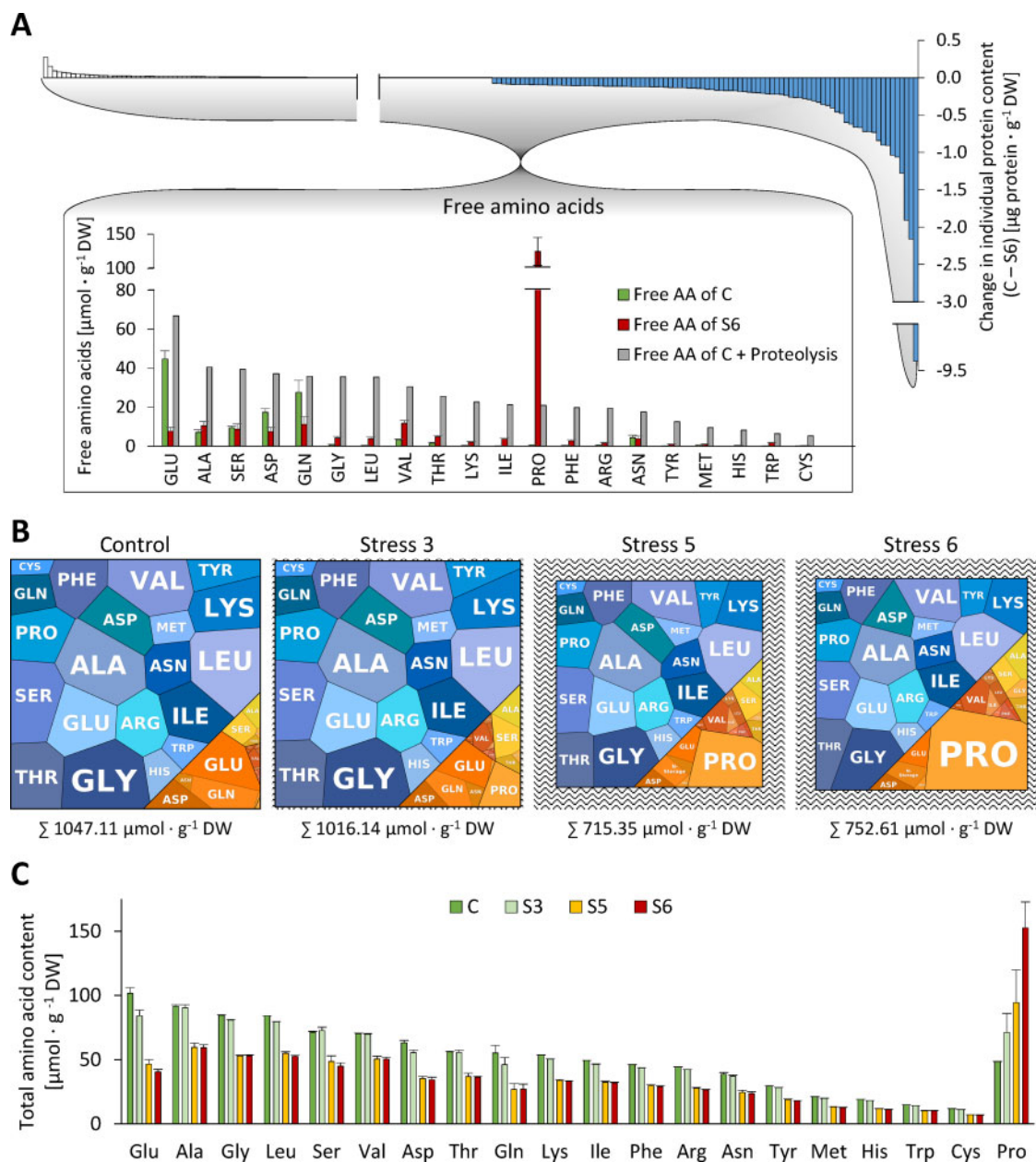


Figure 7 Interconnection of amino acid pools during progressive drought stress. **(A)** Effect of proteolysis on free amino acid homeostasis. The quantitative composition of the degraded fraction of the proteome (blue bars) was used to calculate the theoretical composition of the free amino acid pool (gray bars) that would result from massive proteolysis during drought stress (control versus maximum tolerable stress) without any metabolic conversion of the amino acids produced. The actual free amino acid profiles in the leaves of control plants (green bars) and of severely stressed plants (red bars) were analyzed by HPLC. **(B)** “AMINOmaps” illustrating pool sizes and compositions of the free (orange colors) and protein-bound (blue colors) amino acid pools during progressive drought stress. Amino acids are shown as polygons whose sizes represent the molar fractions. Free amino acid contents were quantified by HPLC, and quantitative amino acid composition of the proteome was calculated on the basis of molar composition of the proteome (see [Supplemental Dataset S1](#)) as detailed in the “Materials and methods” section. **(C)** Total amino acid contents (protein bound plus free) during progressive drought stress. The amino acid contents in proteins were calculated based on iBAQ values. Free amino acid profiles were analyzed by HPLC. Error bars indicate the variability (SD , $n = 7$) in the free amino acid pool (see [Supplemental Datasets S6, S7](#)). AA, amino acid.

chain amino acids, Cys, Lys, and Arg were indeed increased by drought stress, as were Pro and GABA metabolism (Figure 8, A and [Supplemental Dataset S8](#)). Statistical evaluation based on LFQ values showed that 8 of the 31 amino acid catabolic enzymes included in our dataset increased significantly in their relative abundance during stress

and none significantly decreased ([Supplemental Dataset S8](#), column W). In contrast, enzymes involved in amino acid synthesis and primary nitrogen assimilation (e.g. nitrate reductase, nitrite reductase, and Gln synthase) were significantly decreased, indicating that de novo synthesis of amino acids from inorganic nitrogen is negligible. The respiratory

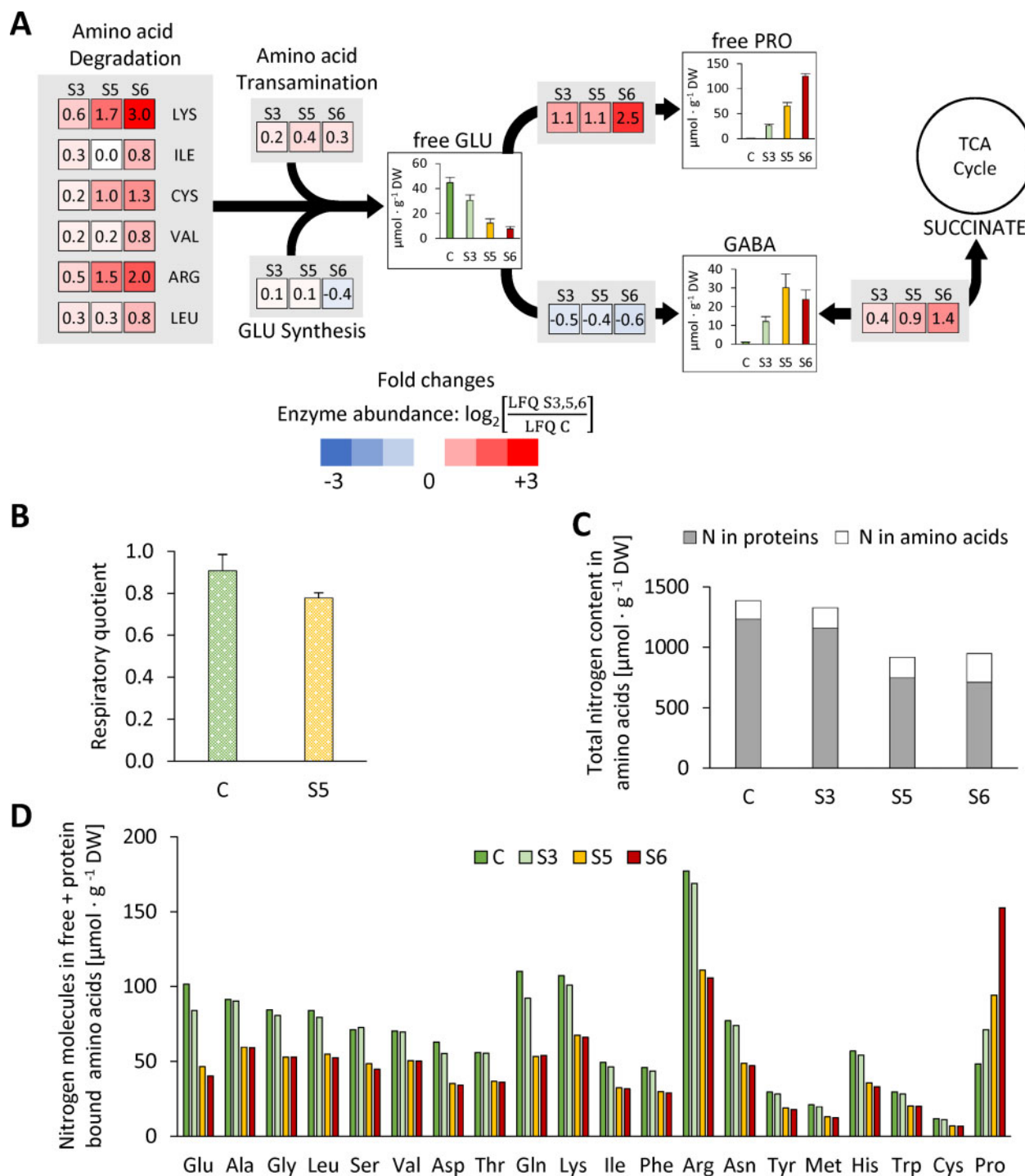


Figure 8 Drought stress-induced amino acid degradation delivers nitrogen and glutamate for the production of proline and GABA as osmolytes as well as alternative substrates for mitochondrial respiration. **(A)** Heatmap squares show LFQ-based \log_2 -fold changes in abundances of enzymes involved in amino acid metabolism at the selected stress levels. Red colors: increase with respect to the control fraction. Blue colors: decreased with respect to the control fraction. Abundance of currently known enzymes involved in amino acid synthesis and degradation pathways were extracted from the proteomics dataset (Supplemental Dataset S1, column “Amino acid pathway”). The colored squares represent the means of all changes in the abundance of enzymes involved in the respective branch of the pathway (see Batista-Silva et al. [2019] for a complete map of plant amino acid metabolism). Bar charts show free amino acid contents (means \pm SD, $n = 7$) in the leaves [$\mu\text{mol} \cdot \text{g}^{-1}$ DW]. **(B)** RQ (CO_2 production/ O_2 consumption) of rosette leaves under control conditions (green bar) and at stress level S5 (yellow bar). Values are means \pm SD, $n = 3$. **(C)** Total leaf nitrogen content [$\mu\text{mol} \cdot \text{g}^{-1}$ DW] included in the free and protein-bound amino acid pools of control and stressed plants. **(D)** Estimation of the nitrogen content of individual (bound and free) amino acids [$\mu\text{mol} \cdot \text{g}^{-1}$ DW] (Supplemental Dataset S7). GABA, γ -amino-butyric acid; GLU, L-glutamate; and PRO: L-proline.

quotient (RQ; RC = carbon dioxide production/oxygen consumption) can be used as an indicator of which substrates are mainly being metabolized, since complete oxidation of carbohydrates consumes less oxygen per carbon dioxide released (RC = 1.0) than the oxidation of proteins (RC = 0.8) or lipids (RC = 0.7). We measured a RQ of 0.91 ± 0.08 in the leaves of control plants, which decreased to 0.78 ± 0.03 in severely stressed plants (stress level S5; Figure 8, B). This result thus supports a substrate shift from mainly carbohydrate-based respiration to a larger contribution of proteins and lipids during drought stress. In order to develop an idea about how long plants would be able to keep up their regular mitochondrial respiration rate when using exclusively the amino acids released by protein degradation as substrates, we calculated the total number of electrons that would be transferred to oxygen via the mitochondrial respiratory chain during complete oxidation of the specific set of amino acids released during drought stress (Supplemental Dataset S7; Hildebrandt et al., 2015). This oxidation process would lead to a total oxygen consumption of $1,062 \mu\text{mol O}_2 \cdot \text{g}^{-1}$ DW and thus, on the basis of a mean leaf respiration rate of $3.4 \text{ nmol O}_2 \cdot \text{g}^{-1}$ fresh weight (FW) $\cdot \text{s}^{-1}$ (O'Leary et al., 2017), could fully sustain leaf energy metabolism for about 7 h.

Discussion

The number of protein molecules in a plant cell

Common sense indicates that cells require an adequate set of proteins to function properly. However, the literature did not allow us to deduce a comprehensive picture of what this protein infrastructure of a plant cell might look like. Thus, we calculated the average protein copy number in a plant cell based on published information about the size and number of cells in an average Arabidopsis leaf using two independent approaches. Both calculations consistently revealed that an average mesophyll cell in a mature Arabidopsis leaf contains ~ 25 billion protein molecules.

A major function of leaf mesophyll cells is photosynthesis, and this is reflected by the large fraction of proteins (20 billion) localized in the ~ 100 chloroplasts present in each cell, corresponding to ~ 200 million proteins per chloroplast, and again, the largest fraction of these proteins are included in ~ 3.4 million RubisCO hexadecamers (Königer et al., 2008). The high abundance of RubisCO in leaves is well established. Recent estimations suggest that its total mass on earth is ~ 0.7 Gt, and RubisCO accounts for $\sim 3\%$ of leaf DW (Bar-On and Milo, 2019). Adding up the mass content of all RubisCO subunits in our MS dataset (Supplemental Dataset S1, B) results in a very similar estimate of $21.4 \text{ mg} \cdot \text{g DW}^{-1}$. The dominant position of RubisCO within the leaf proteome is also illustrated by gel-based proteomic approaches (Supplemental Figure S2, B).

Interestingly, the protein copy number we calculated for the cytosol of a plant cell (~ 3.2 billion) matches almost exactly the total number of proteins reported for animal cells (Kulak et al., 2014; Supplemental Figure S1). According to

our estimation, a mesophyll cell contains about 495 million mitochondrial proteins (Table 1). Assuming that between 300 and 450 mitochondria are present in a plant cell, depending on the leaf age (Preuten et al., 2010), a single mitochondrion would harbor 1.1–1.7 million protein molecules, which is in perfect agreement with previous results (Fuchs et al., 2020).

Strengths and limitations of the proteomics approach and its different evaluation strategies

For statistical analysis to identify significant differences between the stress levels we used LFQ, an algorithm optimized for accurate horizontal comparisons between different samples including multiple levels of normalization (Cox et al., 2014). This approach helps to identify, e.g. a set of extracellular proteases that might be particularly relevant during drought stress response or to estimate the regulation of amino acid catabolic pathways (Figure 8). However, LFQ-based data interpretation is not suitable for vertical comparisons of the abundance of different protein species and therefore was not the major focus during our evaluation. Detailed information on significant changes in protein abundances at the different stress levels compared with the control are provided in the Supplemental Material (Supplemental Dataset S1, columns U-AC, S5, and S8). A quantitative perspective on the leaf proteome based on iBAQs enables calculation of mass fractions, molarities, and even copy numbers of individual proteins, but lacks statistical validation. Both quantitation methods are limited by the intrinsic shortcomings of shotgun proteomics, which cannot detect very low abundance proteins, and tends to underestimate membrane proteins since the biochemical properties of their peptides, such as high hydrophobicity, are unfavorable for ionization and detection (Schwanhäusser et al., 2011; Krey et al., 2014; Fabre et al., 2014). Furthermore, the extraction procedure may also introduce a bias against, e.g. membrane and membrane-associated proteins. Every proteomics dataset therefore has to be regarded as a representative fraction of the complete picture. We can estimate on the basis of labeled peptides that the fraction detectable by our approach covers more than 80% of the protein mass in a leaf. Thus, it is suitable to provide a realistic impression of the total number of protein molecules in a cell, as well as the general behavior of high to medium abundance proteins during drought stress. Recent large-scale MS surveys with a focus on covering the largest possible fraction of protein groups present in different Arabidopsis tissues were able to detect 8,700 or even 13,826 different proteins by fractionation of individual leaf samples (Zhang et al., 2019; Mergner et al., 2020). For studies focusing on individual pathways or low abundance proteins, it is thus reasonable to increase the sensitivity of the MS analysis by including sample fractionation or targeted approaches.

Proteostasis under challenging conditions—a focus on subcellular compartments and metabolic pathways

Plants use various physiological adaptation mechanisms to cope with insufficient water supply (Gupta et al., 2020). They restrict the number and size of leaves and close their stomata to reduce water consumption. In addition, they increase the root-to-shoot ratio to improve water uptake from the soil. Osmotic adjustment preserves the cell turgor, and antioxidants are produced to attenuate oxidative damage. Even at the lowest stress level analyzed in this study (S3), plant rosettes had already stopped growing, accumulated the osmoprotectant proline, and significantly changed the abundance of at least 291 proteins. The drastic effects on the total leaf protein content and amino acid profile analyzed here are characteristic for the late phase of severe dehydration (stress levels S5 and S6).

How to focus on the relevant pathways during severe drought stress

Combined information about protein abundance and expression levels illustrates the general strategies employed by leaf cells to adjust their protein setup to the challenges posed by insufficient water supply. Specific stress-related proteins, such as individual heat shock proteins and dehydrins and those involved in secondary metabolism, are induced at the expression level. Similarly, cells increase the abundance of pathways that are barely used under control conditions but important to make alternative energy sources accessible, such as protein, amino acid, and lipid catabolism by de novo synthesis of catabolic enzymes. In contrast, the basic mitochondrial functions fulfilled by TCA cycle and respiratory chain are not required to be more active during stress than under control conditions, they just change their initial substrate from carbohydrates to amino acids and lipids. Therefore, it makes perfect sense that these pathways are preserved from degradation rather than up-regulated at the transcriptional level. Protection from degradation might be achieved by selective autophagy of specific organelles. During developmental senescence, autophagic vesicles have been shown to preferentially contain RubisCO, entire chloroplasts, and also ribosomes, whereas mitochondrial integrity and function is preserved until very late stages (Chrobok et al., 2016; Marshall and Vierstra, 2018). Our results are in good agreement with these findings since we observed stronger than average decrease rates in plastid and ribosomal proteins during progressive drought stress but very little effect on mitochondrial proteins. Ribosomes are among the most stable proteins under control conditions (Li et al., 2017). However, they tie up a substantial fraction of cellular resources since they account for a majority of the cell's RNA and also ~3% of the protein mass. Thus, the turnover of ribosomes in eukaryotes is activated by nutritional stress such as carbon, nitrogen, or phosphate deficiency (Floyd et al., 2016). Conveniently, this measure also serves the purpose of down-regulating protein synthesis rates during stress. Apart from selective autophagy, the stability of individual proteins can be regulated via ubiquitinylation and is

also affected by other post-translational modifications, substrate, or cofactor binding, so that less busy enzymes are degraded faster (Nelson and Millar, 2015).

Proteolytic systems and their contribution to stress-induced protein turnover

Autophagy and proteasomes are considered to be the two major proteolytic systems in a cell. However, due to the sheer abundance of chloroplasts, the plastid proteases, according to our evaluation, represent the major share of proteolytic enzymes in a leaf cell under control conditions. Thus, they would be suitable for contributing considerably to the regular turnover of chloroplast proteins. Since amino acid synthesis is also localized mainly in these organelles, they are perfectly equipped for exporting the amino acids resulting from proteolysis (Pottosin and Shabala, 2016). However, the frequency of proteases per total number of proteins is comparatively low in chloroplasts and in contrast to other subcellular compartments does not increase during stress. Bulk degradation of chloroplast proteins during severe dehydration therefore requires additional capacities outside the chloroplast, and these can be provided by the lytic vacuoles that strongly increase their protease content and are able to hydrolyze proteins delivered by autophagic vesicles (Michaeli and Galili, 2014; Marshall and Vierstra, 2018).

In contrast to plastids, the extracellular space is extremely rich in protease molecules per total proteins. Apart from maintaining the cell wall, major functions of the apoplast are signaling and defense against pathogens, which both involve proteolysis. Extracellular plant proteases hydrolyze proteins of invading pathogens to inactivate them and to release signal peptides, triggering immune reactions (Balakireva and Zamyatnin, 2018). Plant peptide hormones are usually produced as pre-protein and need to be activated by proteolytic cleavage (Stührwohldt and Schaller, 2019). This function has been shown to be particularly relevant for drought tolerance. Extracellular subtilisin-like proteases are involved in the regulation of stomatal density and distribution in response to environmental stimuli (Berger and Altmann, 2000; Engineer et al., 2014). In addition, the subtilase Senescence-Associated Subtilisin Protease (SASP) degrades and thus inactivates OST1 (Open Stomata 1), a kinase activated by abscisic acid (ABA), and therefore acts as a negative regulator in ABA signaling (Wang et al., 2018). Our dataset shows a strong induction of SASP during drought stress and identifies 14 additional extracellular proteases that are significantly increased and thus might be relevant for stress tolerance. The apoplast proteome is remarkably stable even during severe dehydration. This finding might indicate a specific relevance of extracellular proteins during drought stress, which is clearly the case for proteases. An alternative explanation could be that apoplast proteins simply evade the intracellular bulk degradation systems autophagy and proteasome due to their remote localization. Since our proteomics dataset covers only a fraction

of all cellular proteases, it has to be kept in mind that these insights do not show the complete picture. Additional stress relevant compounds of proteolytic systems, which were not detected here, may be involved.

Amino acid homeostasis under challenging conditions—massive adjustments to the free pool provide osmolytes and ATP

The free pool represents only about 11% of all cellular amino acids under control conditions but strongly gains impact in the course of the drought stress response. Also, despite massive proteolysis the relative composition of the proteome looks roughly similar before and after stress (Supplemental Figure S7), whereas changes on the metabolite level are rapid and drastic (Figure 7, B). Taken together these observations illustrate that homeostasis has a different meaning with regard to free amino acids and proteins. Proline is a well-known compatible osmolyte in plants and also in some euryhaline animals (Szabados and Savouré, 2010; Wiesenthal et al., 2019). Free proline accumulated 219-fold, and even its total amount (free plus bound in proteins) increased from 48 to 153 $\mu\text{mol} \cdot \text{g}^{-1}$ DW during progressive drought stress, indicating extensive de novo synthesis (Supplemental Dataset S7 and Figure 7, C). In contrast, the total contents of all other 19 proteinogenic amino acids (except Pro) clearly decreased during the stress phase indicating that they are most likely not synthesized during stress, but accumulate in the free pool as a consequence of proteolysis (Supplemental Figure S6, B). An exception might be those amino acids that serve as precursors for secondary metabolites such as the aromatic amino acids (Tzin and Galili, 2010). The total amount of nitrogen contained in amino acids decreases by about one-third during progressive drought stress (Figure 8, C). Taken together with the down-regulation of enzymes involved in primary nitrogen assimilation, it becomes clear that protein degradation can most likely cover the full nitrogen demand for the synthesis of proline (Figure 8, D), GABA, and additional metabolites involved in stress response.

The sum of all amino acids dropped by 29% during stress, most likely due to their use as alternative respiratory substrates and precursors for secondary metabolites (Araújo et al., 2011; Hildebrandt, 2018). The drop in the RQ in stressed compared with control leaves also suggests that respiratory substrates other than carbohydrates (i.e. proteins and lipids) are used during drought. Our estimation based on published respiration rates of Arabidopsis leaves (O'Leary et al., 2017) indicates that amino acid oxidation could fully sustain leaf energy metabolism for about 7 h. However, leaf respiration rates tend to decrease during dehydration (Pinheiro and Chaves, 2011), so that amino acid catabolism, in addition to some residual photosynthetic activity and the oxidation of lipids and chlorophyll, can be anticipated to make a substantial contribution to the ATP supply of drought stressed plants. A shift in the respiratory substrate

can thus provide an efficient means to counterbalance carbohydrate limitation in Arabidopsis during drought stress.

Conclusion

Our estimation of the quantitative protein and amino acid composition of a plant leaf cell provides an initial idea of scales and dimensions. On this basis, the dynamic interconnection of protein and amino acid homeostasis during severe drought stress could be monitored and quantified on absolute scales. The current understanding of protein copy numbers in individual plant cells will be refined in the future based on single cell approaches and the analysis of different tissues, developmental stages, and stress conditions.

Materials and methods

Plant growth and drought stress treatment

Arabidopsis (*Arabidopsis thaliana*) Columbia-0 plants were grown for 2 weeks in pots (200 cm^3) in a phytochamber (22–24°C, 16-h light, 8-h darkness, 110 $\mu\text{mol s}^{-1} \text{m}^{-2}$ light). The stress treatment started with soaking the substrate (Steckmedium, Klasmann-Deilmann GmbH) with tap water to a distinct weight (150 g). A uniform desiccation process was achieved by monitoring pot weights and reorganizing the positions of the pots in the chamber every other day. After 10 d without watering, leaf material (complete rosettes) was harvested on a daily basis in the middle of the light period (Figure 2). During late stages of severe drought stress (S4–S7), plants were additionally sub-classified according to their leaf phenotype (S4: 4–7 rolled leaves S5: 8–10 rolled leaves, S6: >10 rolled leaves). For each stress level, seven stressed plants and three controls were harvested individually. The leaf material of each individual plant is considered as a biological replicate. In addition, three stressed plants were re-watered to test their viability and harvested after 24 h.

Determination of RWC

The method used is based on Smart and Bingham (1974). The weight of a leaf was measured immediately after harvest (FW), after overnight incubation in distilled water (turgor weight, TW), and after overnight drying at 37°C (DW). RWC was calculated according to the following formula:
$$\text{RWC} [\%] = \frac{(\text{FW} - \text{DW})}{(\text{TW} - \text{DW})} \times 100.$$

Determination of the RQ

Dark respiration of rosette leaf discs was measured at 25°C in a reaction mixture containing 1-mM NaHCO_3 and 100-mM KCl using an O2K respirometer (Oroboros Instruments, Innsbruck, Austria). The oxygraph chamber was additionally equipped with a FiveEasy pH meter (Mettler Toledo) to detect O_2 consumption and CO_2 production simultaneously. The increase in CO_2 was calculated on the basis of the pKs value 6.4 and divided by the concurrent decrease in the oxygen concentration of the reaction mixture to determine the RQ (RC).

Extraction and quantification of total protein

In total, 5 mg of lyophilized plant rosette powder was dissolved in 700 μL methanol and incubated for 20 min shaking at 80°C. After centrifugation (10 min, 4°C, 18,800 \times g), the pellet was washed twice in 1-mL ethanol (70%, v/v) and resuspended in 400- μL NaOH (0.1 M). The solution was incubated for 1 h shaking at 95°C and centrifuged again. The protein content of the supernatant was quantified using Ready-to-use Coomassie Blue G-250 Protein Assay Reagent (ThermoFisher) and Albumin Standard 23209 (ThermoFisher).

Quantification of free amino acids by HPLC

Free amino acids were extracted as described in [Batista-Silva et al. \(2019\)](#). The pre-column derivatization with *o*-phthalaldehyde (OPA) and fluorenylmethoxycarbonyl (FMOC) was based on the application note “Automated amino acids analysis using an Agilent Poroshell HPH-C18 Column” by Agilent. The samples were injected onto a 100 mm \times 3 mm InfinityLab Poroshell HPH-C18 column (2.7 μm) using an Ultimate 3000 HPLC system (ThermoFisher). HPLC settings were set as described in [Batista-Silva et al. \(2019\)](#). Cysteine was quantified after derivatization with the fluorescent dye monobromobimane, using the same HPLC system ([Fahey et al., 1980](#); [Newton et al., 1981](#)). Five milligrams of lyophilized plant powder was mixed with 10 μL bromobimane (46 mM in acetonitrile), 100 μL acetonitrile, and 200 μL buffer (160-mM HEPES, 16-mM EDTA, pH 8.0), and incubated on a shaker for 30 min in darkness before adding 100 μL methanesulfonic acid (65 mM). Samples were separated on a LiChrospher 60 RP-select Hibar RT 5 μm column (Merck) at 18°C using a gradient of two solvents (0.25% [v/v] acetic acid [pH 4] and methanol). Labeled thiols were detected using a fluorescence detector 3400 RS (ThermoFisher) at 380 nm for excitation and 480 nm for emission.

Protein extraction and label-free quantitative shotgun MS

For protein extraction, about 5 mg of the lyophilized rosette powder was used (C, S3, S5, S6; $n = 4$). Protein extraction, sample preparation, and LC–MS/MS were performed as previously described ([Thal et al., 2018](#)) using a Q-Exactive mass spectrometer coupled to an Ultimate 3000 UPLC (ThermoFisher). Peptides were first bound to a 2-cm C18 reversed phase trap column (Acclaim PepMap100, diameter: 100 μm , granulometry: 5 μm , pore size: 100 Å; Thermo Fisher Scientific, Waltham, MA, USA). Separation took place on a 50-cm C18 reversed phase analytical column (Acclaim PepMap100, diameter: 75 μm , granulometry: 3 μm , pore size: 100 Å; Thermo Fisher Scientific) eluted using a non-linear 5–36% acetonitrile gradient containing 0.1% (v/v) formic acid. Peptides were transferred into a Q-Exactive mass spectrometer (Thermo Fisher Scientific, Dreieich, Germany) by electrospray ionization (ESI) using a NSI source (Thermo Fisher Scientific, Dreieich, Germany) equipped with a stainless steel nano-bore emitter (Thermo Fisher Scientific,

Dreieich, Germany). The data-dependent duty cycle involved a top-10 method, using resolutions set to 70,000 for MS1 (AGI set to 1,000,000) and 17,500 for MS2 (AGI set to 100,000). Profile mode was used during data acquisition.

Protein identification by MaxQuant and data processing via Perseus software

The LC–MS/MS spectra were analyzed using MaxQuant (Version 1.5.5.1, [Cox and Mann, 2008](#)) and protein identification was based on the TAIR10 database (35,387 proteins plus the common contaminants trypsin, bovine serum albumin (BSA), and keratin). The search parameters were set to: carbamidomethylation (C) as fixed modification, oxidation (M) and acetylation (protein N-term) as variable modifications. The specific digestion mode was set to trypsin (P) and a maximum of two missed cleavage sites was allowed. A positive peptide identification was required to contain a minimum of seven amino acids. The mass tolerances of the precursor ion were set to 20 and 4.5 ppm for the first and main searches, respectively. The mass tolerances of the fragment ions were set to 40 ppm. FDR at the protein and PSM level was set to 1%. The minimum number of unique peptides per protein group was 1. In total, 3,472 protein groups were identified (1,298–1,655 per sample). Unique and razor peptides were used for protein quantification. The iBAQ function of MaxQuant was enabled, “log fit” disabled. Further analyses and statistical evaluation based on LFQ and iBAQ values generated by MaxQuant were performed in Perseus (version 1.6.1.1), ([Tyanova et al., 2016](#)). Changes in the relative abundance of individual proteins were estimated via label-free quantification (LFQ; [Cox et al., 2014](#)). This approach is suitable for identifying proteins that are induced and thus might be particularly relevant during the conditions tested. iBAQs were used as a basis for calculating mass and molar contents of the individual proteins. MaxQuant output tables were filtered to remove non-plant contaminants, reversed sequences, and proteins that were only identified based on modified peptides. Proteins were excluded from further analysis if they were not detected in at least three of four replicates in at least one group (C, S3, S5, S6). Missing protein intensities were then considered as too low for proper quantification and replaced by very low values from a normal distribution. Finally, a list of 1,399 proteins ([Supplemental Dataset S1](#)) was used for all further calculations. Statistical analysis of the MS dataset was performed in Perseus using two-sample *t* tests ($P < 0.05$).

Calculating absolute contents of individual proteins based on iBAQ values

Raw iBAQ values generated by MaxQuant were multiplied with the molecular weight of the respective protein [kDa]. These individual weighted iBAQs were then divided by the sum of weighted iBAQs of all detected proteins for normalization, and means of the four biological replicates in each sample group were calculated. The mean mass fractions were then multiplied with the total protein content of the

sample [$\text{mg} \cdot \text{g}^{-1}$ DW] to determine the mass content of each individual protein [$\mu\text{g} \cdot \text{g}^{-1}$ DW]. The mass contents were divided by the molecular weight of the respective protein to calculate the molar protein contents [$\text{nmol} \cdot \text{g}^{-1}$ DW]. Protein copy numbers in an individual mesophyll cell were calculated by multiplying the molar protein contents with the mean leaf DW and the Avogadro constant, and dividing it by the mean number of mesophyll cells per leaf. A more detailed description of the calculation methods is provided in [Supplemental Figure S1](#).

Calculating protein-bound amino acid contents based on individual protein contents

The amino acid composition of each protein was determined on the basis of its sequence. The molar content of the protein was then multiplied with the number of each of the 20 amino acids present in this protein to calculate the molar contents of the individual amino acids. The resulting molar amino acid contents were summed up for all identified proteins in a sample. The total numbers of amino acids released due to proteolysis were calculated by subtracting contents of protein-bound amino acids in stressed and control plants.

Quantification of RubisCO using parallel reaction monitoring targeted proteomics

In order to verify the iBAQ-based calculation of absolute amounts of individual proteins, the ribulose-bisphosphate carboxylase/oxygenase large subunit (RubisCO LS) was quantified in control samples via parallel reaction monitoring (PRM) in a targeted MS approach. Three unique peptides of RubisCO LS were selected, based on their intensity, peak symmetry, and the absence of miscleavages and modification sites ([Rauniyar, 2015](#)). The following isotopically heavy labeled peptides were provided by New England Peptides (Gardner, MA, USA): (1) DTDLILAAFR*, (2) LTYYPPEYETK*, (3) ESTLGFVDLLR* (R* = Arg, $^{13}\text{C}_6$, $^{15}\text{N}_4$; K* = Lys, $^{13}\text{C}_6$, $^{15}\text{N}_2$). The peptides were mixed equally and diluted with plant sample matrix for calibration (1,600–25 fmol/ μL). An inclusion list containing the masses of the labeled and the natural peptides in addition to their retention times was implemented. For the absolute quantification of RubisCO LS, the digested plant samples were spiked with heavy peptides to a final concentration of 400 fmol/ μL . Chromatograms were extracted and evaluated with Skyline (V20.1.0.155, [MacLean et al., 2010](#)). Peak areas of three transition fragments per peptides were quantified against the calibration of the heavy labeled peptides and subsequently divided by the total peptide content of the individual sample ([Supplemental Dataset S2](#)). Due to low and inconsistent signal intensity, the third peptide (ESTLGFVDLLR*) could not be used for quantitation. The total peptide content of the digested leaf samples was determined by using the Pierce Quantitative Colorimetric Peptide Assay (ThermoFisher).

Calculating mitochondrial oxygen consumption with amino acids as alternative respiratory substrates

To estimate mitochondrial respiration in leaves that exclusively use the set of amino acids released by protein degradation during drought stress as substrates, total leaf amino acid contents of stressed plants were subtracted from those of control plants. For each amino acid this difference was multiplied with the number of electrons transferred to the respiratory chain during complete oxidation ([Hildebrandt et al., 2015](#)) and divided by four to calculate the total amount of oxygen consumed ([Supplemental Dataset S7](#)).

Genevestigator datasets

The following three microarray datasets were used for estimating gene expression levels during drought stress: (1) AT-00684_1 ([Ludwików et al., 2009](#); long-day conditions, start: 3 weeks, samples after 5 d of dehydration in soil); (2) AT-00626_1 ([Pandey et al., 2013](#); long-day conditions, start: 3 weeks, samples after 10 d of dehydration in soil); (3) AT-00292_1 ([Perera et al., 2008](#); short-day conditions, start: 6 weeks, samples after 7 d of dehydration in soil).

Data availability statement

The MS proteomics data have been deposited to the ProteomeXchange Consortium (<http://proteomecentral.proteomexchange.org>) via the PRIDE partner repository ([Perez-Riverol et al., 2019](#)) with the dataset identifier PXD021563.

Accession numbers

Sequence data from this article can be found in the GenBank/EMBL data libraries under the accession numbers listed in [Supplemental Dataset S1](#).

Supplemental data

Supplemental Figure S1. Calculation of individual protein contents and copy numbers.

Supplemental Figure S2. Estimation of the absolute content of RubisCO large subunit.

Supplemental Figure S3. Principal component analysis of the MS dataset.

Supplemental Figure S4. Compartment-specific patterns of stress-induced changes in individual protein abundances: individual protein contents.

Supplemental Figure S5. Compartment-specific patterns of stress-induced changes in individual protein abundances: fold change ratios.

Supplemental Figure S6. Protein-bound and free amino acids during progressive drought stress in Arabidopsis rosette leaves.

Supplemental Figure S7. Changes in the quantitative composition of the leaf proteome during drought stress.

Supplemental Dataset S1. Complete MS dataset: LFQ and iBAQ values, relative protein abundances, mass contents [$\mu\text{g} \cdot \text{g}^{-1}$ DW], molar contents [$\text{nmol} \cdot \text{g}^{-1}$ DW], and copy

numbers [million proteins per cell] of 1,399 protein species during progressive drought stress.

Supplemental Dataset S2. Quantification of RubisCO LS via PRM in a targeted MS approach.

Supplemental Dataset S3. Quantitative composition of the leaf proteome under control conditions. Mass fractions (%) of metabolic categories.

Supplemental Dataset S4. Combined analysis of protein abundances and expression levels to identify general strategies of leaf cells to adjust their protein setup to the challenges posed by insufficient water supply.

Supplemental Dataset S5. MS dataset of all proteins involved in protein metabolism (extracted from Supplemental Dataset S1).

Supplemental Dataset S6. Free amino acid contents in Arabidopsis rosette leaves during progressive drought stress.

Supplemental Dataset S7. Pools of bound and free proteinogenic amino acids (AA) in Arabidopsis rosette leaves during progressive drought stress.

Supplemental Dataset S8. MS dataset of all proteins involved in amino acid metabolism (extracted from Supplemental Dataset S1).

Acknowledgments

The authors thank Marianne Langer and Dagmar Lewejohann for skillful technical assistance during MS sample preparation and Michael Senkler for IT support.

Conflict of interest statement. The authors have no conflicts of interest to declare.

References

- Alcázar R, Marco F, Cuevas JC, Patron M, Ferrando A, Carrasco P, Tiburcio AF, Altabella T (2006) Involvement of polyamines in plant response to abiotic stress. *Biotechnol Lett* **28**: 1867–1876.
- Araújo WL, Tohge T, Ishizaki K, Leaver CJ, Fernie AR (2011) Protein degradation—an alternative respiratory substrate for stressed plants. *Trends Plant Sci* **16**: 489–498.
- Baerenfaller K, Grossmann J, Grobei MA, Hull R, Hirsch-Hoffmann M, Yalovsky S, Zimmermann P, Grossniklaus U, Gruissem W, Baginsky S (2008) Genome-scale proteomics reveals *Arabidopsis thaliana* gene models and proteome dynamics. *Science* **320**: 938–941.
- Balakireva AV, Zamyatnin AA (2018) Indispensable role of proteases in plant innate immunity. *Int J Mol Sci* **19**:629.
- Bar-On YM, Milo R (2019) The global mass and average rate of rubisco. *Proc Natl Acad Sci U S A* **116**: 4738–4743.
- Batista-Silva W, Heinemann B, Rugen N, Nunes-Nesi A, Araújo WL, Braun H-P, Hildebrandt TM (2019) The role of amino acid metabolism during abiotic stress release. *Plant Cell Environ* **42**: 1630–1644.
- Berger D, Altmann T (2000) A subtilisin-like serine protease involved in the regulation of stomatal density and distribution in *Arabidopsis thaliana*. *Genes Dev* **14**: 1119–1131.
- Chrobok D, Law SR, Brouwer B, Lindén P, Ziolkowska A, Liebsch D, Narsai R, Szal B, Moritz T, Rouhier N, et al. (2016) Dissecting the metabolic role of mitochondria during developmental leaf senescence. *Plant Physiol* **172**: 2132–2153.
- Cox J, Hein MY, Lubner CA, Paron I, Nagaraj N, Mann M (2014) Accurate proteome-wide label-free quantification by delayed normalization and maximal peptide ratio extraction, termed MaxLFQ. *Mol Cell Proteomics* **13**: 2513–2526.
- Cox J, Mann M (2008) MaxQuant enables high peptide identification rates, individualized p.p.b.-range mass accuracies and proteome-wide protein quantification. *Nat Biotechnol* **26**: 1367–1372.
- Dikic I (2017) Proteasomal and autophagic degradation systems. *Annu Rev Biochem* **86**: 193–224.
- Engineer CB, Ghassemian M, Anderson JC, Peck SC, Hu H, Schroeder JI (2014) Carbonic anhydrases, EPF2 and a novel protease mediate CO₂ control of stomatal development. *Nature* **513**: 246–250.
- Fabre B, Lambour T, Bouyssié D, Menneteau T, Monsarrat B, Burllet-Schiltz O, Bousquet-Dubouch M-P (2014) Comparison of label-free quantification methods for the determination of protein complexes subunits stoichiometry. *EuPA Open Proteomics* **4**: 82–86.
- Fahey RC, Newton GL, Dorian R, Kosower EM (1980) Analysis of biological thiols: derivatization with monobromotrimethylammoniumbimane and characterization by electrophoresis and chromatography. *Anal Biochem* **107**: 1–10.
- Floyd BE, Morriss SC, MacIntosh GC, Bassham DC (2016) Evidence for autophagy-dependent pathways of rRNA turnover in Arabidopsis. *Autophagy* **11**: 2199–2212.
- Fuchs P, Rugen N, Carrie C, Elsässer M, Finkemeier I, Giese J, Hildebrandt TM, Kühn K, Maurino VG, Ruberti C, et al. (2020) Single organelle function and organization as estimated from Arabidopsis mitochondrial proteomics. *Plant J* **101**: 420–441.
- Gupta A, Rico-Medina A, Caño-Delgado AI (2020) The physiology of plant responses to drought. *Science* **368**: 266–269.
- Hildebrandt TM (2018) Synthesis versus degradation: directions of amino acid metabolism during Arabidopsis abiotic stress response. *Plant Mol Biol* **98**: 121–135.
- Hildebrandt TM, Nunes Nesi A, Araújo WL, Braun H-P (2015) Amino acid catabolism in plants. *Mol Plant* **8**: 1563–1579.
- Ho B, Baryshnikova A, Brown GW (2018) Unification of protein abundance datasets yields a quantitative *Saccharomyces cerevisiae* proteome. *Cell Syst* **6**: 192–205.e3.
- Hooper CM, Castleden IR, Tanz SK, Aryamanesh N, Millar AH (2017) SUBA4: the interactive data analysis centre for Arabidopsis subcellular protein locations. *Nucleic Acids Res* **45**: D1064–D1074.
- Hruz T, Laule O, Szabo G, Wessendorp F, Bleuler S, Oertle L, Widmayer P, Gruissem W, Zimmermann P (2008) Genevestigator v3: a reference expression database for the meta-analysis of transcriptomes. *Adv Bioinform* **2008**: 420747.
- Jorgensen P, Nishikawa JL, Bretkreutz B-J, Tyers M (2002) Systematic identification of pathways that couple cell growth and division in yeast. *Science* **297**: 395–400.
- Königer M, Delamaide JA, Marlow ED, Harris GC (2008) *Arabidopsis thaliana* leaves with altered chloroplast numbers and chloroplast movement exhibit impaired adjustments to both low and high light. *J Exp Bot* **59**: 2285–2297.
- Krasensky J, Jonak C (2012) Drought, salt, and temperature stress-induced metabolic rearrangements and regulatory networks. *J Exp Bot* **63**: 1593–1608.
- Krey JF, Wilmarth PA, Shin J-B, Klimek J, Sherman NE, Jeffery ED, Choi D, David LL, Barr-Gillespie PG (2014) Accurate label-free protein quantitation with high- and low-resolution mass spectrometers. *J Proteome Res* **13**: 1034–1044.
- Kulak NA, Pichler G, Paron I, Nagaraj N, Mann M (2014) Minimal, encapsulated proteomic-sample processing applied to copy-number estimation in eukaryotic cells. *Nat Methods* **11**: 319–324.
- Kwasniak M, Pogorzelec L, Migdal I, Smakowska E, Janska H (2012) Proteolytic system of plant mitochondria. *Physiol Plant* **145**: 187–195.
- Lam H-M, Wong P, Chan H-K, Yam K-M, Chen L, Chow C-M, Coruzzi GM (2003) Overexpression of the ASN1 gene enhances nitrogen status in seeds of Arabidopsis. *Plant Physiol* **132**: 926–935.
- Li L, Nelson CJ, Trösch J, Castleden I, Huang S, Millar AH (2017) Protein degradation rate in *Arabidopsis thaliana* leaf growth and development. *Plant Cell* **29**: 207–228.

- Liebermeister W, Noor E, Flamholz A, Davidi D, Bernhardt J, Milo R** (2014) Visual account of protein investment in cellular functions. *Proc Natl Acad Sci U S A* **111**: 8488–8493.
- Ludwików A, Kierzek D, Gallois P, Zeef L, Sadowski J** (2009) Gene expression profiling of ozone-treated *Arabidopsis* abi1td insertional mutant: protein phosphatase 2C ABI1 modulates biosynthesis ratio of ABA and ethylene. *Planta* **230**: 1003–1017.
- MacLean B, Tomazela DM, Shulman N, Chambers M, Finney GL, Frewen B, Kern R, Tabb DL, Liebler DC, MacCoss MJ** (2010) Skyline: an open source document editor for creating and analyzing targeted proteomics experiments. *Bioinformatics* **26**: 966–968.
- Marshall RS, Vierstra RD** (2018) Autophagy: the master of bulk and selective recycling. *Annu Rev Plant Biol* **69**: 173–208.
- McClellan AJ, Tam S, Kaganovich D, Frydman J** (2005) Protein quality control: chaperones culling corrupt conformations. *Nat Cell Biol* **7**: 736–741.
- Merchante C, Stepanova AN, Alonso JM** (2017) Translation regulation in plants: an interesting past, an exciting present and a promising future. *Plant J* **90**: 628–653.
- Mergner J, Frejno M, List M, Papacek M, Chen X, Chaudhary A, Samaras P, Richter S, Shikata H, Messerer M, et al.** (2020) Mass-spectrometry-based draft of the *Arabidopsis* proteome. *Nature* **579**: 409–414.
- Michaeli S, Galili G** (2014) Degradation of organelles or specific organelle components via selective autophagy in plant cells. *Int J Mol Sci* **15**: 7624–7638.
- Nelson CJ, Millar AH** (2015) Protein turnover in plant biology. *Nat Plants* **1**: 15017.
- Newton GL, Dorian R, Fahey RC** (1981) Analysis of biological thiols: derivatization with monobromobimane and separation by reverse-phase high-performance liquid chromatography. *Anal Biochem* **114**: 383–387.
- Nishimura K, Kato Y, Sakamoto W** (2016) Chloroplast proteases: updates on proteolysis within and across suborganellar compartments. *Plant Physiol* **171**: 2280–2293.
- O’Leary BM, Lee CP, Atkin OK, Cheng R, Brown TB, Millar AH** (2017) Variation in leaf respiration rates at night correlates with carbohydrate and amino acid supply. *Plant Physiol* **174**: 2261–2273.
- Pandey N, Ranjan A, Pant P, Tripathi RK, Ateek F, Pandey HP, Patre UV, Sawant SV** (2013) CAMTA 1 regulates drought responses in *Arabidopsis thaliana*. *BMC Genomics* **14**: 216.
- Perez-Riverol Y, Csordas A, Bai J, Bernal-Llinares M, Hewapathirana S, Kundu DJ, Inuganti A, Griss J, Mayer G, Eisenacher M, et al.** (2019) The PRIDE database and related tools and resources in 2019: improving support for quantification data. *Nucleic Acids Res* **8**: D442–D450.
- Perera IY, Hung C-Y, Moore CD, Stevenson-Paulik J, Boss WF** (2008) Transgenic *Arabidopsis* plants expressing the type 1 inositol 5-phosphatase exhibit increased drought tolerance and altered abscisic acid signaling. *Plant Cell* **20**: 2876–2893.
- Pinheiro C, Chaves MM** (2011) Photosynthesis and drought: can we make metabolic connections from available data? *J Exp Bot* **62**: 869–882.
- Pottosin I, Shabala S** (2016) Transport across chloroplast membranes: optimizing photosynthesis for adverse environmental conditions. *Mol Plant* **9**: 356–370.
- Preuten T, Cincu E, Fuchs J, Zoschke R, Liere K, Börner T** (2010) Fewer genes than organelles: extremely low and variable gene copy numbers in mitochondria of somatic plant cells. *Plant J* **64**: 948–959.
- Rauniyar N** (2015) Parallel reaction monitoring: a targeted experiment performed using high resolution and high mass accuracy mass spectrometry. *Int J Mol Sci* **16**: 28566–28581.
- Schwanhäusser B, Busse D, Li N, Dittmar G, Schuchhardt J, Wolf J, Chen W, Selbach M** (2011) Global quantification of mammalian gene expression control. *Nature* **473**: 337–342.
- Smart RE, Bingham GE** (1974) Rapid estimates of relative water content. *Plant Physiol* **53**: 258–260.
- Stührwoldt N, Schaller A** (2019) Regulation of plant peptide hormones and growth factors by post-translational modification. *Plant Biol* **21**(Suppl 1): 49–63.
- Suraweera A, Münch C, Hanssum A, Bertolotti A** (2012) Failure of amino acid homeostasis causes cell death following proteasome inhibition. *Mol Cell* **48**: 242–253.
- Szabados L, Savouré A** (2010) Proline: a multifunctional amino acid. *Trends Plant Sci* **15**: 89–97.
- Thal B, Braun H-P, Eubel H** (2018) Proteomic analysis dissects the impact of nodulation and biological nitrogen fixation on *Vicia faba* root nodule physiology. *Plant Mol Biol* **97**: 233–251.
- Thimm O, Bläsing O, Gibon Y, Nagel A, Meyer S, Krüger P, Selbig J, Müller LA, Rhee SY, Stitt M** (2004) MAPMAN: a user-driven tool to display genomics data sets onto diagrams of metabolic pathways and other biological processes. *Plant J* **37**: 914–939.
- Tyanova S, Temu T, Sinitcyn P, Carlson A, Hein MY, Geiger T, Mann M, Cox J** (2016) The Perseus computational platform for comprehensive analysis of (prote)omics data. *Nat Methods* **13**: 731–740.
- Tzin V, Galili G** (2010) New insights into the shikimate and aromatic amino acids biosynthesis pathways in plants. *Mol Plant* **3**: 956–972.
- van der Hoorn RAL** (2008) Plant proteases: from phenotypes to molecular mechanisms. *Annu Rev Plant Biol* **59**: 191–223.
- Vierstra RD** (2009) The ubiquitin-26S proteasome system at the nexus of plant biology. *Nat Rev Mol Cell Biol* **10**: 385–397.
- Wang Q, Guo Q, Guo Y, Yang J, Wang M, Duan X, Niu J, Liu S, Zhang J, Lu Y et al.** (2018) *Arabidopsis* subtilase SASP is involved in the regulation of ABA signaling and drought tolerance by interacting with OPEN STOMATA 1. *J Exp Bot* **69**: 4403–4417.
- Wiesenthal AA, Müller C, Harder K, Hildebrandt J-P** (2019) Alanine, proline and urea are major organic osmolytes in the snail *Theodoxus fluviatilis* under hyperosmotic stress. *J Exp Biol* **222**: jeb193557.
- Wuyts N, Palauqui J-C, Conejero G, Verdeil J-L, Granier C, Massonnet C** (2010) High-contrast three-dimensional imaging of the *Arabidopsis* leaf enables the analysis of cell dimensions in the epidermis and mesophyll. *Plant Methods* **6**: 1–14.
- Zhang H, Liu P, Guo T, Zhao H, Bensaddek D, Hebersold R, Xiong L** (2019) *Arabidopsis* proteome and the mass spectral assay library. *Sci Data* **6**: 278.

A How to calculate the mass content of individual proteins in the leaf:

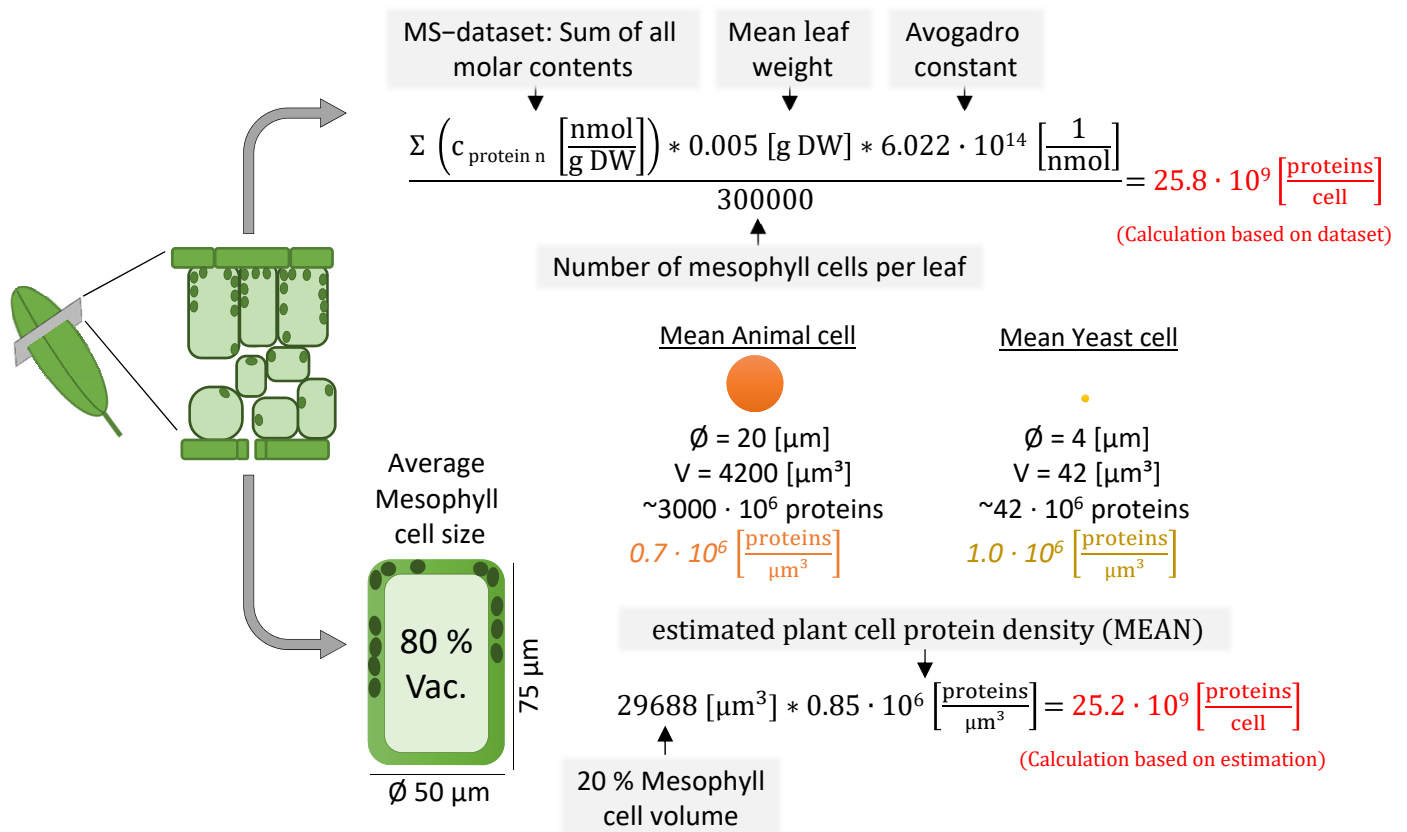
$$\frac{\text{Raw iBAQ} \cdot \text{Molecular weight}}{\sum (\text{iBAQ}_{\text{protein n}} \cdot \text{MW}_{\text{protein n}})} * \text{Protein content} * 1000 = \text{mass content}_{\text{protein A}}$$

Sum of all weighted iBAQs of MS sample

B How to calculate the molar content of individual proteins in the leaf:

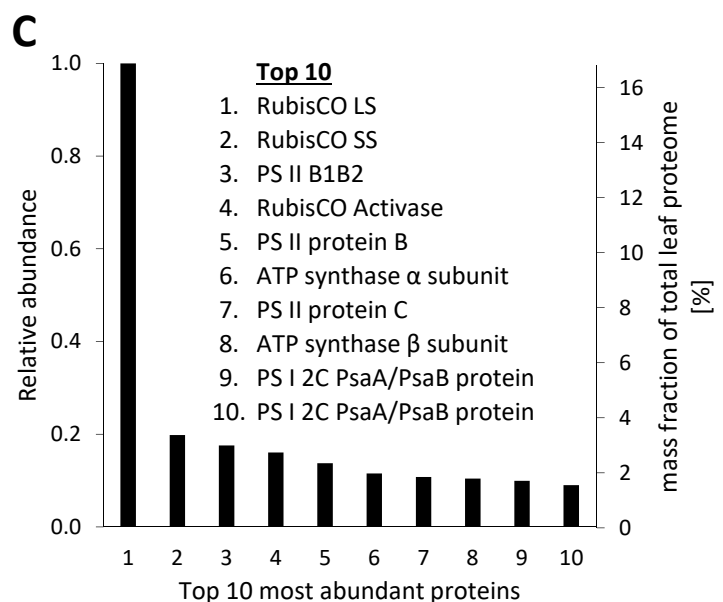
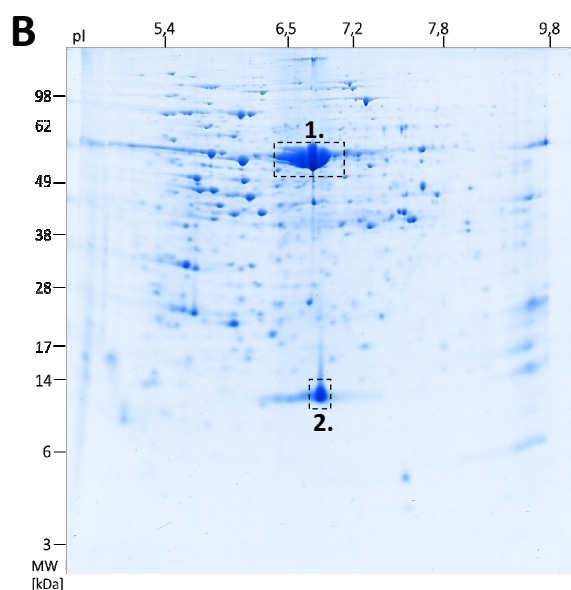
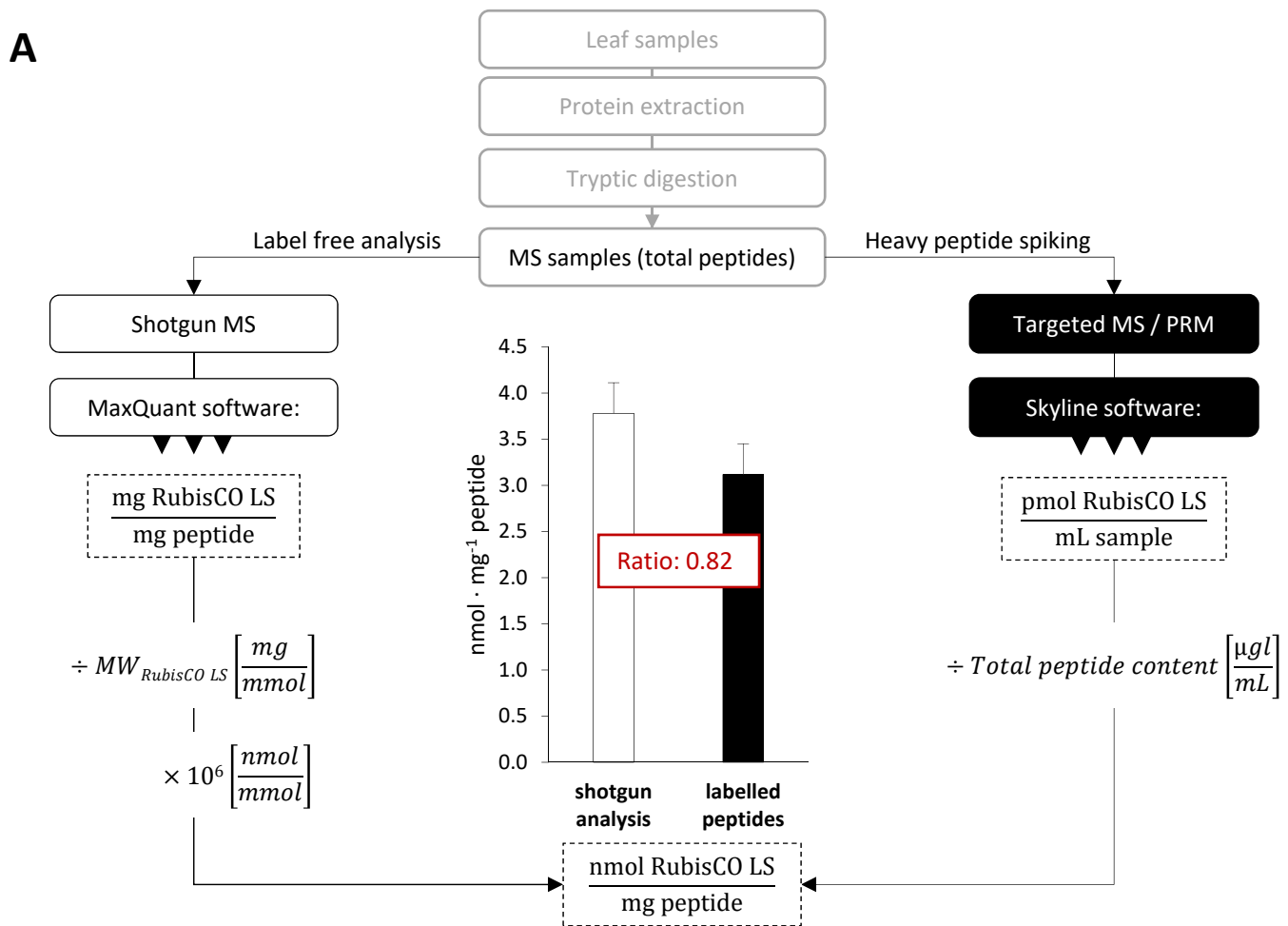
$$\frac{\text{mass content}_{\text{protein A}}}{\text{MW}_{\text{protein A}}} * 1000 = \text{molar content}_{\text{protein A}}$$

C How to calculate protein copy numbers per cell:



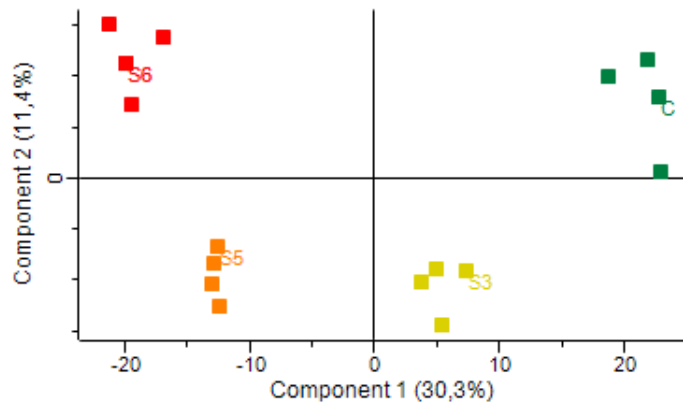
Supplemental Figure S1: Calculation of individual protein contents and copy numbers

A, Raw iBAQ values generated by MaxQuant were multiplied with the molecular weight of the respective protein [$\text{g} \cdot \text{mol}^{-1}$]. These individual weighted iBAQs were then divided by the sum of weighted iBAQs of all detected proteins for normalization and means of the four biological replicates in each sample group were calculated. The mean mass fractions were then multiplied with the total protein content of the sample [$\text{mg} \cdot \text{g}^{-1} \text{ DW}$] to determine the mass content of each individual protein [$\mu\text{g} \cdot \text{g}^{-1} \text{ DW}$]. B, Individual protein molar contents could be calculated by dividing the individual mass protein contents by the respective molecular weight C, Upper arrow: The sum of all molar protein contents (iBAQ based) was multiplied with the Avogadro constant and an average leaf dry weight (200 mm², 20 d, long-day conditions). The product divided by the cell number leads to the total protein copy number. Considering the low protein content of epidermis cells, the average cell number and cell size were focused only on mesophyll cells. Lower arrow: A theoretical estimation of the total protein count. The average volume of a mesophyll cell (mean palisade and spongy, without vacuole) was multiplied with an estimated value for the protein density in a plant cell based on protein densities calculated from published datasets of animal (orange) and yeast cells (yellow). Results are highlighted in red.



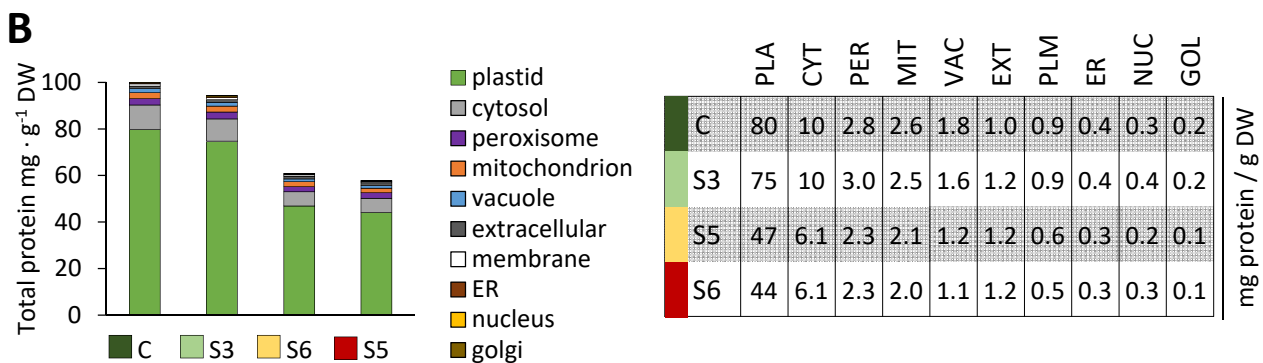
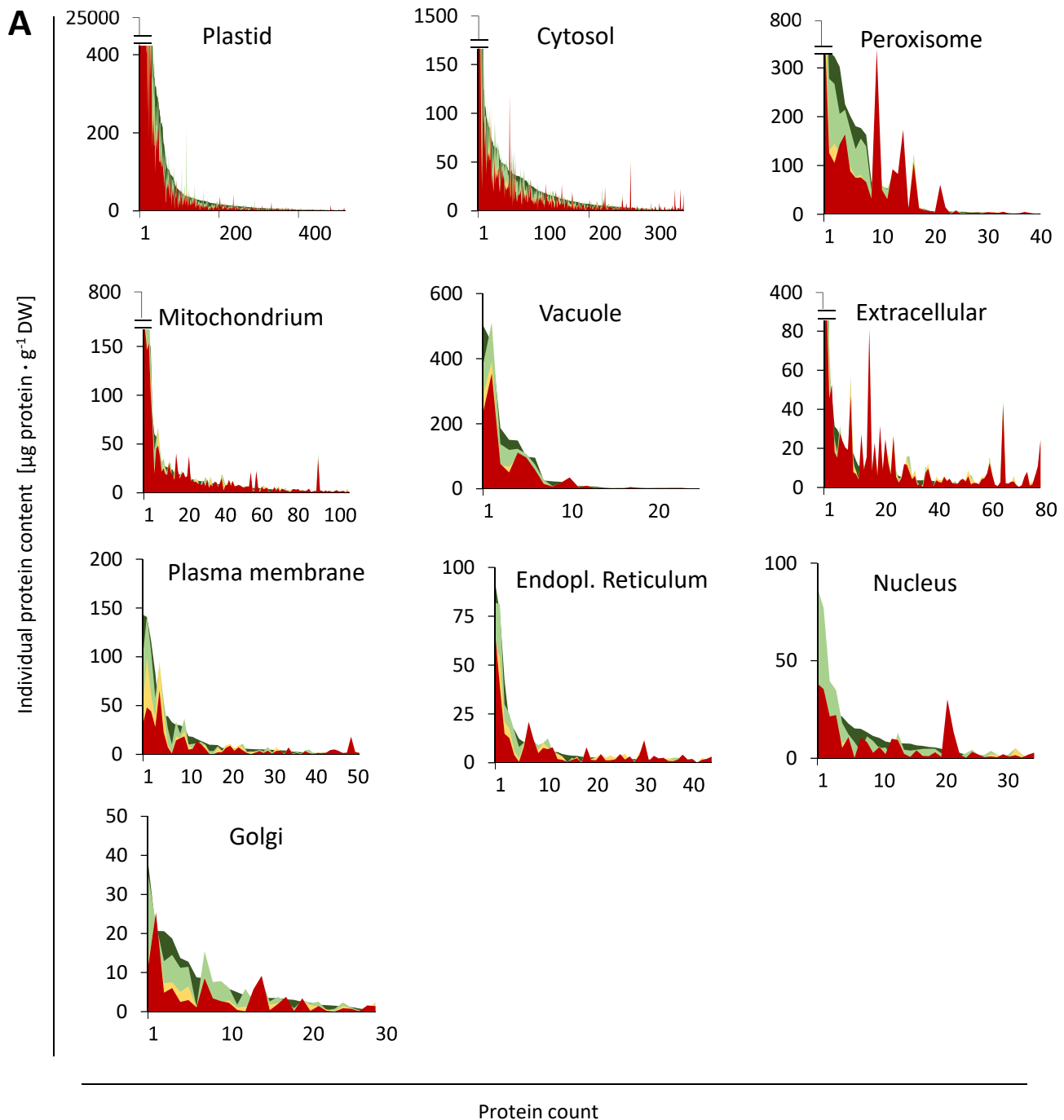
Supplemental Figure S2: Estimation of the absolute content of RubisCO large subunit

A, Estimation based on labeled peptides: The content of RubisCO LS (Atcg00490) in the MS samples of control plants [nmol RubisCO LS/mg peptide] was determined in two ways: 1. based on iBAQ values derived from shotgun MS (white bar, workflow on the left hand side of the graph) and 2. by spiking of the samples with labeled peptides (black bar, workflow on the right hand side of the graph). The ratio between the RubisCO LS content determined using labeled peptides and the one derived from shotgun MS represents the mass fraction of the leaf proteome detectable by our MS shotgun approach. Values are means \pm SD (n = 4). B, Estimation based on visual impression: IEF/SDS PAGE of Arabidopsis total leaf extract. Protein extraction and gel electrophoresis were performed as described in Mihr and Braun (2003; doi: 10.1007/978-1-59259-414-6_28). C, Relative mass abundance of the ten most abundant leaf proteins according to our shotgun proteomic results. The second Y-axis indicates the mass fraction of the total leaf proteome. The two largest spots on the gel correspond to the first two hits in the MS dataset (1. RubisCO LS, 2. RubisCO SS) and no additional spots of larger or similar size are visible. Thus, the estimation of RubisCO abundance in leaves based on our MS dataset seems to be realistic. (MW; molecular weight, PRM; parallel reaction monitoring)



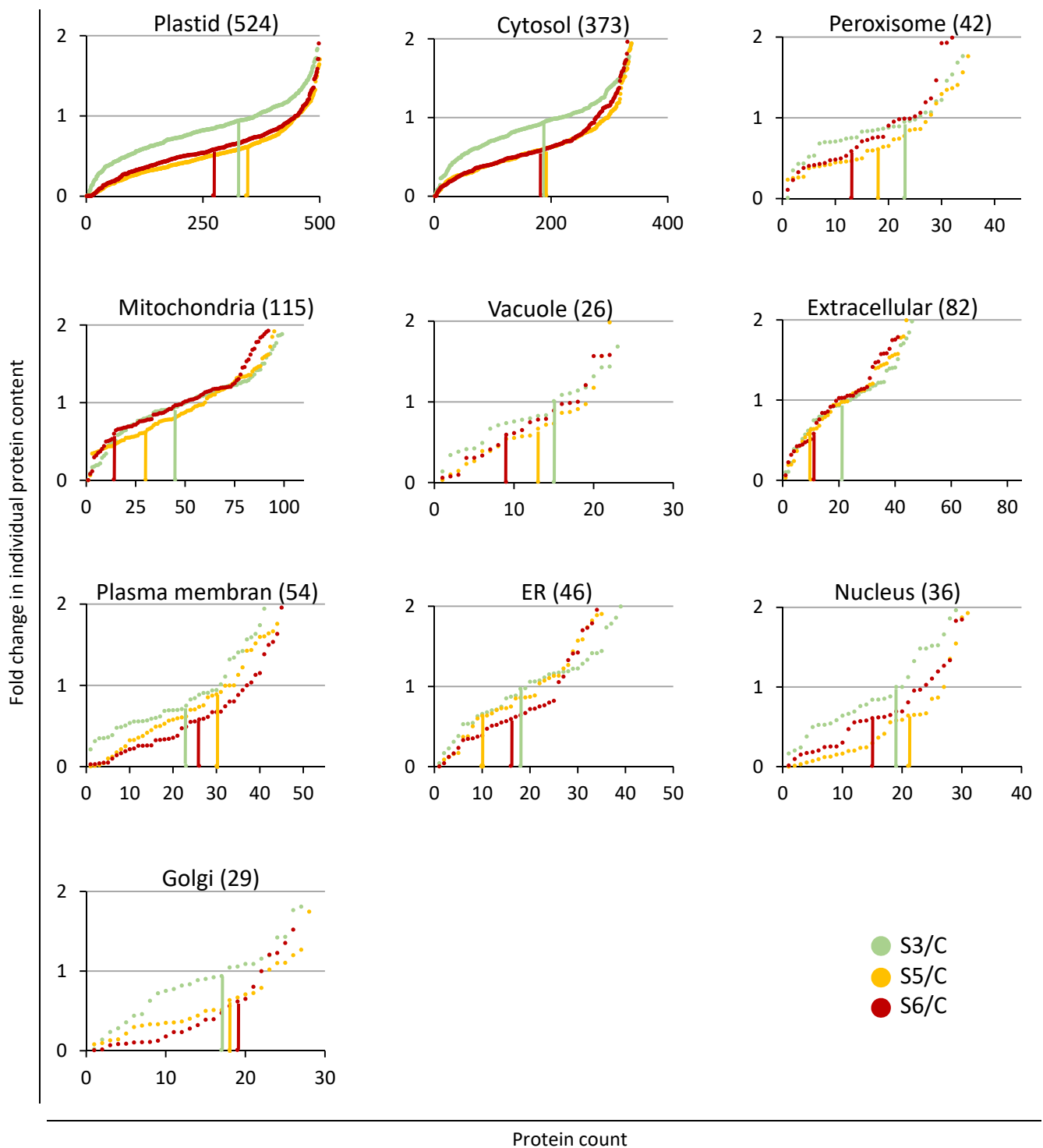
Supplemental Figure S3: Principal component analysis of the MS dataset

Principle component analysis (PCA; with PERSEUS software) of MS dataset (C, S3, S5, S6). Samples were harvested during progressive drought stress of *Arabidopsis thaliana* (n=4). Green: Control - watered, Yellow: S3 – mild stress, Orange: S5 – moderate stress, Red: S6 – severe stress.



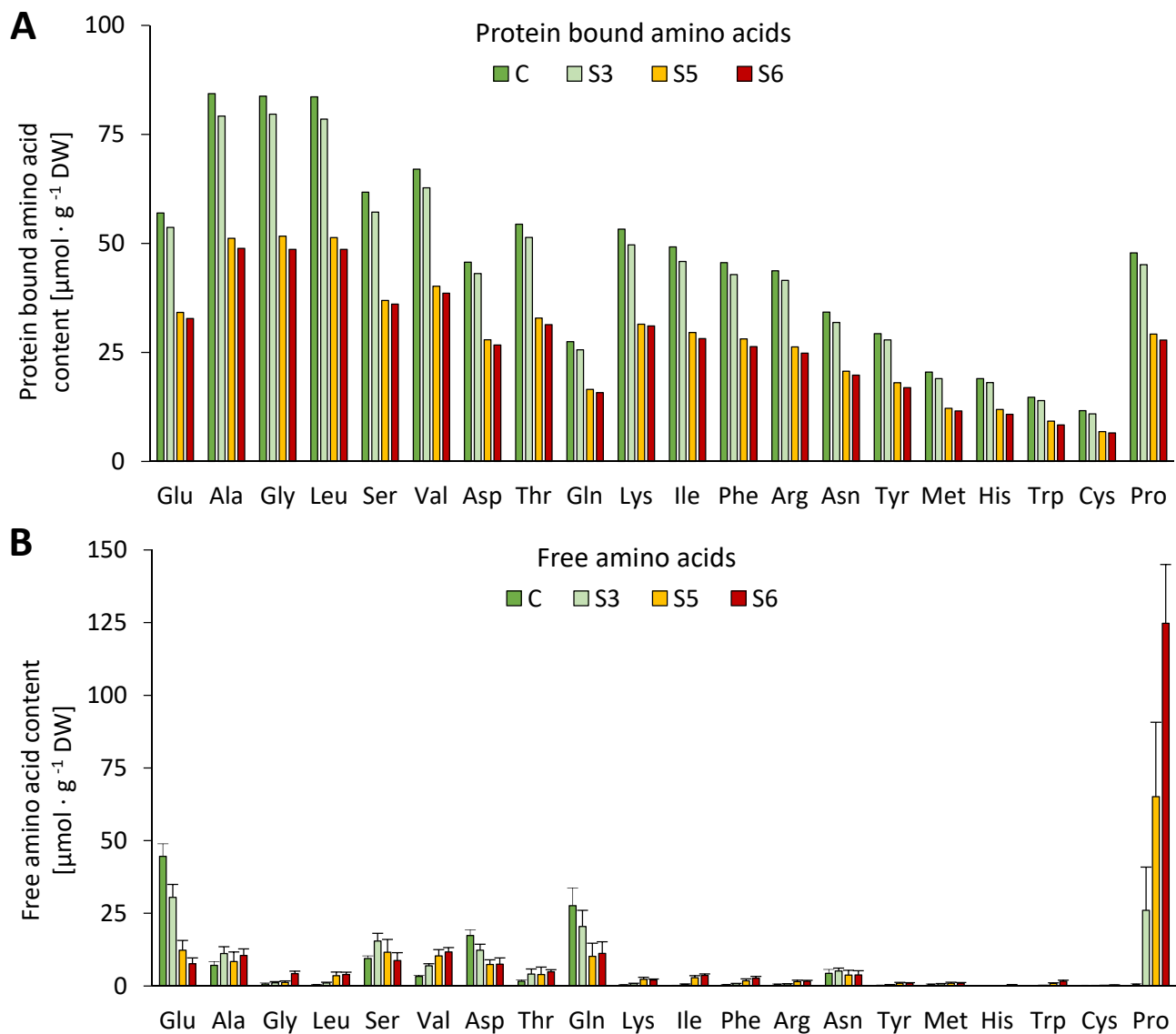
Supplemental Figure S4: Compartment-specific patterns of stress-induced changes in individual protein abundances: Individual protein contents

A, Absolute contents [$\mu\text{g protein} \cdot \text{g}^{-1} \text{DW}$] of all individual proteins detected by shotgun proteomics in descending order (under control conditions) for subcellular compartments. Protein contents under control and stress conditions are shown in superimposed graphs (corresponding colors are shown in B). B, Shares of subcellular compartments to the total protein content of control and stressed plants. The subcellular localization of the individual proteins has been predicted by SUBA4 (Hooper et al. 2017).



Supplemental Figure S5: Compartment-specific patterns of stress-induced changes in individual protein abundances: Fold change ratios

Fold change ratios of individual protein contents in stressed vs. control plants. In order to visualize the fraction of proteins with average, high or low degradation rates, changes in individual protein contents were sorted in ascending order for each stress level. Vertical lines indicate proteins that correspond exactly to the decrease in total protein content, i.e., 0.94 for stress level S3 (light green), 0.61 for S5 (orange), and 0.58 at S6 (red). The subcellular localization of the individual proteins has been predicted by SUBA4 (Hooper et al. 2017). Only proteins with unambiguous assignments are shown. The fold changes in individual protein contents were calculated using absolute protein contents based on iBAQ values (Supplemental Dataset S1).



Supplemental Figure S6: Protein bound and free amino acids during progressive drought stress in Arabidopsis rosette leaves

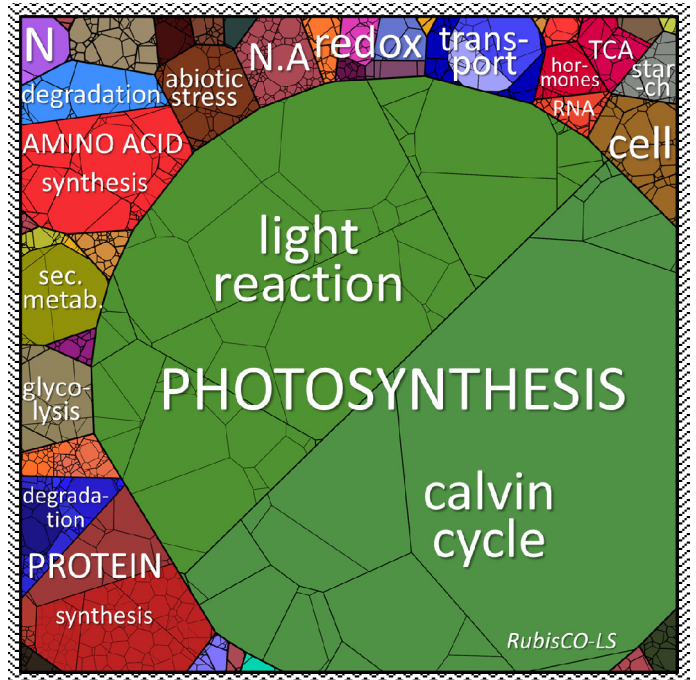
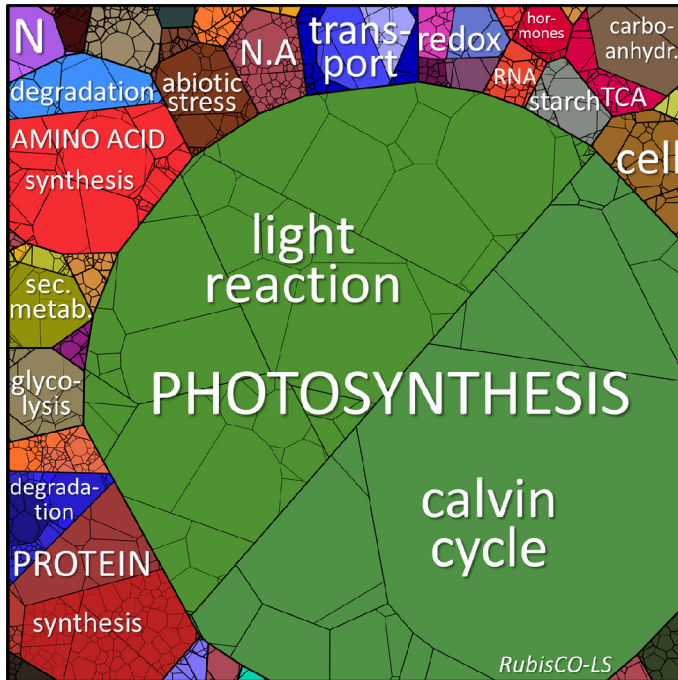
A, Free amino acids were quantified by HPLC. B, Protein bound amino acids were calculated from the amino acid composition and the leaf content of all individual proteins detected by shot-gun proteomics. The complete dataset can be found in Supplemental Dataset S6 and Supplemental Dataset S7. Values are means \pm SD (n = 4).

Control

102 mg protein · g⁻¹ DW

Stress 3

96 mg protein · g⁻¹ DW

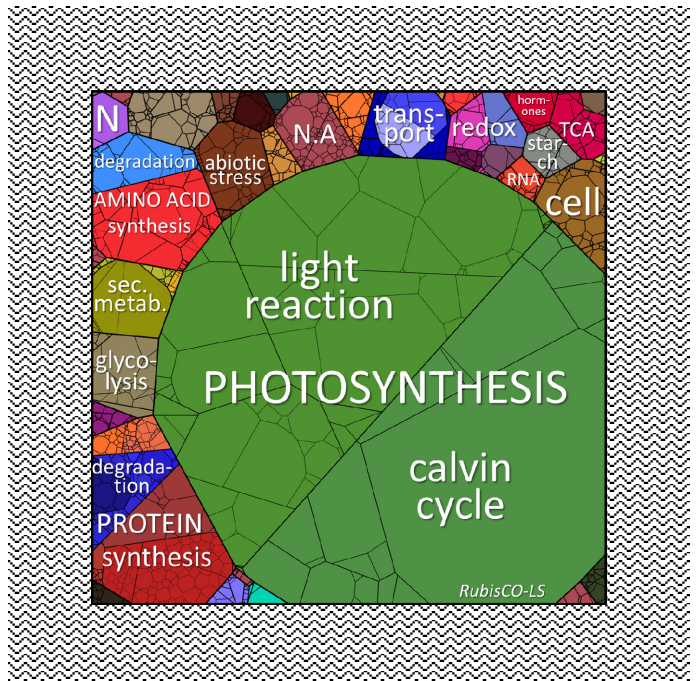
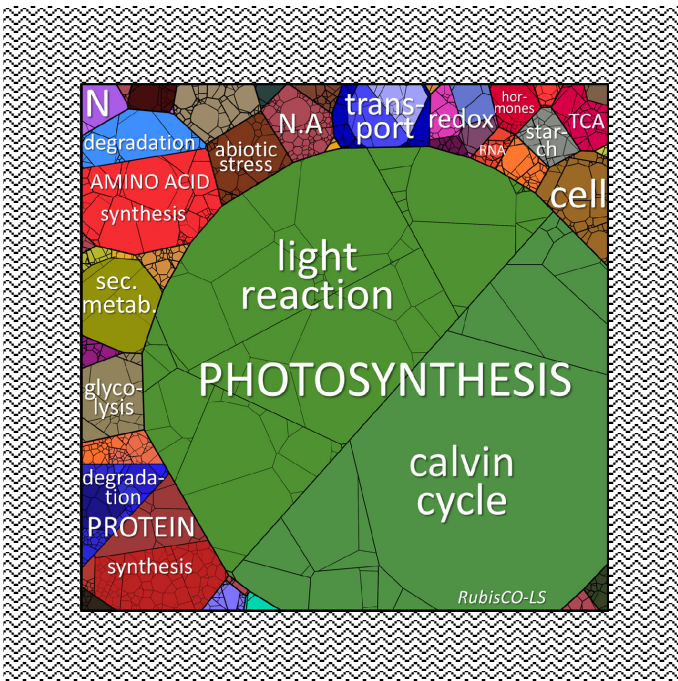


Stress 5

62 mg protein · g⁻¹ DW

Stress 6

59 mg protein · g⁻¹ DW



Supplemental Figure S7: Changes in the quantitative composition of the leaf proteome during drought stress

A curated MapMan annotation list (<https://mapman.gabipd.org>) was used as main database for protein categories (33,600 entries). Relative iBAQ values [%] calculated with the MS-dataset (C, S3, S5, S6; 1399 proteins) were then uploaded and aligned to create PROTEOmaps (<https://bionic-vis.biologie.uni-greifswald.de>). Sizes are adjusted to the leaf total protein content to allow a quantitative comparison across the samples. Shaded areas represent the fraction of the proteome degraded during drought stress. Proteins involved in similar cellular functions according to the MapMan annotation file (version Ath_AGI_LOCUS_TAIR10_Aug2012, Thimm et al. 2004) are arranged in adjacent locations and visualized by colors. Mass fractions of the functional categories [%] are provided in Supplemental Dataset S3

2.3 The role of amino acid metabolism in signaling and metabolic adaption to stress induced energy deficiency in plants

Heinemann, B. and Hildebrandt, T.M.

Institute of Plant Genetics, Leibniz Universität Hannover, Hannover, Germany

Type of authorship:	First author
Type of article:	Invited mini review
Share of the work:	30 %
Contribution to the publication:	Analyzed data and prepared figures, participated in writing the manuscript
Journal:	Journal of experimental botany
Impact factor:	5.908 (2019)
Date of Publication:	16.05.2021
DOI:	10.1093/jxb/erab182
PubMed-ID:	33993299

EXPERT VIEW

The role of amino acid metabolism in signaling and metabolic adaptation to stress-induced energy deficiency in plants

Björn Heinemann^{ID} and Tatjana M. Hildebrandt^{*ID}

Institute for Plant Genetics, Department of Plant Proteomics, Leibniz University Hannover, Herrenhäuser Straße 2, 30419 Hannover, Germany

* Correspondence: hildebrandt@genetik.uni-hannover.de

Received 25 November 2020; Editorial decision 20 April 2021; Accepted 26 April 2021

Editor: Karl-Josef Dietz, Bielefeld University, Germany

Abstract

The adaptation of plant metabolism to stress-induced energy deficiency involves profound changes in amino acid metabolism. Anabolic reactions are suppressed, whereas respiratory pathways that use amino acids as alternative substrates are activated. This review highlights recent progress in unraveling the stress-induced amino acid oxidation pathways, their regulation, and the role of amino acids as signaling molecules. We present an updated map of the degradation pathways for lysine and the branched-chain amino acids. The regulation of amino acid metabolism during energy deprivation, including the coordinated induction of several catabolic pathways, is mediated by the balance between TOR and SnRK signaling. Recent findings indicate that some amino acids might act as nutrient signals in TOR activation and thus promote a shift from catabolic to anabolic pathways. The metabolism of the sulfur-containing amino acid cysteine is highly interconnected with TOR and SnRK signaling. Mechanistic details have recently been elucidated for cysteine signaling during the abscisic acid-dependent drought response. Local cysteine synthesis triggers abscisic acid production and, in addition, cysteine degradation produces the gaseous messenger hydrogen sulfide, which promotes stomatal closure via protein persulfidation. Amino acid signaling in plants is still an emerging topic with potential for fundamental discoveries.

Keywords: Abiotic stress, alternative respiration, amino acid metabolism, branched-chain amino acid degradation, energy deficiency, lysine degradation, signaling, SnRK, TOR.

Introduction

Plants are confronted with a broad spectrum of unfavorable environmental conditions ranging from drought to flooding, high salinity, or extreme temperatures. Often, these abiotic stresses occur not individually but in combination (e.g. dry heat), and they might even coincide with attacks by various pathogens. Being sessile, plants had to develop a sophisticated metabolic defense system to differentiate between the various

threats, correctly assess them, and adapt their defense strategy accordingly. Many aspects of this complex regulatory system are still unknown. Several strategies to cope with the different challenges of abiotic stress require major adaptations in amino acid metabolism (Fig. 1). The proteome has to be modified to shift from growth to defense, including increased synthesis of proteins required for stress tolerance and damage control at

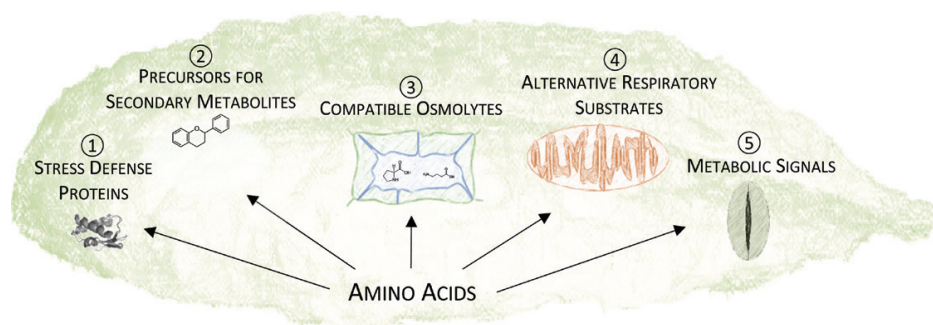


Fig. 1. Major functions of amino acid metabolism during the abiotic stress response in plants. During abiotic stress, amino acids are required as precursors for stress-induced proteins (1) and secondary metabolites (2), and as osmoprotectants (3), substrates for mitochondrial ATP production (4), and signaling molecules (5). This review mainly focuses on aspects 4 and 5.

the expense of a decrease in the photosynthetic apparatus and anabolic enzymes (Less *et al.* 2011; Gururani *et al.*, 2015). This shift inevitably leads to large fluxes through the free amino acid pool and changes in its composition. At the same time, *de novo* nitrogen assimilation and amino acid synthesis are often restricted by low transpiration rates and limited availability of energy (Araus *et al.*, 2020). Still, a sufficient supply of the 20 proteinogenic amino acids is required for the synthesis of stress-relevant proteins.

In addition to proteins, the spectrum of defense compounds derived from amino acids includes a highly diverse set of secondary metabolites with often complex structures. Several classes of secondary metabolites have been reported to accumulate under diverse stressful environmental conditions but their exact functions are largely not clear (Box 1). Osmotic stress during severe drought or high salinity leads to a loss in cell turgor, which can be counteracted by increasing the amount of non-toxic small molecules. Thus, a low water potential strongly induces the synthesis of compatible solutes to maintain cell turgor and stabilize membrane and protein integrity (Singh *et al.*, 2015). Proline acts as a major osmoprotectant in plants (Szabados and Savouré, 2010). During severe drought it constitutes 20% of the total amino acid pool and thus ties up valuable resources but also acts as a nitrogen store (Heinemann *et al.*, 2021). Proline accumulation in the cytosol might also be relevant for balancing the increased vacuolar osmolarity due to autophagic degradation of macromolecules during stress (Signorelli *et al.*, 2019).

A major problem in coping with diverse stressful conditions is energy deprivation. Resources are scarce due to restricted photosynthetic activity and have to be diverted from growth into defense and stress tolerance, leading to a general decrease in cellular energy levels (Biswal *et al.*, 2011; Gururani *et al.*, 2015). Stress may also require prioritizing the growth of specific organs over others and thus cause a local energy deficit. For example, increasing root growth at the expense of flowers or leaves may improve the water supply sufficiently for the plant to survive limited periods of severe drought. Metabolic adaptation to energy deprivation utilizes amino acids as signaling

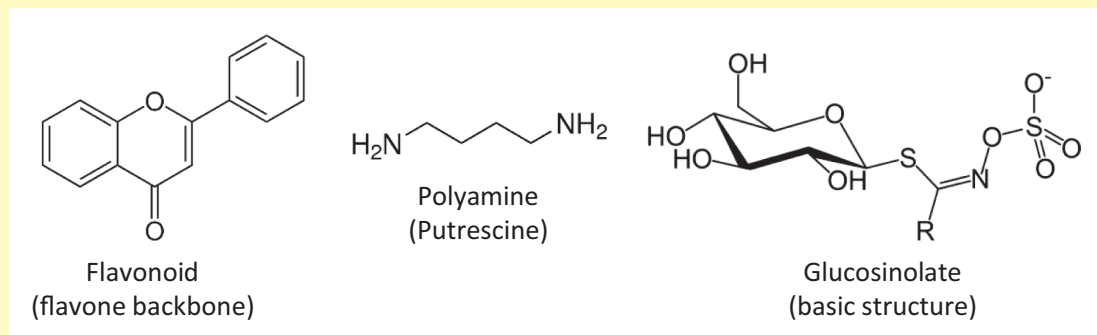
molecules and alternative substrates, and these aspects will be the focus of this short review.

Plants cope with energy shortage by activating respiratory pathways that use amino acids as alternative substrates

When carbohydrate stores are depleted, plants induce catabolic pathways (autophagy, lipid and protein degradation) to provide alternative substrates for ATP production. The induction of the respective pathways during different stress conditions associated with energy deprivation, such as drought or low light conditions, has repeatedly been demonstrated on a transcript and a protein level (Less and Galili, 2008; Angelovici *et al.*, 2013). Mutants with defects in the autophagy apparatus show poor growth and early senescence when exposed to carbon and/or nitrogen starvation, drought, or high salinity, demonstrating the physiological relevance of this bulk degradation pathway for energy homeostasis during stress (Liu and Bassham, 2012; Izumi *et al.*, 2013; Hirota *et al.*, 2018; Tang and Bassham, 2018). Severe dehydration can lead to a substantial loss in protein mass, indicating that the demand for the resources tied up in proteins is high (Heinemann *et al.*, 2021). Amino acid degradation produces tricarboxylic acid cycle intermediates or precursors and thus contributes to the production of substrates for mitochondrial respiration. Notably, the oxidation of amino acids with a complex structure (branched-chain and aromatic amino acids) provides comparable amounts of energy for ATP synthesis to those provided by glucose (Hildebrandt *et al.*, 2015). The catabolic pathways of branched-chain amino acids (BCAAs), lysine, and proline are even physically connected to the mitochondrial respiratory chain, since individual reaction steps transfer electrons into the ubiquinone pool. However, not all the enzymes required for amino acid degradation in plants are known yet, and the mechanisms of their regulation remain partially elusive, hampering progress in fully understanding—let alone exploiting—their role in stress tolerance.

Box 1. Amino acids as precursors for secondary metabolites during abiotic stress

The role of secondary metabolites derived from amino acid metabolism in abiotic stress tolerance is a large field with many open questions. Most importantly, specific functions of these highly complex and diverse molecules, beyond ROS scavenging, have to be addressed.



Flavonoids derived from phenylalanine or tyrosine strongly accumulate under various abiotic stress conditions such as UV, temperature, salt, and drought (Nabavi *et al.*, 2020; Falcone Ferreyra *et al.*, 2012). Flavonoids are ubiquitous in the plant kingdom, and estimations suggest that ~20% of the total carbon flux accounts for this pathway (Haslam, 1993). A total of 54 different flavonoids have been identified in *Arabidopsis*, among them 11 anthocyanins, which cause the characteristic purple color that indicates suboptimal conditions (Saito *et al.*, 2013). Their postulated functions in stress defense are ROS scavenging and the storage of resources. However, since the process of synthesis of aromatic amino acids and their subsequent conversion to secondary metabolites is quite complex and expensive in terms of energy requirement, there might be additional, more specific, benefits during stress that are yet to be discovered.

Polyamines are synthesized from arginine and strongly increase during abiotic stress (reviewed by Alcázar *et al.*, 2010). The overexpression of enzymes involved in polyamine synthesis pathway leads to higher stress tolerance indicating a protective role. However, their function is largely unknown and possibly involves signaling.

Glucosinolates are synthesized from a range of amino acids, including methionine, tryptophan, and phenylalanine specifically in Brassicaceae (reviewed by Halkier and Gershenzon, 2006). They are well known for their contribution to herbivore tolerance, since breakdown upon tissue damage leads to the production of toxic and highly reactive compounds. However, auxin signaling maintains the expression of enzymes involved in glucosinolate biosynthesis during drought, indicating an additional function of these secondary metabolites in abiotic stress resistance. Indeed, increased levels of aliphatic glucosinolates improve drought tolerance in *Arabidopsis*, and a breakdown product, possibly isothiocyanate, promotes stomatal closure independently of ABA signaling (Salehin *et al.*, 2019).

Recently, there has been some clear progress with respect to lysine and BCAA catabolism (Fig. 2; see also Box 2). These amino acids can feed electrons into the mitochondrial respiratory chain via the electron-transfer flavoprotein (ETF)-ubiquinone oxidoreductase complex (ETFQO) (Ishizaki *et al.*, 2005). The initial four reaction steps in lysine catabolism leading to 2-oxoadipate are conserved between animals and plants (Fig. 2, left). An unusual oxidative decarboxylation and hydroxylation reaction is subsequently performed by a recently identified hydroxyglutarate synthase, producing D-2-hydroxyglutarate, which can then be oxidized to 2-oxoglutarate by D-2-hydroxyglutarate dehydrogenase, transferring electrons to the ETF/ETFQO system (Thompson *et al.*, 2020). Lysine can also

be converted to the immune signal *N*-hydroxyphenylpyruvic acid via three recently identified reaction steps (Ding *et al.*, 2016; Chen *et al.*, 2018; Hartmann and Zeier, 2018).

The catabolism of the three BCAAs to acetyl-CoA combines shared reaction steps that use intermediates from leucine, valine, and isoleucine degradation as a substrate with individual, amino-acid-specific steps (Fig. 2, right). Although several enzymes involved in BCAA degradation have been identified during the past 3 years, the pathway is still not complete (see Box 2, Fig. 2). The identification of the last missing steps is hampered by the large number of candidates derived from homology searches, which additionally have multiple isoforms that might be redundant.

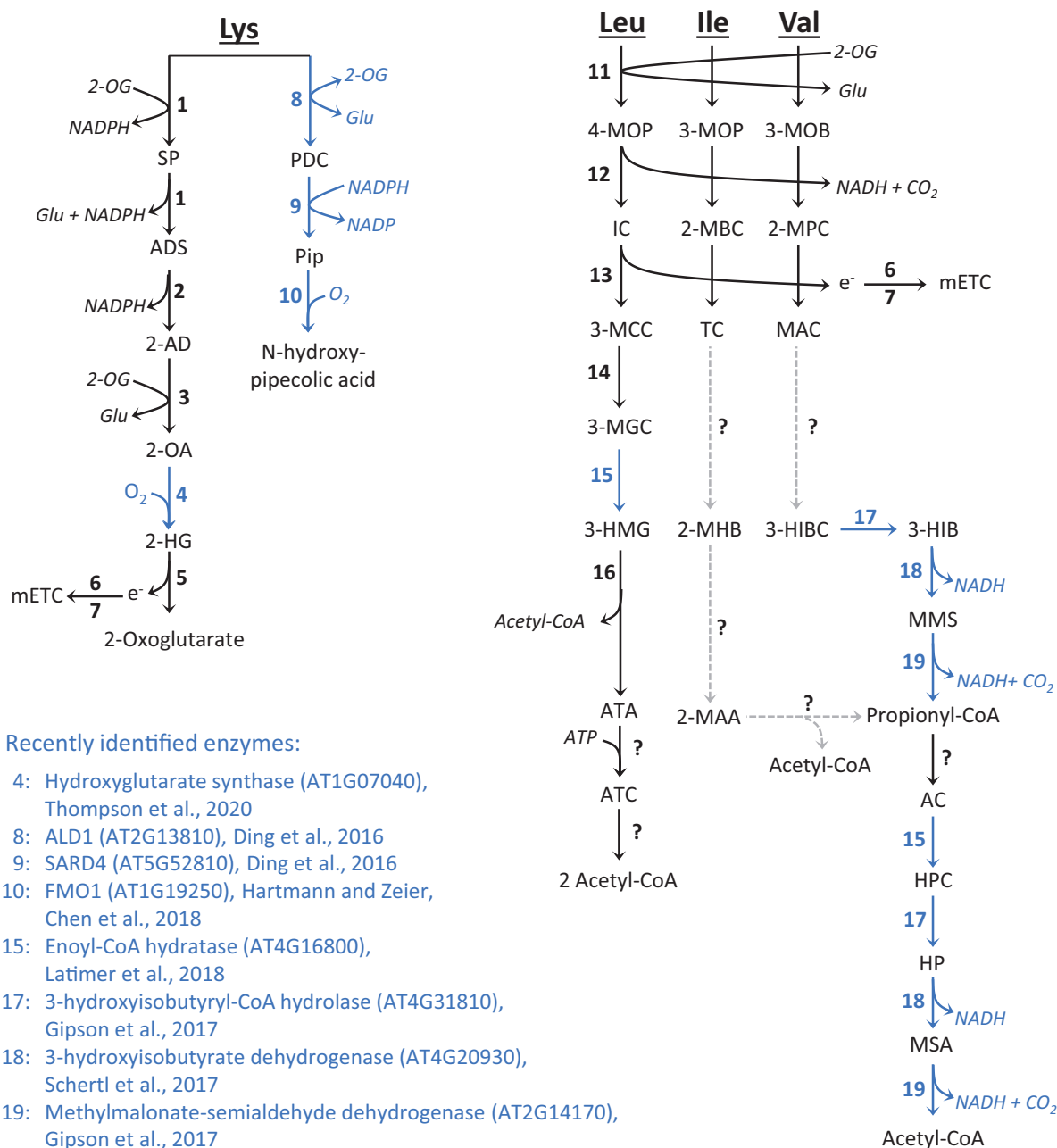


Fig. 2. An update on the catabolic pathways for lysine and branched-chain amino acids in plants. Recently identified reaction steps are shown in blue (see also Box 2). Published information about the previously known steps is summarized in Hildebrandt et al. (2015). Previously identified enzymes: 1, lysine-ketoglutarate reductase/saccharopine dehydrogenase (AT4G33150); 2, aldehyde dehydrogenase 7B4 (AT1G54100); 3, GABA transaminase (AT3G22200); 5, D-2-hydroxyglutarate dehydrogenase (AT4G36400); 6, electron transfer flavoprotein (AT1G50940, AT5G43430); 7, electron-transfer flavoprotein:ubiquinone oxidoreductase (AT2G43400); 11, BCAA transaminase (AT1G10060, AT1G10070, AT3G49680, AT3G19710, AT5G65780, AT1G50110, AT1G50090); 12, branched-chain alpha-keto acid dehydrogenase (AT5G09300, AT1G21400, AT3G13450, AT1G55510, AT3G06850); 13, isovaleryl-CoA-dehydrogenase (AT3G45300); 14, methylcrotonyl-CoA carboxylase (AT1G03090, AT4G34030); 16, hydroxymethylglutaryl-CoA lyase (AT2G26800); ?, Unknown reaction steps. Metabolites: 2-AD, 2-aminoadipate; 2-HG, D-2-hydroxyglutarate; 2-MAA, 2-methylacetoacetyl-CoA; 2-MBC, 2-methylbutanoyl-CoA; 2-MHB, 2-methyl-3-hydroxybutyryl-CoA; 2-MPC, 2-methylpropanoyl-CoA; 2-OA, 2-oxoadipate; 2-OG, 2-oxoglutarate; 3-HIB, 3-hydroxyisobutyrate; 3-HIBC, 3-hydroxyisobutyryl-CoA; 3-HMG, 3-hydroxymethylglutaryl-CoA; 3-MCC, 3-methylcrotonyl-CoA; 3-MGC, 3-methylglutaconyl-CoA; 3-MOB, 3-methyl-2-oxobutanoate; 3-MOP, 3-methyl-2-oxopentanoate; 4-MOP, 4-methyl-2-oxopentanoate; AC, acrylyl-CoA; ADS, 2-aminoadipate-6-semialdehyde; ATA, acetoacetate; ATC, acetoacetyl-CoA; HP, hydroxypropionate; HPC, hydroxypropionyl-CoA; IC, isovaleryl-CoA; MAC, methylacrylyl-CoA; MMS, methylmalonate semialdehyde; MSA, malonate semialdehyde; PDC, L-Δ1-piperidine-2-carboxylate; Pip, L-pipecolate; SP, saccharopine; TC, tiglyl-CoA. mETC, mitochondrial electron transport chain.

Box 2. Key developments in understanding the role of amino acid metabolism in signaling and metabolic adaptation to stress-induced energy deficiency

• Completing knowledge on the lysine catabolic pathway in plants

Thompson *et al.* (2020) identified the last missing step in the lysine degradation pathway in plants, which is catalyzed by a hydroxyglutarate synthase (AT1G07040; Fig. 2). This enzyme, an iron (II)-dependent oxygenase, uses an unusual catalytic mechanism to perform the oxidative decarboxylation and hydroxylation of 2-oxoadipate to D-2-hydroxyglutarate. It strongly responds to both abiotic and biotic stress on a transcriptional level.

• New insights into branched-chain amino acid catabolism in plants

Three recent studies improved our understanding of branched-chain amino acid metabolism substantially (Fig. 2). Using comparative genomics, Latimer *et al.* (2018) identified a 3-methylglutaconyl-CoA hydratase (AT4G16800) catalyzing the dehydration of 3-hydroxymethylglutaryl-CoA to 3-methylglutaconyl-CoA during leucine degradation. Schertl *et al.* (2017) characterized a 3-hydroxybutyrate dehydrogenase (AT4G20930), which can also metabolize 3-hydroxypropionate and is thus involved in both valine and isoleucine degradation. Two additional enzymes required for the degradation of valine, a 3-hydroxyisobutyryl-CoA hydrolase (AT4G31810) and a methylmalonate-semialdehyde dehydrogenase (AT2G14170), were identified and functionally characterized by Gipson *et al.* (2017).

• The molecular mechanism of activating alternative mitochondrial respiration pathways during energy deprivation

SnRK1 kinases act as central metabolic regulators during adaptation to low-energy stress. Pedrotti *et al.* (2018) demonstrated that in response to extended darkness SnRK1 phosphorylates group C bZIP transcription factors, leading to the formation of a complex containing SnRK1, C bZIP, and an additional S1 bZIP transcription factor. This complex coordinates the strong induction of genes involved in the oxidation of branched-chain amino acids, which serve as alternative respiratory substrates during carbohydrate starvation (Figs 3, 4).

• Amino acids activate TOR signaling in plants

Liu *et al.* (2021) demonstrated that 15 of the 20 proteinogenic amino acids activate TOR signaling in the leaf primordia of inorganic-nitrogen-starved seedlings, albeit with different capacities. Both inorganic nitrogen and amino acids require the plant-specific small GTPase ROP2 for TOR induction. O'Leary *et al.* (2020) performed long-term measurements of oxygen consumption rates in Arabidopsis leaves and discovered a regulatory mechanism based on the balance between individual amino acid levels. Proline and alanine, which accumulate to high concentrations during abiotic stress conditions, stimulate respiration via transcriptional up-regulation of their respective degradation pathways. Other amino acids, such as isoleucine and methionine, block this induction by activating TOR signaling.

• Cysteine triggers ABA production and stomatal closure during drought stress

Batool *et al.* (2018) described a new role of cysteine signaling in the physiological water limitation response in Arabidopsis. During soil drying, sulfate is transported to the guard cells via the xylem and incorporated into cysteine. Increased cysteine concentrations stimulate ABA biosynthesis in the leaves by activating two enzymes in the synthesis pathway (NCED3 and AAO3). Zhou *et al.* (2021), Chen *et al.* (2020), and Shen *et al.* (2020) report additional downstream regulatory steps in cysteine-induced stomatal closure mediated by post-translational activation of the protein kinase SnRK2.6, the NADPH oxidase RbohD, and the transcription factor ABI4 (ABA-INSENSITIVE 4) via persulfidation (Fig. 3).

The degradation of BCAAs and lysine is thought to be particularly relevant during stress-induced energy deficiency, since knockout lines for several reaction steps can be distinguished from the wild type by their shorter survival time in complete darkness (Ishizaki *et al.*, 2005, 2006; Araújo *et al.*, 2010; Peng *et al.*, 2015; Hirota *et al.*, 2018). They may also show decreased drought tolerance under specific growth conditions (Pires *et al.*, 2016), which, however, seems to be a less robust phenotype, since it was not observable under our experimental drought setup (Heinemann *et al.*, 2021). The defects in seed development and/or germination reported for several lines may be caused by the accumulation of toxic intermediates such as methacrylyl-CoA during embryogenesis or by starvation prior to the full establishment of photosynthesis (Ding *et al.*, 2012; Angelovici *et al.*, 2013; Peng *et al.*, 2015; Gipson *et al.*, 2017). In addition, the production of storage lipids during seed filling seems to be compromised by defects in BCAA catabolism, but the reason for this effect is not clear yet (Gipson *et al.*, 2017).

The adaptation of amino acid metabolism to energy deprivation is mediated by the balance between TOR and SnRK1 signaling

Plants need to monitor their nutritional status and integrate this information with environmental stress signals in order to react appropriately and find the best balance between growth and defense to guarantee survival and reproduction. Adapting amino acid catabolism to energy requirements is one of these tasks. The protein kinase complexes SnRK1 (Snf1-related protein kinase 1) and TOR (target of rapamycin) are to a large extent evolutionarily conserved in eukaryotes and act as central metabolic regulators (for recent reviews, see Broeckx *et al.* 2016; Baena-González and Hanson, 2017; Shi *et al.*, 2018; Wurzinger *et al.*, 2018; Caldana *et al.*, 2019; Jamsheer *et al.*, 2019; Margalha *et al.*, 2019; Rodriguez *et al.*, 2019; Ryabova *et al.*, 2019; Wu *et al.*, 2019; Fu *et al.*, 2020; Pacheco *et al.*, 2021; Sharma *et al.*, 2021). In general, TOR promotes growth when the supply of nutrients is sufficient, whereas SnRK1 acts antagonistically and restores energy homeostasis during stress (Fig. 3, Box 3).

Reciprocal regulation by TOR and SnRK1 signaling adapts plant protein and amino acid metabolism to the availability of energy and nutrients (Fig. 3). Growth-promoting conditions lead to increased TOR activity, which induces amino acid synthesis and the reinitiation of translation of specific mRNAs, but represses autophagy and amino acid degradation (van Leene *et al.*, 2019; Schepetilnikov *et al.*, 2013; Xiong *et al.*, 2013). In contrast, energy deprivation activates SnRK1 signaling, which represses TOR and induces autophagy (Nukarinen *et al.*, 2016; Huang *et al.*, 2019). Recent evidence suggests that the coordinated induction of key enzymes in amino acid catabolic pathways in response to carbohydrate starvation is also mediated by SnRK1 signaling as part of a general energy-saving program

(Pedrotti *et al.*, 2018; Dietrich *et al.*, 2011). Transcriptional induction of a core set of eight enzymes involved in BCAA, proline, and tyrosine degradation requires the formation of a ternary complex between SnRK1 and a heterodimer of two basic leucine zipper (bZIP) transcription factors. A group C bZIP is phosphorylated by SnRK1 and acts as a bridge to an additional bZIP of the S1 group, which in turn directly controls the transcription of the genes encoding amino acid catabolic enzymes via binding to the G-box promoter elements (Pedrotti *et al.*, 2018; see also Box 2). The mechanism of induction is not known in such detail for the other amino acid degradation pathways. However, the transcriptional response of plants with induced or inhibited TOR and SnRK1 pathways (Fig. 4) indicates that reciprocal regulation by these kinases may adapt the general direction of amino acid metabolism (*de novo* synthesis versus degradation) to the environmental conditions.

Amino acids serve as signaling molecules to coordinate growth and stress responses

Amino acids are well known as signaling molecules in animals. Glutamate, aspartate, γ -aminobutyric acid (GABA), and glycine act as neurotransmitters (Hyman *et al.*, 2005). One of the mammalian TOR complexes (mTORC1) is activated by leucine, arginine, and *S*-adenosylmethionine (SAM) derived from methionine via complex sensing mechanisms (Kim and Guan, 2019). Amino acids are an adequate signal of good nutritional status in humans, who are not able to synthesize all 20 proteinogenic amino acids but have to acquire some essential amino acids (aromatic amino acids and BCAAs, histidine, lysine, methionine, and threonine) in their diet. In plants, the sulfur and nitrogen status is used as a TOR input signal of good nutrient availability instead (Dong *et al.*, 2017; Liu *et al.*, 2021). Equivalents of the mammalian amino acid sensors and TOR activation pathways have not been identified in plants so far (Shi *et al.* 2018). However, some recent findings indicate that the plant TOR pathway can nevertheless be induced by specific amino acids via the small GTPase ROP2 (Rho-related protein from plants 2) (Liu *et al.*, 2021). In addition to nitrate and ammonium, a total of 15 proteinogenic amino acids were able to restore TOR activity in the leaf primordia of nitrogen-starved *Arabidopsis* seedlings, with glutamine, alanine, glycine, and cysteine being the strongest activators (Fig. 3). Proline and alanine accumulate during osmotic stress and hypoxia, respectively. They transcriptionally induce their own degradation pathways to allow rapid removal after stress release. This induction can be blocked by increased contents of some other amino acids (e.g. methionine and isoleucine) in a TOR-dependent manner. O'Leary *et al.* (2020) confirmed the activation of the *Arabidopsis* TOR kinase by isoleucine and glutamine using an S6K phosphorylation assay. In addition, over-accumulations of BCAAs were reported to trigger rearrangements of the actin cytoskeleton during vacuole morphogenesis in *Arabidopsis*

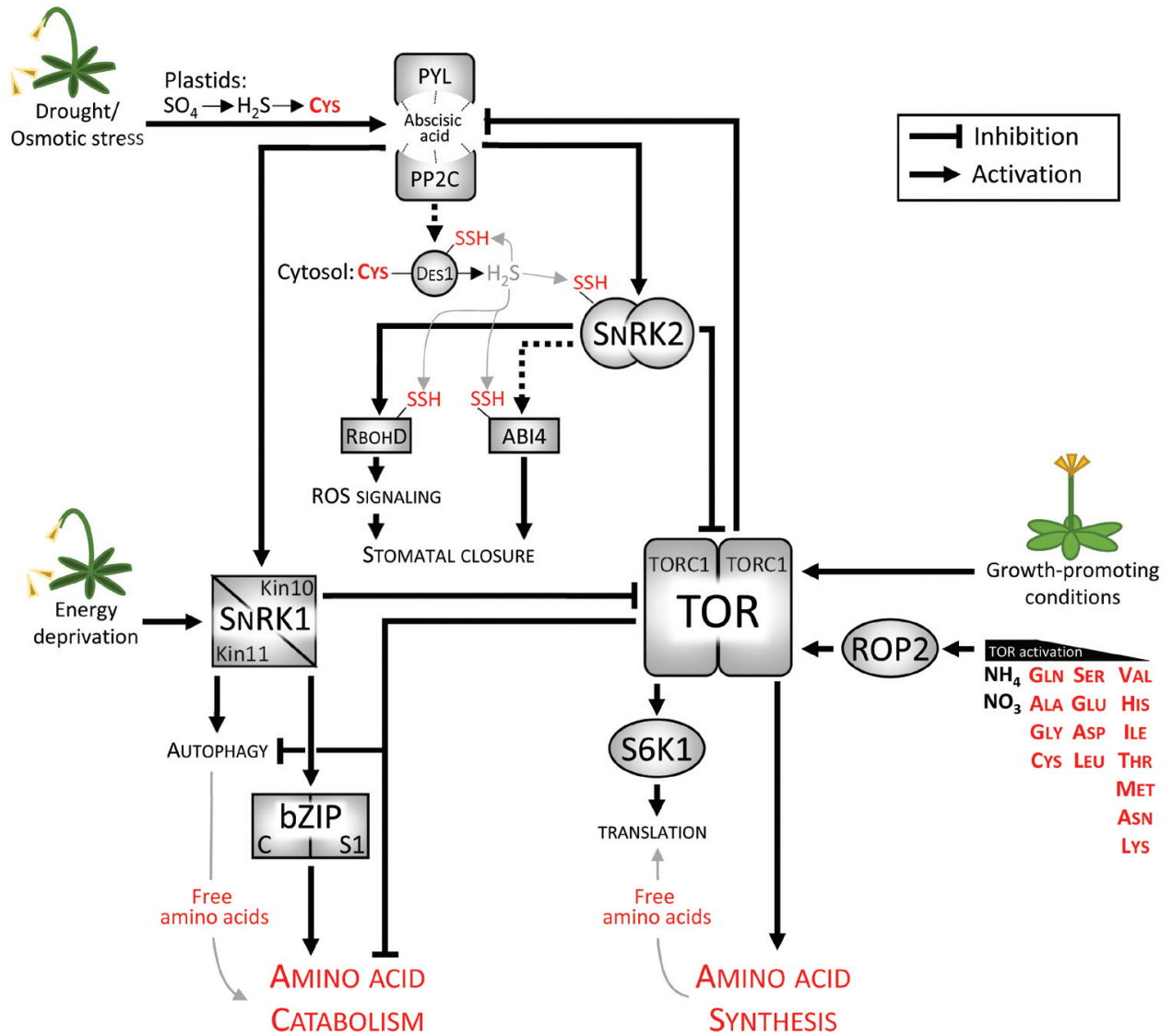


Fig. 3. The role of amino acids in metabolic regulation by TOR and SnRK signaling during abiotic stress. Metabolic adaptation to the environmental conditions is achieved by the antagonistic protein kinases TOR and SnRK. TOR signaling induces amino acid synthesis pathways and represses autophagy as well as amino acid catabolism in response to optimal growth conditions. Individual amino acids act as TOR activators (Cao *et al.*, 2019; O’Leary *et al.*, 2020; Liu *et al.*, 2021). Under unfavorable conditions, SnRKs are activated and repress TOR signaling. During energy deficiency, SnRK1 induces amino acid degradation pathways via bZIP transcription factors (Pedrotti *et al.*, 2018). Increased cysteine synthesis in the guard cells contributes to the activation of ABA signaling during drought (Batool *et al.*, 2018; Rajab *et al.*, 2019). Cysteine degradation produces the gaseous signaling molecule hydrogen sulfide (H₂S), which persulfidates and thus activates SnRK2.6, ABI4, and the NADPH oxidase RbohD, ultimately leading to stomatal closure and other physiological stress responses (Chen *et al.*, 2020; Shen *et al.*, 2020; Zhou *et al.*, 2021). In addition, inhibition of PP2C by ABA results in SnRK1 activation and thus promotes SnRK1 signaling during stress (Rodrigues *et al.*, 2013). Dashed arrows indicate indirect or postulated interactions. Intersections with amino acid metabolism are highlighted in red. ABI4, abscisic acid insensitive 4; bZIP, basic leucine zipper transcription factor; Des1, L-cysteine desulfhydrase 1; PYL, pyrabactin resistance 1-like (ABA receptor); PP2C, protein phosphatase type 2C; RbohD, respiratory burst oxidase homolog protein D; ROP2, rho-related protein from plants 2; ROS, reactive oxygen species; S6K1, S6 kinase 1; SnRK1, Snf1-related protein kinase 1; SnRK2, Snf1-related protein kinase 2; -SSH, persulfidation of cysteine residue; TOR, target of rapamycin.

(Cao *et al.*, 2019). This effect was blocked by TOR silencing but independent of the adapter protein RAPTOR (regulatory-associated protein of TOR). The mechanism and additional components mediating these signaling events still need to be discovered.

Additional input parameters are required to fully assess and integrate the environmental conditions. The plant, for example, needs to distinguish between osmotic stress and optimal growth conditions, which both lead to high levels of glucose and free amino acids. SnRK2 (Snf1-related protein

Box 3. TOR and SnRK1 signaling in plants**TOR (target of rapamycin)**

Two structurally and functionally distinct TOR protein complexes with several regulatory partners have been identified in eukaryotes. Plants contain only one of them, the TORC1 complex consisting of the TOR kinase and the regulatory subunits Raptor (regulatory-associated protein of TOR) and LST8 (lethal with SEC13 protein 8) (reviewed by [Fu et al., 2020](#); [Caldana et al., 2019](#); [Wu et al., 2019](#)).

A key function of TORC1 in plants is integrating different signals indicating growth-promoting environmental conditions such as nutrient and light availability to induce anabolic processes. TOR signaling is involved in the regulation of several plant-specific processes, such as the glyoxylate cycle, cell wall synthesis, and nitrogen and sulfur assimilation ([Wu et al., 2019](#)). During activation of the stem cells at the shoot apical meristem, plant TOR kinase integrates light availability with the universal TOR-activating signal, glucose, via auxin signaling ([Li et al., 2017](#); [Pfeiffer et al., 2016](#)). In contrast, sugar energy signaling is sufficient for TOR activation in the root apex ([Li et al., 2017](#)).

SnRK1 (Snf1-related protein kinase 1)

The SNF1/AMPK/SnRK1 family forms heterotrimeric holoenzymes containing a catalytic α -subunit and non-catalytic β - and γ -subunits. Arabidopsis expresses two isoforms of the SnRK1 catalytic α -subunit (AKIN10 and AKIN11), three β -subunits, and one γ -subunit (reviewed by [Wurzinger et al., 2018](#); [Emanuelle et al., 2016](#)).

SnRK1 kinase activity is induced by starvation conditions and activates an energy-saving program including autophagy and catabolic pathways. A distinct pattern of regulation of plant SnRK1 compared with its mammalian and yeast counterparts, AMPK and SNF1, allows adaptation to plant-specific metabolic requirements. SnRK1 activity is repressed by high-energy sugar-phosphates such as trehalose-6-phosphate, whereas SNF1 and AMPK sense the adenylate charge ([Baena-González and Lunn, 2020](#); [Emanuelle et al., 2016](#)). The plant SnRK1 has a unique autophosphorylation activity and thus is constitutively active unless repressed by high energy status. Low-energy stress triggers nuclear translocation of the catalytic subunit, leading to induced target gene expression ([Ramon et al., 2019](#)). There is also evidence indicating direct redox-regulation of conserved cysteine residues in the kinase subunit in response to ROS signaling ([Broeckx, 2018](#); [Wurzinger et al., 2017](#)).

kinase 2) kinases allow an additional fine-tuning during osmotic stress in plants, in particular, the inhibition of TOR signaling in the presence of sugar. TOR kinase phosphorylates abscisic acid (ABA) receptors and thus represses stress responses under growth-promoting conditions and during stress release. SnRK2s in turn phosphorylate Raptor, a regulatory component in the TOR complex, to inhibit TOR activity and prevent growth during environmental stress ([Fig. 3](#)) ([Wang et al., 2018](#)). The metabolism of the sulfur-containing amino acid cysteine is highly interconnected with TOR and SnRK signaling, and thus might act as an additional adjusting screw ([Fig. 3](#)). The cellular cysteine concentration is generally kept at a low micromolar level, and this can probably be achieved by a coordinated regulation of the different synthesis and degradation pathways ([Hildebrandt et al., 2015](#)). Isoforms of the hetero-oligomeric cysteine synthase complex consisting of *O*-acetylserine(thiol)lyase and serine acetyltransferase subunits are present in chloroplasts, mitochondria, and the cytosol ([Heeg et al., 2008](#)). In addition, several catabolic routes have been identified in the different subcellular compartments ([Hildebrandt et al., 2015](#); [Gotor et al., 2019](#)). Limitation of the

sulfur precursor for cysteine synthesis inhibits TOR activity indirectly by down-regulating glucose metabolism ([Dong et al., 2017](#)). In contrast, a decreased flux of cysteine into glutathione synthesis leads to TOR activation and stimulates protein translation ([Speiser et al., 2018](#)).

Recently, there have been several new insights into the role of cysteine as a signaling molecule during drought ([Fig. 3](#); see also [Box 2](#)). Sulfate acts as a mobile signal to report a low soil water content to the leaves. This signal is translated into increased sulfate reduction and cysteine synthesis in guard cell chloroplasts, which in turn induces ABA production ([Batoool et al., 2018](#); [Chen et al., 2019](#); [Rajab et al., 2019](#)). ABA then triggers the expression of DES1, a cytosolic cysteine desulfurase catalyzing the degradation of cysteine to pyruvate and the gaseous signaling molecule hydrogen sulfide (H₂S) ([Chen et al., 2020](#)). H₂S regulates the activity and/or stability of multiple proteins via persulfidation of regulatory cysteine residues ([Gotor et al., 2019](#)). In the guard cells, two central players in ABA-induced stomatal closure have been shown to be regulated by this post-translational modification. Persulfidation of the NADPH oxidase RbohD

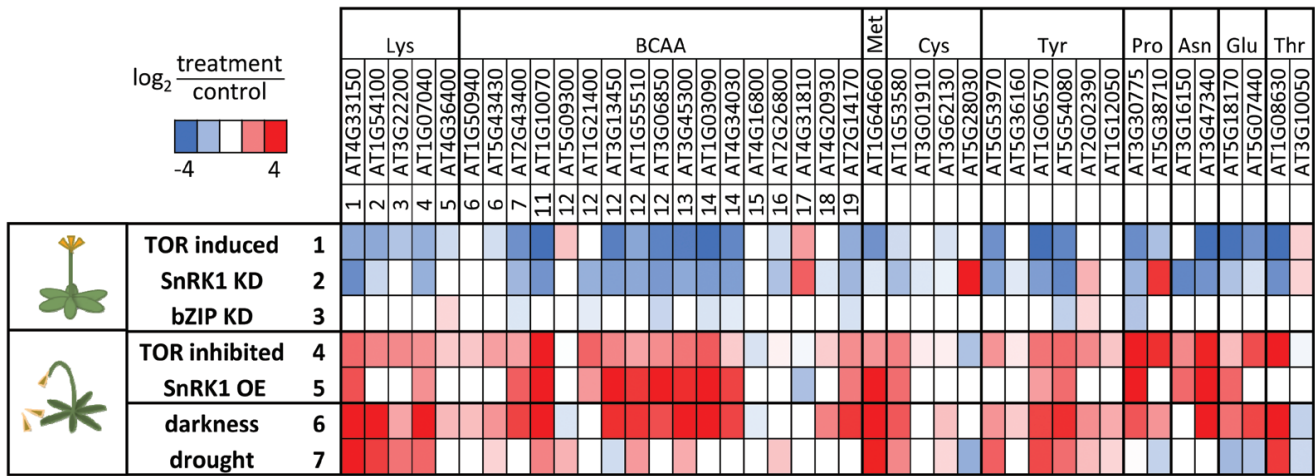


Fig. 4. Regulation of amino acid catabolic pathways in response to the energy status by TOR and SnRK1 signaling in *Arabidopsis thaliana*. Enzymes involved in amino acid degradation are regulated by the antagonistic action of TOR and SnRK1 signaling. TOR induction (dataset 1) as well as knockdown of SnRK1 (dataset 2) or downstream transcription factors of the bZIP group (dataset 3) generally lead to a transcriptional repression of amino acid catabolic enzymes (indicated by blue colors). The opposite effect, that is, an induction of amino acid catabolism (indicated by red colors), is caused by TOR inhibition (dataset 4) or SnRK1 overexpression (dataset 5), and also becomes apparent in datasets of plants subjected to stress conditions that are associated with energy deficiency [extended darkness (dataset 6) and drought (dataset 7)]. Gene IDs and, in addition, the numbers used in Fig. 2 for lysine and BCAA catabolic enzymes are indicated at the top. The colored squares represent log₂-fold changes in mRNA abundance (treatment versus control) compiled from the following datasets: 1, TOR induction by treatment with glucose (Xiong *et al.*, 2013); 2 and 3, knockdown lines for SnRK1 (*snrk1α1/α2*) and S1 bZIPs (*bZIP1/2/11/44/53*) after 6 h of extended darkness (Pedrotti *et al.*, 2018); 4, inhibition of TOR by AZD8055 (Dong *et al.*, 2015); 5, overexpression of the SnRK1 subunit KIN10 (Baena-González *et al.*, 2007); 6, extended darkness (means from six time points, 2–48 h; Usadel *et al.*, 2008); 7, drought (means from three experiments, 5–10 days of dehydration; Perera *et al.*, 2008; Ludwików *et al.*, 2009; Pandey *et al.*, 2013). KD, knockdown; OE, overexpression, SnRK1, Snf1-related protein kinase 1; TOR, target of rapamycin.

leads to increased reactive oxygen species (ROS) signaling, and persulfidation of two cysteine residues exposed on the surface close to an activation loop promotes the activity of the protein kinase SnRK2.6 and its interaction with ABA response element-binding factor2 (ABF2), a transcription factor downstream of ABA signaling (Chen *et al.*, 2020; Shen *et al.*, 2020). The transcription factor ABI4 (ABSCISIC ACID INSENSITIVE 4) is also activated by persulfidation (Zhou *et al.*, 2021). In addition, ABA-dependent persulfidation of the cysteine protease ATG4 seems to be involved in the regulation of autophagy (Laureano-Marín *et al.*, 2020). However, H₂S is also a potent inhibitor of cytochrome *c* oxidase (Birke *et al.* 2012). Thus, increased sulfide concentrations would lead to a down-regulation of mitochondrial respiration, and efficient detoxification mechanisms are required in the mitochondria to maintain or restore ATP production during stress (Birke *et al.*, 2015). The high level of interconnection between cysteine metabolism and ABA signaling is not restricted to the drought response in stomata. Endogenous ABA levels are decreased in germinating seedlings of several sulfur-assimilation mutants, and these lines are also hypersensitive to salt stress. ABA in turn induces the transcription of sulfate transporters and other genes associated with sulfur metabolism (Cao *et al.* 2014).

Several additional amino acids, such as methionine, lysine, histidine, and BCAAs, are normally present in low concentrations and would thus be suitable as signaling molecules. Imbalances in

the homeostasis of specific amino acids (e.g. glutamine, phenylalanine, and cysteine) elicit a strong immune reaction, indicating a potential signaling function in the biotic stress response (Pilot *et al.*, 2004; Liu *et al.*, 2010; Álvarez *et al.*, 2012; Pajeroska-Mukhtar *et al.*, 2012). Ca²⁺ influx mediated by glutamate receptor-like channels is involved in the regulation of several physiological processes in plants, such as pollen tube growth, root meristem proliferation, wound responses, and modulating ABA sensitivity during seed germination (Wudick *et al.*, 2018; Qiu *et al.*, 2020; Grenzi *et al.* 2021). These Ca²⁺-channels are not specific for L-glutamate but can also be activated by D-serine and the L-enantiomers of several other amino acids (Michard *et al.*, 2011; Alfieri *et al.*, 2020). Additional potential amino-acid-sensing mechanisms in plants are the GCN2 (general control non-derepressible 2) kinase pathway, which is activated by uncharged tRNAs, and the plastid-localized PII protein involved in the regulation of arginine and fatty acid biosynthesis (reviewed by Gent and Forde, 2017). There are also indications that proline might act as a signaling molecule to regulate specific aspects of the stress response and plant development (reviewed by Szabados and Savaure, 2010). Experimentally interfering with proline catabolism, for example, leads to developmental defects in seeds, leaves, and inflorescences (Nanjo *et al.*, 1999; Székely *et al.*, 2008). Proline might directly induce the expression of a set of genes that are relevant during recovery from drought by interaction with specific transcription factors (Oono *et al.*, 2003; Satoh *et al.*, 2004; Weltmeier *et al.*, 2006). In addition, local accumulation of

proline during pathogen infection can act as an apoptotic signal and trigger a hypersensitive response via its degradation intermediate pyrroline-5-carboxylate (Fabro *et al.*, 2004). Research on amino acid signaling in plants is still at an early stage and has much potential for fundamental discoveries.

Conclusion

In the past few years, great progress has been made in understanding the role of amino acid metabolism in signaling and stress-induced energy deficiency. However, several key questions remain unanswered with respect to basic metabolic events as well as their potential to be utilized in agriculture. How do plants correctly interpret the different metabolic signals and balance the levels of individual amino acids to fulfill their diverse roles? Which amino acids act as signals, and how does amino acid signaling work mechanistically? How can plants sense amino acid levels? Do any particular pathways or enzymes act as bottlenecks during stress tolerance that might be addressed to improve the performance of crops under increasingly stressful growth conditions? What is the role of amino acids during growth–defense trade-offs, and can they contribute to uncoupling these processes, if necessary? Why do attempts to increase the seed contents of essential amino acids often lead to severe growth phenotypes, and how can this effect be reduced? What happens to the nitrogen released during amino acid catabolism? Thus, research addressing amino acid metabolism in plants has the potential to advance the fields of stress physiology as well as plant energy biology in the near future.

Acknowledgements

We thank Hans-Peter Braun for critical reading of the manuscript. Research in TMH's group is supported by the Deutsche Forschungsgemeinschaft (HI 1471).

References

- Alcázar R, Altabella T, Marco F, Bortolotti C, Reymond M, Koncz C, Carrasco P, Tiburcio AF. 2010. Polyamines: molecules with regulatory functions in plant abiotic stress tolerance. *Planta* **231**, 1237–1249.
- Alfieri A, Doccula FG, Pederzoli R, *et al.* 2020. The structural bases for agonist diversity in an *Arabidopsis thaliana* glutamate receptor-like channel. *Proceedings of the National Academy of Sciences, USA* **117**, 752–760.
- Álvarez C, Ángeles Bermúdez M, Romero LC, Gotor C, García I. 2012. Cysteine homeostasis plays an essential role in plant immunity. *New Phytologist* **193**, 165–177.
- Angelovici R, Lipka AE, Deason N, Gonzalez-Jorge S, Lin H, Cepela J, Buell R, Gore MA, Dellapenna D. 2013. Genome-wide analysis of branched-chain amino acid levels in *Arabidopsis* seeds. *The Plant Cell* **25**, 4827–4843.
- Araújo WL, Ishizaki K, Nunes-Nesi A, *et al.* 2010. Identification of the 2-hydroxyglutarate and isovaleryl-CoA dehydrogenases as alternative electron donors linking lysine catabolism to the electron transport chain of *Arabidopsis* mitochondria. *The Plant Cell* **22**, 1549–1563.
- Araus V, Swift J, Alvarez JM, Henry A, Coruzzi GM. 2020. A balancing act: how plants integrate nitrogen and water signals. *Journal of Experimental Botany* **71**, 4442–4451.
- Baena-González E, Hanson J. 2017. Shaping plant development through the SnRK1–TOR metabolic regulators. *Current Opinion in Plant Biology* **35**, 152–157.
- Baena-González E, Lunn JE. 2020. SnRK1 and trehalose 6-phosphate – two ancient pathways converge to regulate plant metabolism and growth. *Current Opinion in Plant Biology* **55**, 52–59.
- Baena-González E, Rolland F, Thevelein JM, Sheen J. 2007. A central integrator of transcription networks in plant stress and energy signalling. *Nature* **448**, 938–942.
- Batool S, Uslu VV, Rajab H, *et al.* 2018. Sulfate is incorporated into cysteine to trigger ABA production and stomatal closure. *The Plant Cell* **30**, 2973–2987.
- Birke H, Haas FH, De Kok LJ, Balk J, Wirtz M, Hell R. 2012. Cysteine biosynthesis, in concert with a novel mechanism, contributes to sulfide detoxification in mitochondria of *Arabidopsis thaliana*. *Biochemical Journal* **445**, 275–283.
- Birke H, Hildebrandt TM, Wirtz M, Hell R. 2015. Sulfide detoxification in plant mitochondria. *Methods in Enzymology* **555**, 271–286.
- Biswal B, Joshi PN, Raval MK, Biswal UC. 2011. Photosynthesis, a global sensor of environmental stress in green plants: stress signalling and adaptation. *Current Science* **101**, 47–56.
- Broeckx T. 2018. Upstream regulators of the plant energy sensor SnRK1. PhD thesis, KU Leuven.
- Broeckx T, Hulsmans S, Rolland F. 2016. The plant energy sensor: evolutionary conservation and divergence of SnRK1 structure, regulation, and function. *Journal of Experimental Botany* **67**, 6215–6252.
- Caldana C, Martins MCM, Mubeen U, Urrea-Castellanos R. 2019. The magic ‘hammer’ of TOR: the multiple faces of a single pathway in the metabolic regulation of plant growth and development. *Journal of Experimental Botany* **70**, 2217–2225.
- Cao MJ, Wang Z, Zhao Q, Mao JL, Speiser A, Wirtz M, Hell R, Zhu JK, Xiang CB. 2014. Sulfate availability affects ABA levels and germination response to ABA and salt stress in *Arabidopsis thaliana*. *The Plant Journal* **77**, 604–615.
- Cao P, Kim S-J, Xing A, Schenck CA, Liu L, Jiang N, Wang J, Last RL, Brandizzi F. 2019. Homeostasis of branched-chain amino acids is critical for the activity of TOR signaling in *Arabidopsis*. *eLife* **8**, e50747.
- Chen S, Jia H, Wang X, Shi C, Wang X, Ma P, Wang J, Ren M, Li J. 2020. Hydrogen sulfide positively regulates abscisic acid signaling through persulfidation of SnRK2.6 in guard cells. *Molecular Plant* **13**, 732–744.
- Chen YC, Holmes EC, Rajniak J, Kim JG, Tang S, Fischer CR, Mudgett MB, Sattely ES. 2018. *N*-hydroxy-pipecolic acid is a mobile metabolite that induces systemic disease resistance in *Arabidopsis*. *Proceedings of the National Academy of Sciences, USA* **115**, E4920–E4929.
- Chen Z, Zhao PX, Miao ZQ, *et al.* 2019. SULTR3s function in chloroplast sulfate uptake and affect ABA biosynthesis and the stress response. *Plant Physiology* **180**, 593–604.
- Dietrich K, Weltmeier F, Ehlert A, Weiste C, Stahl M, Harter K, Dröge-Laser W. 2011. Heterodimers of the *Arabidopsis* transcription factors bZIP1 and bZIP53 reprogram amino acid metabolism during low energy stress. *The Plant Cell* **23**, 381–395.
- Ding G, Che P, Ilarslan H, Wurtele ES, Nikolau BJ. 2012. Genetic dissection of methylcrotonyl CoA carboxylase indicates a complex role for mitochondrial leucine catabolism during seed development and germination. *The Plant Journal* **70**, 562–577.
- Ding P, Rekhter D, Ding Y, *et al.* 2016. Characterization of a pipecolic acid biosynthesis pathway required for systemic acquired resistance. *The Plant Cell* **28**, 2603–2615.

- Dong P, Xiong F, Que Y, Wang K, Yu L, Li Z, Ren M.** 2015. Expression profiling and functional analysis reveals that TOR is a key player in regulating photosynthesis and phytohormone signaling pathways in *Arabidopsis*. *Frontiers in Plant Science* **6**, 677.
- Dong Y, Silbermann M, Speiser A, et al.** 2017. Sulfur availability regulates plant growth via glucose-TOR signaling. *Nature Communications* **8**, 1174.
- Emanuelle S, Doblin MS, Stapleton DI, Bacic A, Gooley PR.** 2016. Molecular insights into the enigmatic metabolic regulator, SnRK1. *Trends in Plant Science* **21**, 341–353.
- Fabro G, Kovács I, Pavet V, Szabados L, Alvarez ME.** 2004. Proline accumulation and *AtP5CS2* gene activation are induced by plant-pathogen incompatible interactions in *Arabidopsis*. *Molecular Plant-Microbe Interactions* **17**, 343–350.
- Falcone Ferreyra ML, Rius SP, Casati P.** 2012. Flavonoids: biosynthesis, biological functions, and biotechnological applications. *Frontiers in Plant Science* **3**, 222.
- Fu L, Wang P, Xiong Y.** 2020. Target of Rapamycin signaling in plant stress responses. *Plant Physiology* **182**, 1613–1623.
- Gent L, Forde BG.** 2017. How do plants sense their nitrogen status? *Journal of Experimental Botany* **68**, 2531–2539.
- Gipson AB, Morton KJ, Rhee RJ, et al.** 2017. Disruptions in valine degradation affect seed development and germination in *Arabidopsis*. *The Plant Journal* **90**, 1029–1039.
- Gotor C, García I, Aroca Á, Laureano-Marín AM, Arenas-Alfonseca L, Jurado-Flores A, Moreno I, Romero LC.** 2019. Signaling by hydrogen sulfide and cyanide through post-translational modification. *Journal of Experimental Botany* **70**, 4251–4265.
- Grenzi M, Bonza MC, Alfieri A, Costa A.** 2021. Structural insights into long-distance signal transduction pathways mediated by plant glutamate receptor-like channels. *New Phytologist* **229**, 1261–1267.
- Gururani MA, Venkatesh J, Tran LS.** 2015. Regulation of photosynthesis during abiotic stress-induced photoinhibition. *Molecular Plant* **8**, 1304–1320.
- Halkier BA, Gershenzon J.** 2006. Biology and biochemistry of glucosinolates. *Annual Review of Plant Biology* **57**, 303–333.
- Hartmann M, Zeier J.** 2018. L-lysine metabolism to *N*-hydroxypipicolinic acid: an integral immune-activating pathway in plants. *The Plant Journal* **96**, 5–21.
- Haslam E.** 1993. Shikimic acid: metabolism and metabolites. Chichester: Wiley.
- Heeg C, Kruse C, Jost R, Gutensohn M, Ruppert T, Wirtz M, Hell R.** 2008. Analysis of the *Arabidopsis* *O*-acetylserine(thiol)lyase gene family demonstrates compartment-specific differences in the regulation of cysteine synthesis. *The Plant Cell* **20**, 168–185.
- Heinemann B, Künzler P, Eubel H, Braun HP, Hildebrandt TM.** 2021. Estimating the number of protein molecules in a plant cell: protein and amino acid homeostasis during drought. *Plant Physiology* **185**, 385–404.
- Hildebrandt TM, Nunes Nesi A, Araújo WL, Braun HP.** 2015. Amino acid catabolism in plants. *Molecular Plant* **8**, 1563–1579.
- Hirota T, Izumi M, Wada S, Makino A, Ishida H.** 2018. Vacuolar protein degradation via autophagy provides substrates to amino acid catabolic pathways as an adaptive response to sugar starvation in *Arabidopsis thaliana*. *Plant & Cell Physiology* **59**, 1363–1376.
- Huang X, Zheng C, Liu F, et al.** 2019. Genetic analyses of the *Arabidopsis* ATG1 kinase complex reveal both kinase-dependent and independent autophagic routes during fixed-carbon starvation. *The Plant Cell* **31**, 2973–2995.
- Hyman SE.** 2005. Neurotransmitters. *Current Biology* **15**, R154–R158.
- Ishizaki K, Larson TR, Schauer N, Fernie AR, Graham IA, Leaver CJ.** 2005. The critical role of *Arabidopsis* electron-transfer flavoprotein:ubiquinone oxidoreductase during dark-induced starvation. *The Plant Cell* **17**, 2587–2600.
- Ishizaki K, Schauer N, Larson TR, Graham IA, Fernie AR, Leaver CJ.** 2006. The mitochondrial electron transfer flavoprotein complex is essential for survival of *Arabidopsis* in extended darkness. *The Plant Journal* **47**, 751–760.
- Izumi M, Hidema J, Makino A, Ishida H.** 2013. Autophagy contributes to nighttime energy availability for growth in *Arabidopsis*. *Plant Physiology* **161**, 1682–1693.
- Jamsheer K M, Jindal S, Laxmi A.** 2019. Evolution of TOR–SnRK dynamics in green plants and its integration with phytohormone signaling networks. *Journal of Experimental Botany* **70**, 2239–2259.
- Kim J, Guan KL.** 2019. mTOR as a central hub of nutrient signalling and cell growth. *Nature Cell Biology* **21**, 63–71.
- Latimer S, Li Y, Nguyen TTH, Soubeyrand E, Fatihi A, Elowsky CG, Block A, Pichersky E, Basset GJ.** 2018. Metabolic reconstructions identify plant 3-methylglutaconyl-CoA hydratase that is crucial for branched-chain amino acid catabolism in mitochondria. *The Plant Journal* **95**, 358–370.
- Laureano-Marín AM, Aroca A, Perez-Perez ME, Yruela I, Jurado-Flores A, Moreno I, Crespo JL, Romero LC, Gotor C.** 2020. Abscisic acid-triggered persulfidation of cysteine protease ATG4 mediates regulation of autophagy by sulfide. *The Plant Cell* **32**, 3902–3920.
- Less H, Angelovici R, Tzin V, Galili G.** 2011. Coordinated gene networks regulating *Arabidopsis* plant metabolism in response to various stresses and nutritional cues. *The Plant Cell* **23**, 1264–1271.
- Less H, Galili G.** 2008. Principal transcriptional programs regulating plant amino acid metabolism in response to abiotic stresses. *Plant Physiology* **147**, 316–330.
- Li X, Cai W, Liu Y, Li H, Fu L, Liu Z, Xu L, Liu H, Xu T, Xiong Y.** 2017. Differential TOR activation and cell proliferation in *Arabidopsis* root and shoot apices. *Proceedings of the National Academy of Sciences, USA* **114**, 2765–2770.
- Liu G, Ji Y, Bhuiyan NH, Pilot G, Selvaraj G, Zou J, Wei Y.** 2010. Amino acid homeostasis modulates salicylic acid-associated redox status and defense responses in *Arabidopsis*. *The Plant Cell* **22**, 3845–3863.
- Liu Y, Bassham DC.** 2012. Autophagy: pathways for self-eating in plant cells. *Annual Review of Plant Biology* **63**, 215–237.
- Liu Y, Duan X, Zhao X, Ding W, Wang Y, Xiong Y.** 2021. Diverse nitrogen signals activate convergent ROP2-TOR signaling in *Arabidopsis*. *Developmental Cell* doi: [10.1016/j.devcel.2021.03.022](https://doi.org/10.1016/j.devcel.2021.03.022)
- Ludwików A, Kierzek D, Gallois P, Zeef L, Sadowski J.** 2009. Gene expression profiling of ozone-treated *Arabidopsis abi1td* insertional mutant: protein phosphatase 2C ABI1 modulates biosynthesis ratio of ABA and ethylene. *Planta* **230**, 1003–1017.
- Margalha L, Confraria A, Baena-González E.** 2019. SnRK1 and TOR: modulating growth–defense trade-offs in plant stress responses. *Journal of Experimental Botany* **70**, 2261–2274.
- Michard E, Lima PT, Borges F, Silva AC, Portes MT, Carvalho JE, Gilliam M, Liu LH, Obermeyer G, Feijó JA.** 2011. Glutamate receptor-like genes form Ca^{2+} channels in pollen tubes and are regulated by pistil α -serine. *Science* **332**, 434–437.
- Nabavi SM, Šamec D, Tomczyk M, et al.** 2020. Flavonoid biosynthetic pathways in plants: versatile targets for metabolic engineering. *Biotechnology Advances* **38**, 107316.
- Nanjo T, Kobayashi M, Yoshida Y, Sanada Y, Wada K, Tsukaya H, Kakubari Y, Yamaguchi-Shinozaki K, Shinozaki K.** 1999. Biological functions of proline in morphogenesis and osmotolerance revealed in anti-sense transgenic *Arabidopsis thaliana*. *The Plant Journal* **18**, 185–193.
- Nukarinen E, Nägele T, Pedrotti L, et al.** 2016. Quantitative phosphoproteomics reveals the role of the AMPK plant ortholog SnRK1 as a metabolic master regulator under energy deprivation. *Scientific Reports* **6**, 31697.
- O’Leary BM, Oh GJK, Lee CP, Millar AH.** 2020. Metabolite regulatory interactions control plant respiratory metabolism via Target of Rapamycin (TOR) kinase activation. *The Plant Cell* **32**, 666–682.
- Oono Y, Seki M, Nanjo T, et al.** 2003. Monitoring expression profiles of *Arabidopsis* gene expression during rehydration process after dehydration using ca. 7000 full-length cDNA microarray. *The Plant Journal* **34**, 868–887.

- Pacheco JM, Canal MV, Pereyra CM, Welchen E, Martínez-Noël G, Estevez JM.** 2021. The tip of the iceberg: emerging roles of TORC1 and its regulation in plant cells. *Journal of Experimental Botany* **72**, 4085–4101.
- Pajeroska-Mukhtar KM, Wang W, Tada Y, Oka N, Tucker CL, Fonseca JP, Dong X.** 2012. The HSF-like transcription factor TBF1 is a major molecular switch for plant growth-to-defense transition. *Current Biology* **22**, 103–112.
- Pandey N, Ranjan A, Pant P, Tripathi RK, Ateek F, Pandey HP, Patre UV, Sawant SV.** 2013. CAMTA 1 regulates drought responses in *Arabidopsis thaliana*. *BMC Genomics* **14**, 216.
- Pedrotti L, Weiste C, Nägele T, et al.** 2018. Snf1-RELATED KINASE1-controlled C/S₁-bZIP signaling activates alternative mitochondrial metabolic pathways to ensure plant survival in extended darkness. *The Plant Cell* **30**, 495–509.
- Peng C, Uygun S, Shiu SH, Last RL.** 2015. The impact of the branched-chain ketoacid dehydrogenase complex on amino acid homeostasis in *Arabidopsis*. *Plant Physiology* **169**, 1807–1820.
- Perera IY, Hung CY, Moore CD, Stevenson-Paulik J, Boss WF.** 2008. Transgenic *Arabidopsis* plants expressing the type 1 inositol 5-phosphatase exhibit increased drought tolerance and altered abscisic acid signaling. *The Plant Cell* **20**, 2876–2893.
- Pfeiffer A, Janocha D, Dong Y, et al.** 2016. Integration of light and metabolic signals for stem cell activation at the shoot apical meristem. *eLife* **5**, e17023.
- Pilot G, Stransky H, Bushey DF, Pratelli R, Ludewig U, Wingate VP, Frommer WB.** 2004. Overexpression of *GLUTAMINE DUMPER1* leads to hypersecretion of glutamine from hydathodes of *Arabidopsis* leaves. *The Plant Cell* **16**, 1827–1840.
- Pires MV, Pereira Júnior AA, Medeiros DB, et al.** 2016. The influence of alternative pathways of respiration that utilize branched-chain amino acids following water shortage in *Arabidopsis*. *Plant, Cell & Environment* **39**, 1304–1319.
- Qiu XM, Sun YY, Ye XY, Li ZG.** 2020. Signaling role of glutamate in plants. *Frontiers in Plant Science* **10**, 1743.
- Rajab H, Khan MS, Malagoli M, Hell R, Wirtz M.** 2019. Sulfate-induced stomata closure requires the canonical ABA signal transduction machinery. *Plants* **8**, 21.
- Ramon M, Dang TVT, Broeckx T, Hulsmans S, Crepin N, Sheen J, Rolland F.** 2019. Default activation and nuclear translocation of the plant cellular energy sensor SnRK1 regulate metabolic stress responses and development. *The Plant Cell* **31**, 1614–1632.
- Rodrigues A, Adamo M, Crozet P, et al.** 2013. ABI1 and PP2CA phosphatases are negative regulators of Snf1-related protein kinase1 signaling in *Arabidopsis*. *The Plant Cell* **25**, 3871–3884.
- Rodríguez M, Parola R, Andreola S, Pereyra C, Martínez-Noël G.** 2019. TOR and SnRK1 signaling pathways in plant response to abiotic stresses: do they always act according to the “yin-yang” model? *Plant Science* **288**, 110220.
- Ryabova LA, Robaglia C, Meyer C.** 2019. Target of Rapamycin kinase: central regulatory hub for plant growth and metabolism. *Journal of Experimental Botany* **70**, 2211–2216.
- Saito K, Yonekura-Sakakibara K, Nakabayashi R, Higashi Y, Yamazaki M, Tohge T, Fernie AR.** 2013. The flavonoid biosynthetic pathway in *Arabidopsis*: structural and genetic diversity. *Plant Physiology and Biochemistry* **72**, 21–34.
- Salehin M, Li B, Tang M, Katz E, Song L, Ecker JR, Kliebenstein DJ, Estelle M.** 2019. Auxin-sensitive Aux/IAA proteins mediate drought tolerance in *Arabidopsis* by regulating glucosinolate levels. *Nature Communications* **10**, 4021.
- Satoh R, Fujita Y, Nakashima K, Shinozaki K, Yamaguchi-Shinozaki K.** 2004. A novel subgroup of bZIP proteins functions as transcriptional activators in hypoosmolarity-responsive expression of the *ProDH* gene in *Arabidopsis*. *Plant & Cell Physiology* **45**, 309–317.
- Schepetilnikov M, Dimitrova M, Mancera-Martínez E, Geldreich A, Keller M, Ryabova LA.** 2013. TOR and S6K1 promote translation reinitiation of uORF-containing mRNAs via phosphorylation of eIF3h. *The EMBO Journal* **32**, 1087–1102.
- Schertl P, Danne L, Braun HP.** 2017. 3-Hydroxyisobutyrate dehydrogenase is involved in both, valine and isoleucine degradation in *Arabidopsis thaliana*. *Plant Physiology* **175**, 51–61.
- Sharma M, Muhammed JK, Saksena HB, et al.** 2021. Balancing growth and defense. In: Pandey GK, ed. *Protein kinases and stress signaling in plants: functional genomic perspective*. Hoboken: John Wiley & Sons, 105–132.
- Shen J, Zhang J, Zhou M, et al.** 2020. Persulfidation-based modification of cysteine desulfhydrase and the NADPH oxidase RBOHD controls guard cell abscisic acid signaling. *The Plant Cell* **32**, 1000–1017.
- Shi L, Wu Y, Sheen J.** 2018. TOR signaling in plants: conservation and innovation. *Development* **145**, dev160887.
- Signorelli S, Tarkowski ŁP, Van den Ende W, Bassham DC.** 2019. Linking autophagy to abiotic and biotic stress responses. *Trends in Plant Science* **24**, 413–430.
- Singh M, Kumar J, Singh S, Singh VP, Prasad SM.** 2015. Roles of osmoprotectants in improving salinity and drought tolerance in plants: a review. *Reviews in Environmental Science and Bio/Technology* **14**, 407–426.
- Speiser A, Silbermann M, Dong Y, et al.** 2018. Sulfur partitioning between glutathione and protein synthesis determines plant growth. *Plant Physiology* **177**, 927–937.
- Szabados L, Savouré A.** 2010. Proline: a multifunctional amino acid. *Trends in Plant Science* **15**, 89–97.
- Székely G, Abrahám E, Cséplö A, et al.** 2008. Duplicated *P5CS* genes of *Arabidopsis* play distinct roles in stress regulation and developmental control of proline biosynthesis. *The Plant Journal* **53**, 11–28.
- Tang J, Bassham DC.** 2018. Autophagy in crop plants: what's new beyond *Arabidopsis*? *Open Biology* **8**, 180162.
- Thompson MG, Blake-Hedges JM, Pereira JH, et al.** 2020. An iron (II) dependent oxygenase performs the last missing step of plant lysine catabolism. *Nature Communications* **11**, 2931.
- Usadel B, Bläsing OE, Gibon Y, Retzlaff K, Höhne M, Günther M, Stitt M.** 2008. Global transcript levels respond to small changes of the carbon status during progressive exhaustion of carbohydrates in *Arabidopsis* rosettes. *Plant Physiology* **146**, 1834–1861.
- Van Leene J, Han C, Gadeyne A, et al.** 2019. Capturing the phosphorylation and protein interaction landscape of the plant TOR kinase. *Nature Plants* **5**, 316–327.
- Wang P, Zhao Y, Li Z, et al.** 2018. Reciprocal regulation of the TOR kinase and ABA receptor balances plant growth and stress response. *Molecular Cell* **69**, 100–112.e6.
- Weltmeier F, Ehlerdt A, Mayer CS, Dietrich K, Wang X, Schütze K, Alonso R, Harter K, Vicente-Carbajosa J, Dröge-Laser W.** 2006. Combinatorial control of *Arabidopsis* proline dehydrogenase transcription by specific heterodimerisation of bZIP transcription factors. *The EMBO Journal* **25**, 3133–3143.
- Wu Y, Shi L, Li L, Fu L, Liu Y, Xiong Y, Sheen J.** 2019. Integration of nutrient, energy, light, and hormone signalling via TOR in plants. *Journal of Experimental Botany* **70**, 2227–2238.
- Wudick MM, Michard E, Oliveira Nunes C, Feijó JA.** 2018. Comparing plant and animal glutamate receptors: common traits but different fates? *Journal of Experimental Botany* **69**, 4151–4163.
- Wurzinger B, Mair A, Fischer-Schrader K, Nukarinen E, Roustan V, Weckwerth W, Teige M.** 2017. Redox state-dependent modulation of plant SnRK1 kinase activity differs from AMPK regulation in animals. *FEBS Letters* **591**, 3625–3636.
- Wurzinger B, Nukarinen E, Nägele T, Weckwerth W, Teige M.** 2018. The SnRK1 kinase as central mediator of energy signaling between different organelles. *Plant Physiology* **176**, 1085–1094.
- Xiong Y, McCormack M, Li L, Hall Q, Xiang C, Sheen J.** 2013. Glucose-TOR signalling reprograms the transcriptome and activates meristems. *Nature* **496**, 181–186.
- Zhou M, Zhang J, Shen J, et al.** 2021. Hydrogen sulfide-linked persulfidation of ABI4 controls ABA responses through the transactivation of MAPKKK18 in *Arabidopsis*. *Molecular Plant* doi: 10.1016/j.molp.2021.03.007

3 Appendix

3.1 Curriculum Vitae

Björn Heinemann

born 21.02.1991 in Hildesheim / Germany

Address: Berggartenstraße 6, 30419 Hannover,

bjorn-heinemann@gmx.de

School and academic education

1997-2001	Primary school in Barnten, Germany
2001-2005	Secondary school in Nordstemmen, Germany
2005-2010	Secondary school in Sarstedt, Germany; Abitur
2011-2014	Bachelor of Science, Plant Biotechnology Leibniz University Hannover, Germany Thesis: Transformation of <i>Anacyclus pyrethrum</i> via <i>A. rhizogenes</i> (Grade 1,7)
2014-2016	Master of Science: Plant Biotechnology Leibniz University Hannover, Germany Thesis: Profiling the stress-induced amino acid catabolism of <i>A. thaliana</i> (Grade 1,3)
2016-2021	PhD candidate at Department of Plant Proteomics, Institute for Plant Genetics Leibniz University Hannover, Germany Thesis: Amino acid metabolism under drought stress in <i>A. thaliana</i> (Grade: summa cum laude)
Since 2021	Post-Doc at Department of Plant Proteomics, Institute of Plant Genetics, Leibniz University Hannover

Academic appointments

2013-2015	Student Assistant, Institute of Horticultural Production Systems, Leibniz University Hannover, Germany
2013-2014	Member of the iGEM Team of Hannover Project: Expression of a heavy metal binding super protein in <i>A. thaliana</i>
2015-2016	ISAP/DAAD six month scholarship, Microbiology Lab of Prof. Godoy, Institute of Biology, Northeastern University, Boston, USA

3.2 List of publications

- **Heinemann, B.**, Hildebrandt, T.M. (2021):
The role of amino acid metabolism in signaling and metabolic adaptation to stress induced energy deficiency in plants
Journal of Experimental Botany, Vol. 72, Issue 13, Pages 4634–4645
DOI: 10.1093/jxb/erab182
- **Heinemann, B.**, Künzler, P., Eubel, H., Braun, H.P., Hildebrandt, T.M. (2020):
Estimating the number of protein molecules in a plant cell: protein and amino acid homeostasis during drought
Plant Physiology, Vol. 185, Issue 2, Pages 385–404
DOI: 10.1093/plphys/kiaa050
- Batista-Silva, W.* , **Heinemann, B.***, Rugen, N., Nunes-Nesi, A., Araújo, W.L., Braun, H.P., Hildebrandt, T.M. (2019): The role of amino acid metabolism during abiotic stress release. * *Equally contributing first authors*
Plant, Cell & Environment, Vol. 42, Pages 1630-1644
DOI: 10.1111/pce.13518
- Ching, C., Gozzi, K., **Heinemann, B.**, Chai, Y. and Godoy, V. (2017): RNA-mediated cis regulation in *Acinetobacter baumannii* modulates stress-induced phenotypic variation.
Journal of bacteriology, Vol. 199, Issue 11
DOI: 10.1128/JB.00799-16

3.3 Conference contribution

Poster Presentations

- **International Plant Science Conference (Botanikertagung)**
September 15-19, 2019, Rostock (Germany)
Heinemann, B., Braun, H.P., Hildebrandt, T.M.: "A metabolic and proteomic time series of amino acid metabolism during progressive drought stress in *Arabidopsis thaliana*"
- **11th International Conference for Plant Mitochondrial Biology (ICPMB)**
March 10-15, 2019, Ein Gedi (Israel)
Heinemann, B., Braun, H.P., Hildebrandt, T.M.: "Amino acid metabolism under stress: Desiccation vs. Extended Darkness"
- **CropStrengthen Oxidative and Abiotic Stress Symposium**
November 13-14, 2018, Potsdam (Germany)
Heinemann, B., Braun, H.P., Hildebrandt, T.M.: "Between life and death: Arabidopsis amino acid profiles during reversible and fatal drought stress"
- **International Plant Immunity Symposium**
June 14-15, 2018, Göttingen (Germany)
Heinemann, B., Lorenz, C., Hildebrandt, T.M.: "Possible role of mitochondrial persulfide metabolism in plant pathogen response"